CRANFIELD INSTITUTE OF TECHNOLOGY

School of Mechanical Engineering

Ph.D. THESIS

Academic Year 1972 – 1974

A.A. RIZKALLA

THE INFLUENCE OF AIR AND LIQUID PROPERTIES ON AIRBLAST ATOMIZATION

SUPERVISOR: PROFESSOR A.H. LEFEBVRE

September, 1974.

SUMMARY

This thesis reports the results of a detailed programme of research on airblast atomization carried out using a specially designed atomizer in which the liquid is first spread into a thin sheet and then exposed on both sides to high velocity air. The primary aim of the investigation was to examine the influence of air and liquid properties on atomization quality. The work was divided into four main phases:-

(1) The first phase was confined to the effects of liquid properties, namely viscosity, surface tension and density on mean drop size. Special liquids were produced to study the separate effect of each property on atomization quality. They presented a range of values of viscosity from 1.0 to 124 centipoise, while surface tension and density were varied between 26 and 73.5 dynes/cm and 0.8 and 1.8 gm/cm^3 respectively. Atomizing air velocities covered the range of practical interest to the designers of continuous combustion systems and varied between 60 and 125 m/sec.

(2) To obtain experimental data on the influence of air properties, notably air density, on mean drop size, the air temperature was varied between 23 and 151°C at atmospheric pressure in one series of experiments, while a separate study on the effect of air pressure on atomization quality was undertaken, where tests were conducted at constant levels of air velocity and temperature, using a range of liquid flows from 5 to 30 gm/sec, at various levels of air pressure between 1 and 8.5 atm.

(3) In order to provide a comprehensive picture of airblast atomizer performance over a wide range of conditions the separate effects of varying air velocity, liquid flow rate, and hence atomizing air/liquid mass ratio on SMD were examined. This study enabled a better understanding of the effects of changes in operation on the atomizer's performance.

(4) In all three phases above, velocities of both inner and outer atomizing air streams were kept equal. This last phase was aimed at studying the effect of varying the velocity between the inner and outer air streams. Best atomization quality was achieved when 65% of the total atomizing air was flowing through the outer stream.

A detailed description of the light-scattering technique for drop size measurement is included. A discussion on the importance of the results obtained and their direct relevance to the design of airblast atomizers is given.

A dimensional analysis and inspection of all the data obtained on the effects of air and liquid properties on atomization quality showed that over the following range of conditions:

Liquid viscosity	-	1.0	to	44	centipoise
Liquid surface tension	-	26	to	73.5	dynes/cm
Liquid density	-	0.78	to	1.5	gm/cm^3
Air velocity	-	70	to	125	m/sec
Air temperature	-	20	to	151	^oC
Air pressure	-	1.0	to	8.5	kgf/cm^2
Air/liquid ratio	-	2	to	6	

these effects could be described by the dimensionally correct equation:-

$$SMD = 0.33 \frac{(\sigma_\ell \rho_\ell D)^{0.5}}{V_a \rho_a} (1 + W_\ell / W_a) + 0.157 \left(\frac{\eta_\ell^2}{\sigma_\ell \rho_a} \right)^{0.425} D^{0.575} (1 + W_\ell / W_a)^2$$

The ability of this equation to predict values of SMD over the above range of air and liquid properties is also demonstrated.

ACKNOWLEDGEMENTS

The author would like to record his sincere appreciation of the guidance and great interest given to him at every stage by Professor A.H. Lefebvre, without whom this investigation could not have been done.

Many useful suggestions of Professor R.S. Fletcher, Mr. E.R. Norster, Dr. E.M. Goodger, Dr. P.T. Hinde, and Mr. K.W. Nobbs are gratefully acknowledged.

He wishes to express his thanks to the supporting staff of the School of Mechanical Engineering and in particular to Mr. Frank Pearman, Mr. Donald Beattie, Mr. Ray Wilson, and the late Mr. Eric Barnes, who provided every assistance possible. The author thanks the staff of the Library, Instrumentation, Photographic and Computer Sections for their kind co-operation.

And lastly, but by no means least, a special word of thanks goes to Mrs. Elfriede Rizkalla for her continuing support and encouragement, and to Mrs. Lynne Jones for neat typing of the thesis.

CONTENTS

LIST OF TABLES

LIST OF FIGURES

LIST OF PLATES

NOMENCLATURE

$\mathring{A}$	=	Angstrom, ($1\ \mathring{A} = 10^{-7}$ mm)
A.C.	=	Alternating current
A.F.R.	=	Atomizing air / liquid mass flow ratio
cd	=	Candela
D	=	Diameter of airblast atomizer prefilmer, cm
$\bar{D}$	=	Linear mean diameter of spray droplets, microns
D_∞	=	Maximum droplet diameter, microns
$\frac{\bar{D}}{D_\infty}$	=	Skewness in U.L.D.F.
$D_{+\frac{1}{2}}$, $D_{-\frac{1}{2}}$	=	Droplet diameters occuring at half the frequency of the most probable droplet diameter, microns
$\frac{D_{+\frac{1}{2}} - D_{-\frac{1}{2}}}{\bar{D}}$	=	Spread in U.L.D.F.
D.C.	=	Direct current
D_{32}	=	Volume to surface area mean diameter, $= \frac{\Sigma\ nd^3}{\Sigma\ nd^2}$ microns
d	=	Droplet diameter, microns
d_c	=	Collimating aperture diameter in optical bench
F.N.	=	Atomizer flow number
F.No.	=	(Focal length/diameter) ratio of a lens
f	=	Function
f.a.r.	=	Liquid / air mass flow ratio
f_c	=	Collimating lens focal length
f_r	=	Receiver lens focal length
H.T.	=	High tension power
I (θ)	=	Intensity of light at angular displacement θ rad
M.M.D.	=	Mass median diameter, microns, $\simeq$ 1.2 S.M.D.
n	=	Number of drops, the diameter of which is 'd' microns
P	=	Total pressure, kgf/cm^2
ΔP	=	Pressure drop
ΔP_{orif}	=	Pressure drop across orifice plate
p	=	Static pressure
p.s.i.	=	Pounds per square inch

p.s.i.a.	=	Pounds per square inch absolute
p.s.i.g.	=	Pounds per square inch gauge
percent	=	Percentage by volume in liquid properties
Q	=	Volume flow rate, cm^3/sec
r	=	Photomultiplier traverse distance corresponding to 0.1 I (θ)
S.M.D.	=	Sauter mean diameter, microns = $\frac{\Sigma\ nd^3}{\Sigma\ nd^2}$
T	=	Absolute temperature, ^oK
T_{orif}	=	Absolute temperature at orifice plate, ^oK
T_{atom}	=	Absolute temperature at atomizer prefilming edge, ^oK
t	=	Liquid film thickness
U.L.D.F.	=	Upper Limit Distribution Function
V	=	Velocity, m/sec
V_{rel}	=	Relative velocity, m/sec
W	=	Mass flow rate, gm/sec
x	=	Slope of resulting straight lines in log - log graphs

Greek Symbols

μ	=	Micron, ($1\mu = 10^{-3}$ mm)
η	=	Absolute viscosity, centipoise
ν	=	Kinematic viscosity, centistoke
σ	=	Liquid surface tension, dynes/cm
ρ	=	Density, gm/cm^3
θ	=	Angular displacement of monochromatic light beam, rad
λ	=	Wavelength, Angstroms

X

Subscripts

a	=	Air
ℓ	=	Liquid
g	=	Gas
w	=	Water

CHAPTER 1

INTRODUCTION

CHAPTER 1

INTRODUCTION

All progress starts with a need, and in the general history of any important new engineering development there are always many processes meriting more detailed description. The particular field under consideration here is that of fuel atomization and evaporation, the two processes that greatly affect the functioning of combustion systems, described by Lucas (Ref. 55) as the "heart and soul" of the gas turbine power unit.

Probably the most critical component of a combustion chamber is the fuel injector, and in no other is the penalty for inefficiency so severe. Most of the fuel injectors employed in gas turbine engines are of the so-called "pressure" type, e.g. simplex, duplex, and dual-orifice atomizers, in which the fuel is forced under pressure through a small orifice from which it discharges at high velocity into a relatively stagnant combustion zone. Pressure atomizers have many useful assets, not the least being that their atomizing characteristics are fairly well established, largely as a result of the many and detailed studies that have been carried out during the past half century on the effects of atomizer geometry and operating conditions on mean drop size. Unfortunately, experience has shown that with pressure atomizers operating at high combustion pressures, penetration of the spray is reduced, so that instead of the fuel distributing itself evenly across the primary zone, it tends to concentrate at the centre of the liner near the spray nozzle, thereby creating regions of very high fuel/air ratio surrounded by oxygen-deficient combustion products. These conditions give rise to high rates of soot formation in the primary burning zone, leading to severe problems of carbon deposition, high flame radiation and excessive exhaust smoke. An additional problem is that of poor atomization at low fuel flow rates.

Mock and Ganger (Ref. 58) reported that the attainment of a high degree of atomization and evenness of distribution, particularly at low fuel rates, are major needs for gas turbine power plants. Similarly, Lawrence (Ref. 47) stated that a highly atomized fuel is required when the fuel flow rate is least. Accordingly, a key function of an atomizer is to maintain the quality of atomization at low as well as at high fuel deliveries.

In the light of the next generation of gas turbine engines, and the continuing trend towards higher combustion pressures,

higher heat release rates and air loadings, increasing recognition of the limitations of pressure atomizers and the so-called "walking-stick" vaporizers has led in recent years to a renewal of interest in the airblast atomizer in which, in contrast to the pressure atomizer, a high relative velocity is achieved by injecting fuel at low velocity into a high-velocity air stream, which is always readily available due to the combustor differential pressure. The high rates of fuel evaporation and the ultimate homogeneity of the combustible mixture, which are vital to attain high rates of combustion, necessitate a vast and rapid increase in the specific surface area of fuel exposed to air, hence increasing the heat transfer surface area.

Much greater energy can easily be made available with air-blast than with pressure injection. This big difference in the available energy in the two injection systems suggests that atomization is more readily obtained with air-blast than with pressure injection. It is also clear that high viscous losses made it uneconomical to feed the fuel at high pressures, to swirl it or to give it a turbulent motion of any kind. The maximum fuel pressures required by pressure atomizers are well in excess of the values desired by most pump manufacturers.

1.1 AIRBLAST ATOMIZATION

None of the established methods of fuel injection merit serious consideration in relation to the future trends towards engines of higher compression ratio, reinforced by the recent environmental laws on air pollution. As early as 1951, Green (Ref.35) stressed that the main hope for the production of fine and efficient atomization lies in the application of aerodynamic forces, and pointed out that comparatively fine atomization is achieved in the conventional "scent-spray", in which a liquid jet is disintegrated by a high-speed turbulent stream of air.

The airblast atomizer employs a simple concept whereby the fuel is caused to spread at low velocity over a "prefilmer"surface into a thin attenuated sheet of uniform thickness. As the liquid sheet flows over the edge of the prefilmer it is shattered into fine droplets by high velocity air which then enters the combustion zone carrying the atomized fuel along with it. This mechanism will be enlarged upon in Chapters 3 and 4.

An important characteristic of the airblast atomizer, which is an important advantage over the "bent-tube" vaporizer, is that it ensures premixing of fuel and air prior to combustion without having metal parts hanging in the flame. This also effectively prevents the formation of very rich zones that with

pressure atomizers always exist in regions close to the fuel spray, and which are mainly responsible for the observed high levels of exhaust smoke. No initial air-fuel mixing is, of course, possible with a pressure atomizer.

The overall philosophy behind the introduction of airblast atomizers to the gas turbine engine is that they also share many of the advantages of vaporizing systems. The notable ones are:

(a) The fuel droplets entering the combustion zone remain completely airborne, their distribution is dictated mainly by the air-flow pattern and is unaffected by fuel flow, hence the spray angle and penetration are relatively constant over a wide range of fuel flows. This also prevents deposition of liquid on solid surfaces.

(b) The ensuing combustion is characterized by an absence of soot formation and a blue flame of low luminosity, resulting in relatively cool flame-tube walls and worthwhile reductions in exhaust smoke.

(c) The fuel distribution pattern which controls the combustion pattern, and hence the temperature traverse quality at the chamber outlet, remains fairly insensitive to changes of fuel flow.

(d) Atomizer component parts are protected from overheating by the fuel and air (which is at compressor-outlet temperature) flowing over them.

(e) Low fuel pressure requirements.

Furthermore, the airblast atomizer is simple in design, free of moving parts, mechanically robust, and of low initial cost. It also produces much finer atomization than a vaporizor because the atomizing air velocity is typically twice as high.

1.2 SCOPE OF THE PRESENT WORK

A combustion system normally has to operate over a wide range of conditions so that the combustor air employed in atomization may suffer variations in pressure, temperature, and velocity. Also different combustion systems are called upon to burn fuels which may differ widely in the physical properties of viscosity, surface tension and density, all of which affect the degree of atomization.

Unfortunately, from the designers' viewpoint, the prefilming type of airblast atomizer which is dealt with in this work, and now finding increasing application in both aircraft and industrial gas turbines, has not received the same detailed and careful experimental study as that afforded the pressure atomizer. In consequence, comparatively little is known about the effects of air and liquid properties on atomization quality. It was this dearth of information that prompted the present investigation. All aspects of the airblast atomization process have been studied over the range of air and liquid properties encountered in practical combustion systems, using a specially designed form of airblast atomizer which is fully representative of modern gas turbine practice.

It is hoped that the present research will not only serve to highlight the influence of the dominant factors involved in airblast atomization, but will also provide a basis for airblast atomizer design.

CHAPTER 2

LITERATURE SURVEY

CHAPTER 2

LITERATURE SURVEY

The literature on atomization and spray formation theories is voluminous and care was required in selecting the most pertinent and useful references that have a bearing on the physical aspects of shattering by the action of high-speed air.

2.1 THE WORK OF NUKIYAMA AND TANASAWA

One of the earliest and most comprehensive studies of airblast atomization were those conducted by Nukiyama and Tanasawa (Ref. 63). From measurement of droplet sizes and drop size distribution for a range of liquid properties, flow conditions and nozzle sizes and configurations (Fig. 1), they attempted in a photomicrographic study to distinguish three stages of liquid jet disintegration due to the atomizing action of high-speed air:

(1) Dropwise Atomization

At very low air velocities, the relative motion between the air and liquid streams produces bead-like swellings and contractions with continuously increasing amplitude until the liquid jet finally breaks up into several separate drops due to the surface tension forces.

(2) Twisted Ribbon-like Atomization

Increasing the air velocity creates a fluttering action of the jet, forming the shape of a twisted ribbon of liquid. A portion of the ribbon is caught up (say at a point where its surface is ruffled) by the air stream and,being anchored at the other end, it is drawn out into a fine ligament. This ligament is quickly cut off by the rapid growth of a dent in its surface and the separated portions are swiftly drawn up into a spherical drop.

(3) Filmwise Atomization

Further increase in the air velocity causes flattening of the twisted ribbon's horizontal part and thus forms a cobweb-like film, which is so thin that it tears itself apart into microdroplets. A further increase again in the air velocity gradually increases the number of films that are becoming smaller and thinner until finally only the large number of films can be seen.

Droplet diameters were measured by collecting samples of the spray on small oil-coated glass slides, and results were expressed in terms of Sauter mean diameter calculated directly from the equation:

$$D_{32} = \frac{\Sigma\, n\, d^3}{\Sigma\, n\, d^2} \qquad \text{.....(1)}$$

where n = number of droplets, the diameter of which is 'd' microns.

They stressed the importance of drop-size distribution, whether the range of droplet size is quite irregular or whether it follows some law of distribution. Correlation of results obtained from tests on water at high volumetric flow-ratio (Q_a / Q_w) and at fairly high relative velocity was given for a total number of droplets 'n' by a simple empirical formula of the type:

$$d\,n = 0.5n \,.\, b^3 \,.\, x^2 \,.\, \exp(-b\,x) \,.\, d\,x \qquad \text{.....(2)}$$

where x = the mean diameter of a number of droplets 'dn' of diameters lying between the limiting diameters $(x - d\,x / 2)$ and $(x + d\,x/ 2)$, and

dn = a function of the experimental constant 'b'.

Further tests on water using a converging air nozzle (Fig. 1-a) showed that SMD was essentially independent of the size of air and water nozzles, and transition from laminar to turbulent flow conditions in the water-jet appeared to have little effect on drop sizes.

In an attempt to determine the effects of liquid properties on SMD, they conducted tests on gasoline, heavy oil, and solutions of alcohols and glycerine in destilled water over the following range of properties:

Liquid viscosity	-	1.0 to 30 centipoise,
Liquid surface tension	-	30 to 73 dynes/cm, and
Liquid density	-	0.8 to 1.2 gm/cm^3,

Nukiyama and Tanasawa derived the well-known empirical expression for SMD:

$$SMD = 585 \frac{\sqrt{\sigma_\ell}}{V_{rel} \cdot \sqrt{\rho_\ell}} + 597 \left(\frac{\eta_\ell}{\sqrt{\sigma_\ell \rho_\ell}}\right)^{0.45} \cdot \left(1000 \frac{Q_\ell}{Q_a}\right)^{1.5} \quad \ldots\ldots\ldots\ldots \quad (3)$$

They assumed that if the above formula will hold good for gasoline, heavy oils and alcohols, the range of variation for validity of equation (3) will then be:

Liquid viscosity	-	0.3 to 50 centipoise,
Liquid surface tension	-	19 to 73 dynes/cm, and
Liquid density	-	0.7 to 1.2 gm/cm^3.

When the ratio (Q_a/Q_ℓ) is large, then SMD is governed mainly by the first term on the right hand side of equation (3), i.e. SMD is inversely proportional to the relative velocity, whereas the liquid viscosity is of minor importance. But when the ratio (Q_a/Q_ℓ) becomes less, SMD is governed mainly by the second term of the equation and the surface tension has only a slight influence on mean drop size.

However, it should be borne in mind that the most significant effect on airblast atomization, namely that of the air properties was neglected in the experiments of Nukiyama and Tanasawa. The fundamental weakness of their equation is that it is limited to S.T.P. and cannot therefore be applied to practical gas turbine combustion chambers which have to operate over a wide range of air pressures and temperatures. Owing to the difficulties of separating

the three dominant liquid properties, their experiments failed in determining the separate effect of each property on atomization quality and no rigorous conclusions were reached. In any case, their work was centred on single-jet airblast type of nozzles which are not widely used in practice.

2.2 SUPPORT AND EXTENSION TO THE WORK OF NYKIYAMA AND TANASAWA

Although the equation of the Japanese workers is dimensionally inconsistent it has been found by Lewis et al (Ref.54) to successfully correlate their experimental results obtained with different gas-atomizing nozzles. Lewis et al called attention to the "general usefulness for purposes of design and control" of the Nukiyama-Tanasawa equation. In an attempt to establish the effect of gas density on atomization quality, they used compressed gases of nitrogen, ethylene, and helium as atomizing media, and reported that when the gas density was reduced to one-seventh of its original value, at constant gas viscosity and ratio of liquid-to-gas, the SMD of diesel oil sprays was increased by a factor of about two, despite a slight increase in gas velocity.

The effect of gas density on the degree of atomization has been also examined by Lane (Ref. 46), who subjected comparatively large water drops of known initial size (varying from 5.0 to 0.5 mm) to fast air-blasts by means of a blast gun. Using electronic flash and spark photography for drop size measurement, he reported that the secondary droplets into which a drop was shattered were found to be progressively smaller as the velocity of the air stream was increased, and the degree of shatter became higher as the pressure in the blast gun was increased to about 10 atmospheres. Thereafter further increase in pressure caused little improvement on atomization. Lane hoped that his work would help toward a clearer understanding of the action of aerodynamic forces in optimizing the process of atomization of liquid fuels.

The behaviour of liquid sprays from a small airblast atomizer under reduced pressures has also been investigated by Garner and Henny (Ref. 28). Their sprays were formed in chambers held at sub-atomospheric pressures and again the air density was found to be a major controlling factor. These workers reported that as the pressure of the air-blast was reduced, droplets greater than the "critical size" could no longer be broken up by the resistance of low pressure air.

There is no information in the literature about the effect of higher air temperatures on atomization quality; variation in air density has been limited so far to variation in pressure at constant temperature. The pressure of the air stream has been varied from 1 to 5 atmosphere absolute in another series of experiments conducted by Weiss and Worsham (Ref. 76). All available data suggest strongly that droplet sizes fall with increasing the atomizing air pressure, which promotes the formation of liquid ligaments and accelerates their disintegration into fine droplets.

2.3 THE WORK OF WIGG

The most important recent studies of airblast atomization were those carried out by Wigg at the N.G.T.E. (Refs. 78, 79), who reported that the minimum drop size predicted from the Nukiyama-Tanasawa equation is too high and the effect of increasing the ratio of liquid-to-air flow rates is far too great. Wigg emphasized the importance of the atomizing air kinetic energy and considered the difference between the inlet air energy and that of the emerging spray to be the variable which mainly affects the mean drop size.

In an effort to establish the effect of atomizer scale on spray characteristics he tested three large airblast atomizers, made to the same design, but scaled for the diameter of the inner body and the height of the air annulus to give flow areas in the ratios 1 : 4 : 8 . The atomizer design employed in his experiments is shown in Fig. (2). Wigg compared his experimental results with some others of Golitzine et al (Ref. 34), and of Clare and Radcliffe (Ref. 11) using airblast atomizers shown in Figs. (3) and (4) respectively and found that atomizer scale affects atomization only through its influence on liquid and air flow rates. Correlation of his results gave a straight line relationship between the mass median diameter (≃1.2 SMD) and the water/air mass flow ratio of the form:

$$M.M.D. = 4 + (58 + 55\ D^{1.5}) \cdot (W_w/W_a) \qquad \ldots\ldots\ldots(4)$$

where D = the diameter of the inner body (Fig. 2).

With three different water swirlers he tested the effect of increasing water pressure (from 20 to 60 p.s.i.g.) and found no appreciable effect on atomization quality. From an analysis relating the loss of kinetic energy to the energy required to overcome viscous forces, taking recombination of water droplets into account, the following empirical correlation was then proposed:

$$M.M.D. = 2300 \left[\eta_\ell^{0.5} \cdot W_\ell^{0.05} \cdot (1 + W_\ell/W_a)^{0.5} / V_{rel} \right] \cdot \left[1 + 2 (W_\ell/W_a)^{0.7} \cdot W_\ell^{0.25} \right] \quad \ldots\ldots\ldots\ldots (5)$$

This correlation is based on different sets of results obtained by different investigators. Moreover, it does not take account various significant parameters influencing the airblast atomization process such as:

(a) Air density,

(b) Liquid surface tension,

(c) Liquid density, and

(d) Atomizer characteristic dimension.

In later work by Wigg (Ref. 79), he correlated existing data using N.G.T.E. atomizers (Figs. 2 and 4) together with:

i) Nukiyama and Tanasawa results using a sharp-edged air orifice atomizer (Fig. 1-b),

ii) Data of Wood (Ref. 86), who tested a Rolls-Royce airspray atomizer (Fig. 5) spraying molten wax to avoid recombination of drops, and

iii) Results of Ingebo and Foster (Ref.42), who photographed droplets formed by cross-current break-up of iso-octane, JP-5, benzene, carbon tetrachloride (ρ = 1.59 gm/cm^3), and water,

and derived the following dimensionally consistent relationship:

$$\text{M.M.D.} = \frac{200 \quad \nu_\ell^{0.5} \cdot W_\ell^{0.1} \cdot (1+W_\ell/W_a)^{0.5} \cdot h^{0.1} \cdot \sigma_\ell^{0.2}}{\rho_a^{0.3} \cdot V_{rel}}$$

$$= 200\ N \qquad \ldots\ldots\ldots(6)$$

where h = the height of air annulus, cm.

In order to take coalescence of water drops into account, Wigg studied the performance of seven different atomizers (Figs. 1 -b, 2, 3, 4, and 5) using high pressure air (V_a not less than 100 m/sec) and added another term to equation (6) arriving at the following empirical formula:

$$\text{M.M.D.} = 200\ N \left[1 + 2.5\ (W_\ell/W_a)^{0.6} \cdot W^{0.1} \right] \qquad \ldots\ldots\ldots(7)$$

This study carried out by Wigg did much to elucidate the key factors involved in the airblast atomization process, and confirmed the predominant effect of the relative velocity of air and liquid on mean drop size. Unfortunately, his work suffers from the disadvantage that the range of variables covered was fairly narrow, in consequence, the significant effects of air density and liquid properties were not well established, and equations (6) and (7) indicate that the mass median diameter of droplets is only slightly affected by changes in fuel flow and atomizer dimensions. However, and in common with the work of Nukiyama and Tanasawa, the physical form of the atomizer employed in the experiments was different to the airblast atomizers now being developed for gas turbine applications.

2.4 OTHER CONTRIBUTIONS TO THE FUNDAMENTALS OF AIRBLAST ATOMIZATION

Little information has been published on the subject of airblast atomizer design and performance, and only very few of all previous investigations have been of sufficient scope to provide a basis for predicting accurate atomization characteristics outside the narrow ranges tested. One reason is the complexity of the airblast atomization process itself; another is the difficulty involved in separating the dominant parameters influencing this process, and in measurements of spray characteristics, especially in determining the mean drop size. These factors together presented the research workers with a number of problems for further investigation. Fraser, Eisenklam and Dombrowski (Ref. 26) state that : "It is surprising how little of the fundamental principles of disintegration of a liquid in a gas stream has been applied to a great number of designs of twin-fluid atomizers. Their mechanical efficiency is still extremely low and there is an increasing demand for atomizers of greater energy transfer".

On the other hand, efficient atomization by means of air-blasts was confirmed by Hrubecky's experiments (Ref. 41), who reported that injecting the liquid parallel to the surrounding air flow gave the best degree of atomization. His results indicated that when the liquid was injected at the point of maximum air velocity, minimum droplets sizes were achieved. At sonic air velocity, with air-to-fuel volume flow ratio of 5000, droplet sizes of the order 5 to 7 microns could be obtained.

Gretzinger and Marshall, Jr. (Ref. 36) state that: "Airblast nozzles are well suited to the production of sprays with average drop diameters in the less than 30 microns range", and consider the application of Nukiyama-Tanasawa equation to atomization for a drop-size range of 5 to 30 microns as of doubtful value. They reported drop sizes of sprays of an aqueous solution of a black dye sampled in mineral oil, produced by a converging airblast nozzle which was very similar to that used by Nukiyama and Tanasawa, and an airblast impingement nozzle, at liquid rates from 0.5 to 5 gal/hr. The drop size data for each nozzle were then correlated and the following equations were suggested:

(a) Converging airblast nozzle:

$$M.M.D. = 2600 \left[\left(\frac{W_\ell}{W_a} \right) \left(\frac{\eta_a}{V_a L} \right) \right]^{0.4} \quad \ldots\ldots\ldots(8)$$

(b) Airblast impinging nozzle :

$$M.M.D. = 122 \left(\frac{W_\ell}{W_a}\right)^{0.6} \cdot \left(\frac{\eta_a}{V_a L}\right)^{0.15} \qquad .....(9)$$

where L = diameter of the contact periphery of the air and liquid streams.

Gretzinger and Marshall concluded that the correlations above are specific to the liquid and the two types of nozzles designs employed, and are entirely invalid outside the range of M.M.D. from 5 to 29 microns.

Fraser, Dombrowski and Routly (Refs. 22, 23, 24, 25) reported that the production of thin liquid sheets and the increase of area of contact between gas and liquid is an essential pre-requisite to fine atomization. Liquid sheets studied in these references were produced from spinning cups. They also observed that a liquid sheet does not break down upon immediate impact with high-velocity air but is deflected away from it. Waves are initiated at the point of impact and the sheet breaks up into drops through the formation of unstable ligaments. These workers added that atomization at any level of air energy is improved when the air is distributed from a narrower annular gap, while imparting a rotary motion to the atomizing air stream improves both the quality of atomization and spatial dispersion. On this basis efficient designs would have to incorporate prefilming devices whereby an annular gas stream impinges on a thin liquid sheet. The sheet must maintain its form throughout a wide range of operating conditions.

2.5 AIRBLAST ATOMIZATION STUDIES AT CRANFIELD

In recent years the need to reduce exhaust smoke led to renewed interest in airblast atomization. Several research airblast atomizers have been designed and tested at Cranfield to enable parallel studies of combustion and emissions to be made.

Following a series of tests on various types of airblast atomizer, Lefebvre and Miller (Ref.52) concluded that in order to provide maximum physical contact between air and fuel, and to achieve minimum drop sizes the fuel should be spread into a continuous thin sheet and then exposed on both sides to high velocity air. The experimental results obtained at atmospheric conditions and with air velocities available in a low pressure loss combustion chamber indicated that the airblast atomizer is capable of

producing fuel droplets which are comparable in size to those obtained from a swirl-pressure atomizer.

A further experimental study on the effect of ambient pressure on airblast atomization quality has been carried out by Godbole (Ref. 31). His tests on the atomizer shown in Fig. (6) indicated that above a pressure of approximately 30 p.s.i.a., S.M.D. decreased continuously with increasing pressure. Above a pressure of 50 p.s.i.a. there was no measurable effect of increasing A.F.R. on mean drop size. The effect of ambient pressure on S.M.D. was then described by a power law with a pressure index ranging from -0.57 to -0.63 . Godbole's results are in good agreement with the results of Weiss and Worsham (Ref.76), but the average value of the pressure index is higher than that of Wigg (Ref. 79). Throughout the range of ambient pressures tested the effect of shroud air in reducing the mean drop size at high rates of liquid flow was observed, and the advantage to be gained by inclusion of shroud air in atomizer design to improve starting performance was emphasized (Ref. 9). Insufficient experimental evidence was obtained to determine the optimum proportion of shroud air.

CHAPTER 3

MECHANISM OF DROPLET DISINTEGRATION

CHAPTER 3

MECHANISM OF DROPLET DISINTEGRATION

The effect of aerodynamic forces in controlling deformation and break-up may be small under normal atmospheric conditions, but it becomes most important under practical combustion chamber conditions. As this effect is a function of air density, it depends on other variables such as:

(a) Air velocity which affects the magnitude of inertia forces.

(b) Physical properties of the liquid which affect the magnitude of the forces opposing the disruption of a liquid sheet.

(c) Atomizer design which affects the extent to which these forces are effective.

3.1. EFFECT OF AIR FORCES ON AERODYNAMIC ATOMIZATION RATE

Quantitative information on the effect of air forces on the rate of aerodynamic atomization of liquid drops has been reported by Dickerson and Schuman (Ref. 15), who conducted some interesting experiments. Using a high-speed motion camera (14,500 frames/sec) they established a relationship for the time rate of mass loss from a high-grade kerosine droplet of known initial size as a function of the gas stream properties and droplet characteristics. The following expression for the rate of aerodynamic atomization of liquid droplets was proposed:

$$M = 3.53 \times 10^{-5} \ (Re')^{2.8} \ . \ (We)^{-0.42} \qquad \ldots\ldots\ldots (10)$$

Where M = Mass number,

$= \dot{m} D / A_d \ \eta_d$,

$\dot{m}$ = Mass loss rate, gm/sec ,

D = Droplet average diameter, cm,

A_d = Droplet surface area, cm^2 ,

η_d = Droplet viscosity, centipoise,

Re' = Modified Reynold's number,

= $D \cdot V_{rel} \cdot \rho_g \cdot \rho_d^{\frac{1}{2}} / \eta_d$,

V_{rel} = Relative velocity, cm/sec ,

ρ_g , ρ_d = Density of gas and droplet respectively, gm/cm^3 ,

We = Weber number ,

= $\rho_g \cdot V_{rel}^2 \cdot D / \sigma_d$, and

σ_d = Liquid surface tension, dynes/cm.

Unfortunately, only one liquid (RP-1) was used in the development of equation (10) ; its surface tension was 26 dynes/cm, and viscosity was 1.71 centipoise. Caution should thus be taken when applying this equation to liquids having physical properties different from those of RP-1. Dickerson and Schuman added that the aerodynamic atomization process is known to be intimately related to the propagation of capillary waves over the surface of liquid. These capillary waves originate from some small surface disturbance, are caused to grow in amplitude by aerodynamic forces, and eventually crest and disintegrate into a myriad of microdroplets. On account of the surface curvature, divergent propagation of capillary waves from the forward stagnation point, and the magnitude of deformation that occurs when liquid droplets are subjected to high-velocity gas flows, a sound theoretical development would be excessively and perhaps intractably complicated.

The fragmentation of liquid drops behind normal shock waves in a shock tube has been studied experimentally by Engel (Ref. 19); Hanson, Domich, and Adams (Ref. 37); and by Wolfe, and Andersen (Ref. 82) in order to examine the shattering of certain liquid drops. Drop diameters, surface tension, density, and viscosity of the droplets and the Mach number of the shocks were varied. The overall results of these experiments suggest stongly that the major variables affecting the high-speed break-up are the drop diameter, the dynamic pressure of the convective flow, and the liquid properties.

Ranger and Nicholls (Ref. 66) reported that all of the previous experiments were conducted at relatively low primary shock-wave Mach numbers or low dynamic pressures and, therefore, they do not cover the range of conditions characteristic of two-phase detonation. They supplemented and extended earlier experimental and analytical investigations to find the rate of drop shattering, the break-up times, the drop displacement, and the drop deformation for a range of conditions generated by two-phase detonations. In order to photograph the sequence of events leading to the shattering of water drops having diameters of 750 - 4000 microns by shock waves moving at Mach numbers of 1.5 - 3.5, they used a collimated beam of high-intensity light to back-light the drops with both image converter and rotating-drum type cameras. A series of individual shadows and streak photographs taken at different time intervals after the shock wave had intercepted the drop showed that the drop displacement is a smooth, continuously varying function of time and thus the drop velocity is also a continuous function of time. These photographs also demonstrated that the collision between the incident shock and the drop has little, if any, effect of the shattering phenomenon, and thus break-up occurs as a result of the interaction between a drop and the convective flow field established by the shock. A drop that was originally spherical was deformed into a planetary ellipsoid with its major axis perpendicular to the direction of flow. The shearing action exerted by the high-speed flow causes a boundary layer to be formed in the surface of the liquid and the stripping away of this layer accounts for the break-up. It was found that the break-up time (defined as the time required to produce a trace of mist only) is proportional to the drop diameter, inversely proportional to the velocity, and proportional to the square root of the liquid-to-gas density ratio.

On the basis of their experimental observations, Ranger and Nicholls then formulated a model for shock wave-drop interaction and treated the problem simply as a droplet in a steady and incompressible high-speed flow, considering that break-up results from a boundary-layer stripping mechanism. The rate of disintegration is found by integrating over the thickness of the liquid boundary layer to determine the mass flux in the layer. In spite of the approximate nature of their analysis, and the use of approximate relations for the experimental data, Ranger and Nicholls concluded that the agreement between experiment and theory was quite encouraging.

3.2 BEHAVIOUR OF THE GAS-LIQUID INTERFACE IN AIRBLAST ATOMIZATION

An analytical investigation into the mechanism of liquid atomization in high-velocity gas streams has been conducted by Mayer (Ref. 57). By consideration of the development of capillary waves (ripples) that are produced by a high-velocity gas flow along the liquid surface, he pointed out that waves of very small wavelength cannot be developed readily because of viscous dissipation, while waves of very long wavelength are slow to develop because of inertial effects, even though in this case viscous dissipation is negligible. Between the extremely short and long (capillary) wavelengths there exists a spectrum of wavelengths which can be excited to appreciable amplitudes during the action time of the high-velocity gas flow. With given properties of liquid and gas and the wind velocity relative to liquid, he postulated that if such a wavelength 'λ' with a characteristic excitation time τ (λ) has developed to an amplitude comparable with 'λ', the gas stream will erode the wave crest as a ligament from which droplets of diameter comparable in size to 'λ' are formed. Mayer added that by considering a liquid of large surface and great depth, it will be possible to assess the fundamental role of liquid properties in the primary atomization by the action of the high-velocity gas stream. His analysis then was based on the following assumption:

$$D = F \cdot \lambda \qquad \ldots\ldots\ldots\ldots (11)$$

where D = Droplet diameter, and

F = Dimensionless configuration factor, is independent of 'λ'.

On conceptual grounds 'F' is anticipated to be of the order of unity, and preliminary comparison of theoretical results based on equation (11) with experimental data of Weiss and Worsham (Ref. 76), who sprayed molten synthetic wax into hot air streams of sustained high velocity, suggests that 'F' depends somewhat on liquid viscosity but is nearly independent of air velocity and density, and liquid density and surface tension. However, the weakness of this work is that it was based on experiments of very limited range whereby no definite dependence of drop sizes on gas and liquid properties could be ascertained.

Briffa and Dombrowski (Ref. 6) carried out an investigation into the region of disintegration of a liquid sheet through aerodynamic action. Two liquids were employed:

i) iso-octane : η = 0.54 centipoise,

σ = 18.90 dynes/cm,

ρ = 0.69 gm/cm^3, and

ii) tetralin : η = 2.00 centipoise,

σ = 36.00 dynes/cm,

ρ = 0.97 gm/cm^3

With air velocities ranging from 23 to 155 cm/sec, they pointed out that rapidly growing waves are produced on the sheet which subsequently break down at the crests. Fragments of the sheet then rapidly contract into ligaments which disintegrate into drops. A number of drops are also produced at the point of fragmentation; these drops have an additional velocity component resulting from the accelerating wave crest. The break-up length of the sheet depends upon the liquid properties and operating conditions. At low air densities or low air-liquid relative velocities the bulk of the spray may result from drops produced from the sheet edge, and in a cocurrent air stream the path of the drops tends towards that of the air. These authors also found that the measured lengths of the coherent liquid sheet are proportional to the liquid density and surface tension, and inversely proportional to the liquid ejection velocity.

Another effort to investigate the mechanism of disintegration of liquid sheets by York, Stubbs and Tek (Refs. 88, 89) has been added to the literature. Their study was based on instability theories in relation to the forces created from the interaction of two fluids moving along a continuous interface. The velocity difference between the two fluids causes the growth of waves until eventually one fluid mass may disintegrate and be swept away in the other. These authors assume that disturbances in the interface immediately set up an unbalanced opposition of forces. Two sets of forces become effective:

(a) The uniform tension on the perturbed interface acts to squeeze the liquid back to the original boundary to reinstate the original equilibrium.

(b) The gas, assumed to be streaming at constant velocity with respect to the liquid, experiences a local decrease in pressure corresponding to the

increase in velocity in the vicinity of the protuberance. This local low pressure acts to move the liquid still farther from the plane, to increase the amplitude of the disturbance, and to make the equilibrium unstable.

Additional assumptions made in this study, using air and water as the two fluids, are stated as follows:

i) Both fluids are assumed to be frictionless, i.e. viscosities are zero.

ii) Both fluids are assumed to be incompressible, i.e. densities are constant.

iii) The undisturbed interfaces are assumed to be plane.

iv) The infinite sheet of water is considered to be stationary with respect to the coordinate system.

v) The amplitudes of original disturbances on the interface are assumed to be small compared to their wave lengths, and their time rate of change is small.

vi) The general motion of both fluids is two-dimensional and irrotational (or potential), and the bulk velocities are constant.

Evaluation of the opposing forces mentioned above begins with an instantaneous force balance across the interface, involving only the pressures of liquid and gas with the pressure resulting from the interfacial tension and curvature. For this case, the balance is:

$$p_w - p_a = -\sigma \left(\frac{\partial^2 b}{\partial x^2} \right) \qquad \text{.....(12)}$$

where σ = the interfacial tension, and

$\frac{\partial^2 b}{\partial x^2}$ = the curvature of liquid sheet with respect to the x-axis (direction of air flow).

For a mathematical solution of their model they assumed that the wave amplitudes in the liquid sheet are increasing exponentially. This case of instability is most destructive of the fluid mass, and the principal waves growing on the liquid sheet surface will have a wavelength corresponding to the greatest growth rate and will dominate the disturbances until the sheet disintegrates. In order to justify their analysis, York et al have photographed actual disintegration of an unsupported liquid sheet produced by a swirl-chamber spray nozzle at exposures of about one microsecond, and observed strong wave action leading to disintegration of the sheet. The waves cause rings and holes to appear in the sheet with extremely rapid growth of the holes resulting in separation of thick rings. These rings then break up into drops under the action of surface tension alone, since the air velocity is now normal to the ring itself and no longer contributes aerodynamic forces to the ring disintegration. York et al added that it does not seem possible to accurately predict the time required for a liquid sheet under normal operation to break up, or to calculate the size of drops in the spray. In spite of the many assumptions in their analysis, they concluded that the results are reasonable and verifiable at least qualitatively.

Gretzinger and Marshall, Jr. (Ref. 36) state that the lack of a suitable atomization theory by the disruptive action of high velocity air stream on thin liquid films or filaments has contributed to a state of confusion in this field, and a large amount of work still remains to be done. Additional studies of other pneumatic nozzle designs, studies on the effect of liquid properties on drop size, studies of the effect of air density on drop size, and studies of other drop size ranges all need to be made; and it is with these aspects that the present investigation is largely concerned.

CHAPTER 4

EXPERIMENTAL

AIRBLAST ATOMIZER
DROP SIZE MEASUREMENT
EXPERIMENTAL PROGRAMME
SPECIAL LIQUIDS
ATMOSPHERIC TESTS
HIGH TEMPERATURE TESTS
HIGH PRESSURE TESTS

CHAPTER 4

EXPERIMENTAL

4.1 THE AIRBLAST ATOMIZER

Fortunately, the atomization of a liquid by means of high-speed air-blasts is fairly easy to accomplish. Basically it is simply a matter of creating a high relative velocity between the liquid and the surrounding air. In general the higher the relative velocity the smaller is the mean drop size. In a low-pressure-loss combustion system, a 3 percent pressure drop across the liner produces an air injection velocity of between 70 and 115 m/sec, depending on the air inlet temperature. Therefore, an airblast atomizer design should utilize these available air velocities efficiently, ensure the presence of maximum air velocity at the atomizing edge, and maintain it during the initial disintegration process.

A cross-sectional drawing of the atomizer employed is shown in Fig. (7) and the atomizer mount in the atmospheric test rig in Plate (1). In this design the liquid flows through six equispaced tangential ports, each of 0.8 mm square cross section (Fig. 8), into a weir from which it spills over the prefilming surface (Fig. 9) before being discharged at the atomizing edge. In order to subject both sides of the liquid sheet to high velocity air (Ref. 52), it is necessary to provide two separate air flow paths through the atomizer. Thus it simply consists of two co-axial pipes of 1.5 inch (3.81 cm) and 2.5 inch (6.35 cm) outer diameter. In the design shown in Fig. (7), one air stream flows through the central circular duct and is deflected radially outwards by a pintle (Fig. 10) before striking the inner surface of the liquid sheet, while another air stream flows through an annular passage surrounding the main body of the atomizer. This passage has its minimum flow area in the plane of the atomizing lip in order to impart a high velocity to the air where it meets the outer surface of the liquid sheet.

In addition to providing maximum physical contact between air and fuel this method has a further useful advantage in that, after formation, the liquid drops tend to remain airborne and are not

deposited on adjacent metal surfaces. This is why it has been widely adopted in many practical designs and is an essential feature of the atomizer employed in the present investigation.

4.2 DROP SIZE MEASUREMENT

One of the key properties of any atomizer and a measure of how effectively it performs is the mean drop size achieved. The ideal characterization of sprays and a suitable parameter for expressing the quality of atomization is given by the Sauter mean diameter (Ref. 71) which is essentially an expression of surface area per unit volume, since this governs the rate of evaporation and hence the rate of combustion.

The ideal droplet sampling technique would be one which involves removing at random a number of droplets from the spray, without disturbing it in any way, at a position at which the information is required, and to measure their individual diameters. Just sufficient droplets should be removed to give a reliable indication of S.M.D. However, most of the sampling techniques employed can lead to false results due to the introduction of some form of collecting apparatus into the spray. These techniques present many difficulties, particularly if the assessment is to be made on sprays produced under actual combustion chamber operating conditions.

Mean drop sizes were measured mainly using the light scattering technique due to Dobbins, Crocco and Glassman (Ref. 17), supplemented by a few experiments with the drop-freezing technique. The main advantage of the optical method is that it does not disturb the droplet flow pattern, nor does it affect secondary atomization as in physico-chemical techniques, e.g. freezing.

4.2.1 PRINCIPLES OF THE LIGHT SCATTERING TECHNIQUE

This method is based on the forward scattering of a parallel beam of monochromatic light which has been passed through a spray. Dobbins et al (Ref. 17) found that for sprays described by the Upper Limit Distribution Function (U.L.D.F.) defined by Mugele and Evans (Ref.59) having characteristic parameters of spread and skewness within specified limits, the scattered

light intensity profiles were coincident and the S.M.D. could be obtained from the distance traversed by the beam to have one-tenth of the intensity of scattered light at the optical axis. Cohen and Webb (Ref. 12) showed that Dobbins' method is accurate for the wider range of droplet distributions produced by a swirl-pressure atomizer. Roberts and Webb (Refs. 69, 70) extended its scope to a greater range of spread and skewness in the U.L.D.F. and found that the least deviation between experiment and theory in determining S.M.D. of sprays occured at one-tenth normalized intensity in the scattered profile.

4.2.2 THE OPTICAL BENCH

The optical system is shown diagrammatically in Fig. (11) and in Plates (2, 3 and 4). As a light source the system employs a 100 Watt super high pressure mercury arc lamp, type HBO 100 W/1, manufactured by Osram. This light source is specially designed having a high luminous efficiency combined with very high brightness and arc stability. The emission spectrum is composed of known mercury lines of high density. A vapour pressure of up to 70 atmospheres is being utilized in the bulb to achieve the above qualities. The lamp is found to be of adequate brightness for spray densities expected from airblast atomizers.

It is necessary to mount the lamp in an enclosed housing in order to protect the operators eyes from dangerous U.V. radiation. The lamp is to be inserted with its anode (stamped base) downwards, making sure that no twisting or bending forces are transferred to the lamp body. If the lamp envelope is inadvertently touched, it must be cleaned to avoid reduction in the light output. The housing should allow for adjustments in both vertical and horizontal directions. It should also allow for adequate ventilation during operation together with freedom for the lamp to expand when hot.

In practice, it was found necessary to allow a period of at least 30 minutes before maximum stability of output was achieved. The spatial distribution of luminance depends primarily on the type of power supply. With a D.C. supply the spot of highest luminance is formed adjacent to the negative electrode, however, a maximum is formed adjacent to each electrode when the lamp is operated on rectified A.C. Thus, the lamp must be supplied by stabilized power with minimum A.C. ripple to prevent any variation in the luminous output. Its average life is 100

hours, and caution should be taken to replace it when 100 working hours are elapsed. Other details of the lamp are to be found in (Ref. 32).

Referring to Fig. (11), the amount of light passing through a single element plano-convex condenser lens of 2.25 inch diameter and 3.00 inch focal lenth, and also the beam diameter are controlled by an iris diaphragm. The condenser lens focusses the light beam through a Barr and Stroud interference filter which only allows the 4358 Å wavelength line of the mercury arc spectrum to pass onto a collimating aperture. The filter should be of the narrow band interference type, be mounted normal to the parallel beam of light emerging from the condenser lens, and should match the potomultiplier characteristics. In order to arrange for a compact condenser lens, iris diaphragm and filter unit, they are mounted together in one box (Fig. 12). If the three components within the unit are mounted accurately in relation to each other and to the optical centre line of the unit, no further adjustment of the components themselves is required during the setting-up procedure. Any alignment operations are carried out by adjusting the position of the complete unit, thus saving setting-up time.

The collimating aperture diameter 'd_c' controls the sharpness of the beam edge cut off. A number of trial collimating apertures were tested prior to finally choosing the present 0.020 inch (508 microns) diameter one, which gives the most acceptable results. This collimating aperture, when illuminated from behind, acts as a point source of light at the focal point of the 27 inch focal length plano - convex achromatic collimator lens. Thus, a parallel beam of monochromatic light of 4358 Å wavelength emerges from the collimator lens.

If 'f_c' is the collimating lens focal length, the ratio (f_c/d_c) decides the degree of parallility of the system. In the original apparatus of Dobbins et al (Ref. 17) the value of 1250 was used for this ratio, while in the present system this figure has been improved to 1350. This value has significance in deciding the upper limit of S.M.D. that can be measured; higher values improve the measureable upper limit, i.e. the focal length of the collimator lens should be as long as is practical. It is essential that the geometric and the optical axes should be coincident so that stray reflections are minimized. The traverse control on the light source helps the setting-up procedure. The parallility in the system is checked by measuring the beam cross-sectional size at distances over 15 feet away from the collimating lens (see Appendix B).

This parallel beam of monochromatic light of 4358 Å wavelength is relfected through the spray under investigation to a receiver lens by a 45°, 90°, 45°prism mounted on light springs (Fig. 13) at 45° to the original axis of the beam, hence forming an L-shaped optical path, giving the system more practical overall dimensions. This also helps when setting-up the complete bench as it is divided into two convenient parts by the prism. The receiver lens, exactly identical to the collimator lens, focusses this beam onto a 65 micron aperture in an otheriwse light-tight photomultiplier box. The multiplier phototube is of the type 1P21, manufactured by R.C.A. It should be of high sensitivity while retaining a linear response. The spectral response of 1P21 covers the range from about 300 to 6200 Å as shown in Fig. (14). Maximum response occurs at approximately 4000 Å, very near to the wavelength of the interference filter, i.e. the photomultiplier should be chosen so that its spectral sensitivity curve peaks very near to the wavelength of the interference filter being used. Its dark current should be low, and no extraneous light should be allowed to enter; its only source light coming from the small aperture situated on the focal plane of the receiver lens. This aperture should be made as small as possible. In fact there is great difficulty in making a circular aperture in shim stock of smaller diamter than 65 microns. If it is found possible to produce a circular aperture of smaller size, then it should be used although the diameter of the collimating aperture may have to be decreased. With a stabilized H.T. supply the output current of the 1P21 is a linear function of the exciting illumination which is a function of the mean drop size of spray.

4.2.3 DIRECT READOUT OF LIGHT INTENSITY PROFILE

The photomultiplier box is mounted on a trolley which may be traversed in a plane at right angles to the optical axis. A dial test indicator is mounted giving the position of the trolley relative to the optixal axis to an accuracy of 0.001 inch. Recent improvements by the author include the use of a logarithmic amplifier module, type Bryans 26236 together with an X-axis transducer, type Hewlett-Packard 7 DCDT - 1000, a pre-amplifier module of maximum sensitivity 0.4 mV/cm, type Bryans 26103 to an X-Y plotter, main frame A4, and single pen, type Bryans 26001 for plotting the light intensity profile. In addition to allowing a system symmetry and a scattering symmetry to be made, this new arrangement allows a direct reading of the one-tenth intensity point on the scattered profile. These components are shown in Plate (3).

The position of the light beam (i.e. of the photomultiplier trolley) is indicated on the X-axis of the plotter while the Y-axis records its intensity $I(\theta)$ corresponding to an angular displacement (θ). The sensitivity range control of the logarithmic amplifier should be adjusted to give a traverse distance of the photomultiplier trolley of 0.100 inch over, say, 5 cm on the X-axis of five-cylce log-linear graph paper (see Appendix C). Typical plots of the light intensity profile are shown in Figs. (15 - 18).

In accordance with the work of Roberts and Webb (Refs. 69, 70), by measuring the traverse distance 'r' between the Y-axis and a point on the profile at which the light intensity is equal to one-tenth of the normalized intensity in the scattered profile, the S.M.D. of the spray can be determined using the relationship derived by Roberts and Webb and plotted in Fig. (19).

The need to accurately focus the optical system through the condenser, collimator and receiver lenses onto the photomultiplier cannot be over emphasized. The plane of the photomultiplier aperture is so adjusted, using the adjusting screws of the prism, as to maximize the photomultiplier output, after correct focussing. All the components should be mounted on a rigid bench, free from external vibrations and preferably isolated from the floor using antivibration mounts. The test room in which the apparatus is mounted should be as free as possible from atmospheric moisture and dust, whilst the optical components used must be of high quality and be kept free of all surface dust and depositions. Two fans at both sides of the spray are used for blowing spray droplets away from optical surfaces. These fans are connected through flexible pipes to the prism mount and receiver lens box. Where possible the instrument must be shielded from stray light and all surrounding surfaces painted matt black to reduce the possibility of ghost images being formed in the lenses.

The light beam passes at right angles to the spray axis, and it is important to ensure that the light beam crosses the spray at the same distance away from the atomizer to ensure that under all test conditions the spray sampled by the beam is in the same state of development. This distance was kept at 2 ins. during the entire experimental programme.

4.3 EXPERIMENTAL PROGRAMME

It has been pointed out in the foregoing chapters that the mechansim of airblast atomization, which determines the mean drop size, is a complex function of independent variables which may be divided into four main groups:

(a) The physical properties of the liquid, namely viscosity, surface tension and density.

(b) The properties of the air, namely velocity, temperature and pressure.

(c) Air and liquid flow rates.

(d) Atomizer characteristic dimension.

The statement that SMD is a function of all these variables may be expreseed by writing:

$$S.M.D. = f\left(\eta_\ell^{\,b},\ \sigma_\ell^{\,c},\ \rho_\ell^{\,e},\ V_a^{\,g},\ T_a^{\,h},\ P_a^{\,i},\ W_a^{\,j},\ W_\ell^{\,k}.\ D^m\right) \qquad \text{.....(13)}$$

The experiments were planned to examine the effect of each particular variable on SMD and to determine the values of the exponents above. The first phase was confined to the separate effects of liquid viscosity, surface tension and density on mean drop size. This was accomplished by preparing special liquids and solutions which exhibited wide variation in one property, but only very slight differences in the other two main physical properties. It was then decided to undertake two series of tests at every level in the range of each property under test. The first series was to examine the effect of varying the atomizing air velocity whilst maintaining the liquid flow rate constant, while the liquid flow rate was varied at a constant atomizing air velocity in the second series.

The two main liquids employed during the entire experimental programme then were:

i) Water (η = 0.998, σ = 73.45, ρ = 0.998)

ii) Kerosine (η = 1.293, σ = 27.67, ρ = 0.784)

The second phase of the work was confined to the effects of air temperature (using an atmospheric test rig), and air pressure (using a high pressure test rig) on mean drop size. It was also planned to undertake two series of tests similar to those of the first phase when investigating the effect of air temperature. The experiments on the effect of high pressure were conducted at constant levels of air velocity and temperature.

The third phase was planned to provide a detailed and comprehensive picture of the airblast atomizer performance. In the first place the air and air/liquid flow characteristics were established over a wide range of air velocities and liquid flows. It was desired to investigate the effects of varying air velocity, liquid flow and hence air/liquid mass ratio on mean drop sizes. This was accomplished on the atmospheric test rig at twelve levels of air velocity ranging from 180 to 400 ft/sec (54.86 to 121.92 m/sec), the intervals being selected to provide equal velocity increments of 20 ft/sec. The liquid flow rate was varied between 0.0100 and 0.0500 lb/sec (4.5 to 22.7 gm/sec) with equal increments of 0.0025 lb/sec, which covered a range of air/liquid mass ratio from 0.98 to 10.80.

In the three phases outlined above the velocities of both inner and outer atomizing air streams (referred to as pintle and shroud air streams respectively) were kept equal. The aim of the fourth phase was to examine the effect of varying the velocity and hence the amount of the outer atomizing air stream on atomization quality, and to determine the percentage of the total atomizing air to flow through the shroud in order to achieve the best atomization quality, which also could be of interest to the designer.

4.4 SPECIAL LIQUIDS

Most of the recent experimental investigations on the effects of the physical properties of liquids on atomization quality were limited to a sutdy of the viscosity effect. The reason for this is the strictly practical one that the surface tension and density of liquid fuels vary over only a very narrow range compared with the range of viscosity. This does not mean that the forces of liquid surface tension and gravity do not play a part in airblast atomization.

4.4.1 MEASUREMENT OF LIQUID PROPERTIES

(a) The kinematic viscosity, in centistokes, is measured using a range of the 1625 PSL calibrated suspended level viscometers of the type BS 188 - BS/IP/SL in accordance with ASTM D445 - IP 71. These viscometers were used in a thermostatically controlled viscometer bath, and all measurements were carried out at 20°C. By measuring the flow time 't' in seconds, the kinematic viscosity in centistokes is determined directly from the equation:

$$\nu = C \cdot t \qquad \ldots\ldots\ldots\ldots\ldots\ldots (14)$$

where C = the calibration constant in centistokes/sec engraved on each viscometer and given in a certificate of calibration.

(b) The surface tension is measured using the surface tension torsion balance type 'OS', manufactured by White Electrical Instruments Co., using a platinum ring or a glass test plate. It is calibrated from 0 to 0.12 Newtons per metre, with 240 equal divisions (each is 0.0005 N/m; 1 N/m = 1000 dynes/cm). Checks on surface tension readings were accomplished by measuring the rise in a range of capillary tubes by means of a travelling microscope.

(c) Measurements of density were carried out using a wide range of hydrometers, and checks were made using standard density bottles together with an electronic balance.

The laboratory equipment used for measuring the physical properties of liquids are shown in Plate (5).

4.4.2 RANGE OF LIQUID PROPERTIES

A large number of different trial solutions were made up to obtain wide variations in each of the three properties while maintaining the other two main properties at substantially the same value. The liquids and solutions found to fulfil the above requirements, and the results of measurements carried out at a temperature of 20°C are presented in Tables (1, 2 and 3). The liquids employed in the first phase of the experimental programme represented a range of values as follows:

(a) Viscosity from 0.998 to 123.921 centipoise.

(b) Surface tension from 26.77 to 73.45 dynes/cm.

(c) Density from 0.784 to 1.830 gm/cm^3.

4.5 THE ATMOSPHERIC TEST RIG

A small rotary compressor supplied air at temperatures ranging from 16 to 25°C, and pressures up to 3 p.s.i.g. The air flow divided through two separate outlets into two co-axial ducts in order to provide two air stream paths through the atomizer. The shroud (outer) air stream mass flow was measured using an orifice plate fitted with D and D/2 pressure tappings in accordance with B.S. 1042. The pintle (inner) air stream mass flow was measured by a precision Fisher-Porter float type flowmeter with its associated pressure and temperature gauges. The mass flow and velocity of both air streams could

be varied using isolation valves and by bleeding off air at the compressor. The velocity of each air stream was measured at the atomizing edge and at full stream by means of two pitot tubes. The temperature of each air stream was also measured at the atomizing edge by means of two thermocouples. The instrumentation on the atomospheric test rig is shown in Plates (1, 2 and 4)

Liquids were supplied to the atomizer through a micro-flow valve which provided very small flow increments. Liquid flow rates were measured on precision flowmeters which had been previously calibrated for each liquid at the flow rates tested. The liquid system is shown in Plate (6). Liquid temperature and pressure were recorded by temperature and pressure gauges displayed on the control panel.

4.6 HIGH TEMPERATURE TESTS

It was decided that the simplest and cheapest method of obtaining experimental data on the effect of air density on SMD would be by varying the air temperature using six electric heaters located downstream of the compressor main outlet. This method was adopted and six levels of air temperature between 23 and 151 ^{o}C were satisfactorily accomplished. The atomizing air temperatures at the air velocities tested are presented in Table (4). The heaters arrangement on the atmospheric test rig is shown in Plates (7 and 8).

High temperature tests were conducted with water and kerosine at varying levels of atomizing air velocity for a constant liquid flow rate in one series, and at varying liquid flow rates for a constant air velocity in another.

4.7. THE HIGH PRESSURE TEST RIG

The high pressure test rig is shown schematically in Fig. (20) and Plates (9, 10 and 11). High pressure air from a multistage compressor is fed to the rig through an isolation

valve. The total air mass flow rate is measured by means of an orifice plate made to B.S. 1042 standards. The pressure and temperature tappings, located in accordance with B.S. 1042, feed the manometer, pressure and temperature gauges mounted on the control panel. The air flow divides into two parallel paths formed by two co-axial pipes. The inner copper pipe is supported between the venturi support spider at the upstream end and atomizer support spider at the down stream end. This inner pipe accomodates a venturimeter made to B.S. 1042 specifications to measure the pintle air mass flow. The pressure tappings, brought out of the inner duct through the venturi support spider, feed an inclined manometer and a pressure gauge mounted on the control panel.

The cylindrical observation section, with offset observation windows having armour plate glass, is shown in Fig. (21). The offsetting allows inspection of a bigger area of the spray for the same size of windows. In order to achieve a stable spray at the higher levels of pressure in the observation section, recent improvements include the use of a co-axial cone to divide the outer air flow into two paths. The small end of the cone is connected to the shroud air flow duct in the atomizer, and one air flow passing around the inner (pintle) copper pipe flows through the shroud. The remaining air flow of the outer duct flows past a flame tube mounted in the observation section across the annulus. A static pressure tapping in the cone gives an additional indication of air pressure. The important function of the flame tube is that it gives a well developed spray and prevents deposition of droplets on the glass windows of the observation section. With this method the optical path is kept well clear of any disturbances.

High pressure tests were conducted with water and kerosine at constant levels of velocity and temperature, using a range of liquid flows from 5 to 30 gm/sec, at various levels of pressure between 1.3 and 8.51 atm (19 and 125 p.s.i.a.)

During the entire experimental programme a number of tests were repeated to confirm repeatability and accuracy of the results obtained.

CHAPTER 5

RESULTS

CHAPTER 5

R E S U L T S

All the data reported in this thesis are generally presented in terms of Sauter mean diameter, since this is the most significant average figure describing a spray for use in combustion studies.

5.1 AIRBAST ATOMIZER AIR AND AIR/LIQUID FLOW CHARACTERISTICS

Prior to starting the experimental programme on the atmospheric test rig, the air flow characteristics for the range of atomizing air velocities under test were established. The mean values of mass flow rate for shroud air, pintle air, and total atomizing air streams (at equal velocities for both shroud and pintle air streams) are tabulated in Table (5) and plotted in Fig. (22). The levels of air velocity were chosen to be from 55 to 125 m/sec in order to cover the range of natural air velocities attainable in modern, low-pressure-loss, combustion systems.

The range of liquid flow rates was chosen to be from 4.5 to 30 gm/sec (ca. 35 to 240 lb/hr). The values of A.F.R. and f.a.r. are given in Table (6) and the A.F.R. values are plotted against air velocity for various levels of liquid flow rate in Fig.(23). Both Figs. (22 and 23) illustrate the linear and uniform performance of the airblast atomizer with varying air velocities and liquid flows.

5.2 EFFECT OF LIQUID PROPERTIES

All the data obtained in this phase were at atmospheric pressure and room temperature. The effects of each property on atomization quality are presented separately.

5.2.1 EFFECT OF LIQUID VISCOSITY

In general, viscosity forces tend to oppose the disintegration of ligaments into drops and to resist the further disintegration of drops already formed. This adverse effect of viscosity on atomization quality is shown in Fig. (24) in which SMD is plotted against viscosity in centipoise for various levels of air velocity at a constant liquid flow rate of 15 gm/sec (ca. 120 lb/hr). This figure also demonstrates the well known beneficial effect of an increase in air velocity in reducing SMD.

The effect of varying the liquid flow rate while maintaining the air flow constant (V_a = 100 m/sec) is illustrated in Fig. (25). As might be expected increase in liquid flow rate markedly reduces atomization quality especially with liquids of high viscosity.

5.2.2 EFFECT OF LIQUID SURFACE TENSION

Surface tension forces tend to impair atomization quality by opposing any distortion or irregularity on the liquid surface, thereby delaying the onset of ligament formation. This effect is shown quantitatively in Figs. (26 and 27). Fig. (26) shows the separate effects of surface tension and air velocity on SMD, for a constant liquid flow rate of 15 gm/sec, while Fig. (27) shows the separate effects of surface tension and liquid flow rate on SMD for a constant air velocity of 100 m/sec. Both figures exhibit an increase in SMD with increase in surface tension, especially at low liquid flow rates and low values of surface tension.

5.2.3 EFFECT OF LIQUID DENSITY

The influence of liquid density on mean drop size is illustrated in Figs. (28 and 29). Fig (28) shows the separate effects of liquid density and air velocity on SMD, for a constant liquid flow rate of 15 gm/sec, while Fig. (29) shows the separate effects of liquid density and liquid flow rate on SMD for a constant air velocity of 100 m/sec. All the data obtained show the same general trend, namely an increase in SMD with density

up to a value of around 1.5 gm/cm^3, above which SMD tends to diminish with further increase in density. This characteristic may be attributed to a variation with density in the relative magnitude of its various influence on SMD. For example, it is known from the work of Briffa and Dombrowski (Ref. 6) that the length of the coherent liquid sheet downstream of the atomizing edge increases with density, so that sheet disintegration occurs under conditions of lower relative velocity between the air and the liquid. Moreover, an increase in density at constant flow rate produces a more compact spray that is less exposed to the atomizing action of the high velocity air. Both these effects combine to produce the observed increase in SMD with density up to around 1.5 gm/cm^3 as shown in Figs. (28 and 29). However, an increase in liquid density can also lower SMD by reducing the thickness of the liquid sheet at the atomizing edge, and this may be a dominant factor in the density range above 1.5 gm/cm^3.

5.3 EFFECT OF AIR TEMPERATURE

The effect of air temperature on mean drop size is illustrated in Fig. (30) in which SMD is plotted against air temperature in deg. Centigrade for various levels of air velocity at a constant water flow rate of 15 gm/sec. This figure shows again that increase in air velocity is beneficial in reducing SMD. The effect of air temperature on SMD for a constant air velocity of 100 m/sec and varying water flow rate is illustrated in Fig. (31). The deleterious effect of increase in water/air ratio on atomization quality is clearly brought out in this figure.

Figures (32) and (33) show corresponding data to Figures (30) and (31) respectively for kerosine. These results show exactly the same trends as those observed with water, but the absolute values of SMD are lower due to the lower density and surface tension of kerosine as compared to water.

By plotting the data obtained in this series of experiments for both water and kerosine at a constant liquid flow rate of 15 gm/sec as log (SMD) versus log (air temperature) the slopes of the resulting straight lines were found to be in the range of 0.920 to 0.980 for water, and 0.870 to 0.997 for kerosine at air velocities ranging from 125 to 60 m/sec

respectively. The actual slopes obtained are shown in Fig. (34). Similarly, Figs. (35) and (36) show the actual slopes obtained for both water and kerosine at a constant air velocity of 100 m/sec. The slopes of the resulting straight lines were found to be quite close to the value of 1.0.

5.4 EFFECT OF AIR PRESSURE

The results of measurements of the high pressure air flow characteristics are given in Table (7). The influence of air pressure on mean drop size is illustrated quantitatively in Fig. (37) in which SMD is plotted against air pressure in atmospheres for various levels of water flow rate. This figure clearly shows the beneficial effect of an increase in air pressure in reducing SMD. Fig. (38) shows corresponding data to Fig. (37) for kerosine. The difference in the absolute values of SMD for kerosine is clearly observed as compared to water.

By plotting the data obtained for both water and kerosine at a liquid flow rate of 30 gm/sec as log (SMD) versus log (air pressure) the slopes of the resulting straight lines were found to be - 0.99 and - 1.02 respectively. Fig. (39) shows the actual slopes obtained.

5.5 PERFORMANCE OF THE AIRBLAST ATOMIZER

Prior to undertaking this series of experiments on both water and kerosine, the range of air velocities and liquid flow rates on the atmospheric test rig has been chosen to be from 54.86 to 121.92 m/sec and from 4.5 to 22.7 gm/sec respectively. The measured values of the atomizing air/liquid mass ratio for the entire range are presented in Table (8) and plotted in Fig. (23).

It is not only the air velocity which determines the mean drop size of a spray but also the liquid flow rate, and hence the atomizing air/liquid mass ratio. For this reason it was decided to present the performance of the airblast atomizer in two ways:

(1-a) S.M.D. is plotted against air velocity for various levels of liquid flow rate (Fig. 40),

(1-b) S.M.D. is plotted against air velocity for various levels of air/liquid ratio (Fig. 41),

(1-c) S.M.D. is replotted against air velocity for various levels of liquid flow rate and air/liquid ratio (Fig. 42), and

(2-a) S.M.D. is plotted against air/liquid ratio for various levels of air velocity (Fig. 43),

(2-b) S.M.D. is plotted against air/liquid ratio for various levels of liquid flow rate (Fig. 44),

(2-c) S.M.D. is replotted against air/liquid ratio for various levels of air velocity and liquid flow rate (Fig. 45).

Figures (46 - 51) show corresponding data to Figures (40 - 45) respectively for kerosine.

After careful consideration of all the data obtained regarding the atomizer performance the following observations can be deduced:

(1) An increase in atomizing air velocity results in reduction in S.M.D. of the spray.

(2) A drop in liquid flow rate at any level of air velocity improves atomization quality.

(3) Atomization quality starts to decline when the air/liquid ratio falls below about four, and deteriorates quite rapidly at air/liquid ratios below about two.

(4) Once the air/liquid ratio exceeds about five, only very slight improvement in atomization quality is gained by the addition of more air.

(5) The data obtained from the tests conducted using kerosine show exactly the same trend as those observed with water, but the absolute values of S.M.D. are lower due to the lower density and surface tension of kerosine as compared to water.

5.6 INFLUENCE OF THE SHROUD AIR STREAM

Since in the airblast atomizer under test a thin continuous sheet of liquid is shattered into drops by the atomizing action of high velocity air on both sides of the liquid sheet, it is of interest to examine the effect of varying the velocity of one air stream while keeping the velocity of the other air stream constant. These experiments were conducted at a certain level of pintle air velocity while the shroud air velocity was varied as much as possible with the small rotary compressor on the atmospheric test rig. The results obtained for water at a liquid flow rate of 11.34 gm/sec are given in Fig. (52) where SMD is plotted against pintle air velocity for various levels of shroud air velocity. This Figure gives a clear quantitative picture of the advantage gained by imparting higher velocity to the shroud air stream. The same data of Fig. (52) were replotted in Fig. (53) together with the same liquid flow line of 11.34 gm/sec at equal velocities for both air streams. The deleterious effect of a drop in the shroud air velocity on atomization quality is clearly brought out in this Figure. The percentage of the total atomizing air stream flowing through the shroud was then calculated and the same data of Figs. (52 and 53) were plotted in Fig. (54). At this stage a quantitative conclusion was found, namely best atomization quality was achieved when 65% of the total atomizing air stream was flowing through the shroud. Figs. (55 - 57) show corresponding data to Figs. (52 - 54) respectively for kerosine. These results confirm the above conclusion.

CHAPTER 6

ANALYSIS OF RESULTS

CHAPTER 6

ANALYSIS OF RESULTS

From inspection of all the data obtained on the effects of air and liquid properties on atomization quality it was possible to draw certain general conclusions concerning the main factors governing SMD of sprays. For example, it was very evident that for liquids of low viscosity the dominent factors are air velocity and air density, SMD being inversely proportional to both (Figs. 34, 35, 36 and 39). It was also apparent from the results obtained over a wide test range, that liquid viscosity has an effect which is quite separate and independent from that of air velocity. This suggested a form of equation in which SMD is expressed as the sum of two terms, the first term being dominated by air velocity and air density and the second term by liquid viscosity.

6.1 DIMENSIONAL ANALYSIS

For a dimensionally correct correlation of SMD with all relevant variables, a dimensional analysis was then applied. The table below shows the dimensions of all variables.

Quantity	Symbol	Dimensions
Sauter mean diameter	SMD	L
Atomizing air Velocity	V_a	$L\ T^{-1}$
Air density	ρ_a	$M\ L^{-3}$
Air mass flow rate	W_a	$M\ T^{-1}$
Liquid viscosity (absolute)	η_ℓ	$M\ L^{-1}\ T^{-1}$
Liquid surface tension	σ_ℓ	$M\ T^{-2}$
Liquid density	ρ_ℓ	$M\ L^{-3}$
Liquid film thickness	t	L
Liquid flow rate	W_ℓ	$M\ T^{-1}$

As SMD must be the sum of two terms both of which must have the dimension of length, the following equation for SMD was derived. The various indices were deduced from the experimental data.

$$SMD = A \frac{(\sigma_\ell \rho_\ell t)^{0.5}}{V_a \rho_a} (1 + W_\ell/W_a) + B \left(\frac{\eta_\ell^2}{\sigma_\ell \rho_a} \right)^{0.425} t^{0.575} (1 + W_\ell/W_a)^2 \quad \ldots\ldots\ldots\ldots (14)$$

where A and B are constants.

For liquids of low viscosity, such as water and kerosine, the first term predominates and SMD thus increases with increase in liquid surface tension, liquid density, liquid film thickness and liquid/air ratio, and declines with increase in air velocity and air density. With liquids of high viscosity the second term acquires greater significance and, in consequence, SMD becomes less sensitive to variation in air velocity and air density.

Unfortunately, as no measurements were made of the liquid film thickness at the prefilming lip, the constants A and B in equation (14) cannot be evaluated. However, by making the not unreasonable assumption that the liquid film thickness is proportional to the diameter of the prefilmer, equation (14) may be rewritten in a more useful form as:

$$SMD = 0.33 \frac{(\sigma_\ell \rho_\ell D)^{0.5}}{V_a \rho_a} (1 + W_\ell/W_a) + 0.157 \left(\frac{\eta_\ell^2}{\sigma_\ell \rho_a} \right)^{0.425} D^{0.575} (1 + W_\ell/W_a)^2 \quad \ldots\ldots\ldots\ldots (15)$$

Equation (15) is dimensionally correct and takes into account all the variables affecting airblast atomization.

6.2 COMPARISON BETWEEN CALCULATED AND EXPERIMENTAL VALUES OF SMD

The ability of equation (15) to predict values of SMD over a wide range of air and liquid properties is demonstrated in Figures (58 to 61). The data in these figures were obtained at atmospheric pressure, with air velocities varying from 70 to 125 m/sec and air/liquid ratios from 2 to 6. Fig. (58) shows an excellent correlation of the experimental data obtained with liquid viscosities varying between 1.0 and 44 centipoise.

The correlation of SMD data for values of liquid surface tension between 26 and 73.5 dynes/cm is also satisfactory as shown in Fig. (59)

The ability of equation (15) to predict the effect of changes in liquid density on SMD is less satisfactory than for the other properties studied, as shown in Fig. (60). However, at the lower levels of density, corresponding to liquids of most practical interest (i.e. liquid density less than 1.2 gm/cm^3), the prediction is reasonably good.

In Fig. (61) the variable of main interest is air temperature which affects SMD through the 'ρ_a' term in equation (15).

In this case, it is of interest to note that the second term in the right-hand side of equation (15) contributes very little to the predicted drop size for both water and kerosine. The correlation achieved is again quite good. The evaporation effects as applied to both the atmospheric and high-temperature test are presented in detail in Appendix (A).

Perhpas the most significant aspect of equation (15) is the prediction that SMD is inversely proportional to air pressure. Fig (39) displays experimental results obtained for both water and kerosine at a liquid flow rate of 30 gm/sec as log (SMD) versus log (air pressure). The actual slopes of the resulting straight lines were found to be - 0.99 and - 1.02 for water and kerosine respectively. These values are quite close to the predicted value of - 1.0 and, therefore, give strong support to the validity of equation (15). This result has direct relevance to the design of airblast atomizers in view of the practical application to the gas turbine engine which has to operate over a wide range of pressures.

Equation (15) provides quantitative relationships between all variables influencing the airblast atomization process, and in so far as it is possible to check this equation against actual experimental data the level of agreement is remarkably good.

CHAPTER 7

CONCLUSIONS

CHAPTER 7

C O N C L U S I O N S

From an extensive investigation carried out on a specially designed airblast atomizer in which the liquid is first spread into a thin continuous sheet and then subjected to high velocity air on both sides the following conclusions were drawn :

(1) The air and air/liquid flow characteristics (Figs. 22 and 23) are linear and uniform which may be attributed to the clean aerodynamic design of the atomizer.

(2) Recent improvements in the optical system provided an instrument capable of giving accurate and consistent results over the range of droplet sizes normally encountered in airblast atomizers. The droplet freezing technique was found to be a slow and tedious process.

(3) The approach adopted in isolating the effects of viscosity, surface tension and density provided a quantitative picture of the influence of each property on atomization quality. The mean drop size of the liquid spray increases with increase in viscosity, surface tension and liquid/air ratio. It also increases with density over the range of densities of most practical interest, and is reduced by an increase in air velocity. These findings are in broad agreement with the results obtained on different types of airblast atomizer by Nukiyama and Tanasawa and Wigg. In combustion systems burning fuels of high viscosity it is suggested that as high an air velocity as possible should be used in atomizing the fuel.

(4) Atomization quality deteriorates with increase in air temperature.

(5) Mean drop sizes decrease rapidly with increase in ambient pressure. For liquids of low viscosity, e.g. water and kerosine, the mean drop sizes obtained with airblast atomizers are inversely proportional to air velocity and air density, and directly proportional to the square root of both liquid density and liquid surface tension. All these factors become less significant with increase in liquid viscosity.

(6) In the design of airblast atomizers for light hydrocarbon fuels, e.g. kerosine or gas oil, the air/liquid ratio should ideally exceed a value of two. However, little improvement in atomization quality is gained by raising the air/liquid ratio above a value of five.

(7) Best atomization quality was achieved when 65% of the total atomizing air was applied through the shroud (outer) air stream.

(8) Over the following range of conditions:

Liquid viscosity	-	1.0	to	44	dentipoise
Liquid surface tension	-	26	to	73.5	dynes/cm
Liquid density	-	0.78	to	1.5	gm/cm^3
Air velocity	-	70	to	125	m/sec
Air temperature	-	20	to	151	^oC
Air pressure	-	1.0	to	8.5	kgf/cm^2
Air/liquid ratio	-	2	to	6	

the mean drop size of the spray may be predicted with reasonable accuracy by the dimensionally correct equation:

$$SMD = 0.33 \frac{(\sigma_\ell \rho_\ell D)^{0.5}}{V_a \rho_a} (1 + W_\ell / W_a) +$$

$$0.157 \left(\frac{\eta_\ell^2}{\sigma_\ell \rho_a} \right)^{0.425} D^{0.575} (1 + W_\ell / W_a)^2$$

CHAPTER 8

RECOMMENDATIONS FOR FUTURE WORK

CHAPTER 8

RECOMMENDATIONS FOR FUTURE WORK

(a) In order to minimize any possible errors in S.M.D. measurements, small but significant improvements should be incorporated in the present optical bench. An He/Ne continuous wave gas laser beam should be used as a light source instead of the mercury arc lamp to reduce any possible arc fluctuations. However, it has been found that these fluctuations can be overcome by the use of a very small damping capacitance in the log-amplifier. Furthermore, an adequate photo detector with integral amplifier should be used instead of the present photomultiplier which can suffer from saturation problems. This problem, however is less significant when enough time (ca. 5 minutes) is allowed for complete discharge of the signal.

(b) Further research on airblast atomization should be continued. A special design of airblast atomizer similar to the design employed in this work should enable measurements to be made of the liquid film thickness at the atomizing edge. It would be of value to study the extent to which the sheet thickness as it emerges to the air streams governs S.M.D.

(c) High-speed photography should be employed to study the mechanism of droplet disintegration by the disruptive action of high velocity air on both sides of a liquid sheet.

(d) Once a conclusive answer has been achieved regarding the two points stated above a suitable model for airblast atomization should be developed.

ADDENDUM

It is clearly desirable to assess the ability of equation (15) to predict the values of S.M.D. obtained by other workers (Refs. 11, 34, 42, 63, 76, 78, 79 and 86). Unfortunately most of the previous studies of airblast atomization were conducted using either single-jet nozzles or other types of atomizer which were significantly different from the atomizer employed in the present research. In some cases the characteristic dimension of the atomizer was chosen to be the liquid orifice diameter which is clearly markedly different from the prefilmer diameter used as the characteristic dimension in the present investigation.

Due to these limitations the only results which appear amenable to analysis are those reported by Wigg (Ref. 78). Three N.G.T.E. airblast atomizers were tested of the type shown in Fig.(2), the values of D being 1.28 , 2.54 and 3.59 cm. The liquid employed was water and the atomizing fluid was air supplied at pressures from 20 to 26 p.s.i.g.

Fig.(69) shows the drop size measurements obtained plotted against the first term only on the right hand side of equation (15), since this is the dominant term for low-viscosity liquids. The correlation is reasonably good except that a constant about three times higher than the present value of 0.33 would have to be used in order to obtain a reasonable fit to the experimental data. The explanation for this is probably that the pressure drop available at the atomizing edge (Fig. 2) is much less than the values quoted due to losses within the atomizer, and no absolute measurements of the air velocity at the atomizing edge were made.

In later work by Wigg (Ref. 79) the characteristic dimension of the atomizer was chosen to be that of the air annulus "h" i.e. the height of the air annulus at the point of impact, and his correlation of existing data resulted in equations (6) and (7). The experimental values of S.M.D. for water and kerosine sprays at atmospheric pressure and temperature obtained in the present investigation are compared with the predictions of equations (6) and (7) in Fig. (70) and show a very satisfactory level of agreement. No attempt was made to plot data at other levels of pressure because it could be seen from inspection of equations (6) and (7) that the level of agreement between predicted and measured values would diminish with increase in air pressure.

REFERENCES

REFERENCES

1. ANSON, D. — "Influence of the Quality of Atomization on the Stability of Combustion of Liquid Fuel Sprays," Fuel, Quarterly Journal of Fuel Science, Vol. 22, 1953, pp. 39 - 51

2. BAHR, D.W. — "Evaporation and Spreading of Iso-octane Sprays in High-Velocity Air Streams," N.A.C.A. RM E53I 14, 1953

3. BATER, K.M.; and POULTON, W.R. — "The Performance of an Airspray Atomizer in the Pimery Zone of a Gas Turbine Combustion Chamber," N.G.T.E. C.P.C. Note No. 23, June 1966

4. BENNET, P.G. — "Airblast Atomization," Cranfield Thesis, Department of Aircraft Propulsion, June 1962.

5. PB-Chemicals International Ltd. — "Hyvis Polybutenes," Technical Booklet No. HB102/2

6. BRIFFA, F.E.J.; and DOMBROWSKI, N. — "Entrainment of Air into a Liquid Spray," A.I.Ch.E. Journal, Vol. 12, No. 4, July 1966 pp. 708 - 717

7. BROWNING, J.A.; and KRALL, W.G. — "Effect of Fuel Droplets on Flame Stability, Flame Velocity, and Inflammability Limits," 5th Sumposium on Combustion (International), 1955, pp. 159 - 163

8. BRYAN, R.H. — "An Experimental Study of an Airblast Atomizer," Cranfield M.Sc. Thesis, Department of Aircraft Propulsion, Oct. 1967

9. BRYAN, R.H.; GODBOLE, P.S.; and NORSTER, E.R. — "Some observations of the Atomizing Characteristics of Airblast Atomizers," Cranfield Inernational Sympsoim Series, Vol. 11, Edited by E.R. Norster, Pergamon Press, 1971.

10. CASTLEMAN, R.A. — " The Mechanism of Atomization of Liquids," National Bureau of Standards Journal of Research (U.S. Dept. of Commerce), Vol. 6, No. 281, 1931, p.369.

11.	CLARE, H.; and RADCLIFFE, A.	"An Airblast Atomizer for Use with Viscous Fuels," Journal of Institute of Fuels, Vol. 27, Oct. 1954, p. 510
12.	COHEN, N.; and WEBB, M.J.	"Evaluation of Swirl Atomizer Spray Characteristics by a Light Scattering Technique," Princeton University Aeronautical Engineering Laboratory Report, No. 597, Feb. 1962
13.	COLLINS, R.D.; MAYER, G.M.; and NEWBY, M.P.	"The Efficiency of Momentum Production by Fluid-Atomizing Burners," Journal of Institute of Fuels, Vol. 26, No. 5 Oct. 1953, pp. 203 - 208
14.	DEISS, W.E.	"The Optical Determination of Particle Sizes Obeying the Upper Limit Distribution Function," Princeton University Thesis, Department of Aeronautical Engineering, May 1960
15.	DICKERSON, R.A.; and SCHUMAN, M.D.	"Rate of Aerodynamic Atomization of Droplets," Journal of Spacecraft, Vol. 2, No. 1, Jan. - Feb. 1965, pp. 99 - 100
16.	DITYAKIN, I.F.; and YAGODKIN, V.I.	"Effect of Periodic Oscillations of Velocity and Density of a Medium on Disintegration of Liquid Jets," N.A.C.A. TT F-63, April 1961
17.	DOBBINS, R.A.; CROCCO, L.; and GLASSMAN, J.	"Measurement of Mean Particle Sizes of Spray from Diffractively Scattered Light," A.I.A.A. Journal, Vol. 1, No. 8, Aug. 1963, pp. 1882 - 1886
18.	DOMBROWSKI, N.; and MUNDAY, G.	"Spray Drying," Biological and Biochemical Engineering Science, Vol. 2, Chapter 16, pp. 209 - 320
19.	ENGEL, O.G.	"Fragmentation of Water Drops in the Zone Behind an Air Shock," National Bureau of Standards Journal of Research, Vol. 60, No. 3, March 1958
20.	FOSTER, H.H.; and INGEBO, R.D.	"Evaporation of JP-5 Fuel Sprays in Air Streams," N.A.C.A. RM E55K02, Nov. 1955
21.	FRASER, R.P.	"Liquid Fuel Atomization," 6th Symposium on Combusion (International), 1957
22.	FRASER, R.P.; DOMBROWSKI, N.; and ROUTLEY, J.H.	"The Mechanism of Disintegration of Liquid Sheets in Cross-Current Air Streams," Applied Science Research, Volumes A11 - A12, 1962 - 1963

23.	FRASER, R.P.; DOMBROWSKI, N.; and ROUTLEY, J.H.	"The Filming of Liquids by Spinning Cups," Chemical Engineering Science, Vol. 18, 1963, pp. 323 - 337
24.	FRASER, R.P.; DOMBROWSKI, N.; and ROUTLEY, J.H.	"The Production of Liquid Sheets from Spinning Cups," Chemical Engineering Science, Vol. 18, 1963, pp. 315 - 321
25.	FRASER, R.P.; DOMBROWSKI, N.; and ROUTLEY, J.H.	"The Atomization of a Liquid Sheet by an Impinging Air Stream," Chemical Engineering Science, Vol. 18, No. 6, June 1963, pp. 339 - 353
26.	FRASER, R.P.; EISENKLAM, P.; and DOMBROWSKI, N.	"Liquid Atomization in Chemical Engineering," British Chemical Engineering, Vol. 2, pp.414 - 417, 496, 536 and 610 - 614, (1957)
27.	FROESSLING, N.	"Ueber die Verdunstung Fallender Tropfen," (On the Evaporation of Falling Droplets), Gerlands Beitraege zur Geophysik, Vol. 52, 1938, pp. 170 - 216
28.	GARNER, F.H.; and HENNY, V.E.	"Behaviour of Sprays Under High Altitude Conditions," Fuel, Quarterly Journal of Fuel Science, Vol. 32, 1953, pp. 151 - 156
29.	GIFFEN, E.	"Atomization of Fuel Sprays" Engineering, Vol.174, July 1952, pp 6 - 10
30.	GIFFEN, E.; and MURASZEW, A.	"The Atomization of Liquid Fuels," Chapman and Hall Ltd., 1953.
31.	GODBOLE, P.S.	"The Effect of Ambient Pressure on Airbalst Atomizer Performance," Cranfield Thesis, Department of Aircraft Propulsion, Sept. 1968
32.	GODFREY, D.	"An Assessment of a Light Scattering Technique for Drop Size Measurement," Cranfield Thesis, Department of Aircraft Propulsion, Sept. 1969
33.	GODSAVE, G.A.E.	"Studies of the Combustion of Drops in a Fuel Spray," 4th Symposium on Combustion (International) 1953, pp. 818 - 830

34.	GOLITZINE, N.; SHARP, R.; and BADHAM, L.G.	"Spray Nozzles for the Simulation of Cloud Conditions in Icing Tests of Jet Engines," N.A.E. Canada, Report 14, 1951
35.	GREEN, H.L.	"Problems in the Atomization of Liquids," Conference on Fluid Flow, Institute of Physics, 1951, pp. 75 - 86
36.	GRETZINGER, J.; and MARSHALL, Jr., W.R.	"Characteristics of Pneumatic Atomization," Journal of the American Institute of Chemical Engineering, Vol.7, No. 2, June 1961, pp. 312 - 318
37.	HANSON, A.R.; DOMICH, E.G.; and ADAMS, H.S.	"An Experimental Investigation of Impact and Shock Wave Break-up of Liquid Drops," Research Report 125, Jan, 1956, Rosemount Aeronautical Laboratory, Minneapolis, Minn.
38.	HEATH, H.; and RADCLIFFE, A.	"The Performance of an Airblast Atomizer," N.G.T.E. Report No. 71, June 1950
39.	HINZE, J.O.	"Fundamentals of the Hydrodynamic Mechanism of Splitting in Dispersion Processes," Journal of the American Institute of Chemical Engineering, Vol. 1, No. 3, Sept. 1955, pp. 289 - 295
40.	HODGKINSON, J.V.	"An Optical Instrument for the Measurement of Mean Droplet Size of Sprays," Cranfield Thesis, Department of Aircraft Propulsion, May 1966
41.	HRUBECKY, H.F.	"Experiments in Liquid Fuel Atomization," Journal of Applied Physics, Vol. 29, 1958
42.	INGEBO, R.D.; and FOSTER, H.H.	"Drop-size Distribution for Cross-current Break-up of Liquid Jets in Air Streams," N.A.C.A. TN 4087, Oct. 1957
43.	JOYCE, J.R.	"Fuel Atomizers for the Gas Turbine," Shell Thornton Research Centre, Miscellaneous 396, 1948
44.	JOYCE, J.R.	"The Atomization of Liquid Fuels for Combustion," Journal of Institute of Fuel, Feb. 1949 pp. 150 - 156
45.	KERKER, M.	"The Scattering of Light," Academic Press, 1969

46. LANE, W.R. "Shatter of Drops in Streams of Air," Industrial and Engineering Chemisty, Vol. 43, No. 6, June 1951, pp.1312 - 1316

47. LAWRENCE, O.N. "Gas Turbine Accessory Systems," Journal of Royal Aeronautical Society, 1948, p.151

48. LEE, D.W.; and SPENCER, R.C. "Photomicrographic Studies of Fuel Sprays" N.A.C.A. Report No. 454, 1933, pp. 215 - 239

49. LEFEBVRE, A.H. "A Proposed Airspray Atomizer for Aircraft Combustion Chambers," Unpublished College of Aeronautics Memorandum, March 1964

50. LEFEBVRE, A.H. "Progress and Problems in Gas Turbine Combustion," 10th Symposium on Combustion, 1965, pp. 1129 - 1137

51. LEFEBVRE, A.H. "Design Considerations in Advanced Gas Turbine Combustion Chambers," Cranfield International Symposium Series, Vol. 10, Edited by E.I. Smith, Pergamon Press, 1968, pp. 3 - 19

52. LEFEBVRE, A.H.; and MILLER, D. "The Development of an Airblast Atomizer for Gas Turbine Application," Cranfield College of Aeronautics Report Aero No. 193, June 1966

53. LEFEBVRE, A.H.; and NORSTER, E.R. "A proposed 'Double Swirler' Atomizer for Gas Turbine Fuel Injection," Cranfield SME Report No. 1, June 1972.

54. LEWIS, H.C.; EDWARDS, D.G.; GOGLIA, M.J.; RICE, R.I.; and SMITH, L.W. "Atomization of Liquids in High Velocity Gas Streams," Industrial and Engineering Chemistry, Vol. 40, No. 1, Jan. 1948, pp.67 - 74

55. LUCAS, J. "The Jet-Engine Fuel System," Flight, Vol. 49, Jan, 1946, p. 41

56. MACEY, W.R. "A Study of the Factors Influencing Fuel Prefilming and Spray Angle in Airblast Atomizers," Cranfield SME M.Sc. Thesis, Sept. 1971

57. MAYER, E. "Theory of Liquid Atomization in High Velocity Gas Streams," A.R.S. Journal, Vol. 31, 1961, pp. 1783 - 1785

58. MOCK, F.C.; and GANGER, D.R. "Practical Conclusions on Gas Turbine Spray Nozzles," S.A.E. Transactions, Vol. 4, No. 3, July 1950, pp. 357 - 367

59 MUGELE, R.A.; and EVANS, H.D. "Droplet Size Distribution in Sprays," Journal of Industrial and Engineering Chemistry, Vol. 43, No. 6, June 1951, pp. 1317 - 1324

60. NEYA, K. "Measuring Methods for the Spray Characteristics of a Fuel Atomizer at Various Conditions of the Ambient Gas," Paper of Ship Research Institute, Tokyo, Japan, No. 23, Sept. 1967.

61. NEYA, K.; and SATO, S. "Effect of Abmient Air Pressure on the Spray Characteristics of Swirl Atomizers," Paper of Ship Research Institute, Tokyo, Japan, No. 27, Feb. 1968

62. NORSTER, E.R.; and LEFEBVRE, A.H. "Effects of Fuel Injection Methods on Gas Turbine Combustor Emissions," Symposium on Emissions from Continuous Combustion Systems, General Motors Research Laboratories, Michigan, U.S.A., 1971.

63. NUKIYAMA, S.; and TANASAWA, Y. "Experiments on the Atomization of Liquid by means of an Air Stream," Transactions of the Society of Mechanical Engineers, (Japan), Reports 1 - 6, Vols. 4 - 6, 1938 - 1940

64. POPOV, M. "Model Experiments on Atomization of Liquids," N.A.S.A. T.T. F.65, July 1961

65. RADCLIFFE, A.; and CLARE, H. "A Correlation of the Performance of Two Airblast Atomizers with Mixing Sections of Different Size," N.G.T.E. Report No. 144, Oct. 1953

66. RANGER, A.A.; and NICHOLLS, J.A. "Aerodynamic Shattering of Liquid Drops," A.I.A.A. Journal, Vol. 7, No. 2, Feb. 1969 pp. 285 - 290

67. RIZKALLA, A.A.; and LEFEBVRE, A.H. "Influence of Liquid Properties on Airblast Atomizer Spray Characteristics," A.S.M.E. Gas Turbine Conference, Zurich, April 1974, to be published in A.S.M.E. Transactions, Journal of Engineering for Power

68. RIZKALLA, A.A.; and LEFEBVRE, A.H. "The Influence of Air and Liquid Properties on Airblast Atomization," A.S.M.E. Symposium on Fluid Mechanics of Combustion, Montreal Conference, May 1974, to be published in A.S.M.E. Transactions, Journal of Fluids Engineering

69. ROBERTS, J.H.; and WEBB "The Use of the Upper Limit Distribution Function in Light Scattering Theory as Applied to Droplet Diameter Measurement," Princeton University Aeronautical Engineering Laboratory Report No. 650, 1963

70. ROBERTS, J.H.; and WEBB, M.J. "Measurement of Droplet Size for Wide Range Particle Distributions," A.I.A.A. Journal, Vol. 2, No. 3, March 1964, pp. 583 - 585

71. SAUTER, J. "Die Groessenbestimmumg der in Gemischnebel von Verbrennungskraftmaschinen vorhandenen Brennstoffeilchen," (Measurement of Fuel Particles in Fuel Sprays for Internal Combustion Engines) Forsch. Geb. Ingenieurwesens, No. 279, 1926

72. STREET, P.J.; and DANAFORD, V.E. "A Technique for Determining Droplet Size Distribution Using Liquid Nitrogen," Journal of Institute of Petroleum, Vol. 54, No. 536, Aug. 1968, pp. 241 - 243

73. TRIKHA, M.M. "Influence of Fuel Injection on Smoke Emission and Flame Radiation in a Gas Turbine Combustion Chamber," Cranfield Thesis, Department of Aircraft Propulsion, Oct. 1970

74. VAN DE HULST, H.C. "Light Scattering by Small Particles," Wiley, New York, 1956

75. WATSON, E.A.; and CLARKE, J.S. "Combustion and Combustion Equipment for Aero Gas Turbines," Journal of Institute of Fuel, Vol. 21, No. 116, Oct. 1947, pp. 1 - 34

76. WEISS, M.A.; and WORSHAM, C.H. "Atomization in High Velocity Air Streams," Applied Science Research, Vol. 29, No. 4, April 1959

77. WELCH, C. "Design of an Optical System for Counting and Sizing Airborne Particles," National Symposium on Instrumental Methods of Analysis, 8th Proceedings, 1962, pp. 173 - 178

78. WIGG, L.D. "The Effect of Scale on Fine Sprays Produced by Large Airblast Atomizers," N.G.T.E. Report No. 236, July 1959

79. WIGG, L.D. "Drop-Size Prediction for Twin-Fluid Atomizers," Journal of the Institute of Fuel, Vol. 27 No. 286, Nov. 1964, pp. 500 - 505

80. WISE, H.; LORELL, J.; and WOOD, B.J. "The Effects of Chemical and Physical Parameters on the Burning Rate of a Liquid Droplet," 5th Symposium on Combustion (International) 1955, pp. 132 - 141

81. WISE, H.; and AGOSTON, G.A. "Burning of a Liquid Droplet," Advances in Chemistry Series, No. 20, (American Chemical Society), 1958, pp. 116 - 135

82. WOLFE, H.; and ANDERSEN, W. "Aerodynamic Break-up of Liquid Drops," Paper SP 70, (American Physical Society), April 1965

83. WOOD, B.J.; WISE, H.; and INAMI, S.H. "Heterogeneous Combustion of Multicomponent Fuels," N.A.S.A. T.N. D-206, 1958

84. WOOD, B.J.; ROSSER Jr., W.A., and WISE, H. "Combustion of Fuel Droplets," A.I.A.A. Journal, Vol. 1, No. 5, 1963, pp. 1076 - 1081

85. WOOD, R. "Spray Characteristics of Nene Atomizers: Results with Four Atomizers Used in the R.A.E. Nene Altitude Tests," Shell Thronton Research Centre, Report No. K. 112, Sept. 1953

86. WOOD, R. "The Rolls-Royce Airspray Atomizer: Spray Characteristics," Shell Thonton Research Centre, Report No. K. 123, July 1954.

87. YASLONIM, I. "Determination of the Size of Particles by Scattering Light," Optics and Spectroscopy, Vol. 8, No. 2, Feb. 1960

88. YORK, J.L; and STUBBS, H.E. "Photographic Analysis of Sprays" Transactions of A.S.M.E., Oct. 1952, pp. 1157 - 1162

89. YORK, J.L.; STUBBS, H.E.; and TEK, M.R. "The Mechanism of Disintegration of Liquid Sheets," A.S.M.E. Paper No. 53-S-40, 1953

X

APPENDICES

APPENDIX (A)

EVAPORATION EFFECTS AS APPLIED TO THE RESULTS AT ATMOSPHERIC PRESSURE

This analytical study aims at examining the influence of air velocity and kerosine flow rate on droplet lifetime and the distance the droplets moved during lifetime. The reason for undertaking this study was to determine the extent to which drop size measurements at a fixed distance downstream of the atomizer (2 inch) are affected by evaporation rates. It was thought that this effect might be of significance as applied to the high temperature tests conducted.

The range of air temperatures tested was between 20 and 151 ^{o}C, thus the cold evaporation mechanism based on mass transfer without chemical reaction is applicable. This case of evaporation in a moving gas stream has been studied extensively by Froessling (Ref. 27), who reported that the mass transfer rate is governed mainly by drop size and gas velocity. Based on his observations Froessling then derived the following well-known expression for mass transfer rates:

$$\frac{d\,m}{d\,t} = -\frac{2\,\pi\,d\,D\,m}{R\,T}\,(P_1 - P_\infty)\,.\,(1 + 0.276\,Sc^{1/3}\,Re^{\frac{1}{2}}) \quad \ldots\ldots\ (1)$$

where $\frac{dm}{dt}$ = mass rate of change in size of drop, gm/sec

d = drop diameter, cm

D = coefficient of diffusion of the vapour through the surrounding atmosphere, cm^2/sec

M = molecular weight of the vapour

R = gas constant, for air $R = 82.0567\ cm^3.atm/mol.^{o}K$

T = absolute temperature of air, ^{o}K

p_1 = partial pressure of the vapour at the surface of drop, atm.

p_∞ = partial pressure of the vapour at infinite distance from the drop, atm.

Sc = Schmidt number of vapour evaporating into the gas stream, based on mass diffusivity, $= \nu_{air} / D_{vap}$

ν_{air} = kinematic viscosity of air, at 20 °C : $\nu_{air} = 0.151$ cm^2/sec

Re = Reynold's number of gas flow past the drop $= V\,d / \nu_{air}$

V = gas velocity past the drop, cm/sec

The validity of Froessling's equation for mass transfer without chemical reaction has been confirmed by numerous investigators Refs. (2, 33, 80, 81, 83, and 84).

A.1 COMPUTATIONS OF DROPLET LIFETIME AT AIR PRESSURE = 1 atm, AND AIR TEMPERATURE = 20 °C

The value of p_∞ is very small compared with p_1 and can be neglected with reasonable accuracy.

For kerosine at 20 °C :

$$p_1 = 0.8 \text{ mm. Hg.}$$

$$= \frac{0.8}{760} \text{ atm.}$$

and $D = 0.05$ cm^2/sec.

From Thermal properties of Petroleum products:

$$M = \frac{44.29\ (S.G.)}{1.03-(S.G.)}$$, S.G. = specific gravity

$$= \frac{44.29 \times 0.795}{1.03 - 0.795}$$

$$= 149.83$$

$$(Sc)^{1/3} = \left[\frac{0.151 \text{ cm}^2/\text{sec}}{0.05 \text{cm}^2/\text{sec}}\right]^{1/3}$$

$$= 1.4454$$

Substituting these values in equation (1), we arrive at the following equation :

$$\frac{d\,m}{d\,t} = -2.0598 \times 10^{-10} \quad d\,(1 + 0.3989\ Re^{\frac{1}{2}}) \quad \ldots\ldots\ldots \quad (2)$$

where d = initial drop diameter, microns.

From the results obtained and plotted in Figs. (46 - 51), (dm/dt) has been computed for air velocities from 54.9 to 121.9 m/sec and kerosine flow rates ranging from 4.5 to 22.5 gm/sec.

It is known that :

$$\frac{d}{d\,t}\ D^2 = \lambda \ \text{cm}^2/\text{sec} \quad \ldots\ldots\ldots \quad (3)$$

where D = droplet diameter at time t, and

λ = average evaoporation constant, cm^2/sec.

so that, $D^2 = D_o^2 - \lambda t$ $\ldots\ldots\ldots$ (4)

where D_o = initial drop diameter, and t in sec.

It is known from the work of Wood and co-workers (Refs. 83 and 84) that (dm/dt) is related to 'λ' by the following equation:

$$\frac{dm}{dt} = \frac{\pi}{4} d \rho_{\ell} \lambda \quad \text{gm/sec} \qquad \ldots\ldots\ldots \quad (5)$$

$$\text{thus} \quad \lambda = 4 (dm/dt) / \pi d \rho_{\ell} \qquad \ldots\ldots\ldots \quad (6)$$

Substituting for all relevant values in equation (6), we arrive at the following equation :

$$\lambda = 330 (1 + 0.3989 \, Re^{\frac{1}{2}}) \quad \mu^2/\text{sec.}$$

$$\ldots\ldots\ldots \quad (7)$$

The values of 'λ', and hence the droplet lifetime 't' have been computed for the above test range and the results are plotted in Figs. (62) and (63). In Fig. (62) the droplet lifetime in milliseconds is plotted against air velocity for various levels of kerosine flow rate, while droplet lifetime is plotted against kerosine flow rate for various air velocities in Fig. (63). Both figures clearly show the beneficial effect of an increase in air velocity and the detrimental effect of an increase in kerosine flow rate on droplet life time.

A.2 COMPUTATIONS OF THE DISTANCE THE DROPLETS MOVE DURING LIFETIME

Air Pressure = 1 atm., and

Air Temperature = 20 ^{o}C

The objective of this study is to derive an expression for the distance the droplet move during its lifetime. It is known from the fundamentals of aerodynamic drag on a sphere that :

$$C_D = \frac{2 F_d \cdot g_c}{\rho_g \cdot u^2 \cdot A} \quad \ldots\ldots\ldots \quad (8)$$

where C_D = drag coefficient

F_d = drag force

g_c = acceleration due to gravity

ρ_g = gas density

u = velocity of droplets relative to air

A = frontal area of the droplets, = $1/4 \; \pi \; D^2$

From equation (8) :

$$F_d = \frac{C_D \cdot \rho_g \cdot u^2 \cdot A}{2 g_c} \quad \ldots\ldots\ldots \quad (9)$$

but $$F_d = \frac{m \cdot a}{g_c} \quad \ldots\ldots\ldots \quad (10)$$

where m = droplet mass, $= \frac{1}{6} \; \pi \; D^3 \; \rho_f$, and

a = droplet acceleration

ρ_f = liquid density.

Thus :

$$\frac{m \cdot a}{g_c} = \frac{C_D \cdot \rho_g \cdot u^2 \cdot A}{2 g_c} \quad \ldots\ldots\ldots \quad (11)$$

Therefore :

$$a = \frac{d\,V}{d\,t} = \frac{C_D \cdot \rho_g \cdot u^2 \cdot A}{2\,m} \qquad \ldots\ldots\ldots \quad (12)$$

where V = droplet velocity, and

the relation between 'u' and 'V' is:-

$$u = U - V \qquad \ldots\ldots\ldots \quad (13)$$

where U = Velocity of the air flow, is constant.

i.e. $V = U - u$

thus: $a = \frac{d}{dt}(U - u)$

$$= \frac{dU}{dt} - \frac{du}{dt}$$

$$= - \frac{du}{dt} \qquad \ldots\ldots\ldots \quad (14)$$

therefore from equation (12) :

$$- \frac{d\,u}{d\,t} = \frac{C_D \cdot \rho_g \cdot u^2 \cdot A}{2\,m} \qquad \ldots\ldots\ldots \quad (15)$$

Integrating equation (15) gives :

$$\int_U^u \frac{d\,u}{u^2} = \int_o^t - \frac{C_D \cdot \rho_g \cdot A}{2\,m}\, d\,t$$

$$- u^{-1}\Big|_U^u = - \frac{C_D \cdot \rho_g \cdot A}{2\,m} \cdot t\Big|_o^t$$

$$-\frac{1}{u} + \frac{1}{U} = -\frac{C_D \cdot \rho_g \cdot A}{2\,m} \cdot t$$

then : $$u = \frac{1}{\frac{C_D \cdot \rho_g \cdot A \cdot t}{2\,m} + \frac{1}{U}} = f(t) = U - V$$

therefore the value of droplet velocity 'V' is :

$$V = U - \frac{1}{\frac{C_D \cdot \rho_g \cdot A \cdot t}{2\,m} + \frac{1}{U}} = f(t) \quad \ldots\ldots\ldots (16)$$

Now let X = droplet position,

$$X = \int V \cdot dt$$

$$= \int \left(U - \frac{1}{\frac{C_D \cdot \rho_g \cdot A \cdot t}{2\,m} + \frac{1}{U}} \right) dt$$

Following integration by parts and the boundary condition :

$$X = o \qquad \text{at} \qquad t = o$$

the following expression of X can be derived :

$$X = U\,t - \frac{2\,m}{C_D \cdot \rho_g \cdot A} \cdot \ln \left[1 + \frac{C_D \cdot \rho_g \cdot A \cdot t}{2\,m} U \right] \ldots\ldots\ldots (17)$$

The classical values of C_D are known from the work of Dickerson and Schuman (Ref. 15) as follows:

$$C_D = 27\ Re^{-0.84}, \quad 0 \leqslant Re \leqslant 80$$

$$C_D = 0.271\ Re^{0.217}, \quad 80 \leqslant Re \leqslant 10^4$$

$$C_D = 2, \quad Re \geqslant 10^4$$

Using the same results obtained for kerosine at atmospheric pressure and air temperature of 20 °C, the distances moved during lifetime have been computed, tabulated in Table (9), and plotted in Figs. (64) and (65). Both figures demonstrate again the beneficial effect of an increase in air velocity and the deleterious effect of an increase in liquid flow rate on these distances.

A.3 EFFECT OF AIR TEMPERATURE ON DROPLET LIFETIME AND DISTANCE MOVED DURING LIFETIME

Following the same procedure and using the data obtained at various levles of atomizing air temperature and plotted in Fig. (32), droplet lifetimes and distances moved during lifetime have been computed, tabluated in Table (10) and plotted in Figs. (66) and (67). Figure (66) indicates clearly the effect of air temperature on droplet lifetime. Fig. (67) demonstrates quantitatively this effect on the distance moved during the time required to reduce the droplet diameter to zero.

At this stage it may be concluded that at 2 inch (0.0508 m) downstream of the atomizer, where SMD measurements were made, evaporation effects are of minor importance. Evaporation rates would be higher at very low liquid flow rates and higher air temperatures.

The study outlined above led to a further analysis of the relationship between the droplet's velocity and the atomizing air velocity. It was of interest to study the rate of increase of the drop velocity and thus the time required for a drop to follow the atomizing air velocity. Using equation (16) the values of drop velocity were computed at varying time intervals and plotted in Fig. (68). It was found that the drop velocity achieves the value of air velocity in less than 0.1 millisecond.

APPENDIX (B)

ALIGNMENT OF THE OPTICAL BENCH

Before optimum results can be expected from the Light Scattering Technique all the system components must lie on the same optical axis. The following procedure, with the exception of part vi), was carried out each time the mercury arc lap was switched on. If during a series of tests the optical bench was disturbed due to some knock or external shock then the alignment procedure should be repeated.

(i) Swich on the mercury arc lamp and allow 30 minutes for the arc to stabilize.

(ii) Swich on the X-Y recorder, and the Photomultiplier H.T. supply on negative polarity.

(iii) Clean all optical surfaces. (Use only approved brushes, cloths, tissues, etc. as every attempt should be made to keep the optical surface clean and free of scratches or other defects.)

(iv) Check that the lamp, condenser lens, iris diaphragm, filter and collimating aperture are all situated on the same optical axis. If not, adjust the components until they are still retaining the beam central in the collimating lens.

(v) Adjust the lamp and/or condenser lens to focus the image of the arc on to the collimating aperture.

(vi) With the prism removed from its mount check that the beam is parallel by measuring its diameter adjacent to the collimator lens and then at some position approximately 15 feet away. If the two diameters are not equal adjust the position of the collimating lens, with respect to the collimating aperture, until the two diameters become euqal.

(vii) Check the beam diameter at the exit from the collimating lens. Adjust to the correct diameter by varying the diameter of the iris diaphragm.

(viii) Replace the prism and adjust it until the beam is central in the receiver lens.

(ix) Check that the beam clears any windows or screening which may be present in the measuring section.

(x) Move the photomultiplier trolley until it is positioned on the optical axis; set the dial test indicator to zero.

(xi) Adjust the photomultiplier H.T. supply to give an output of 700 V.

(xii) With the X-scale on the recorder set to a sensitivity of 40 mV/cm and adjust the range control to give a pen deflection of 0.100 in. over 5 cm. Adjust the X-axis vernier scale until the pen rests at mid position.

(xiii) With the focussed light beam shining on the photomultiplier aperture adjust the prism alternately on all three adjusting screws until a maximum reading is recorded on the Y-axis of the recorder.

(xiv) Traverse the photomultiplier 0.150 in. to either side of the beam centre line, obtaining an unscattered beam profile. If the beam profile is not symmetrical adjust the horizontal positioning of the lamp, very slightly, until a symmetrical profile is obtained.

(xv) The optical system should now be properly aligned. if this is so the beam should give at least 5.00 in. deflection at its centre, for an H.T. supply of 700 V, whilst still retaining its symmetrical shape.

APPENDIX (C)

CALIBRATION AND OPERATING PROCEDURE OF THE LOGARITHMIC AMPLIFIER

Calibration of the X-Y plotter is necessary after installation and should be repeated subsequently each time before use or when it is re-installed in a different axis or recorder main frame. The calibration and operating procedure is done in the following way:

a) With the function switch in the OdB position switch on the recorder and allow 15 minutes warm-up period.

b) Place a sheet of Log 5 cycles x mm paper on the recorder and check that it is held in position by the vacuum.

c) By means of the Pen Offset Control move the pen to half scale.

d) Turn the Range Control to its calibrated position i.e. fully anti-clockwise and switch to Internal Reference.

e) Switch the Internal Reference switch to 100 mV and adjust the sub-panel SET OdB potentiometer with a small screwdriver so that the pen returns to the OdB-line.

f) Switch to 10 V and adjust the CAL potentiometer to give 10 cm deflection corresponding to 2 decades (2 log cycles) i.e. to 40 dB.

g) Switch to 0.316 mV and adjust the CAL 0.316 mV potentiometer to give a deflection of - 12.5 cm corresponding to - 2.5 decades.

h) When calibration is performed, repeated use of the Pen Offset Control is necessary to ensure that the pen does not exceed full scale deflection in either direction.

i) Check the full range of Internal Reference sources from 0.316 mV to 10 V. The Log Amplifier will now be calibrated with a scale factor of 4 dB/cm over the full dynamic range from 0.316 mV to 10 V.

j) After the required 15 minutes warm-up period the Log Amplifier is ready for use. The Log x mm paper is useful for the indication of the actual magnitude of the compressed input signal.

k) Switch to OdB. The input from the photomultiplier is now disconnected from the Log Amplifier and the pen will have taken up a position corresponding to OdB.

l) Move the pen by means of the Pen Offset Control to the maximum desired pen deflection e.g. full scale deflection. This will be the OdB position.

m) Switch to Internal Reference and switch the Internal Reference switch to the level desired for OdB (in this case the highest voltage to be measured).

n) Switch the highest voltage to be measured and rotate the range control until the pen position coincides with the desired lines on the paper for this voltage e.g. zero scale deflection.

o) Switch the Input to plot the input function i.e. the photomultiplier output against the traverse distance.

p) After use switch to either OdB or Internal Reference and disconnect the input signal line from the input terminals before switching off the recorder.

TABLES

TABLE (1)

Solutions of the synthetic hydrocarbon polymer, Hyvis Polybutene No. 05 in kerosine to obtain a wide range of viscosity:

Level tested	Solution	η	σ	ρ
1	Pure kerosine	1.293	27.67	0.784
2	30 % Hyvis 05	2.868	28.67	0.800
3	40 % Hyvis 05	4.286	28.78	0.809
4	50 % Hyvis 05	6.042	28.87	0.812
5	60 % Hyvis 05	9.789	29.17	0.819
6	70 % Hyvis 05	17.014	30.08	0.823
7	80 % Hyvis 05	33.802	30.16	0.828
8	85 % Hyvis 05	44.104	30.27	0.830
9	90 % Hyvis 05	76.541	30.46	0.833
10	95 % Hyvis 05	123.921	30.70	0.838
	Pure Hyvis 05	218.562	30.96	0.840

TABLE (2)

Mixtures of sec-Butyl Alcohol (Butan - 2 - ol) with water to obtain different values of surface tension:

Level tested	Solution	η	σ	ρ
1	Pure water	0.998	73.45	0.998
2	1.48 % Butan-2-ol	1.127	55.94	0.990
3	2.44 % Butan-2-ol	1.131	51.89	0.988
4	3.85 % Butan-2-ol	1.150	46.45	0.986
5	6.98 % Butan-2-ol	1.274	39.45	0.983
6	11.11 % Butan-2-ol	1.404	33.96	0.980
7	16.67 % Butan-2-ol	1.712	29.07	0.978
8	25.93 % Butan-2-ol	2.342	26.77	0.968
	Pure Butan-2-ol	3.468	24.16	0.807

TABLE (3)

Dibromo-ethane (ethylene dibromide) diluted with methylated spirit to obtain a wide range of density:

Level tested	Solution	η	σ	ρ
	Pure methylated spirit	1.530	26.17	0.812
1	9.09 % Dibromo-ethane	1.537	29.86	0.933
2	13.04 % Dibromo-ethane	1.545	30.29	0.978
3	16.67 % Dibromo-ethane	1.552	30.71	1.031
4	23.08 % Dibromo-ethane	1.559	31.14	1.123
5	28.47 % Dibromo-ethane	1.566	31.56	1.213
6	37.50 % Dibromo-ethane	1.574	31.99	1.315
7	44.44 % Dibromo-ethane	1.581	32.42	1.430
8	50.00 % Dibromo-ethane	1.588	32.84	1.503
9	54.00 % Dibromo-ethane	1.597	33.27	1.634
10	60.00 % Dibromo-ethane	1.603	33.70	1.830
	Pure Dibromo-ethene	1.727	42.05	2.180

TABLE (4)

ATOMIZING AIR TEMPERATURES OBTAINED FROM 6 HEATERS

Air Velocity (m/sec) / No. of Heaters switched on	60	70	80	90	100	110	125
1 heater, t_1 °C	58	56	53	50	49	47	44
2 heater, t_2 °C	76	73	70	69	67	63	61
3 heater, t_3 °C	97	91	89	86	81	79	76
4 heater, t_4 °C	116	110	106	104	102	96	89
5 heater, t_5 °C	134	127	123	122	120	113	106
6 heater, t_6 °C	151	146	141	136	132	128	121

TABLE (5)

Mean values of air mass flow rates at equal velocities for both shroud and pintle air streams:

Mass Flow Rate / Air Velocity	$W_{a(shroud)}$ (gm/sec)	$W_{a(pintle)}$ (gm/sec)	$W_{a(total)}$ (gm/sec)
180 ft/sec = 54.86 m/sec	14.5149	8.1193	22.6342
200 ft/sec = 60.96 m/sec	15.6036	8.9811	24.5847
220 ft/sec = 67.06 m/sec	17.1911	9.9790	27.1701
240 ft/sec = 73.15 m/sec	18.3705	10.8408	29.2113
260 ft/sec = 79.25 m/sec	20.0034	11.7027	31.7061
280 ft/sec = 85.34 m/sec	21.4549	12.6099	34.0648
300 ft/sec = 91.44 m/sec	22.9518	13.7438	36.6956
320 ft/sec = 97.54 m/sec	24.4032	14.6510	39.0542
340 ft/sec = 103.63 m/sec	25.7187	15.4675	41.1862
360 ft/sec = 109.73 m/sec	27.3970	16.5107	43.9077
380 ft/sec = 115.82 m/sec	28.8031	17.2819	46.0850
400 ft/sec = 121.92 m/sec	30.3907	17.9622	48.3529

TABLE (6)

VALUES OF AIR FLOW RATE ; A.F.R. and f.a.r.

V_a (m/sec)	$W_{a(total)}$ (gm/sec)	Liquid Flow Rate W_ℓ , (gm/sec)						
		5	10	15	20	25	30	
60	24.3125	4.86	2.43	1.62	1.22	0.97	0.81	A.F.R.
		0.2057	0.4133	0.6170	0.8226	1.0283	1.2339	f.a.r.
70	28.0319	5.61	2.80	1.87	1.40	1.12	0.93	A.F.R.
		0.1784	0.3567	0.5351	0.7135	0.8918	1.0702	f.a.r.
80	32.4318	6.49	3.24	2.16	1.62	1.30	1.08	A.F.R.
		0.1542	0.3083	0.4625	0.6167	0.7708	0.9250	f.a.r.
90	36.4234	7.28	3.64	2.43	1.82	1.46	1.21	A.F.R.
		0.1373	0.2745	0.4118	0.5491	0.6864	0.8236	f.a.r.
100	40.0974	8.02	4.01	2.67	2.00	1.60	1.34	A.F.R.
		0.1247	0.2494	0.3741	0.4988	0.6235	0.7482	f.a.r.
110	44.4066	8.88	4.44	2.96	2.22	1.78	1.48	A.F.R.
		0.1126	0.2252	0.3378	0.4504	0.5630	0.6757	f.a.r.
125	49.0785	9.82	4.91	3.27	2.45	1.96	1.64	A.F.R.
		0.1019	0.2038	0.3056	0.4075	0.5094	0.6113	f.a.r.

TABLE (7)

VALUES OF HIGH PRESSURE AIR FLOW RATE, A.F.R. and f.a.r.

P_a (atm)	W_a (gm/sec)	Liquid Flow Rate W_ℓ (gm/sec)						
		5	10	15	20	25	30	
1.30	353.35	70.67	35.34	23.67	17.67	14.14	11.78	A.F.R.
		0.0142	0.0283	0.0424	0.0566	0.0707	0.0849	f.a.r.
1.70	462.07	92.41	46.21	30.80	23.10	18.48	15.40	A.F.R.
		0.0108	0.0216	0.0326	0.0433	0.0541	0.0649	f.a.r.
2.38	809.48	161.90	80.95	53.97	40.47	32.38	26.98	A.F.R.
		0.0062	0.0124	0.0185	0.0247	0.0309	0.0371	f.a.r.
3.40	1230.68	246.14	123.07	82.05	61.53	49.23	41.02	A.F.R.
		0.0041	0.0081	0.0122	0.0163	0.0203	0.0244	f.a.r.
4.42	1585.07	317.01	158.51	105.67	79.25	63.40	52.84	A.F.R.
		0.0032	0.0063	0.0095	0.0126	0.0158	0.0189	f.a.r.
5.44	1917.01	383.40	191.70	127.80	95.85	76.68	63.90	A.F.R.
		0.0026	0.0052	0.0078	0.0104	0.0130	0.0156	f.a.r.
6.80	2304.42	460.88	230.44	153.63	115.22	92.18	76.81	A.F.R.
		0.0022	0.0043	0.0065	0.0087	0.0108	0.0130	f.a.r.
8.51	2737.91	547.58	273.79	182.53	136.90	109.52	91.26	A.F.R.
		0.0018	0.0037	0.0055	0.0073	0.0091	0.0110	f.a.r.

TABLE (8)

Values of total atomizing air/liquid mass ratio at equal velocities for both shroud and pintle air streams:

Air Velocity (m/sec) / W_ℓ lb/sec	W_ℓ gm/sec	54.86	60.96	67.06	73.15	79.25	85.34	91.44	97.54	103.63	109.73	115.82	121.92
0.0100	4.5	5.03	5.56	6.13	6.61	7.13	7.70	8.22	8.76	9.25	9.80	10.30	10.80
0.0125	5.7	4.07	4.49	4.92	5.31	5.72	6.18	6.60	7.02	7.46	7.92	8.33	8.76
0.0150	6.8	3.32	3.66	4.05	4.39	4.73	5.08	5.43	5.79	6.09	6.44	6.74	7.09
0.0175	7.9	2.85	3.12	3.44	3.76	4.05	4.34	4.63	4.93	5.19	5.50	5.75	6.07
0.0200	9.1	2.51	2.78	3.07	3.30	3.58	3.86	4.14	4.41	4.64	4.91	5.16	5.42
0.0225	10.2	2.24	2.48	2.73	2.94	3.21	3.44	3.70	3.95	4.16	4.41	4.65	4.91
0.0250	11.3	2.00	2.20	2.43	2.61	2.83	3.04	3.26	3.47	3.65	3.88	4.06	4.26
0.0275	12.5	1.81	1.95	2.17	2.36	2.56	2.74	2.95	3.14	3.32	3.54	3.71	3.88
0.0300	13.6	1.66	1.82	2.02	2.18	2.39	2.54	2.72	2.90	3.05	3.24	3.40	3.56
0.0325	14.7	1.56	1.68	1.85	1.98	2.13	2.30	2.46	2.62	2.78	2.94	3.10	3.26
0.0350	15.9	1.43	1.57	1.73	1.86	2.01	2.16	2.32	2.47	2.60	2.76	2.89	3.04
0.0375	17.0	1.33	1.44	1.59	1.70	1.82	1.97	2.09	2.23	2.35	2.49	2.63	2.77
0.0400	18.1	1.25	1.37	1.51	1.63	1.74	1.89	2.00	2.14	2.26	2.39	2.51	2.63
0.0425	19.3	1.15	1.25	1.36	1.48	1.60	1.72	1.84	1.97	2.06	2.20	2.32	2.43
0.0450	20.4	1.10	1.21	1.33	1.44	1.54	1.66	1.78	1.90	2.00	2.12	2.23	2.33
0.0475	21.6	1.01	1.09	1.22	1.31	1.41	1.52	1.64	1.75	1.84	1.96	2.06	2.15
0.0500	22.7	0.98	1.07	1.19	1.29	1.38	1.49	1.60	1.71	1.80	1.90	2.00	2.09

TABLE (9)

DROPLET LIFETIME 't' , AND THE DISTANCE THE DROPLETS MOVED DURING LIFETIME 'X'

LIQUID - KEROSINE, AIR PRESSURE = 1 atm., AIR TEMERATURE = 20°C

V_a (m/sec) / W_ℓ (gm/sec)	54.86	60.96	67.06	73.15	79.25	85.34	91.44	97.54	103.63	109.73	115.82	121.92	
	52.5	49	45	42	40	36	34	31	29	27	25.5	24	d(microns)
4.5	1.2840	1.1010	0.9258	0.7997	0.7151	0.5872	0.5210	0.4383	0.3847	0.3353	0.2998	0.2667	t (sec)
	70.06	66.76	61.75	58.20	56.38	49.85	47.39	42.52	39.66	36.60	34.54	32.34	X (m)
	59	53.5	50	45.5	42.5	39	36	34	31.5	29.5	28	26	d(microns)
9.1	1.5431	1.2629	1.0910	0.9066	0.7865	0.6657	0.5698	0.5074	0.4381	0.3855	0.3471	0.3025	t (sec)
	84.24	76.60	72,80	65.99	62.02	56.53	51.84	49.25	45.17	42.09	40.00	36.69	X (m)
	65	60.5	56	51	47	44.5	41	38	35	33	32	31	d(microns)
13.6	1.7974	1.5331	1.3049	1.0858	0.9227	0.8190	0.6998	0.6038	0.5168	0.4602	0.4280	0.3983	t (sec)
	98.15	93.03	87.10	79.07	72.79	69.58	63.70	58.62	53.51	50.26	49.35	48.34	X (m)
	76.5	71	66	60	55	51	46.5	43	40.5	39	37.5	36.5	d(microns)
18.1	2.3195	1.9702	1.6860	1.6059	1.1792	1.0145	0.8517	0.7325	0.6494	0.5975	0.5490	0.5146	t (sec)
	126.72	119.61	112.60	117.05	93.07	86.23	77.55	71.14	67.02	65.29	63.33	62.49	X (m)
	96.5	85	76.5	68.5	62	55	51	47	44	42	41	40.5	d(microns)
22.7	3.3342	2.6090	2.1244	1.7206	1.4219	1.1418	0.9837	0.8421	0.7395	0.6708	0.6307	0.6056	t (sec)
	182.27	158.46	142.98	125.40	112.26	97.07	89.60	81.81	76.33	73.31	72.77	73.56	X (m)

TABLE (10)

DROPLET LIFETIME 't', AND THE DISTANCE THE DROPLETS MOVED DURING LIFETIME 'X' AT HIGHER AIR TEMPERATURES

KEROSINE FLOW RATE = 15 gm/sec, AIR PRESSURE = 1 atm.

Air Vel. (m/sec) / Air Temp.	60	70	80	90	100	110	125	
40 °C	65.5	60	53	44	41	37	35	d (microns)
	0.1791	0.1460	0.1134	0.0805	0.0689	0.0563	0.0488	t (sec)
	10.39	9.89	8.78	7.00	6.67	5.99	5.91	X (m)
60 °C	70	64	56	49	44	40	37	d (microns)
	0.0828	0.0673	0.0515	0.0397	0.0321	0.0265	0.0222	t (sec)
	4.64	4.41	3.85	3.34	3.00	2.73	2.60	X (m)
80 °C	74	68	59	52	46.5	42	39	d (microns)
	0.0378	0.0310	0.0234	0.0183	0.0146	0.0120	0.0101	t (sec)
	1.97	1.90	1.64	1.44	1.27	1.15	1.11	X (m)
100 °C	78	72	63	55	49	45	41	d (microns)
	0.0208	0.0172	0.0132	0.0101	0.0081	0.0068	0.0055	t (sec)
	0.99	0.96	0.84	0.72	0.64	0.60	0.55	X (m)
120 °C	82.5	76	66	58	51.5	47	43.5	d (Microns)
	0.0115	0.0095	0.0072	0.0056	0.0044	0.0037	0.0031	t (sec)
	0.47	0.46	0.40	0.35	0.30	0.28	0.27	X (m)
150 °C	88.5	82	71	62	55	51	46.5	d (microns)
	0.0056	0.0047	0.0035	0.0027	0.0021	0.0018	0.0015	t (sec)
	0.17	0.17	0.14	0.12	0.11	0.10	0.10	X (m)

FIGURES

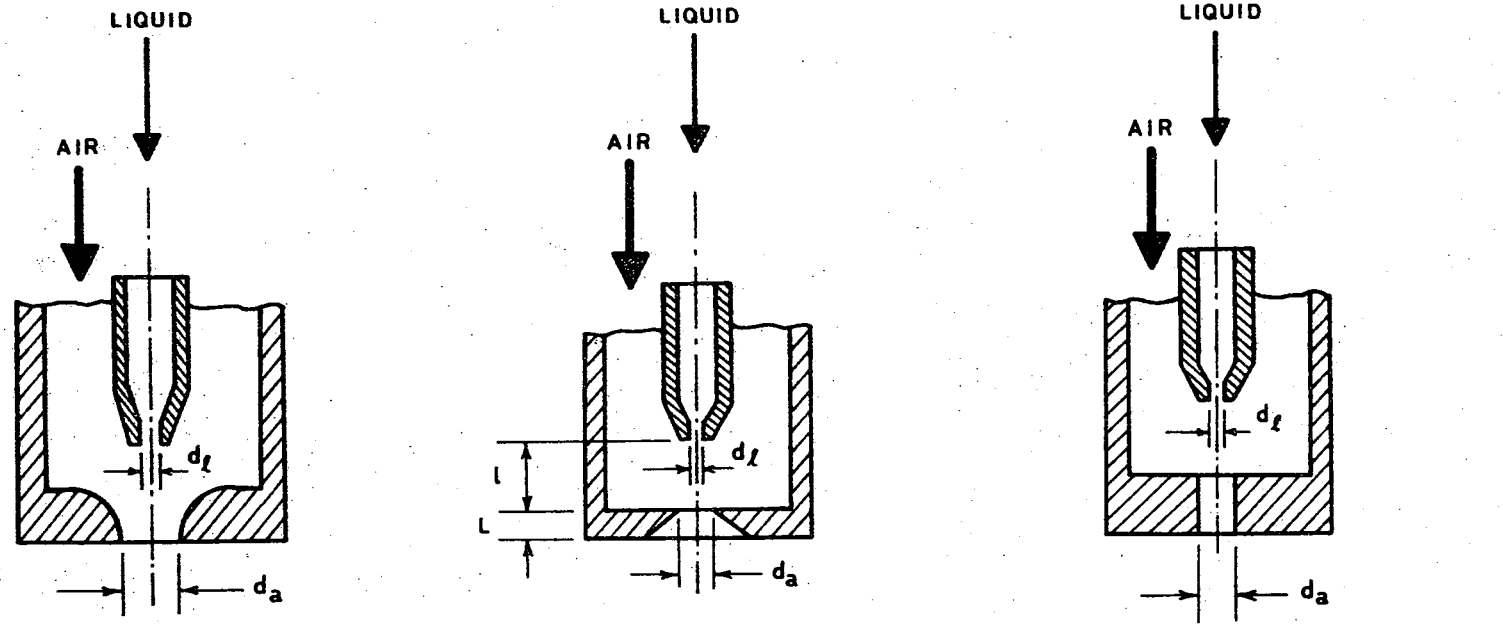

(a) Convergent Air Nozzle (b) 120° Sharp-Edged Orifice (c) Cylindrical Air Nozzle

FIG. 1 NUKIYAMA AND TANASAWA ATOMIZERS

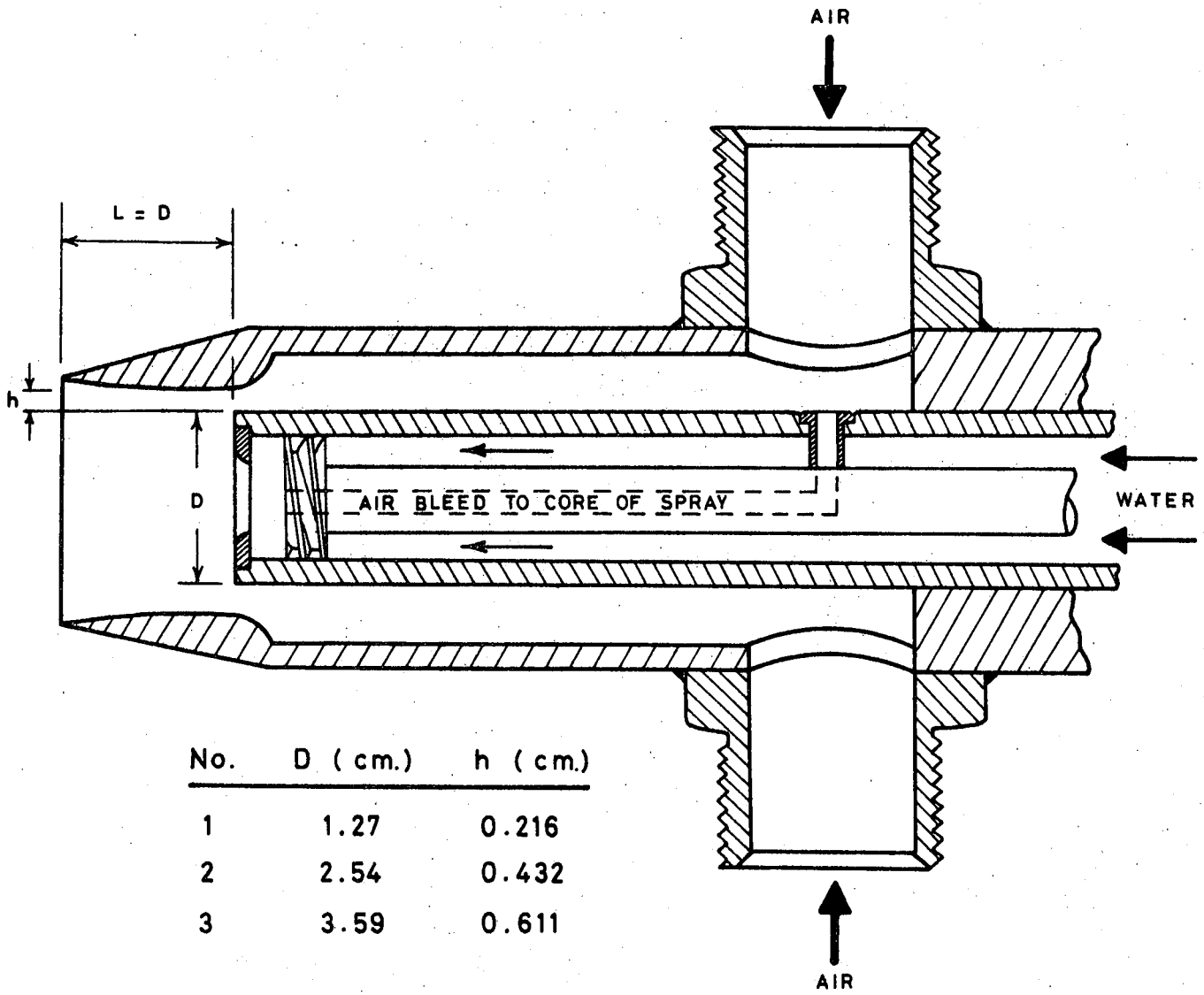

No.	D (cm.)	h (cm.)
1	1.27	0.216
2	2.54	0.432
3	3.59	0.611

FIG. 2 N.G.T.E. AIRBLAST ATOMIZER

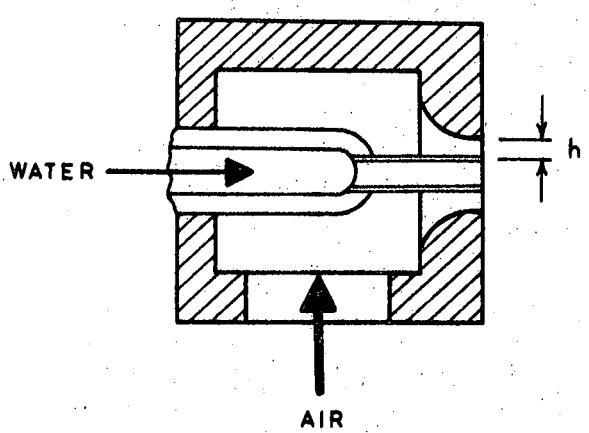

No.	h (cm.)
1	0.061
2	0.099
3	0.144

FIG. 3 N.R.L. CANADA CONVERGENT NOZZLES

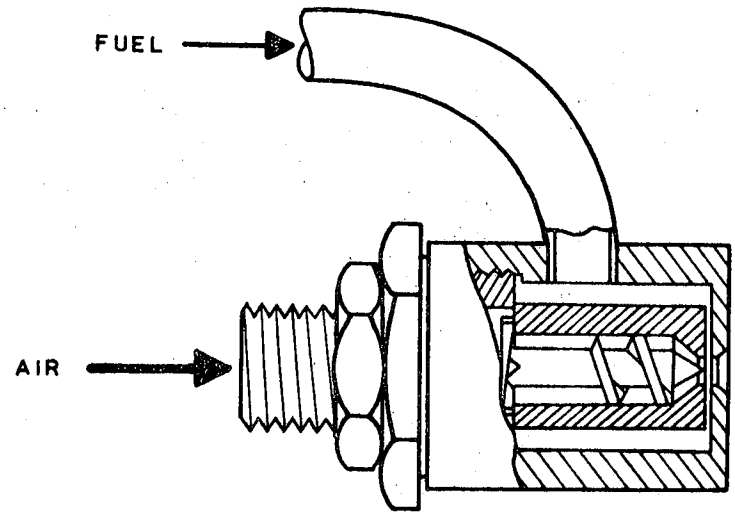

(a) 1/8 - Inch Orifice

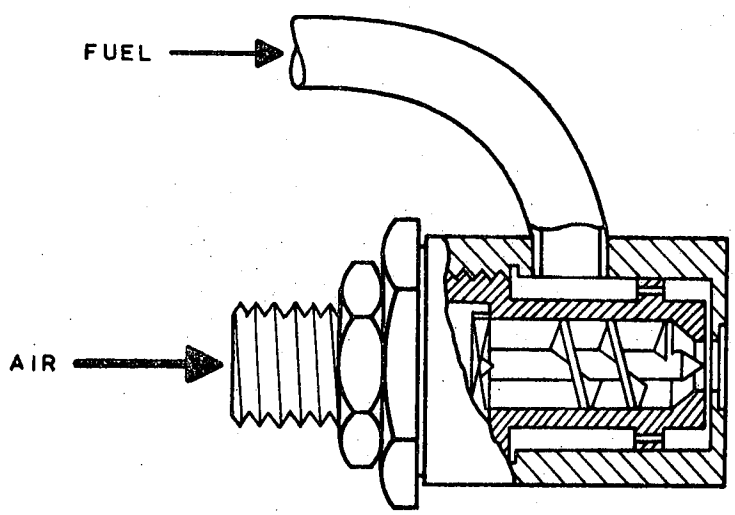

(b) 1/4 - Inch Orifice

FIG. 4 EARLY N.G.T.E. HIGH PRESSURE AIR ATOMIZERS

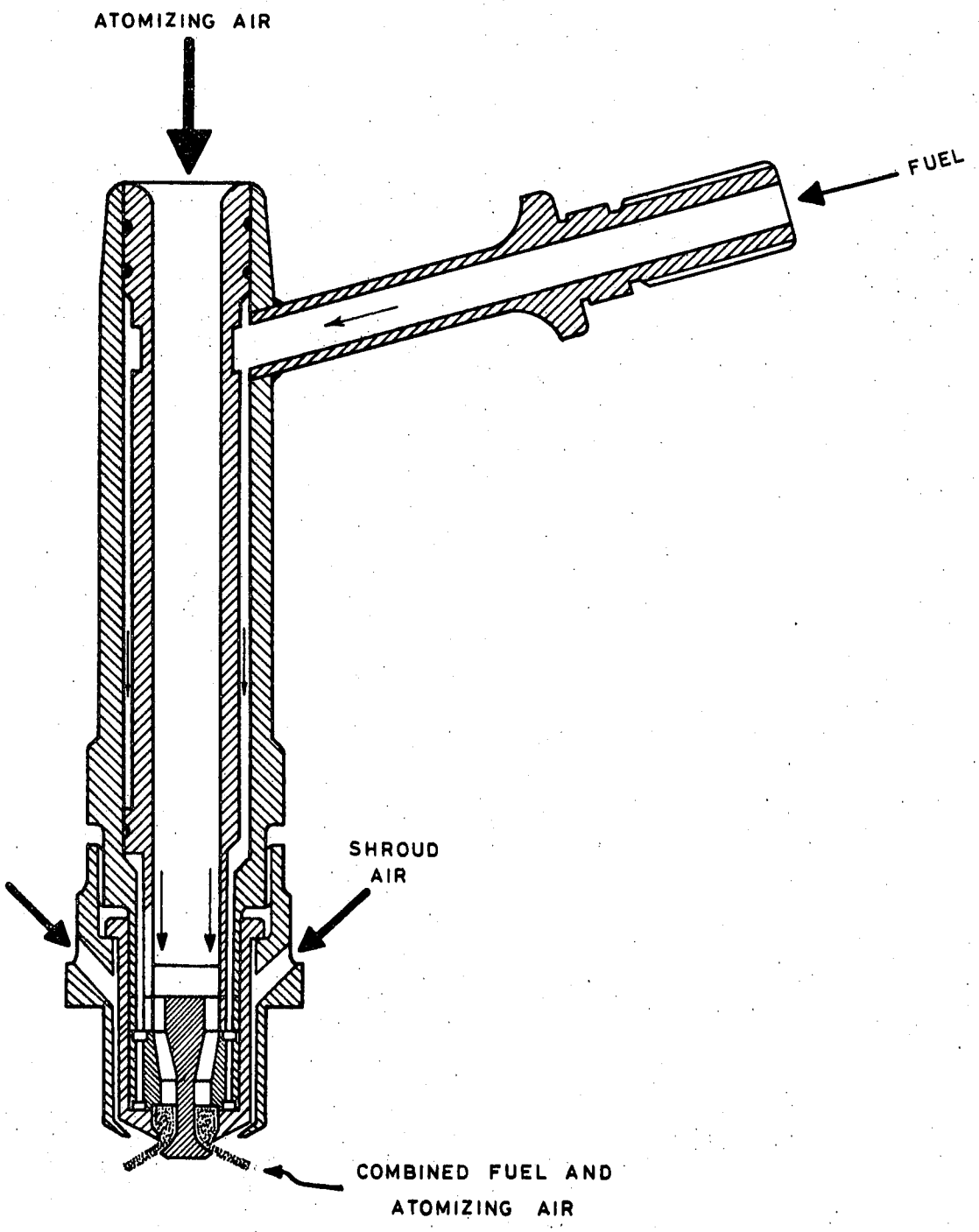

FIG. 5 ROLLS-ROYCE "DART" AIRSPRAY ATOMIZER

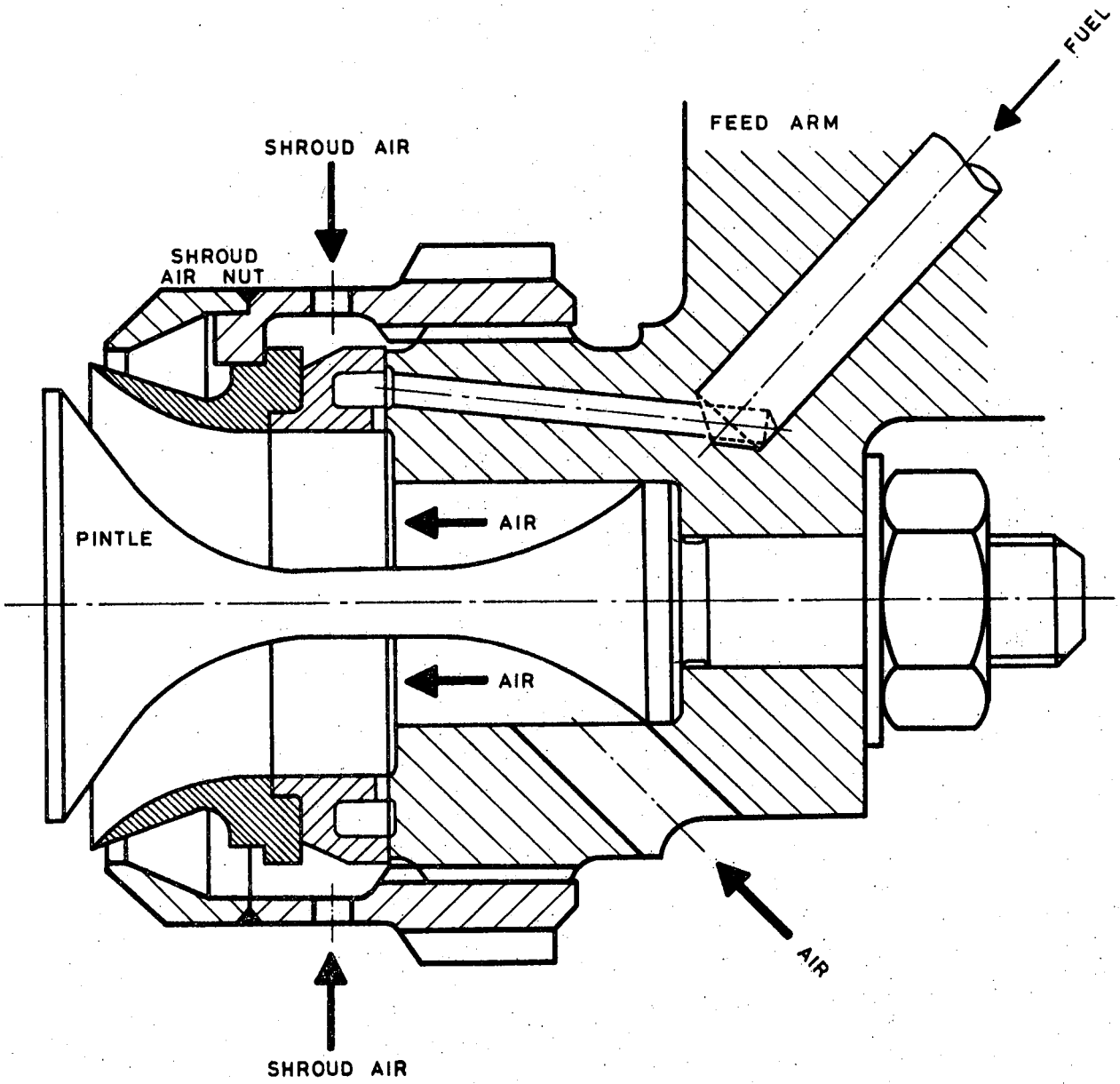

FIG. 6 ATOMIZER NO. 3 [Ref. 8]

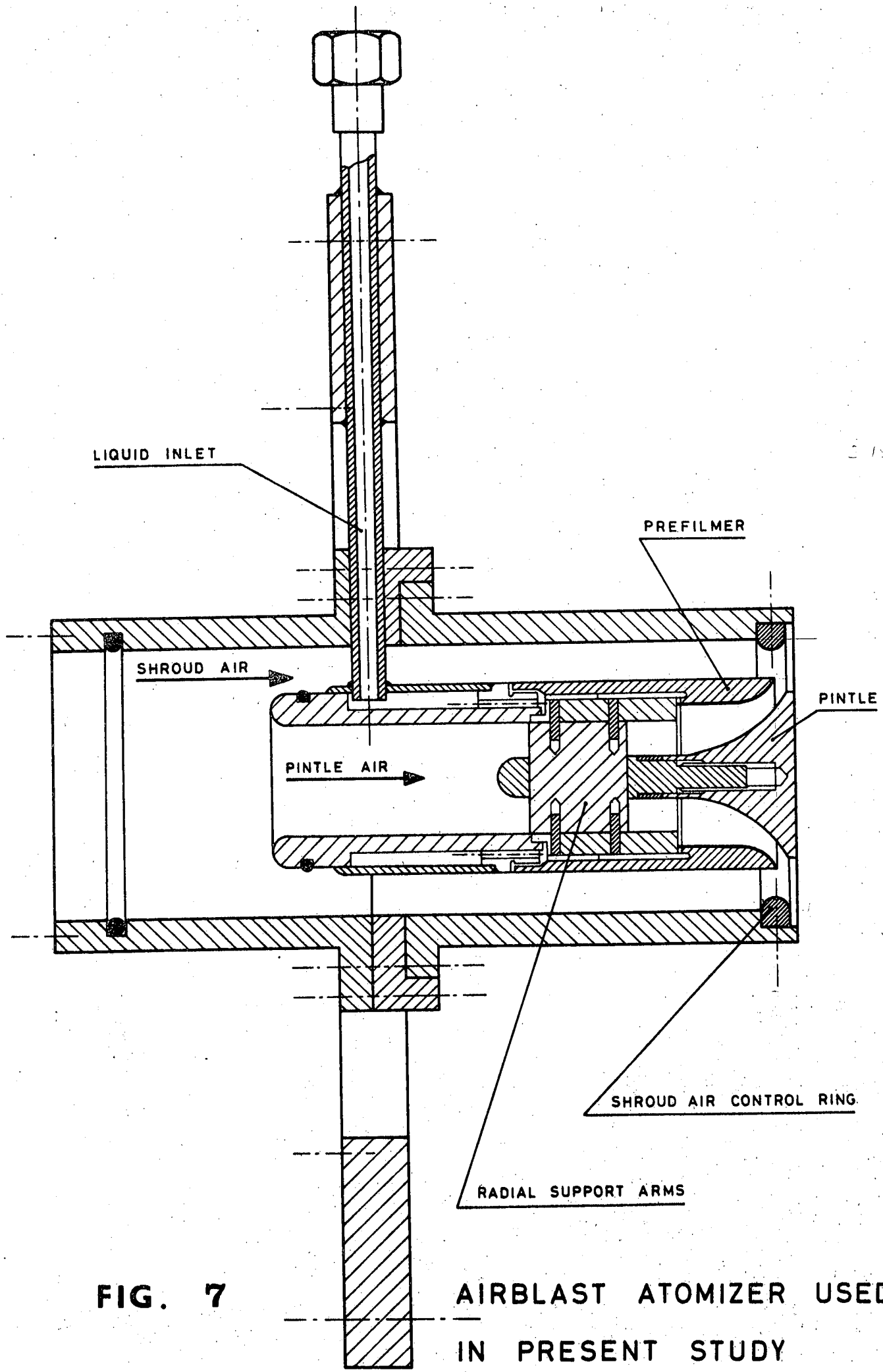

FIG. 7 AIRBLAST ATOMIZER USED IN PRESENT STUDY

(DIMENSIONS IN INCHES)

FIG. 8

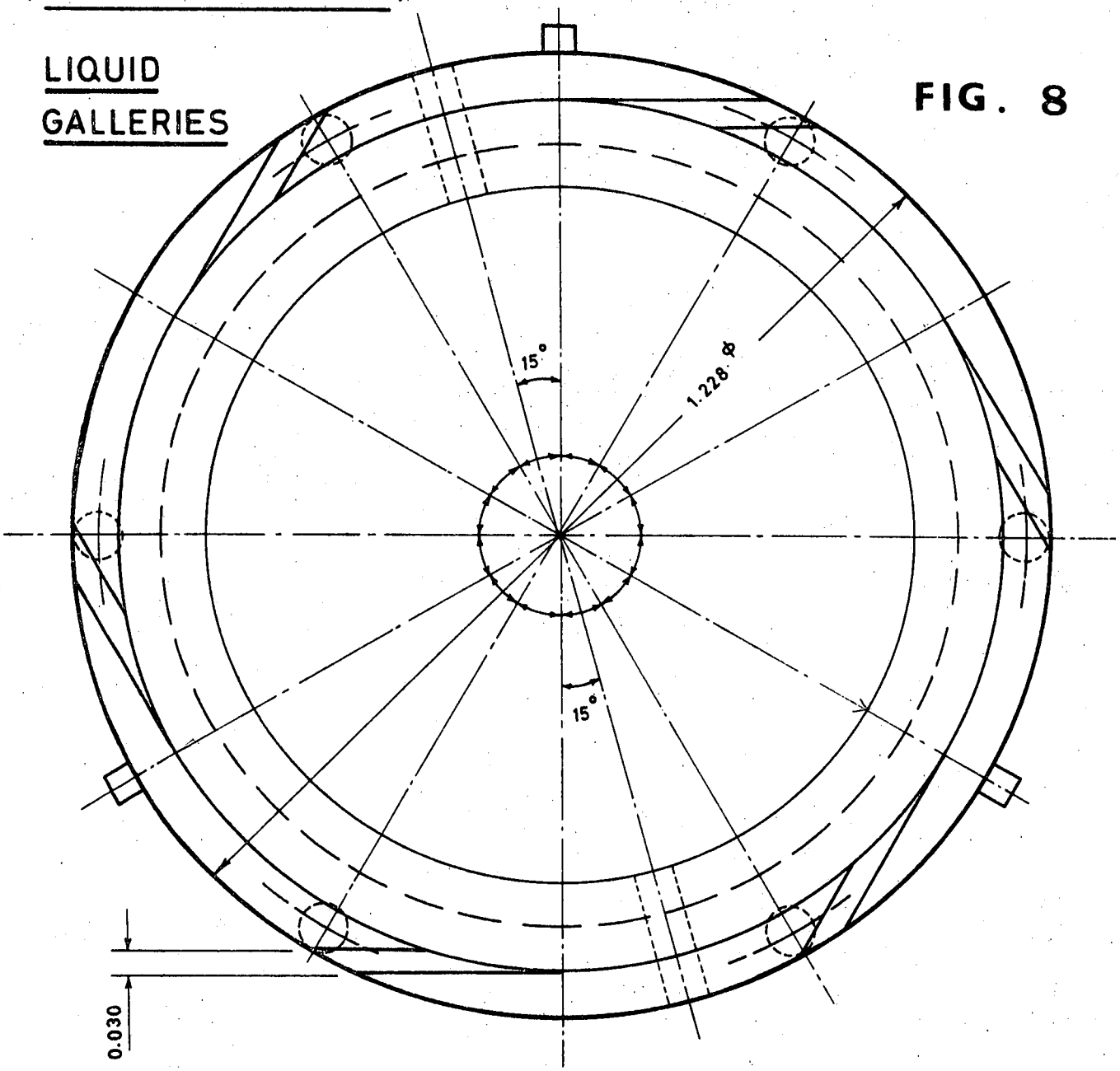

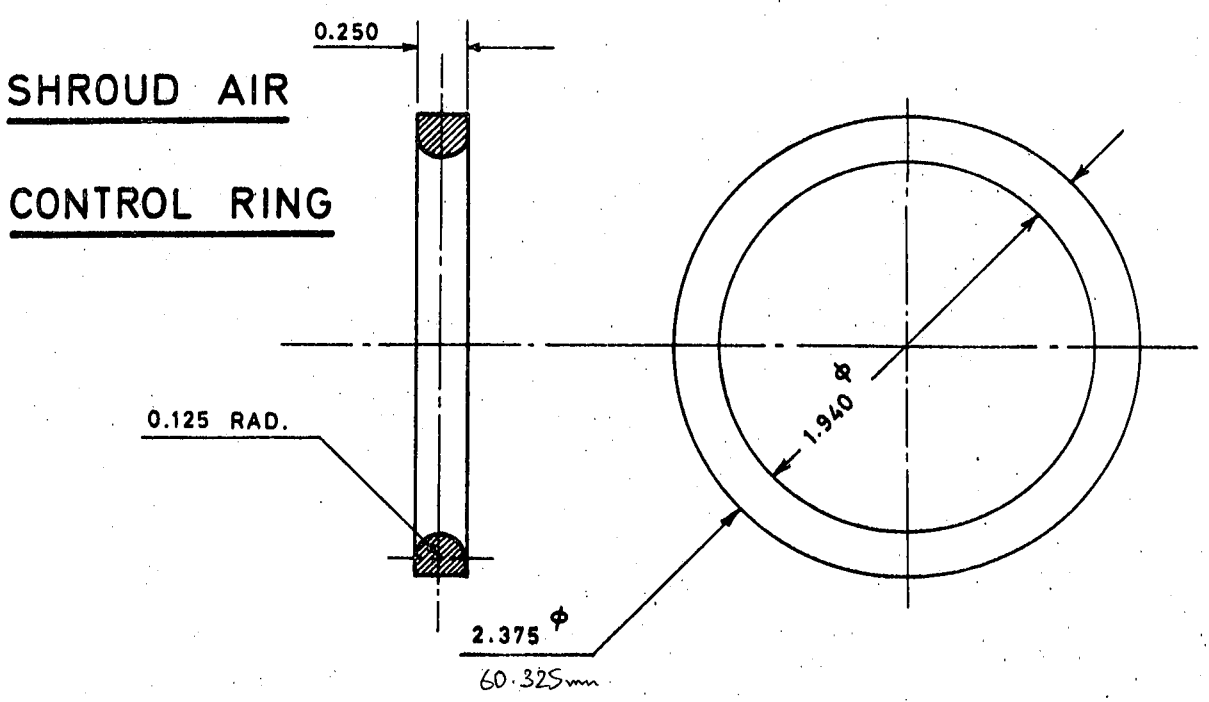

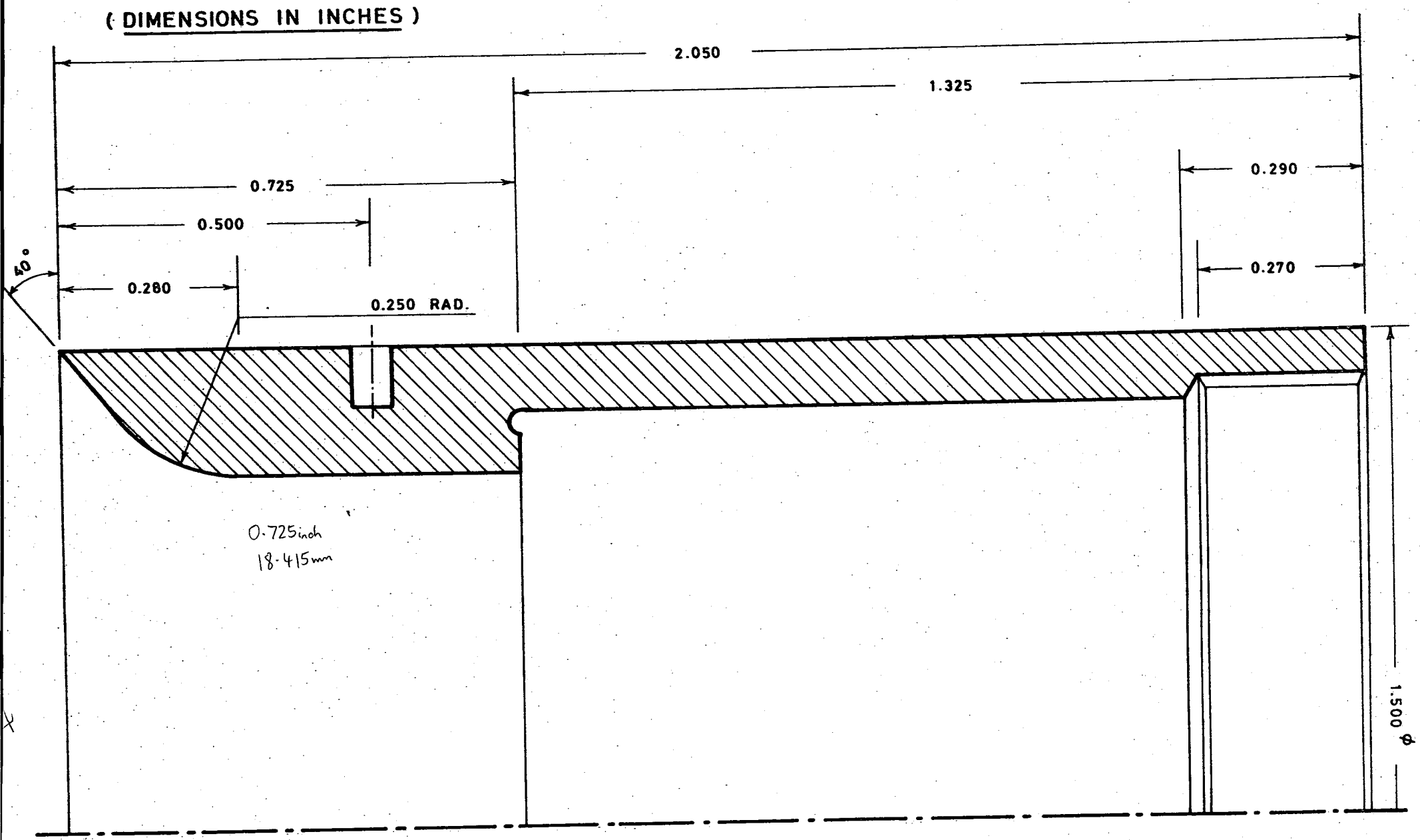

FIG. 9 PREFILMER

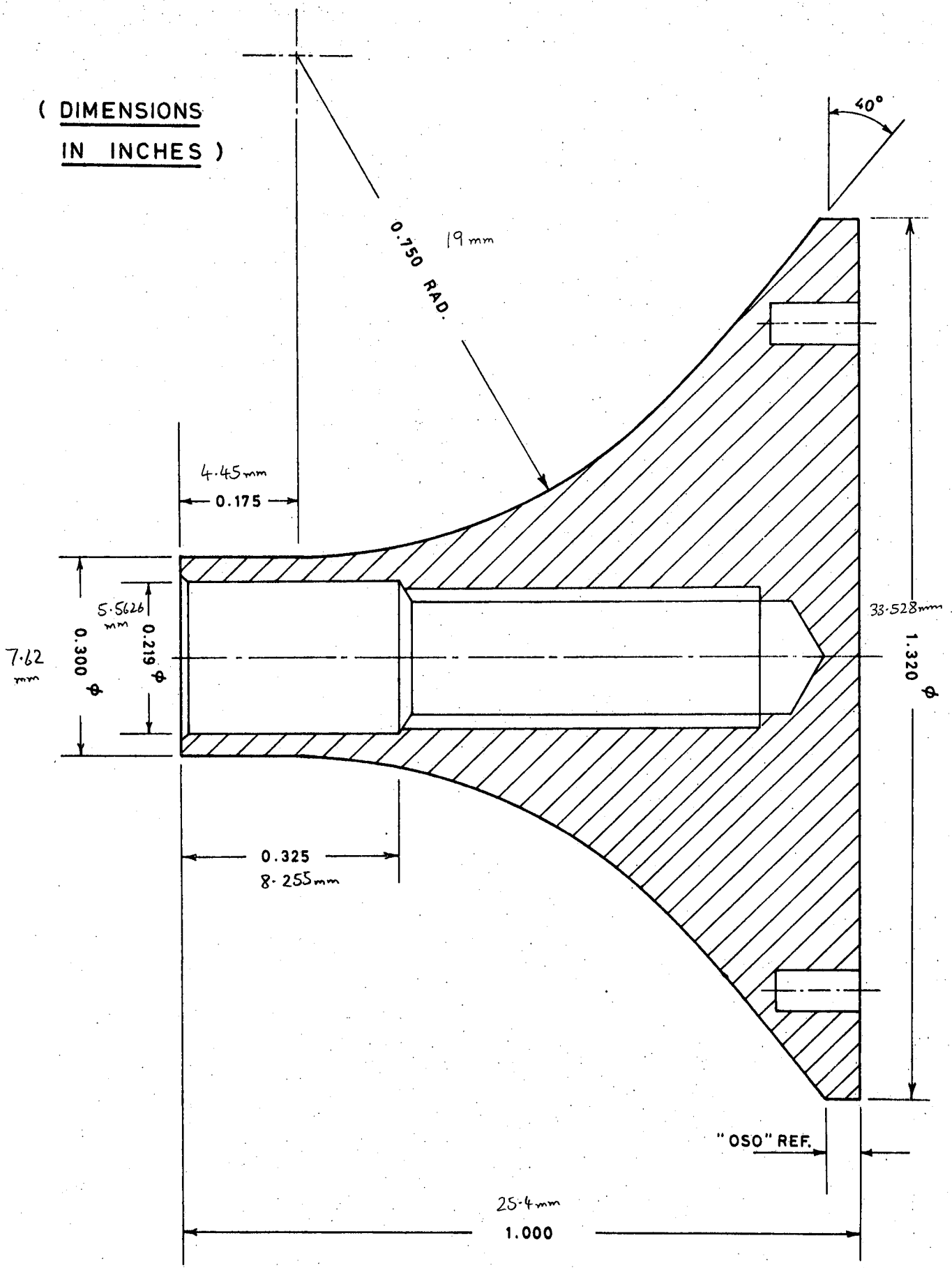

FIG. 10 PINTLE

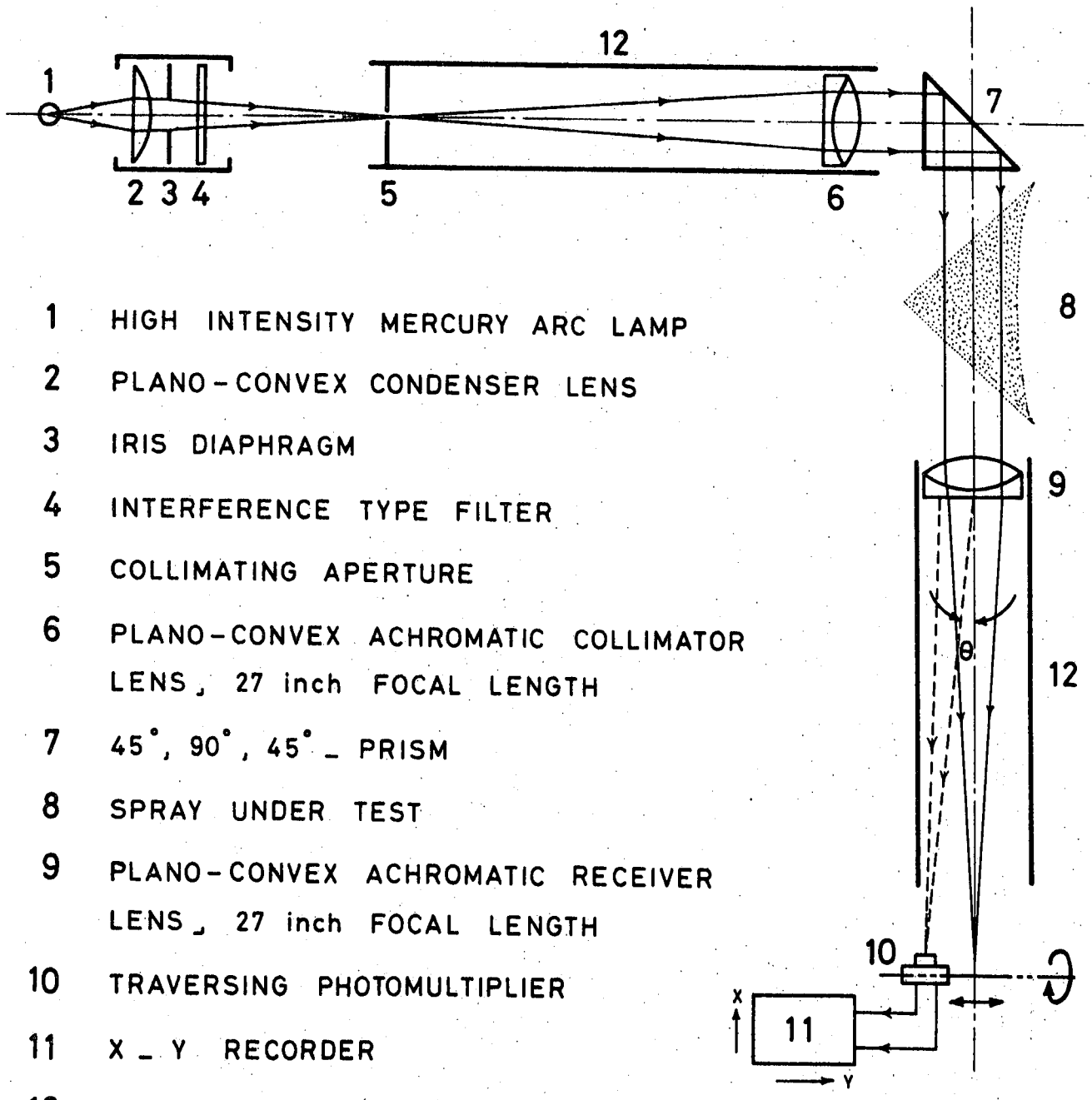

1 HIGH INTENSITY MERCURY ARC LAMP

2 PLANO-CONVEX CONDENSER LENS

3 IRIS DIAPHRAGM

4 INTERFERENCE TYPE FILTER

5 COLLIMATING APERTURE

6 PLANO-CONVEX ACHROMATIC COLLIMATOR LENS, 27 inch FOCAL LENGTH

7 45°, 90°, 45° PRISM

8 SPRAY UNDER TEST

9 PLANO-CONVEX ACHROMATIC RECEIVER LENS, 27 inch FOCAL LENGTH

10 TRAVERSING PHOTOMULTIPLIER

11 X-Y RECORDER

12 STRAY LIGHT SHIELD

FIG. 11 THE OPTICAL BENCH IN DIAGRAMMATIC FORM

SCALE :- FULL SIZE

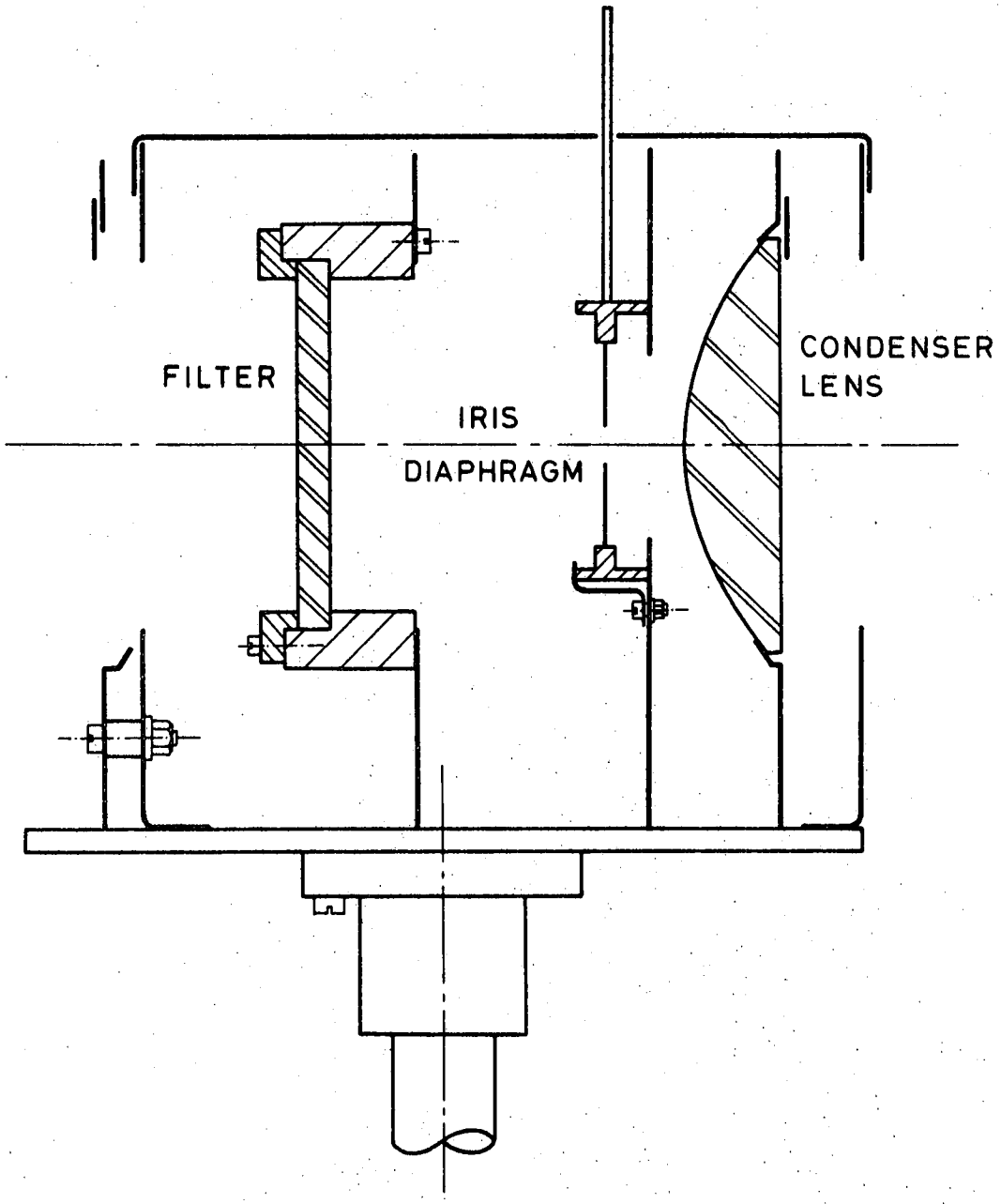

FIG. 12 CONDENSER BOX

SCALE :- FULL SIZE

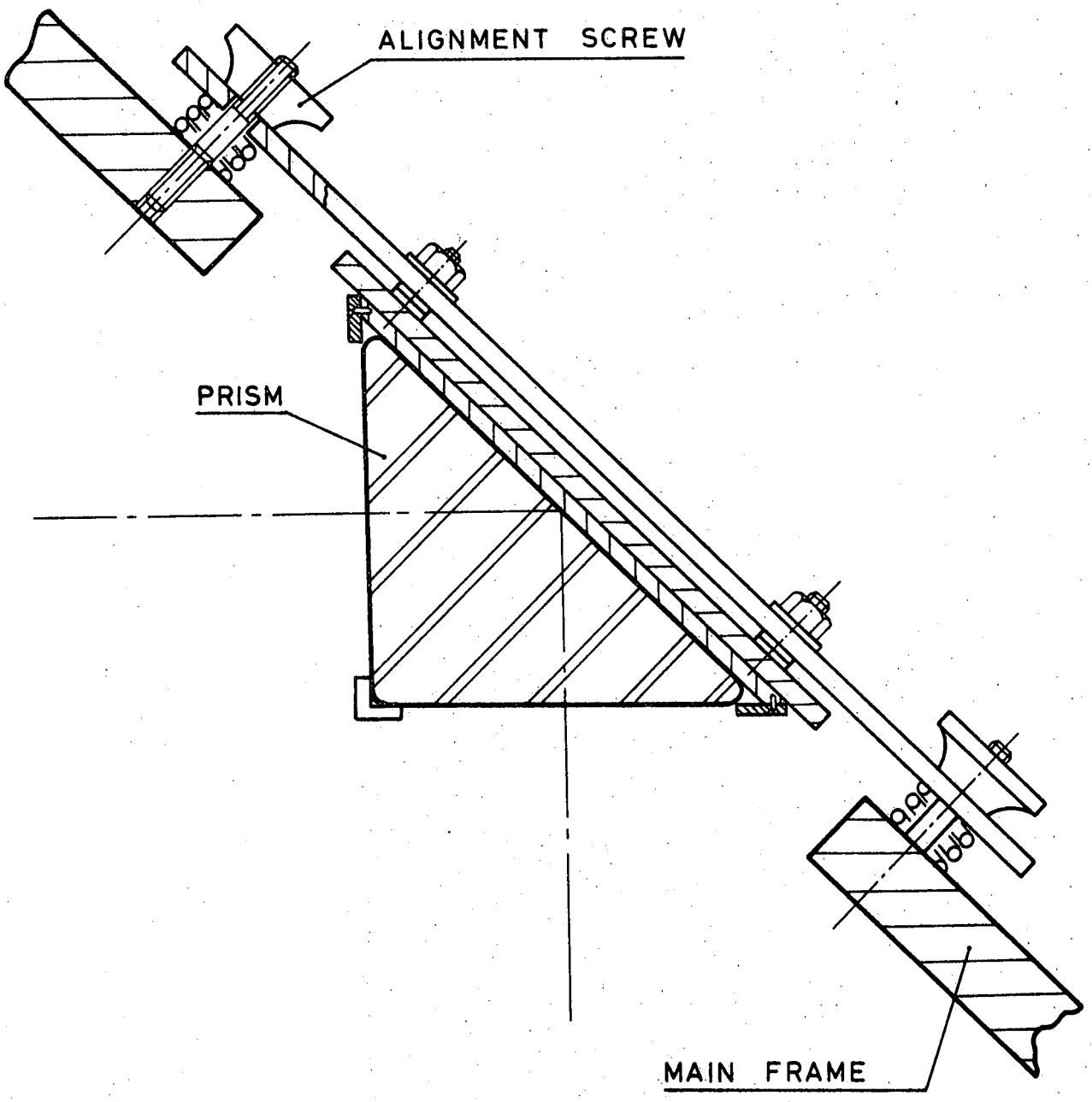

FIG. 13 PRISM AND MOUNT

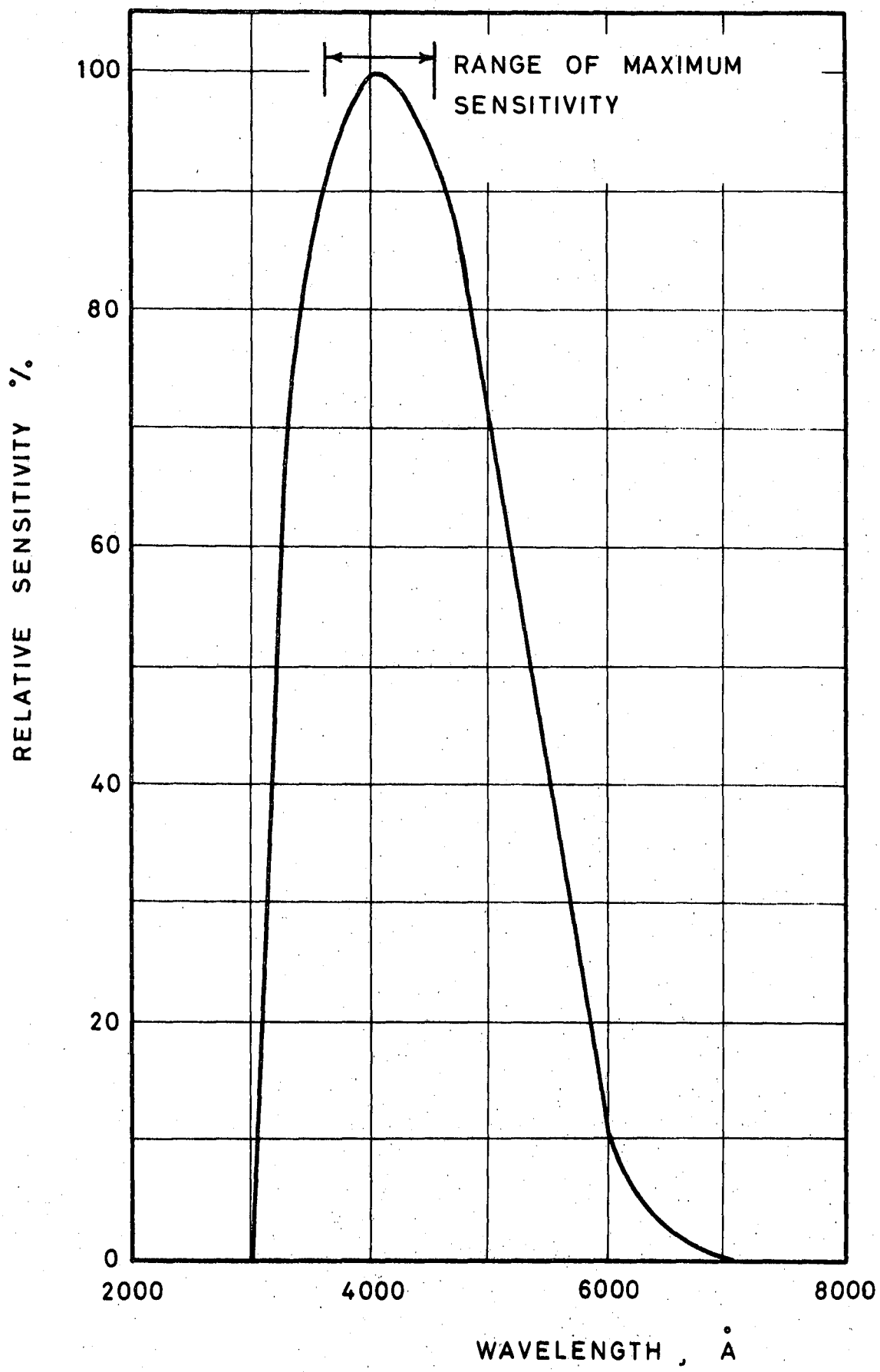

FIG. 14 SPECTRAL SENSITIVITY OF THE 1 P 21 _ PHOTOMULTIPLIER

FIG. 15

Typical X-Y recorder plots
Kerosine Test
Air Velocity : 220 Ft/sec.
Test No.
Wℓ : 0.050 lb/sec
258
Wℓ : 0.045 lb/sec
257
Wℓ : 0.040 lb/sec
256
Wℓ : 0.035 lb/sec
255
V
1 V
μV
100
μV
10
μV
1
300
200
100
0
LIGHT BEAM POSITION (TRAVERSE DISTANCE , Inches x 10^-3)

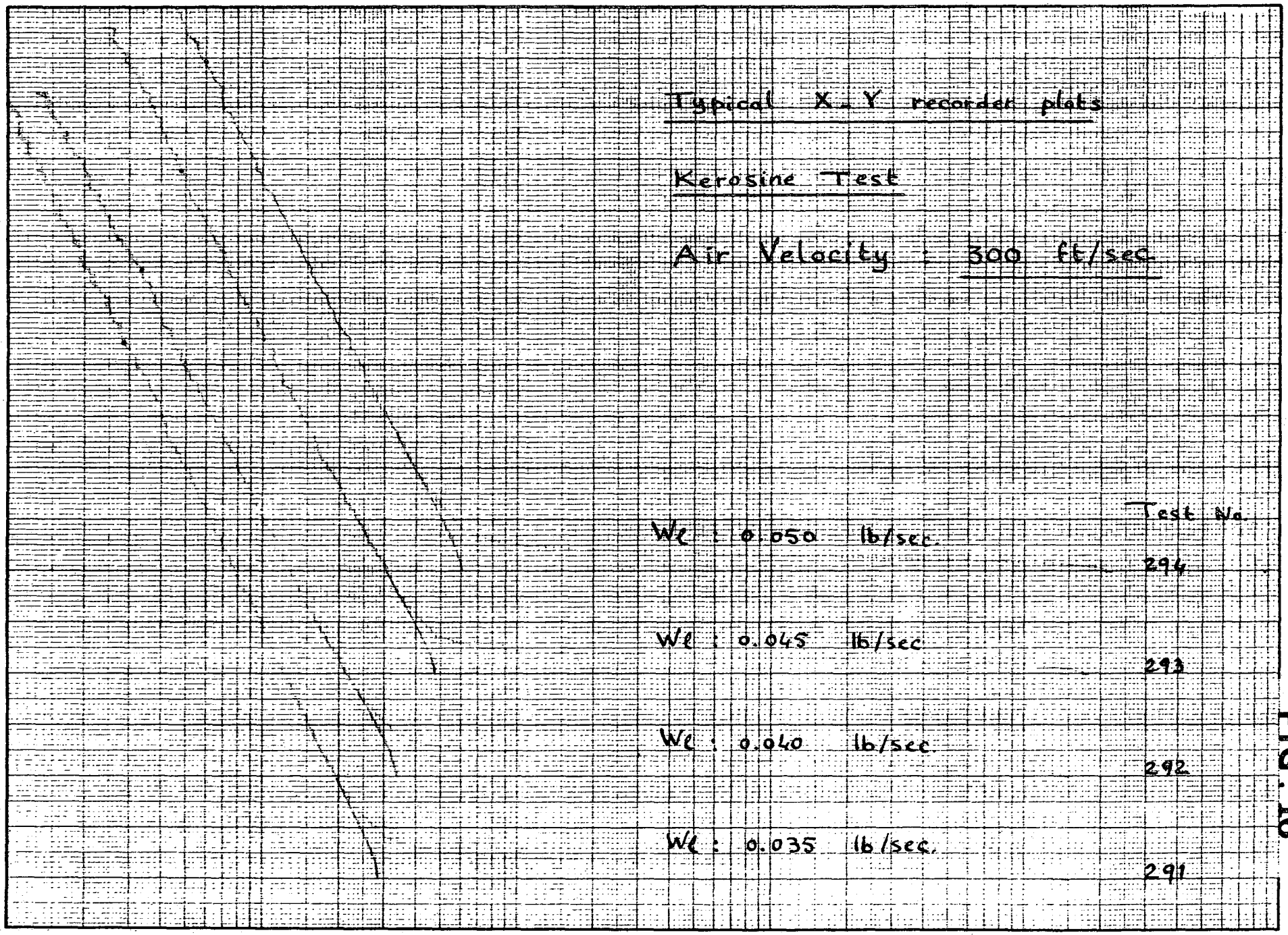
Typical X-Y recorder plots
Kerosine Test
Air Velocity : 300 ft/sec
Test No.
We : 0.050 lb/sec. 294
We : 0.045 lb/sec 293
We : 0.040 lb/sec 292
We : 0.035 lb/sec. 291

FIG. 16

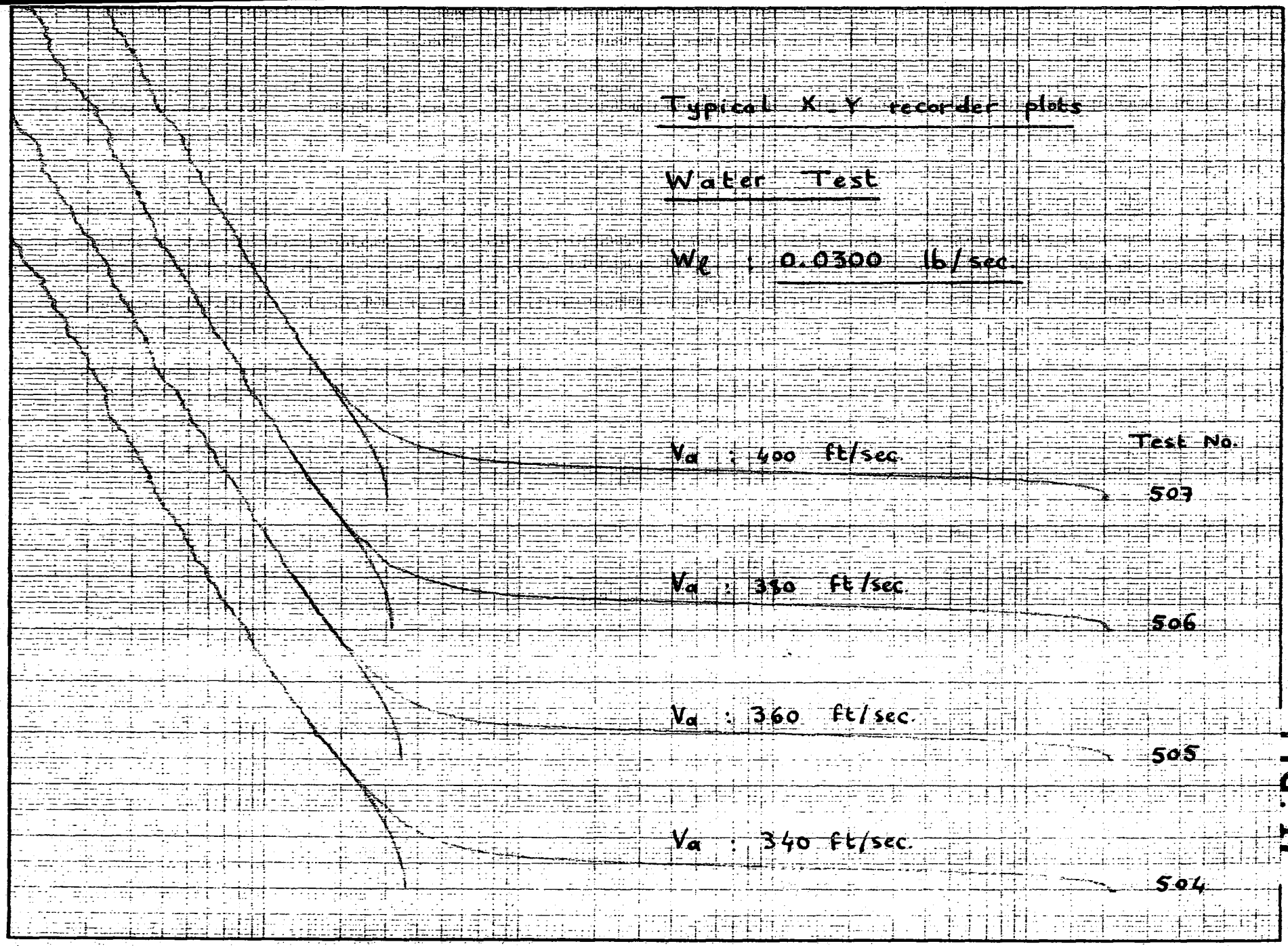
Typical X-Y recorder plots
Water Test
W_ℓ : 0.0300 lb/sec.
V_a : 400 ft/sec.
Test No.
507
V_a : 380 ft/sec.
506
V_a : 360 ft/sec.
505
V_a : 340 ft/sec.
504

FIG. 17

17 APR 1973

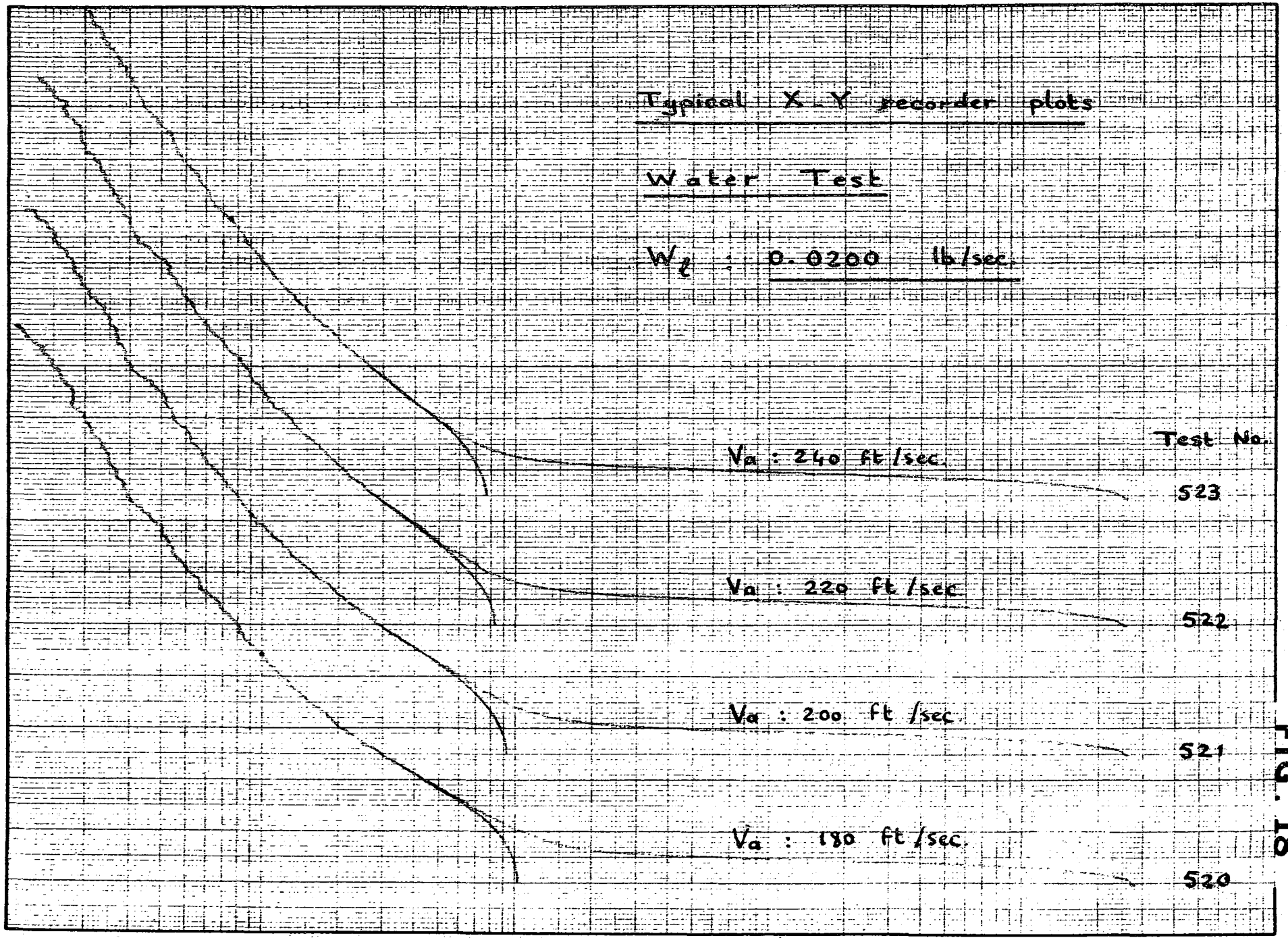

FIG. 18

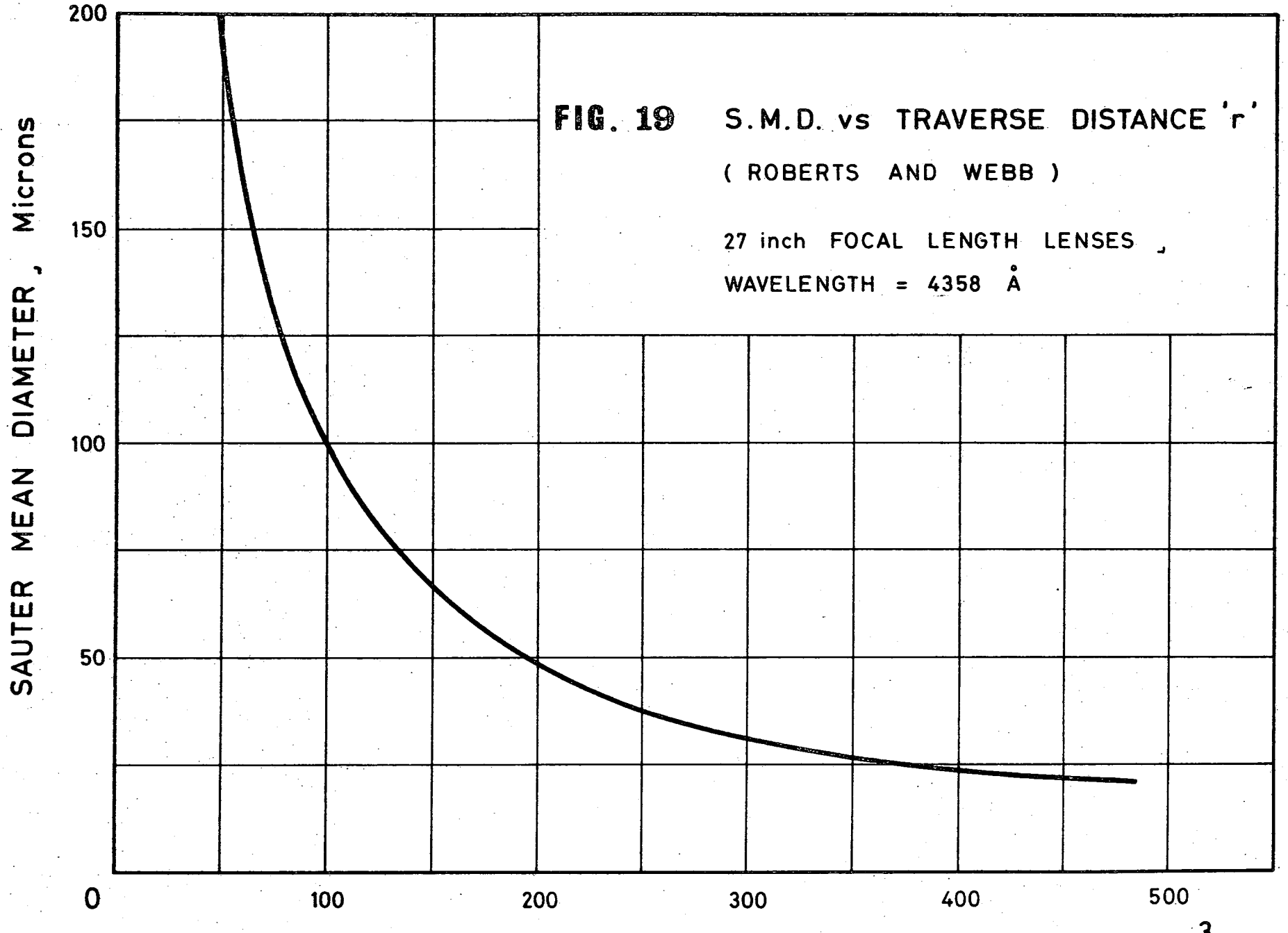
FIG. 19 S.M.D. vs TRAVERSE DISTANCE 'r'
(ROBERTS AND WEBB)
27 inch FOCAL LENGTH LENSES ,
WAVELENGTH = 4358 Å
SAUTER MEAN DIAMETER, Microns
200
150
100
50
0
100
200
300
400
500
TRAVERSE DISTANCE AT 1/10 I(θ) , r , inch x 10^-3

8473.4

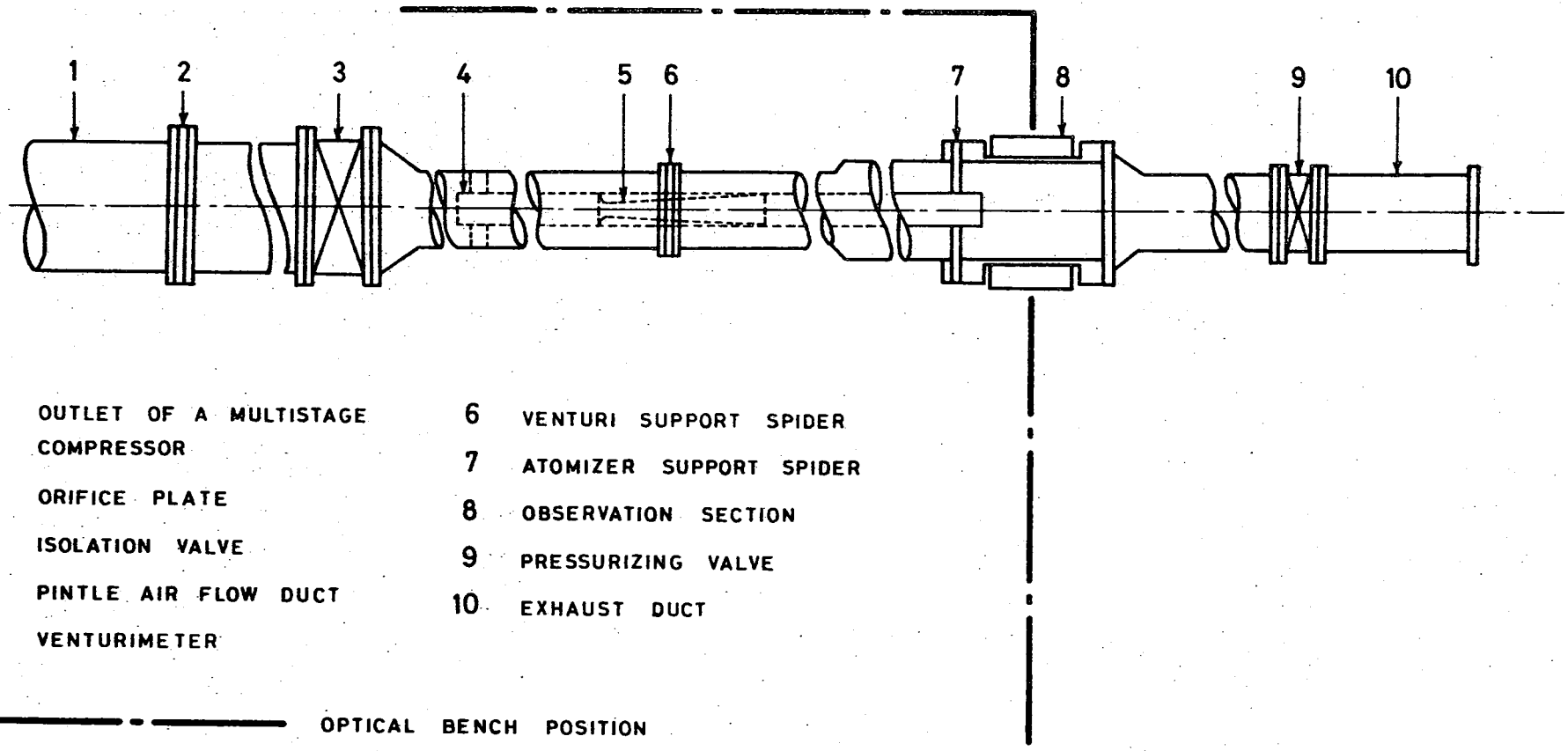

FIG. 20 SCHEMATIC G.A. OF THE HIGH PRESSURE TEST RIG

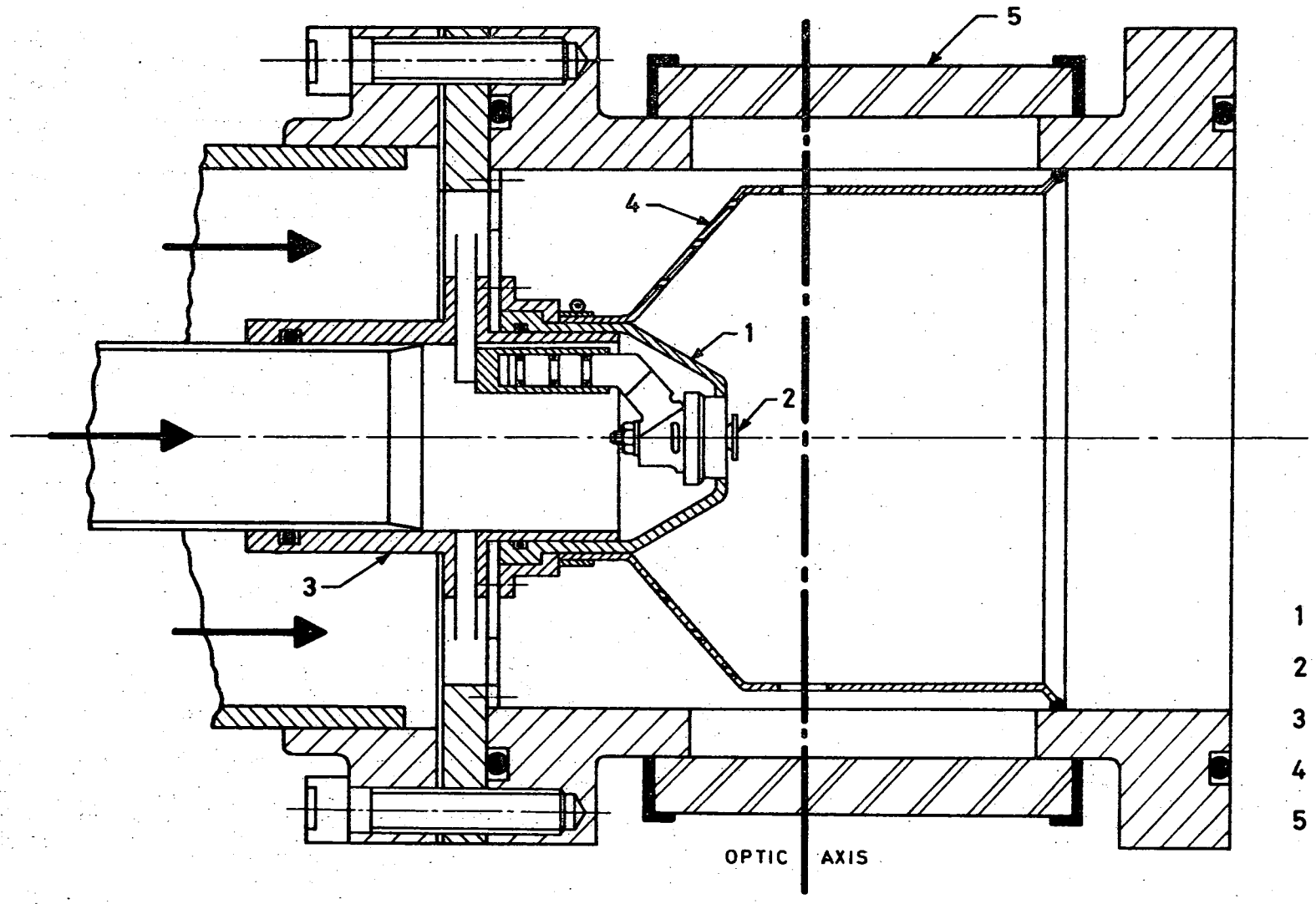

FIG. 21 ATOMIZER MOUNTING WITH FLAME TUBE IN OBSERVATION SECTION (H.P. TEST RIG)

FIG. 22

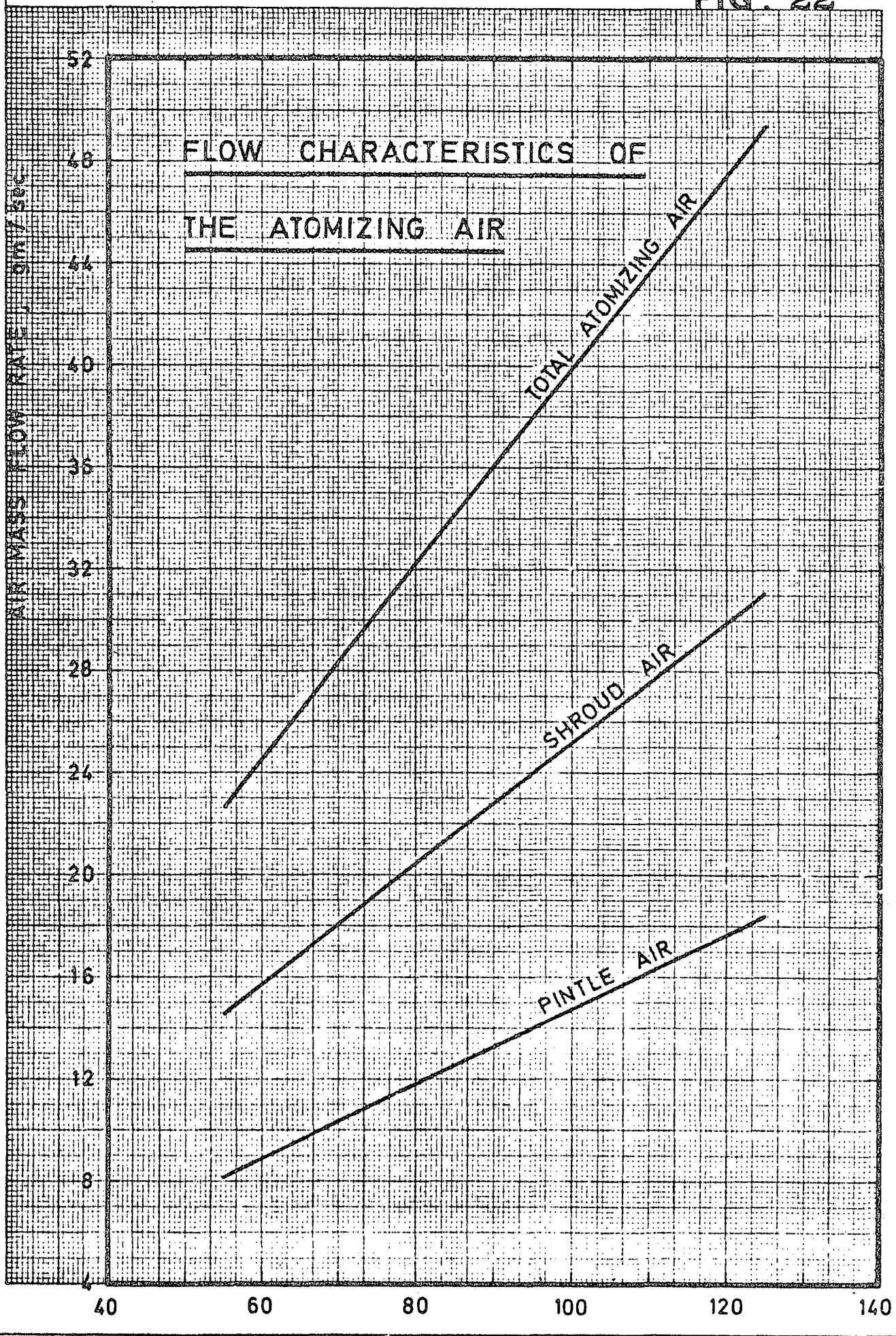
FLOW CHARACTERISTICS OF
THE ATOMIZING AIR
TOTAL ATOMIZING AIR
SHROUD AIR
PINTLE AIR
AIR MASS FLOW RATE, gm / sec.
52
48
44
40
36
32
28
24
20
16
12
8
4
40
60
80
100
120
140
ATOMIZING AIR VELOCITY, m / sec.

FIG. 23

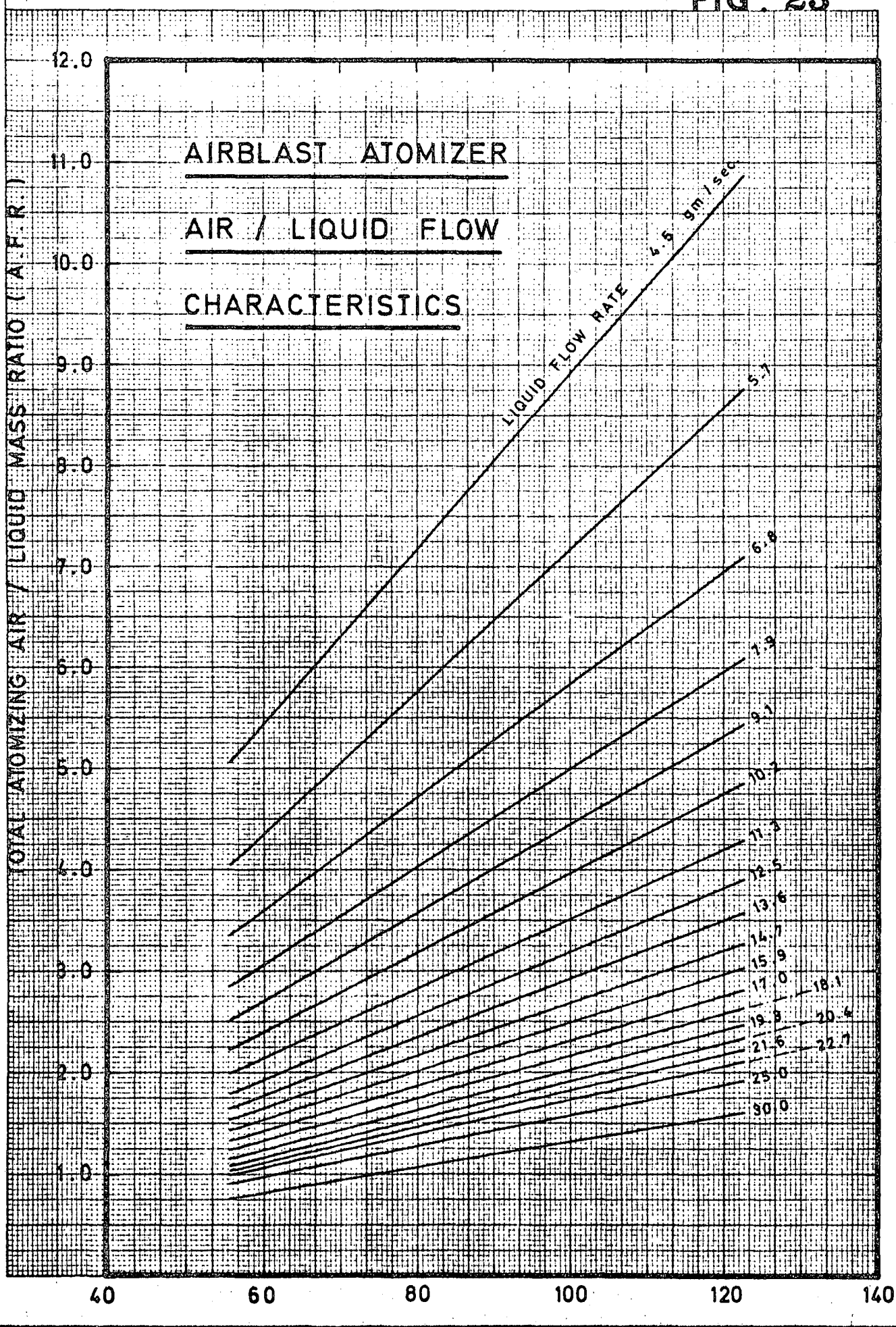
AIRBLAST ATOMIZER
AIR / LIQUID FLOW
CHARACTERISTICS
TOTAL ATOMIZING AIR / LIQUID MASS RATIO (A.F.R.)
12.0
11.0
10.0
9.0
8.0
7.0
6.0
5.0
4.0
3.0
2.0
1.0
LIQUID FLOW RATE 4.5 gm / sec.
5.1
6.8
7.9
9.1
10.2
11.3
12.5
13.6
14.7
15.9
17.0
18.1
19.3
20.4
21.6
22.7
25.0
30.0
40
60
80
100
120
140
ATOMIZING AIR VELOCITY , m / sec.

FIG. 24

VARIATION OF MEAN DROP SIZE WITH LIQUID VISCOSITY FOR A CONSTANT RATE OF LIQUID FLOW

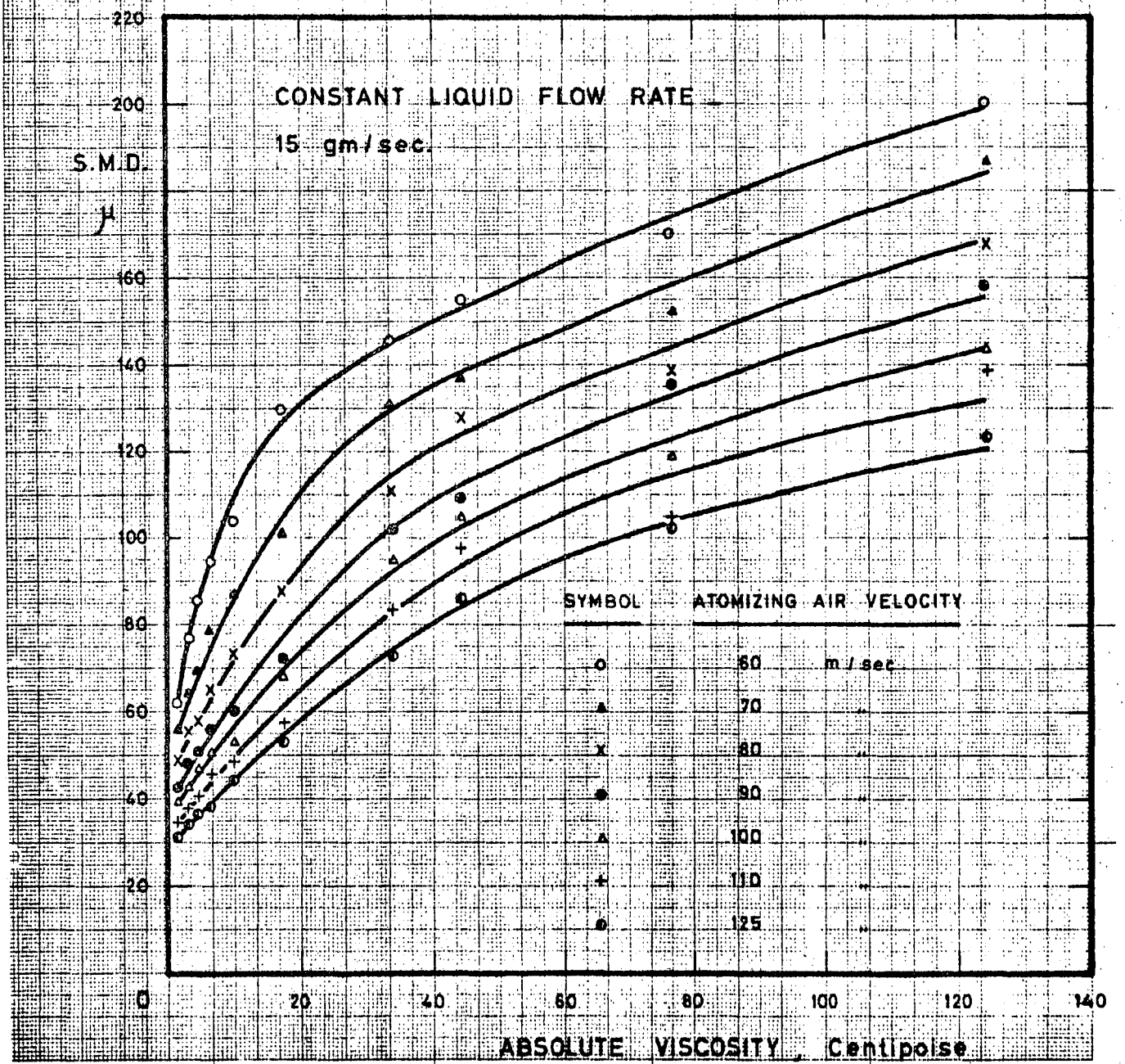

FIG. 25

VARIATION OF MEAN DROP SIZE WITH LIQUID VISCOSITY FOR A CONSTANT ATOMIZING AIR VELOCITY

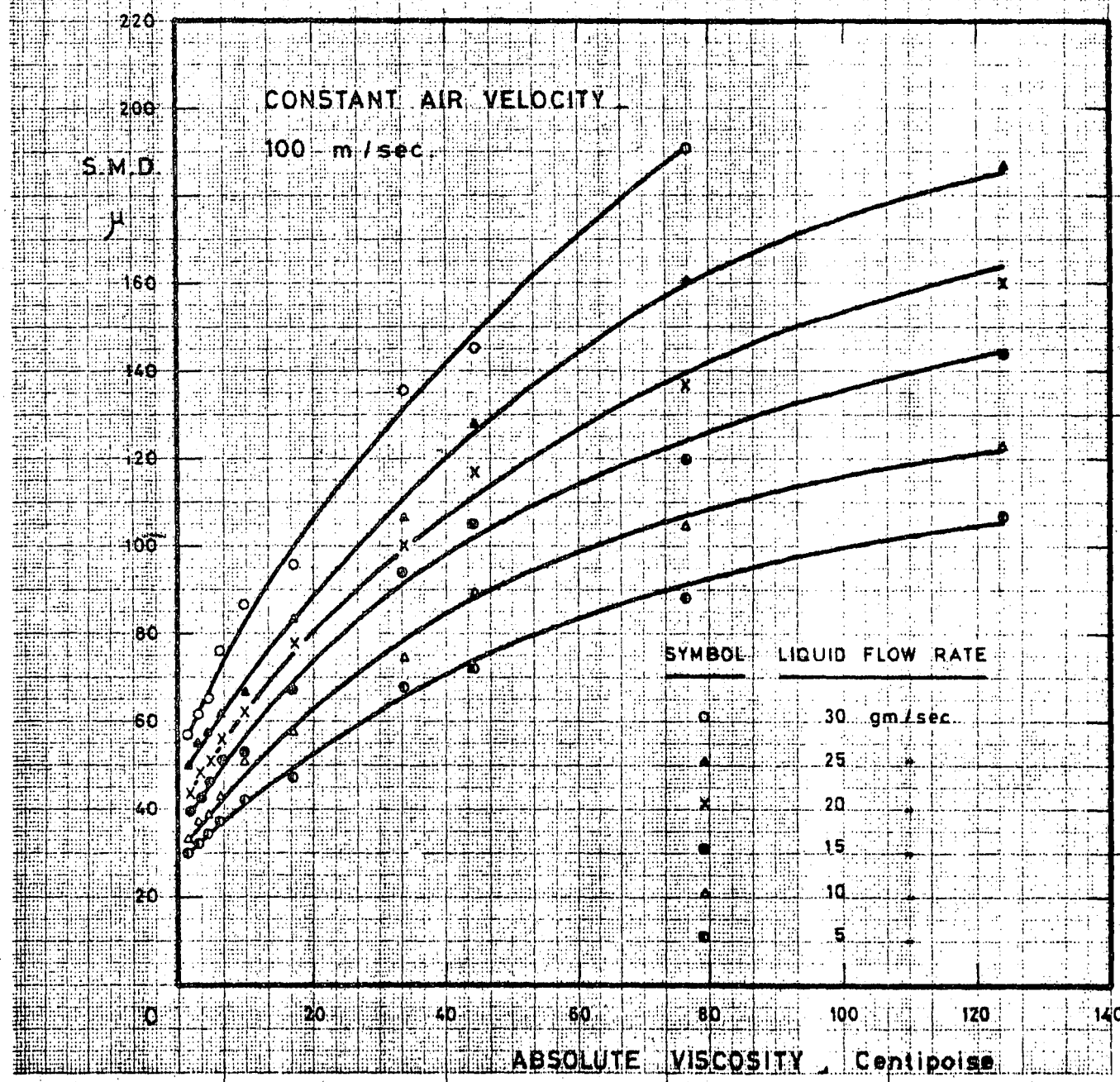

FIG. 26

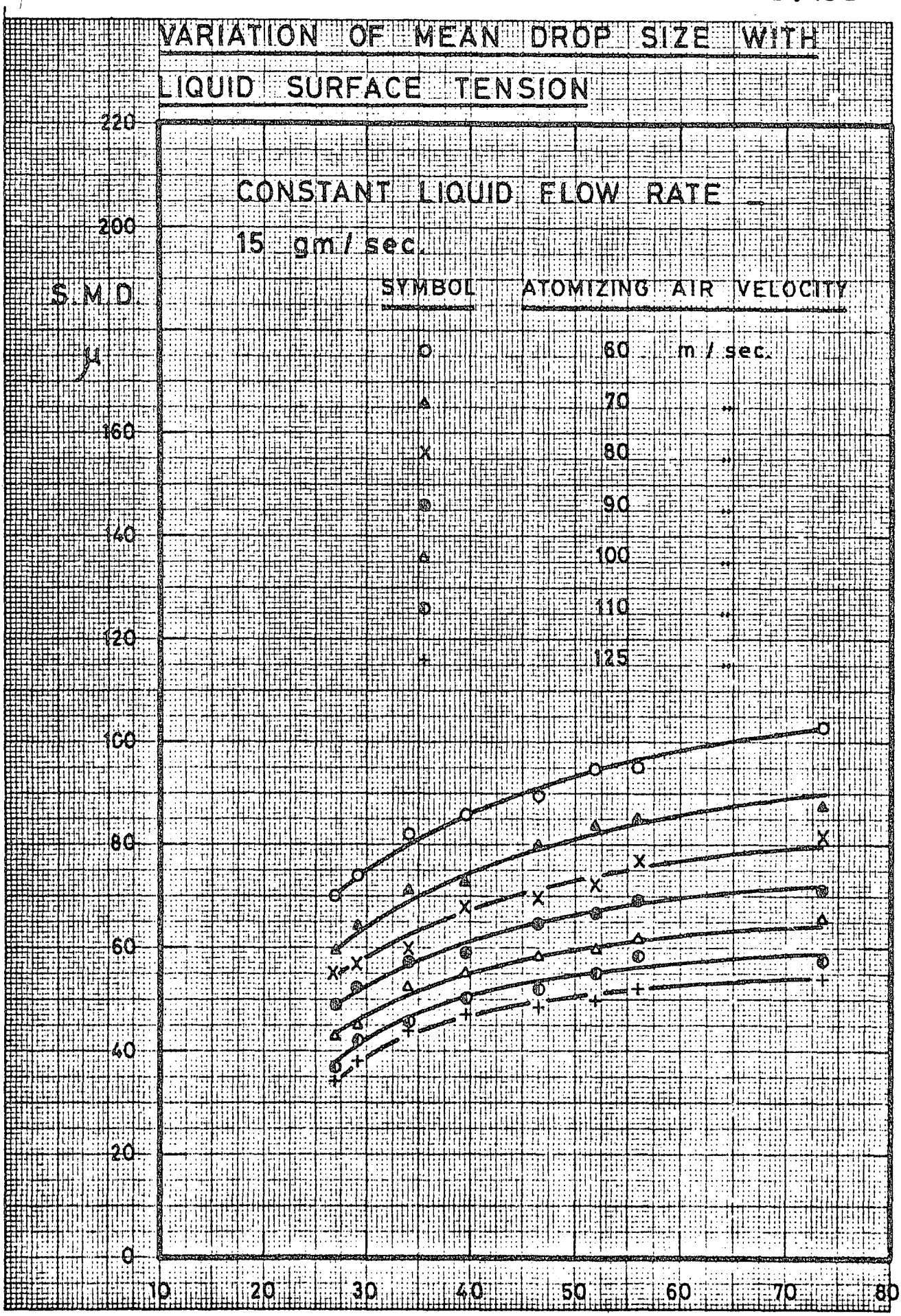
VARIATION OF MEAN DROP SIZE WITH LIQUID SURFACE TENSION
CONSTANT LIQUID FLOW RATE
15 gm / sec.
SYMBOL
ATOMIZING AIR VELOCITY
60 m / sec.
70 "
80 "
90 "
100 "
110 "
125 "
S.M.D. μ
220
200
180
160
140
120
100
80
60
40
20
0
10
20
30
40
50
60
70
80
LIQUID SURFACE TENSION, Dynes / cm.

FIG. 27

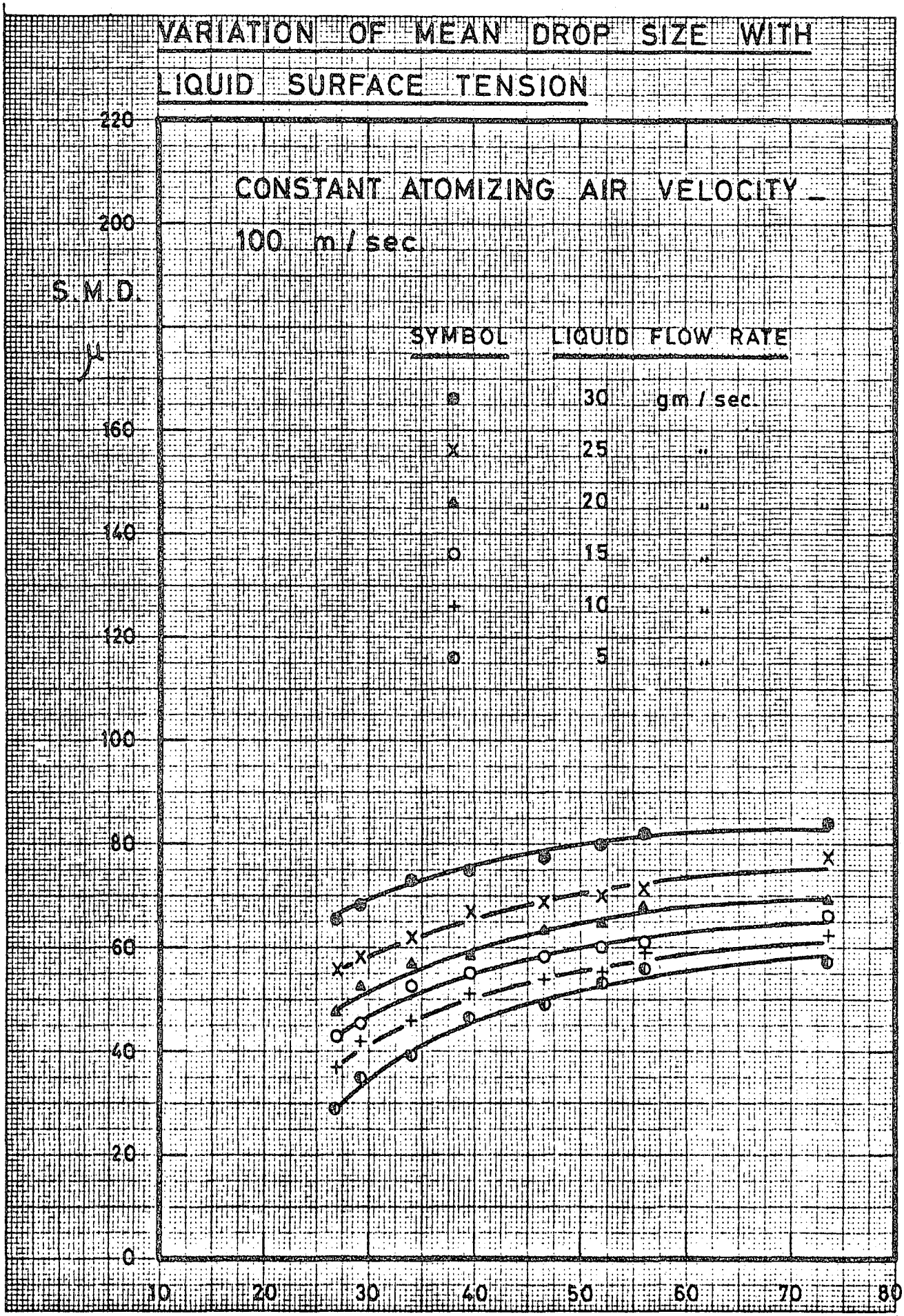
VARIATION OF MEAN DROP SIZE WITH LIQUID SURFACE TENSION
CONSTANT ATOMIZING AIR VELOCITY
100 m / sec.
S.M.D. μ
SYMBOL
LIQUID FLOW RATE
30 gm / sec.
25 "
20 "
15 "
10 "
5 "
220
200
160
140
120
100
80
60
40
20
0
10
20
30
40
50
60
70
80
LIQUID SURFACE TENSION, Dynes / cm.

FIG. 28

VARIATION OF MEAN DROPLET SIZE WITH LIQUID DENSITY

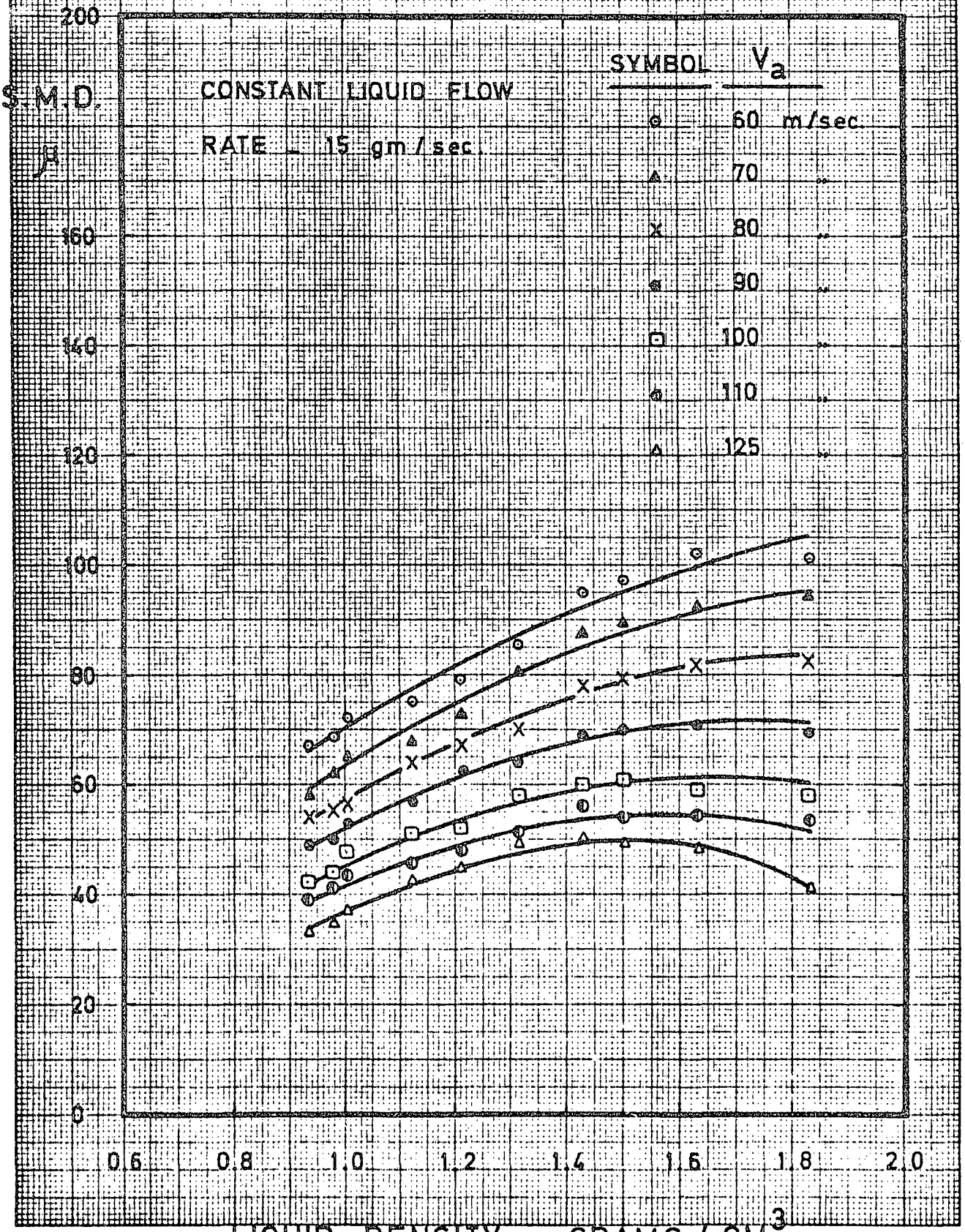

FIG. 29

VARIATION OF MEAN DROPLET SIZE WITH LIQUID DENSITY

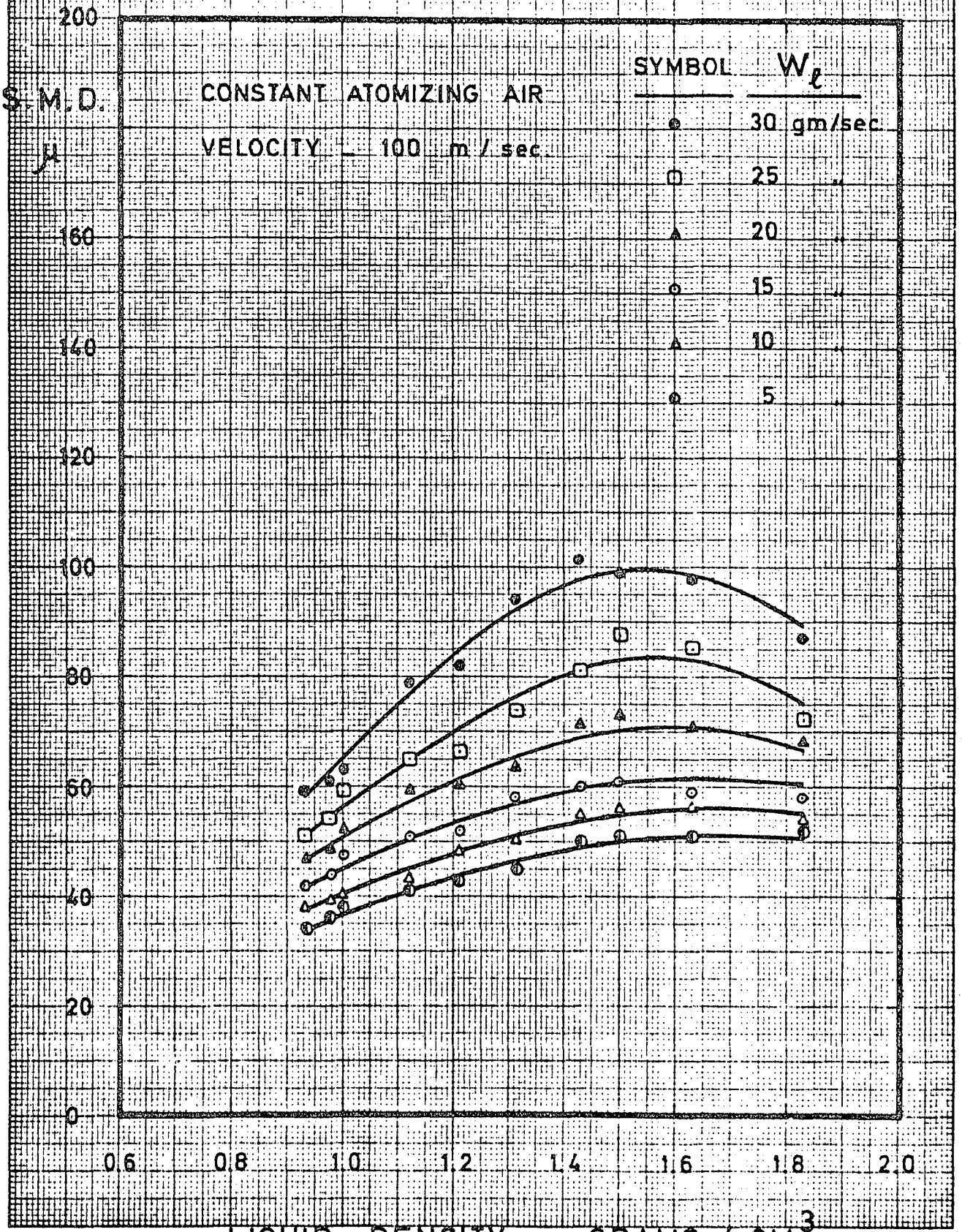

FIG. 30

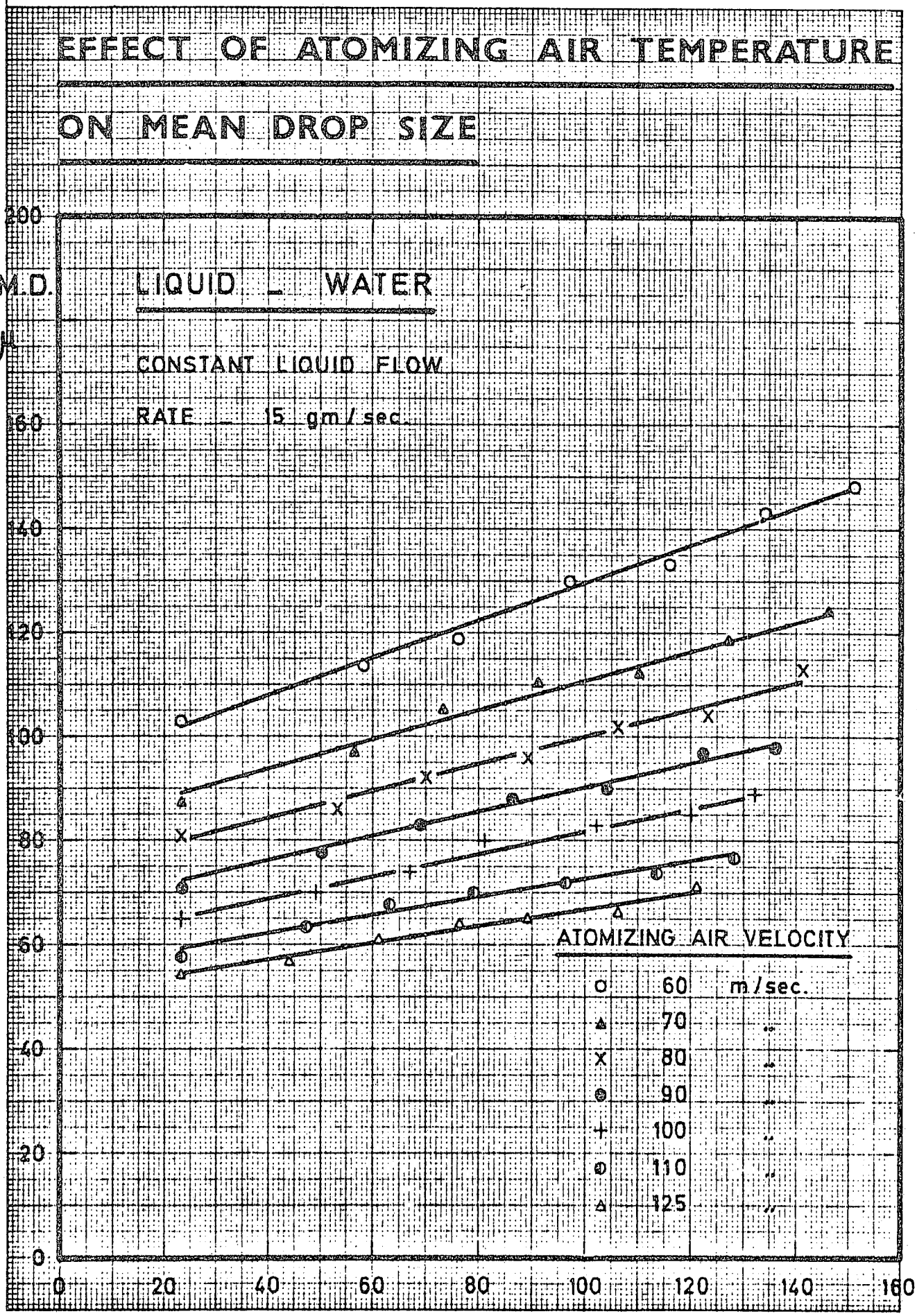
EFFECT OF ATOMIZING AIR TEMPERATURE
ON MEAN DROP SIZE
LIQUID - WATER
CONSTANT LIQUID FLOW
RATE - 15 gm/sec
M.D.
μ
200
160
140
120
100
80
60
40
20
0
0
20
40
60
80
100
120
140
160
ATOMIZING AIR TEMPERATURE, °C.
ATOMIZING AIR VELOCITY
o 60 m/sec.
Δ 70 "
X 80 "
⊙ 90 "
+ 100 "
◎ 110 "
Δ 125 "

FIG. 31

EFFECT OF ATOMIZING AIR TEMPERATURE ON MEAN DROP SIZE

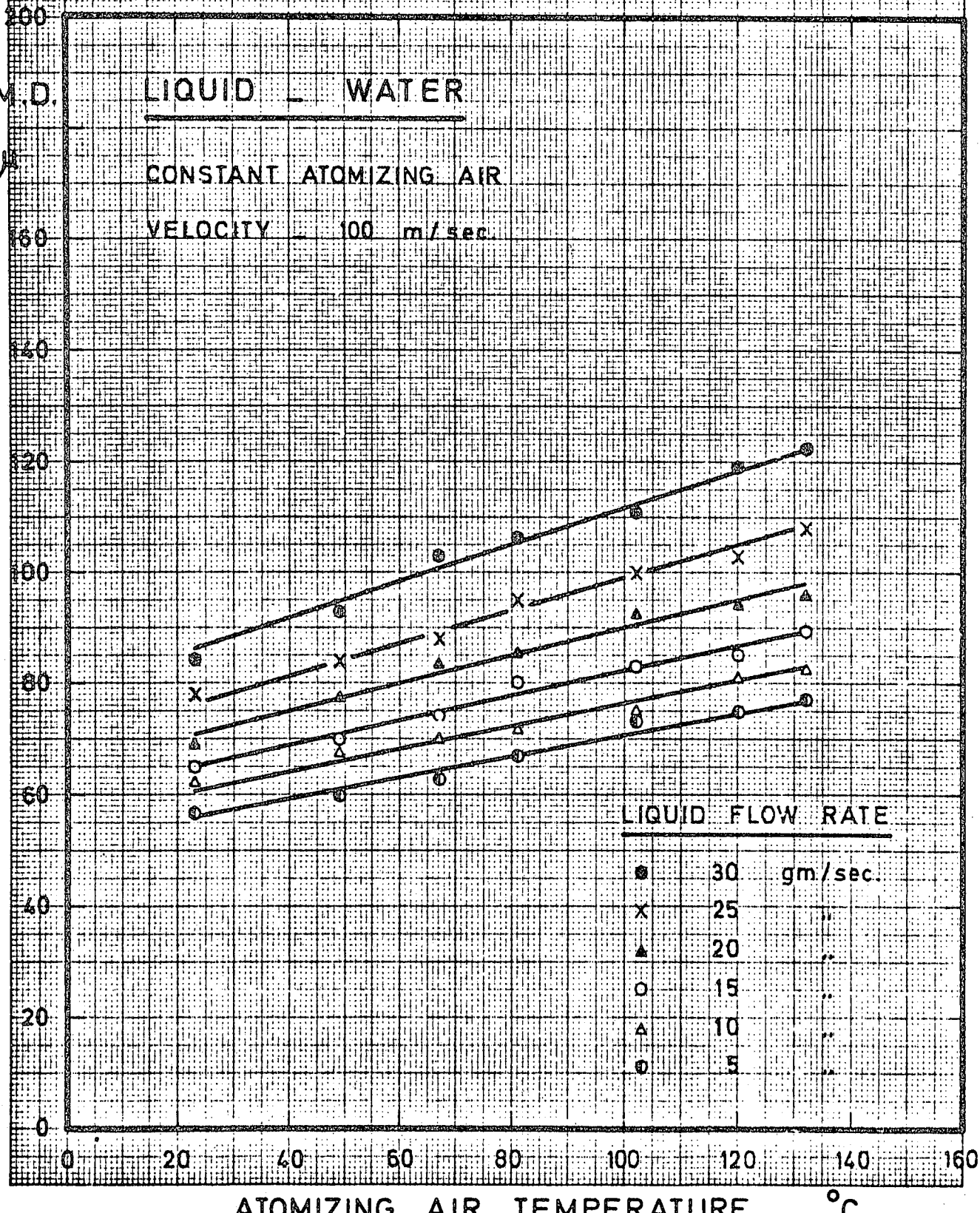

FIG. 32

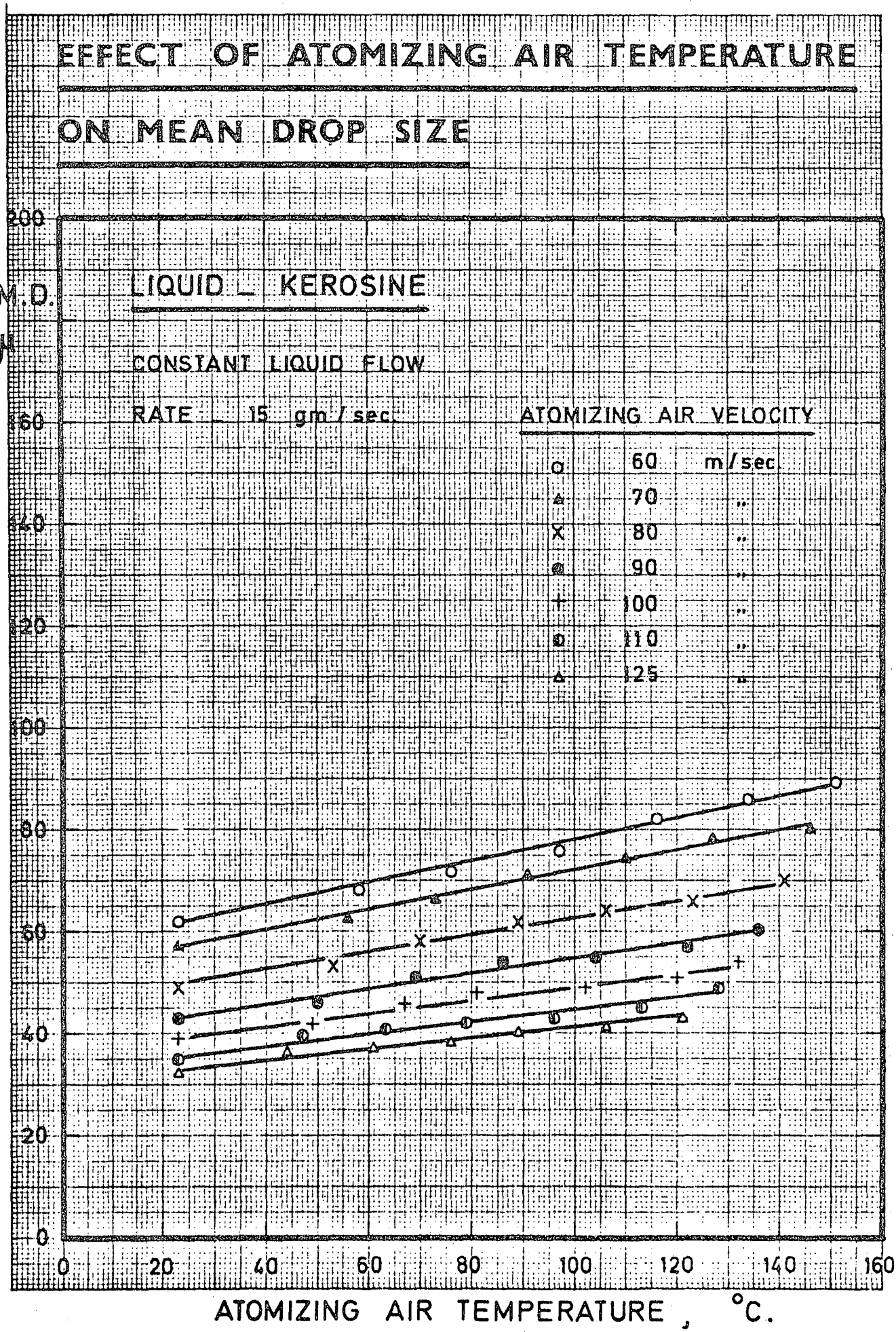
EFFECT OF ATOMIZING AIR TEMPERATURE
ON MEAN DROP SIZE
LIQUID – KEROSINE
CONSTANT LIQUID FLOW
RATE – 15 gm / sec
ATOMIZING AIR VELOCITY
60 m/sec
70 "
80 "
90 "
100 "
110 "
125 "
S.M.D.
μ
200
160
140
120
100
80
60
40
20
0
0
20
40
60
80
100
120
140
160
ATOMIZING AIR TEMPERATURE , °C.

FIG. 33

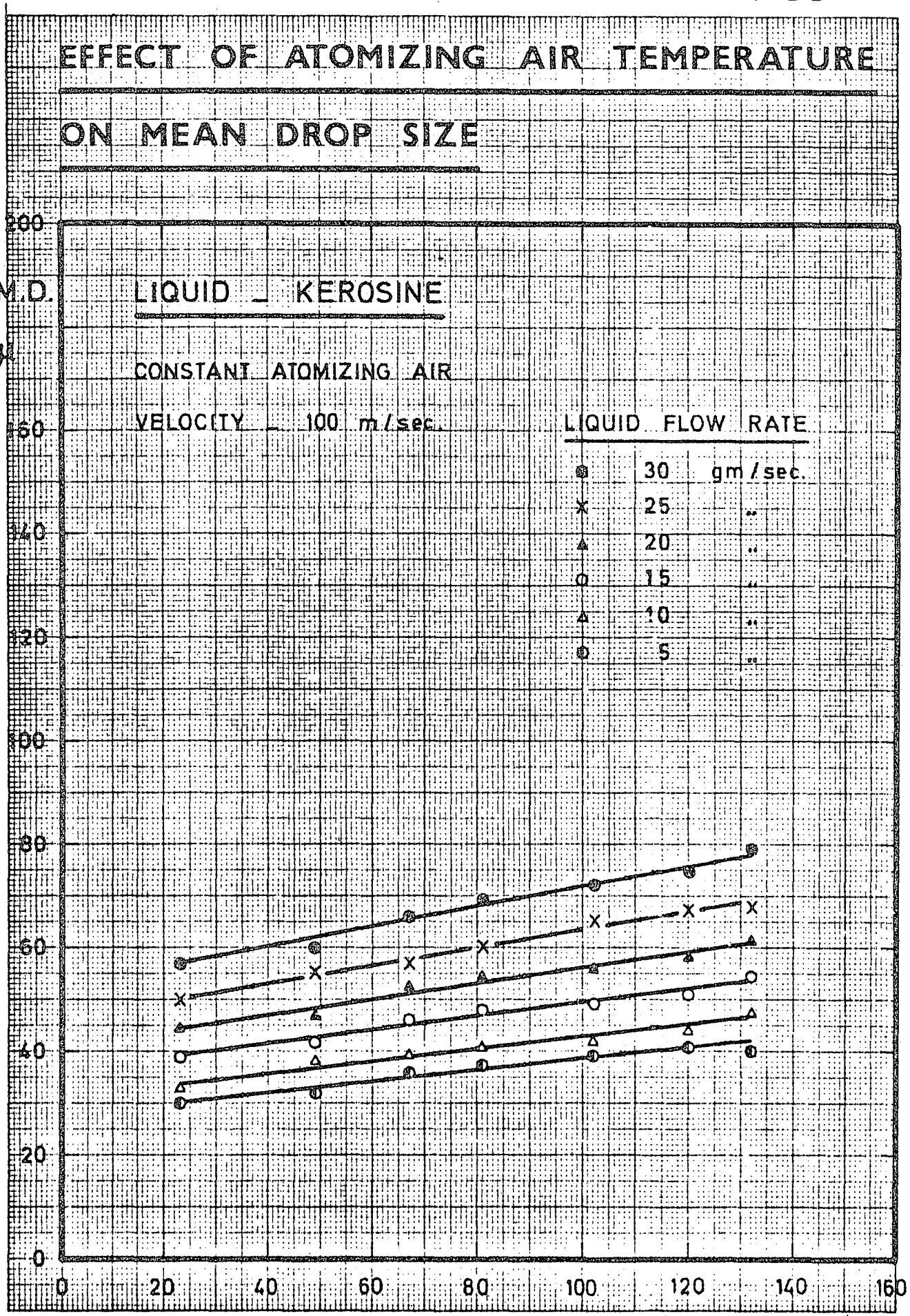
EFFECT OF ATOMIZING AIR TEMPERATURE
ON MEAN DROP SIZE
M.D.
LIQUID - KEROSINE
CONSTANT ATOMIZING AIR
VELOCITY - 100 m/sec.
LIQUID FLOW RATE
30 gm/sec.
25 "
20 "
15 "
10 "
5 "
200
160
140
120
100
80
60
40
20
0
0
20
40
60
80
100
120
140
160
ATOMIZING AIR TEMPERATURE, °C.

ATOMIZING AIR TEMPERATURE RESULTS

FIG. 34

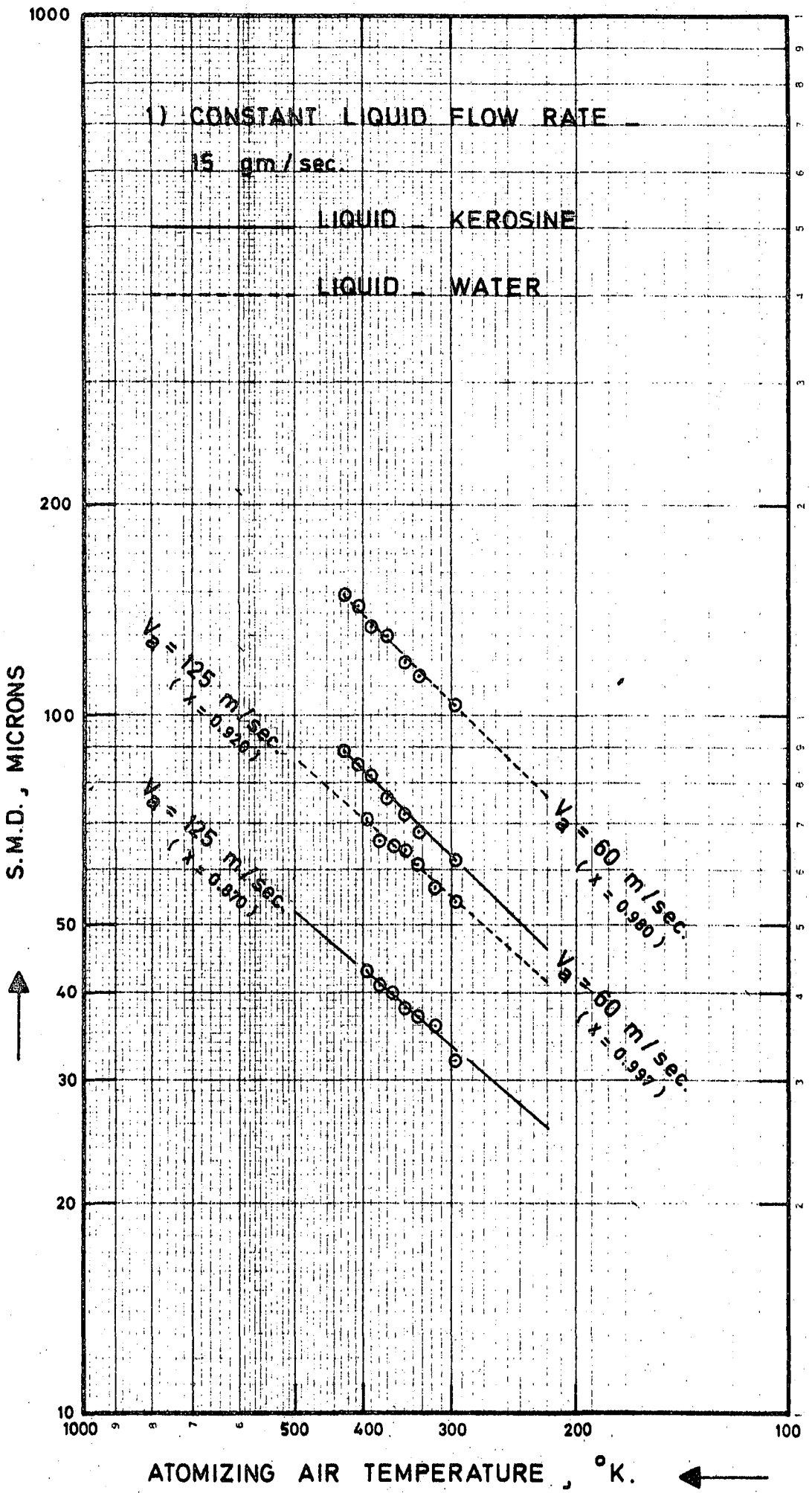

ATOMIZING AIR TEMPERATURE RESULTS

FIG. 35

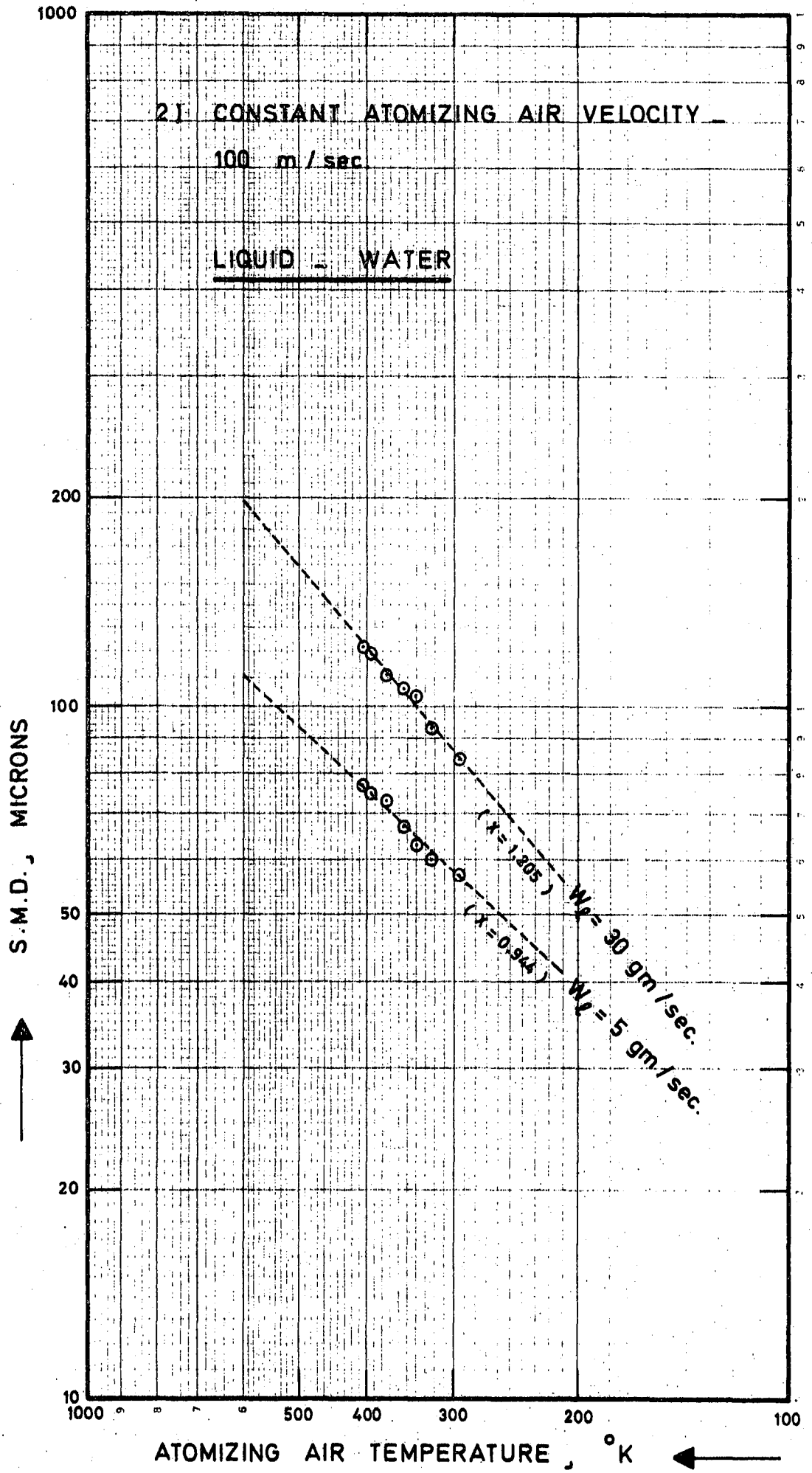

ATOMIZING AIR TEMPERATURE RESULTS

FIG. 36

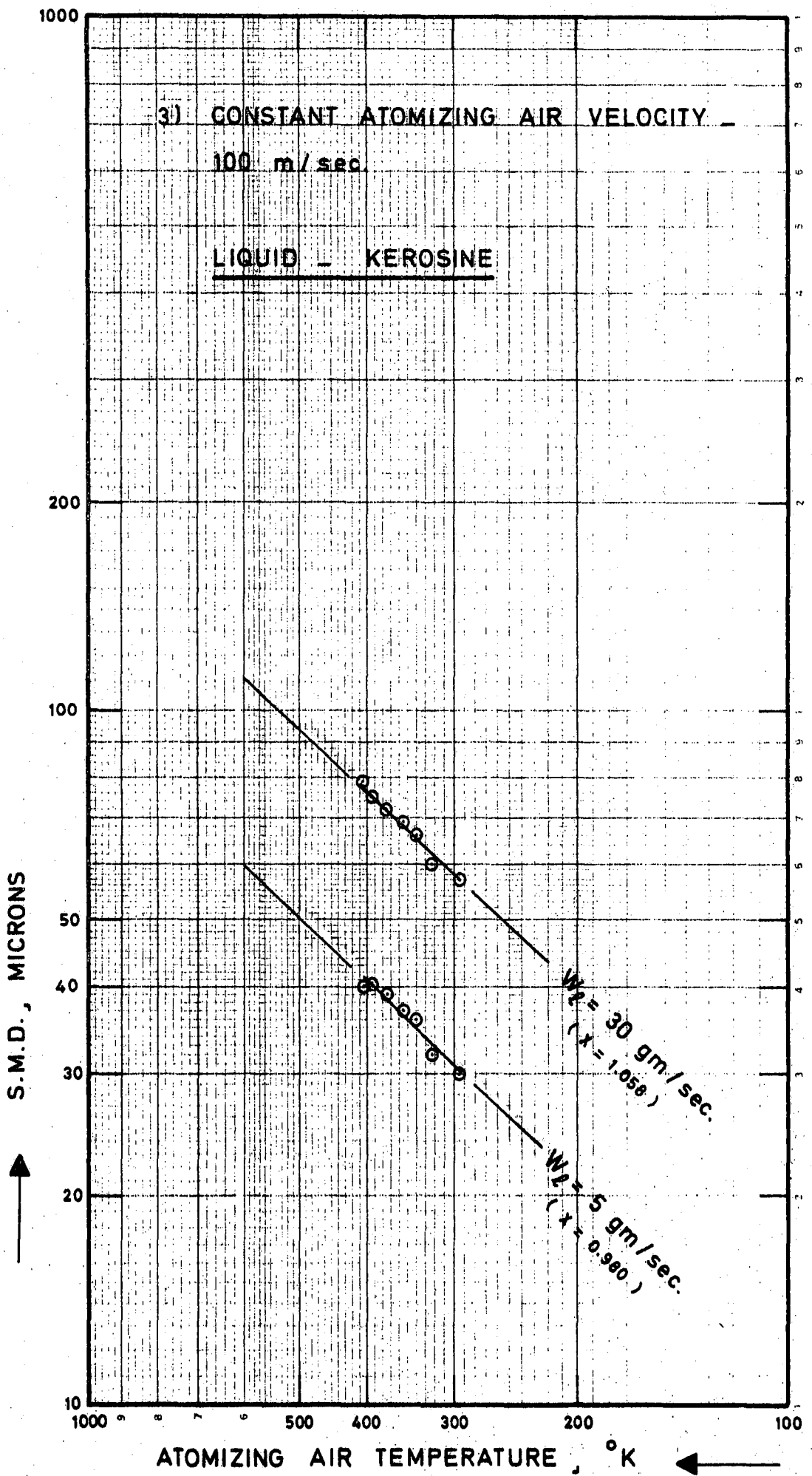

FIG. 37

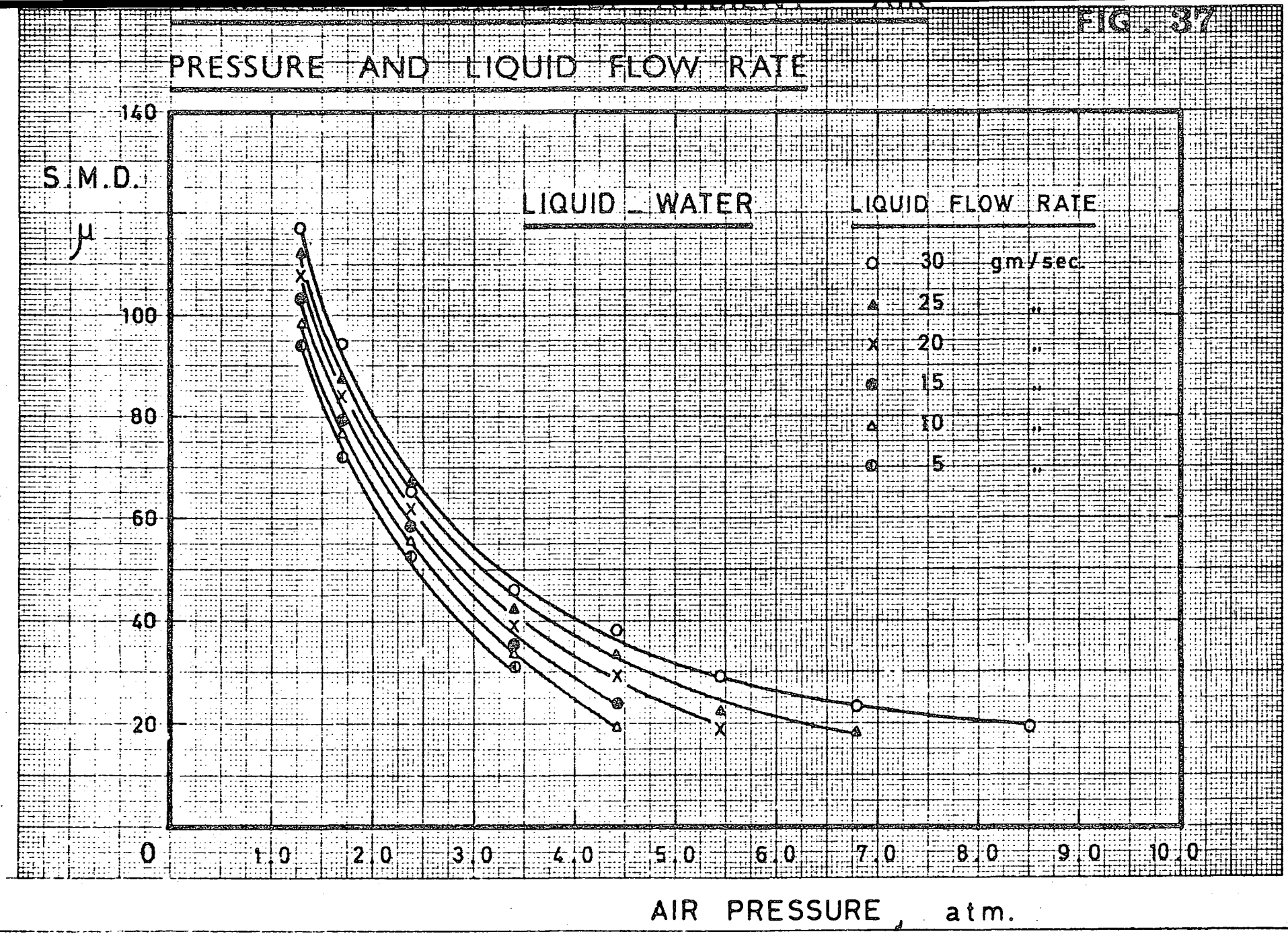
PRESSURE AND LIQUID FLOW RATE
S.M.D.
μ
140
100
80
60
40
20
0
LIQUID _ WATER
LIQUID FLOW RATE
30 gm/sec.
25 "
20 "
15 "
10 "
5 "
1.0
2.0
3.0
4.0
5.0
6.0
7.0
8.0
9.0
10.0
AIR PRESSURE, atm.

INFLUENCE ON S.M.D. OF AMBIENT AIR PRESSURE AND LIQUID FLOW RATE

FIG. 38

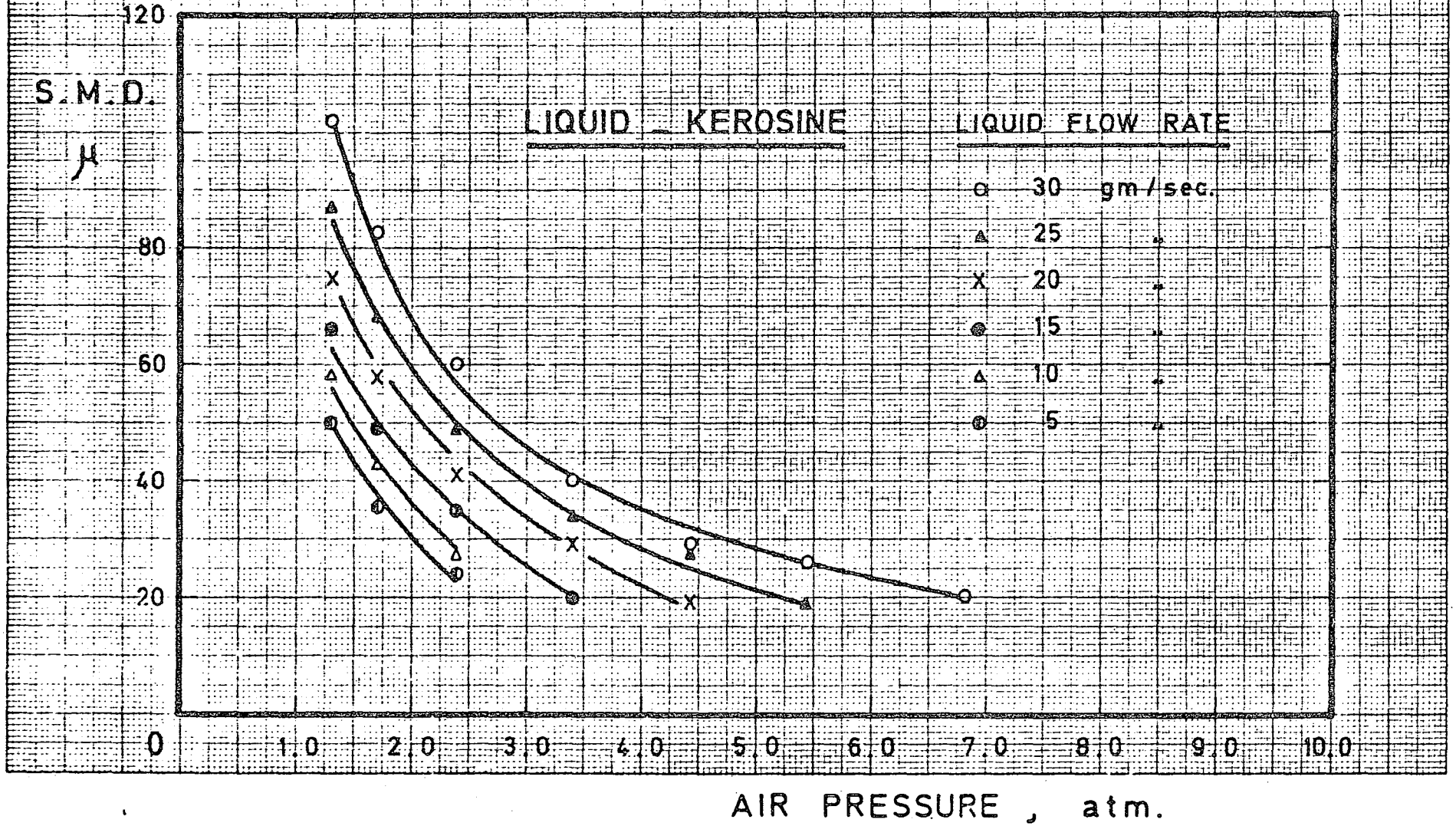

FIG. 39

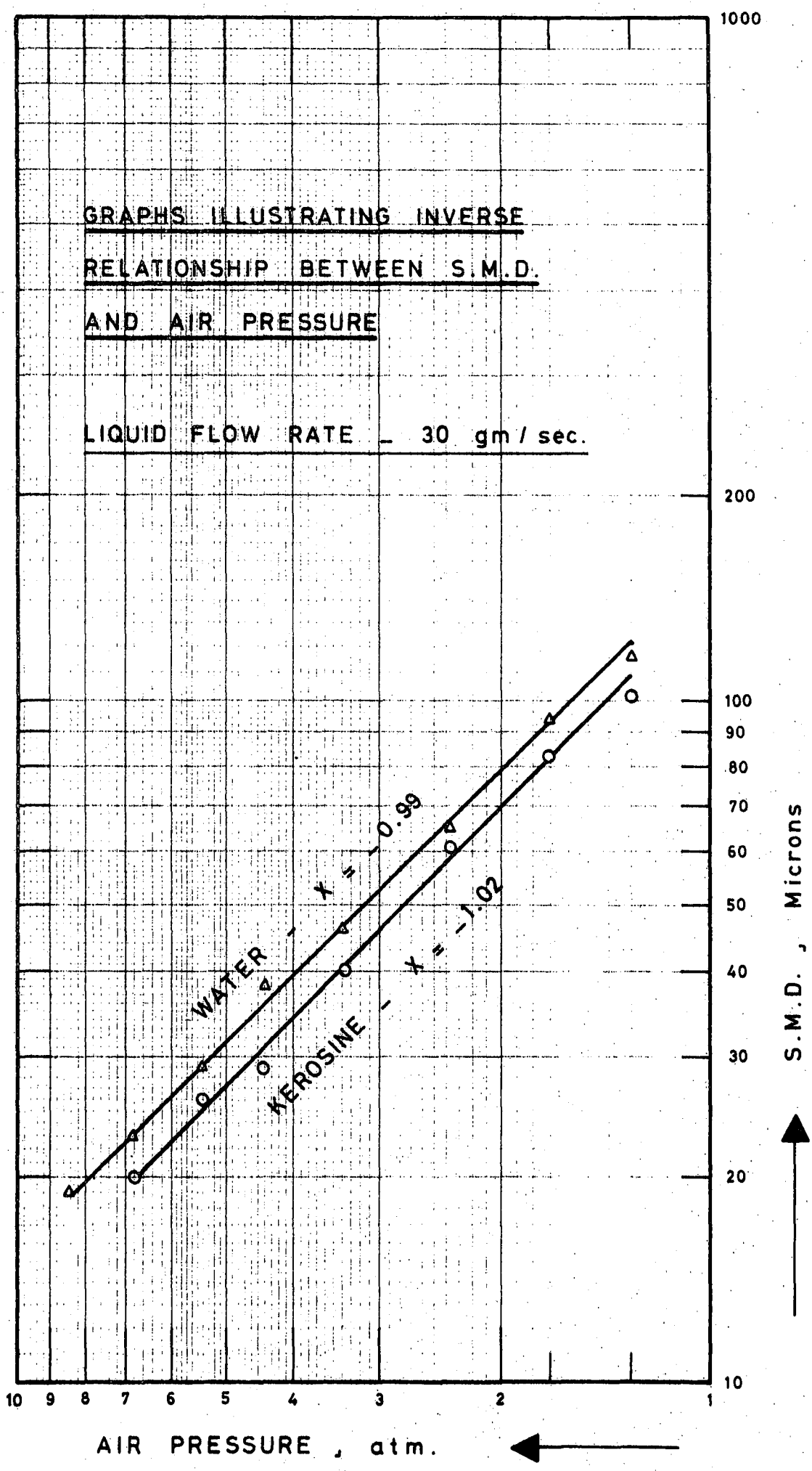
GRAPHS ILLUSTRATING INVERSE
RELATIONSHIP BETWEEN S.M.D.
AND AIR PRESSURE
LIQUID FLOW RATE - 30 gm / sec.
WATER - X = -0.99
KEROSINE - X = -1.02
1000
200
100
90
80
70
60
50
40
30
20
10
10 9 8 7 6 5 4 3 2 1
AIR PRESSURE , atm.
S.M.D. , Microns

FIG. 40

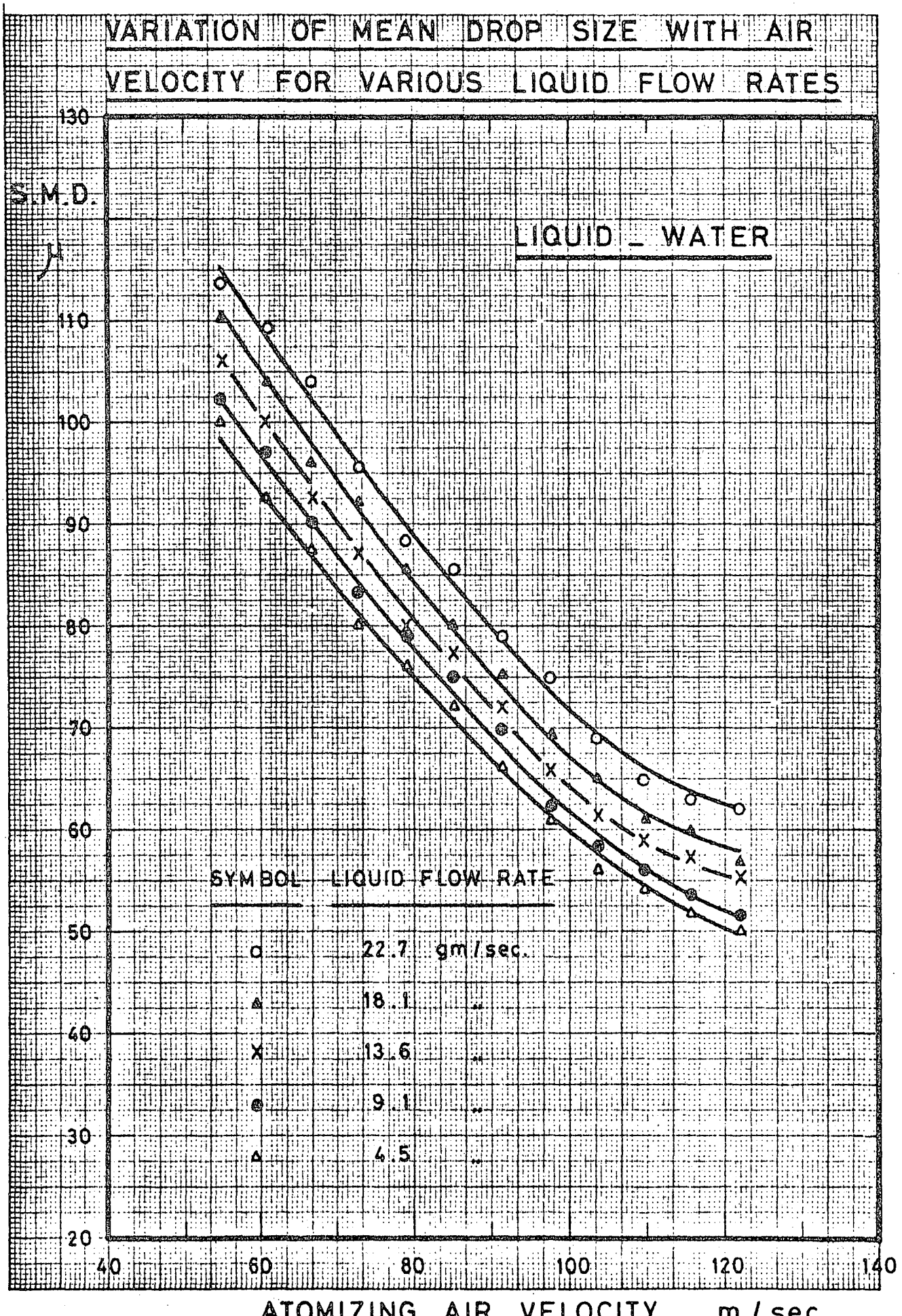
VARIATION OF MEAN DROP SIZE WITH AIR VELOCITY FOR VARIOUS LIQUID FLOW RATES
LIQUID _ WATER
S.M.D. μ
130
110
100
90
80
70
60
50
40
30
20
40
60
80
100
120
140
ATOMIZING AIR VELOCITY , m / sec.
SYMBOL LIQUID FLOW RATE
o 22.7 gm / sec.
Δ 18.1 "
X 13.6 "
● 9.1 "
▲ 4.5 "

FIG. 41

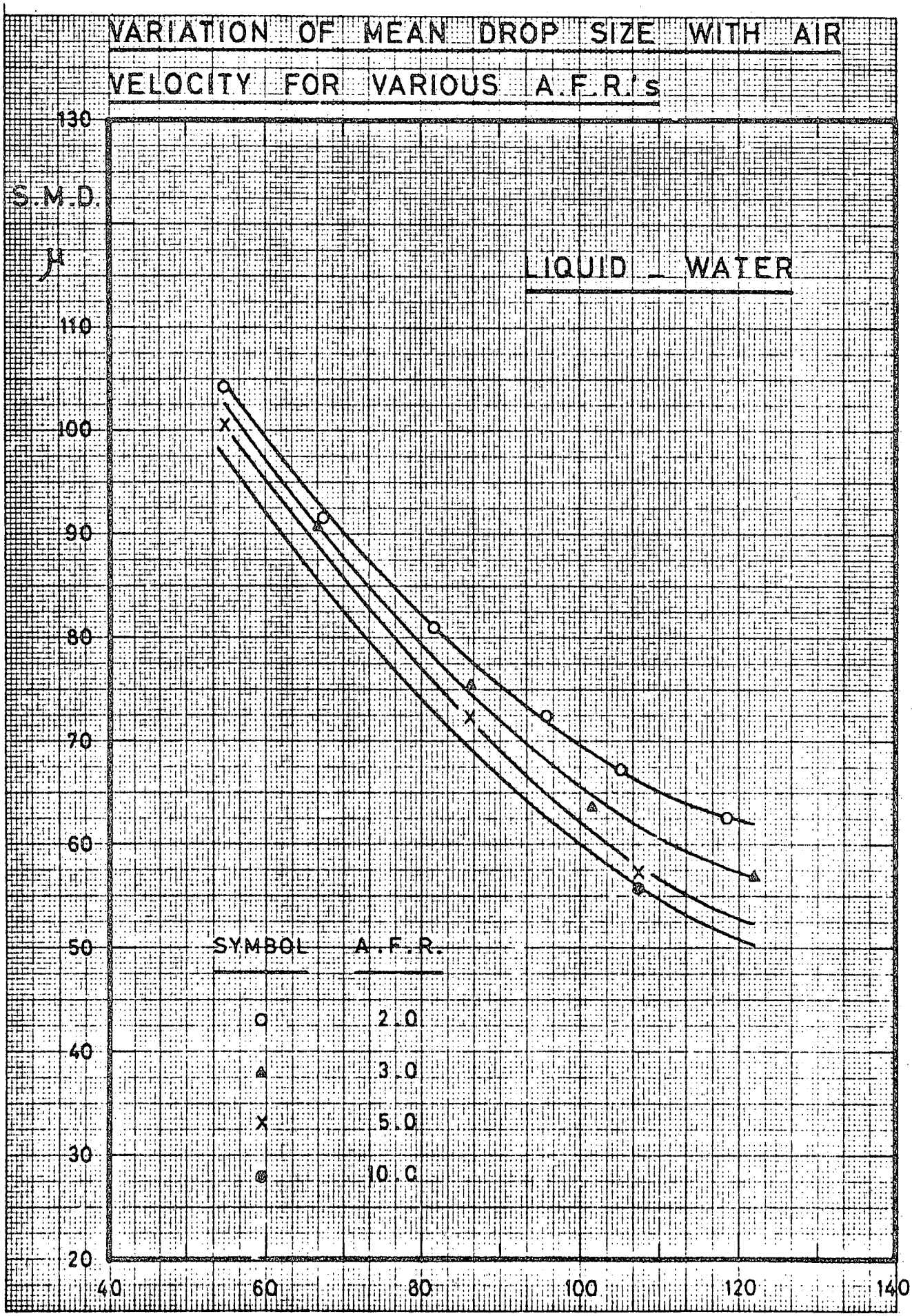
VARIATION OF MEAN DROP SIZE WITH AIR VELOCITY FOR VARIOUS A.F.R.'s
LIQUID - WATER
S.M.D. μ
130
110
100
90
80
70
60
50
40
30
20
SYMBOL
A.F.R.
○ 2.0
△ 3.0
× 5.0
● 10.0
40
60
80
100
120
140
ATOMIZING AIR VELOCITY, m/sec.

FIG. 42

VARIATION OF MEAN DROPLET SIZE WITH AIR VELOCITY FOR VARIOUS LIQUID FLOWS AND A.F.R's

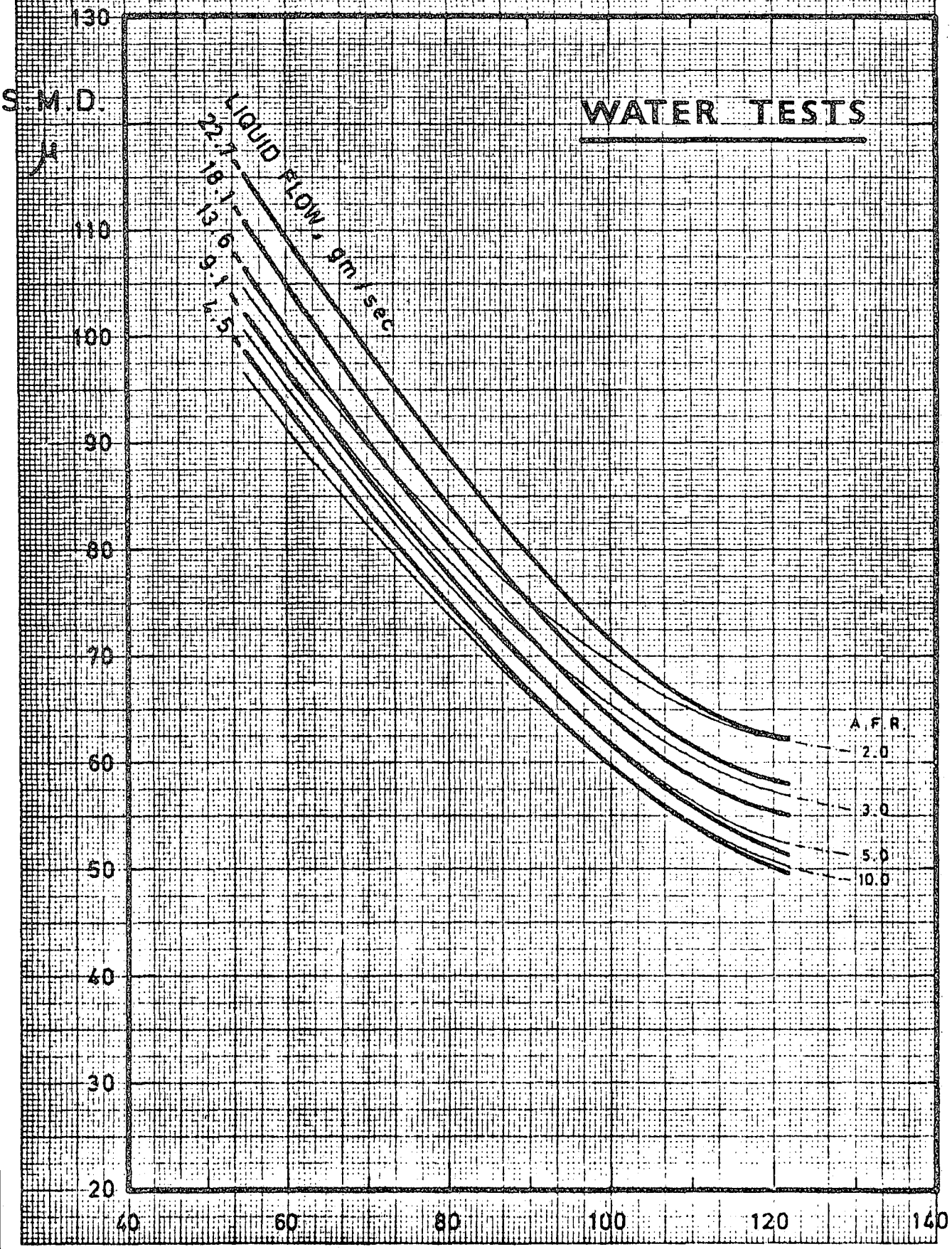

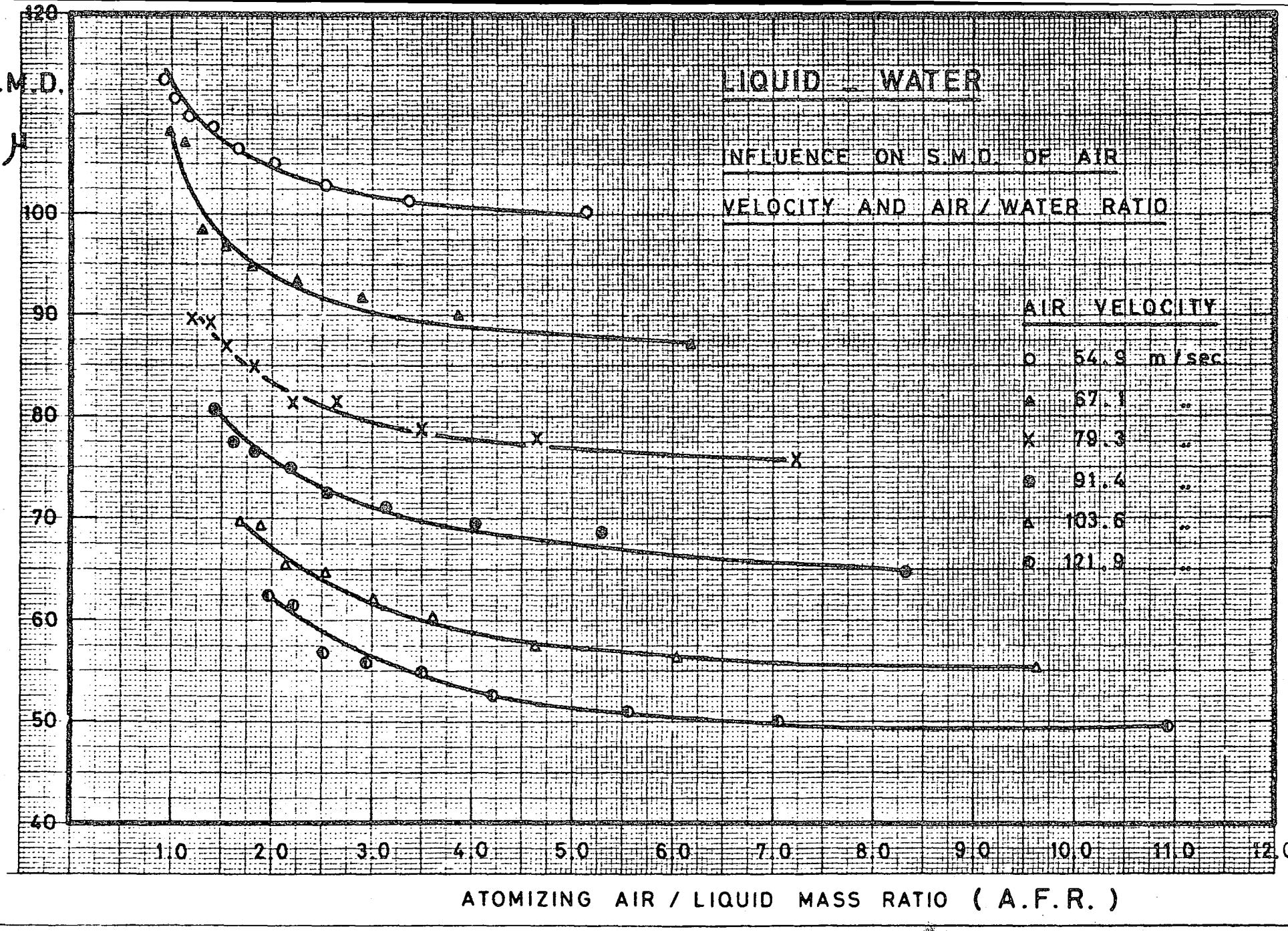
LIQUID — WATER
INFLUENCE ON S.M.D. OF AIR VELOCITY AND AIR / WATER RATIO
AIR VELOCITY
○ 54.9 m/sec.
△ 67.1 ..
X 79.3 ..
◎ 91.4 ..
▲ 103.6 ..
◎ 121.9 ..
S.M.D. μ
120
100
90
80
70
60
50
40
1.0
2.0
3.0
4.0
5.0
6.0
7.0
8.0
9.0
10.0
11.0
12.0
ATOMIZING AIR / LIQUID MASS RATIO (A.F.R.)

FIG. 43

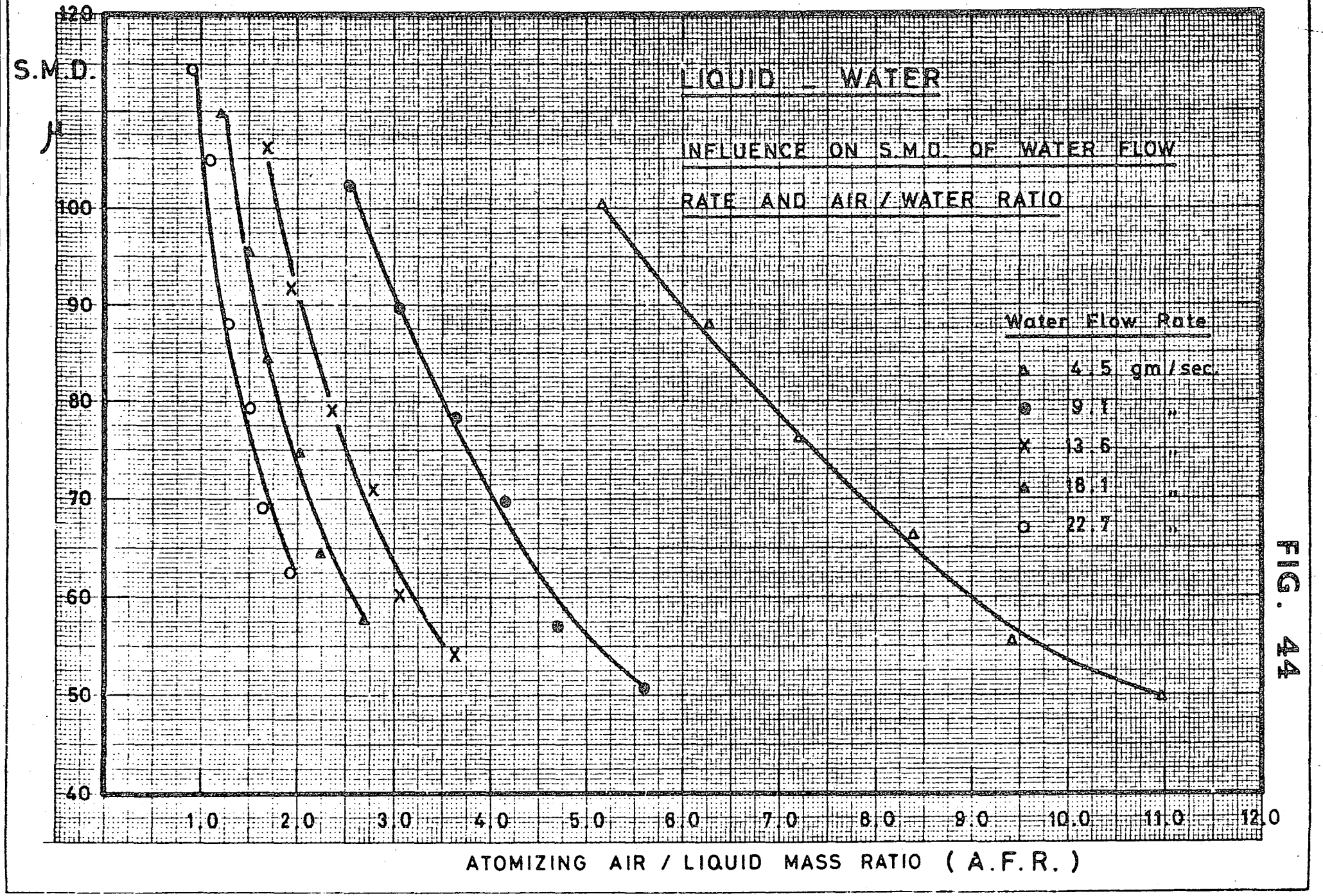
LIQUID - WATER
INFLUENCE ON S.M.D. OF WATER FLOW RATE AND AIR / WATER RATIO
S.M.D. μ
Water Flow Rate
4.5 gm/sec.
9.1 "
13.6 "
18.1 "
22.7 "
120
100
90
80
70
60
50
40
1.0
2.0
3.0
4.0
5.0
6.0
7.0
8.0
9.0
10.0
11.0
12.0
ATOMIZING AIR / LIQUID MASS RATIO (A.F.R.)

FIG. 44

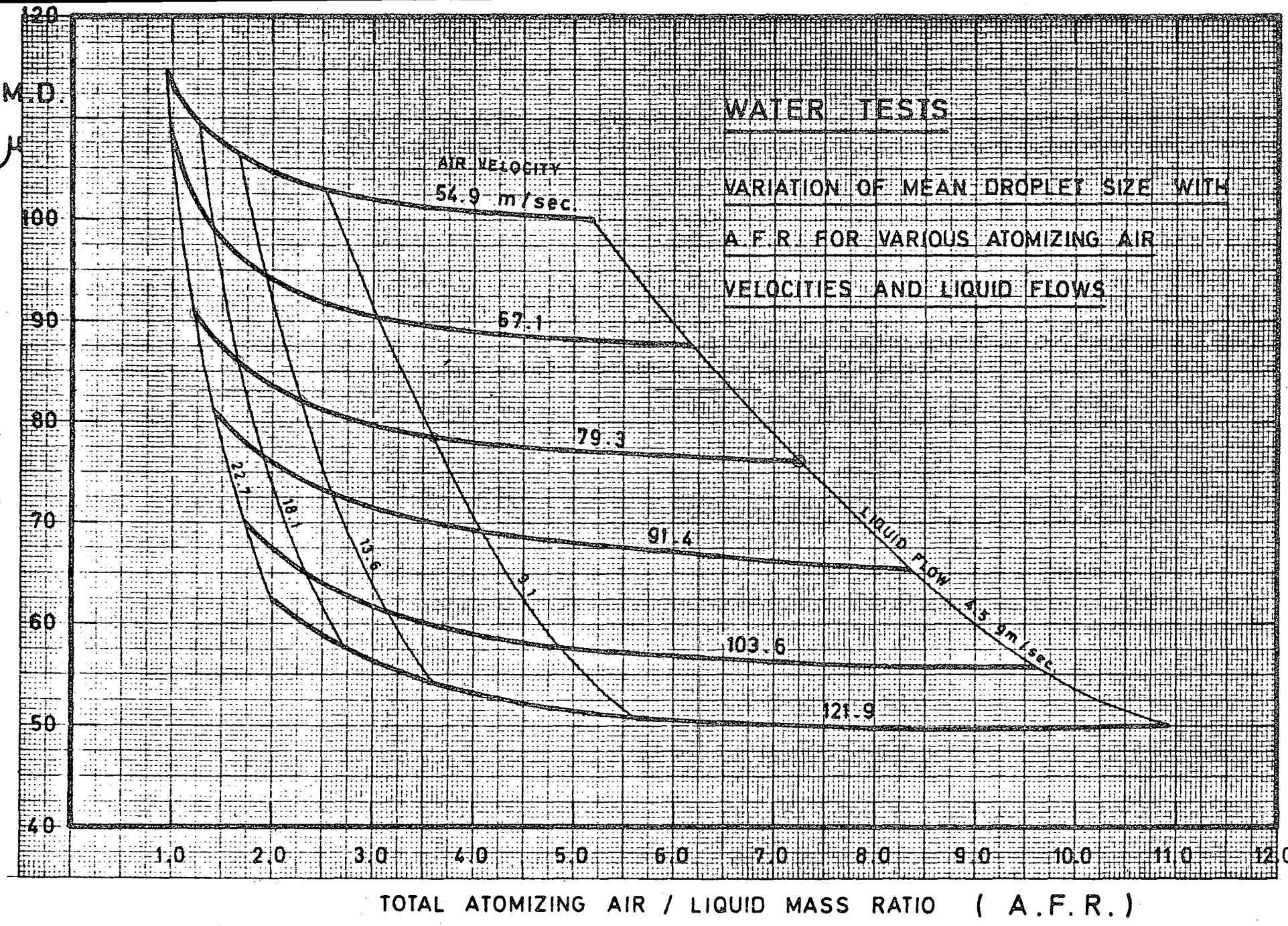
WATER TESIS
VARIATION OF MEAN DROPLET SIZE WITH A.F.R. FOR VARIOUS ATOMIZING AIR VELOCITIES AND LIQUID FLOWS
S.M.D. μ
AIR VELOCITY
54.9 m/sec.
57.1
79.3
91.4
103.6
121.9
22.7
18.1
13.6
9.1
LIQUID FLOW 4.3 gm/sec.
120
100
90
80
70
60
50
40
1.0
2.0
3.0
4.0
5.0
6.0
7.0
8.0
9.0
10.0
11.0
12.0
TOTAL ATOMIZING AIR / LIQUID MASS RATIO (A.F.R.)

FIG. 45

FIG. 46

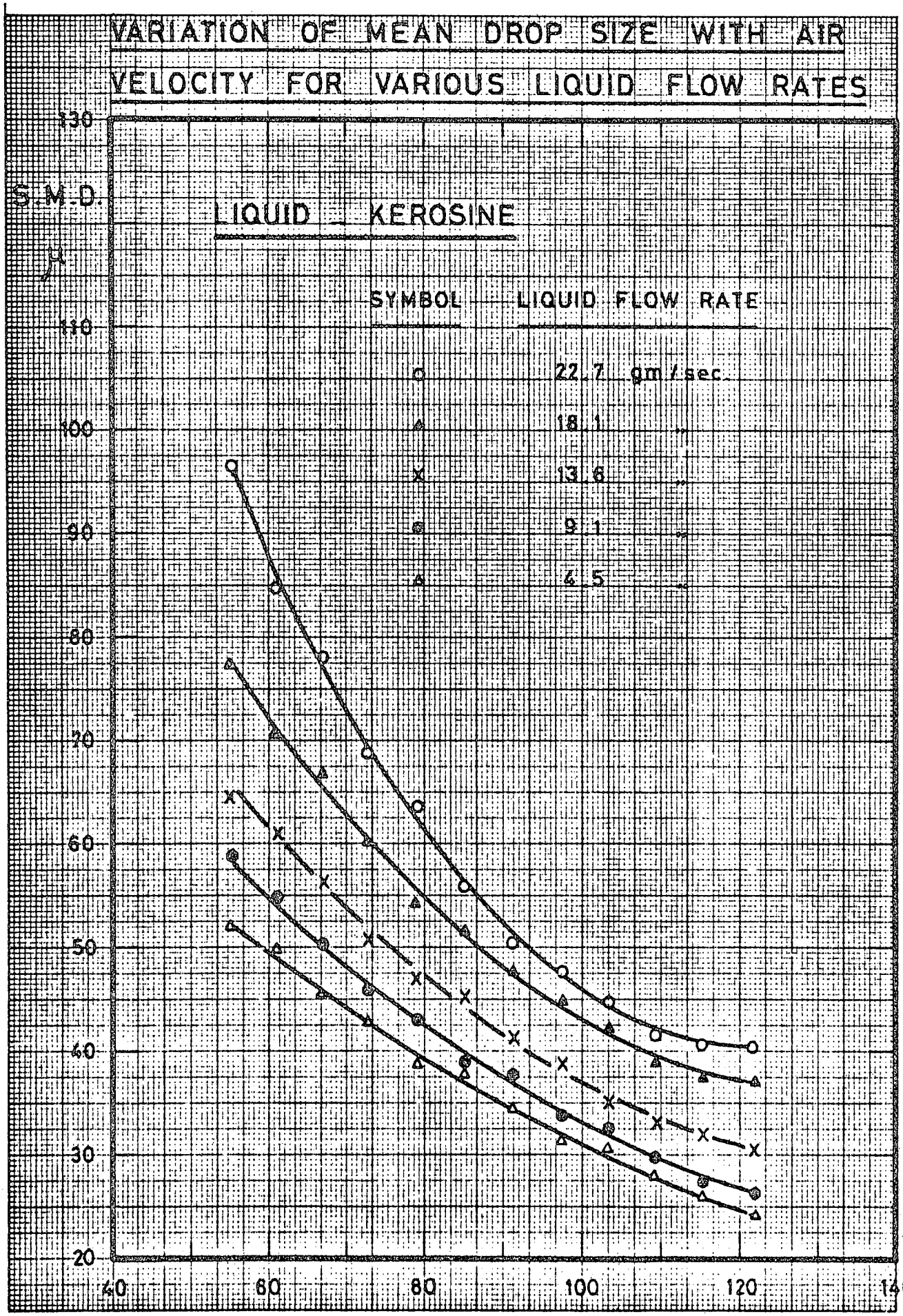
VARIATION OF MEAN DROP SIZE WITH AIR VELOCITY FOR VARIOUS LIQUID FLOW RATES
LIQUID - KEROSINE
SYMBOL
LIQUID FLOW RATE
22.7 gm / sec.
18.1 "
13.6 "
9.1 "
4.5 "
S.M.D. μ
130
110
100
90
80
70
60
50
40
30
20
40
60
80
100
120
140
ATOMIZING AIR VELOCITY, m / sec.

FIG. 47

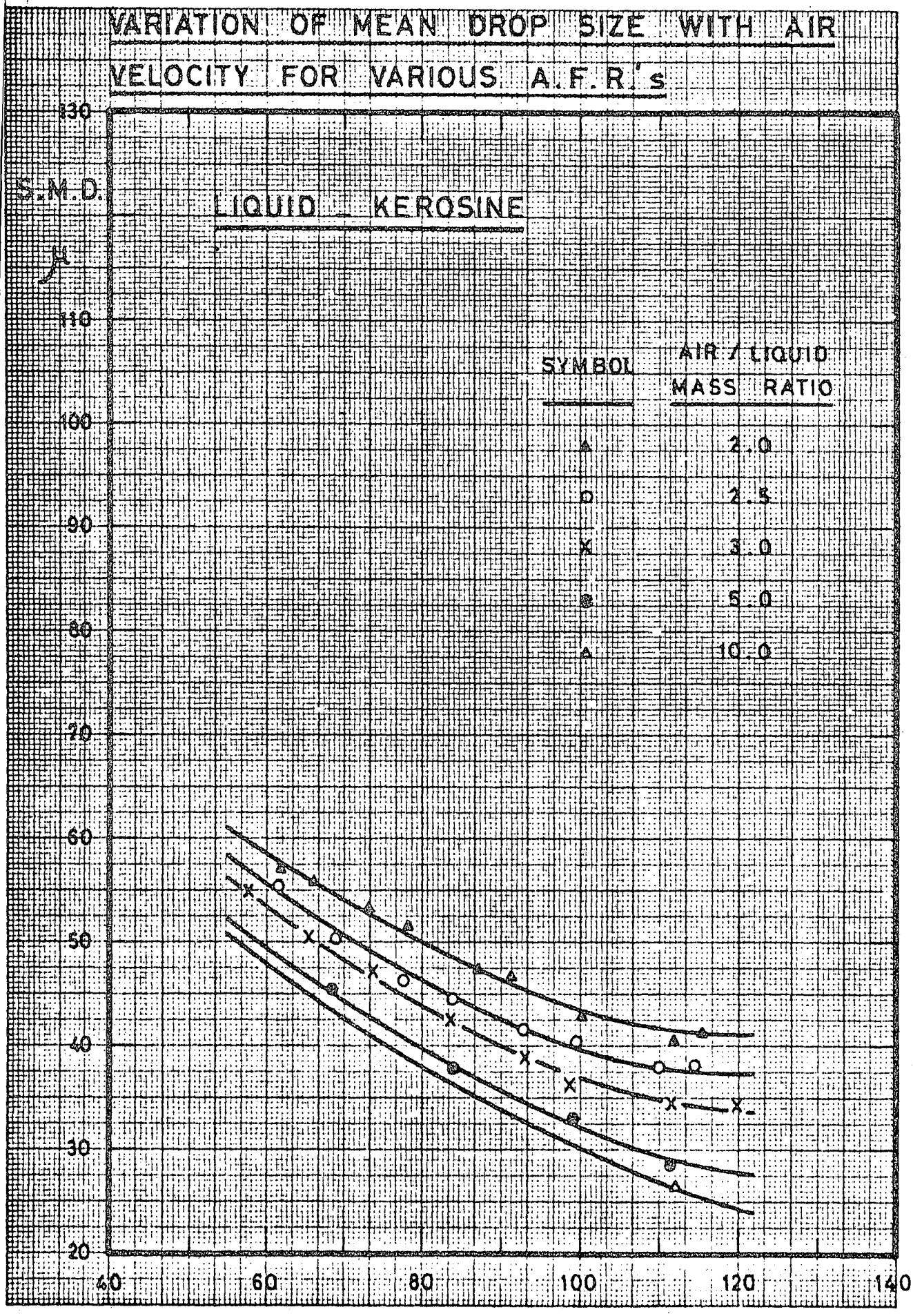
VARIATION OF MEAN DROP SIZE WITH AIR VELOCITY FOR VARIOUS A.F.R.'s
LIQUID - KEROSINE
S.M.D. μ
SYMBOL
AIR / LIQUID MASS RATIO
2.0
2.5
3.0
5.0
10.0
130
110
100
90
80
70
60
50
40
30
20
40
60
80
100
120
140
ATOMIZING AIR VELOCITY, m/sec.

FIG. 48

VARIATION OF MEAN DROPLET SIZE WITH AIR VELOCITY FOR VARIOUS LIQUID FLOWS AND A.F.R.s

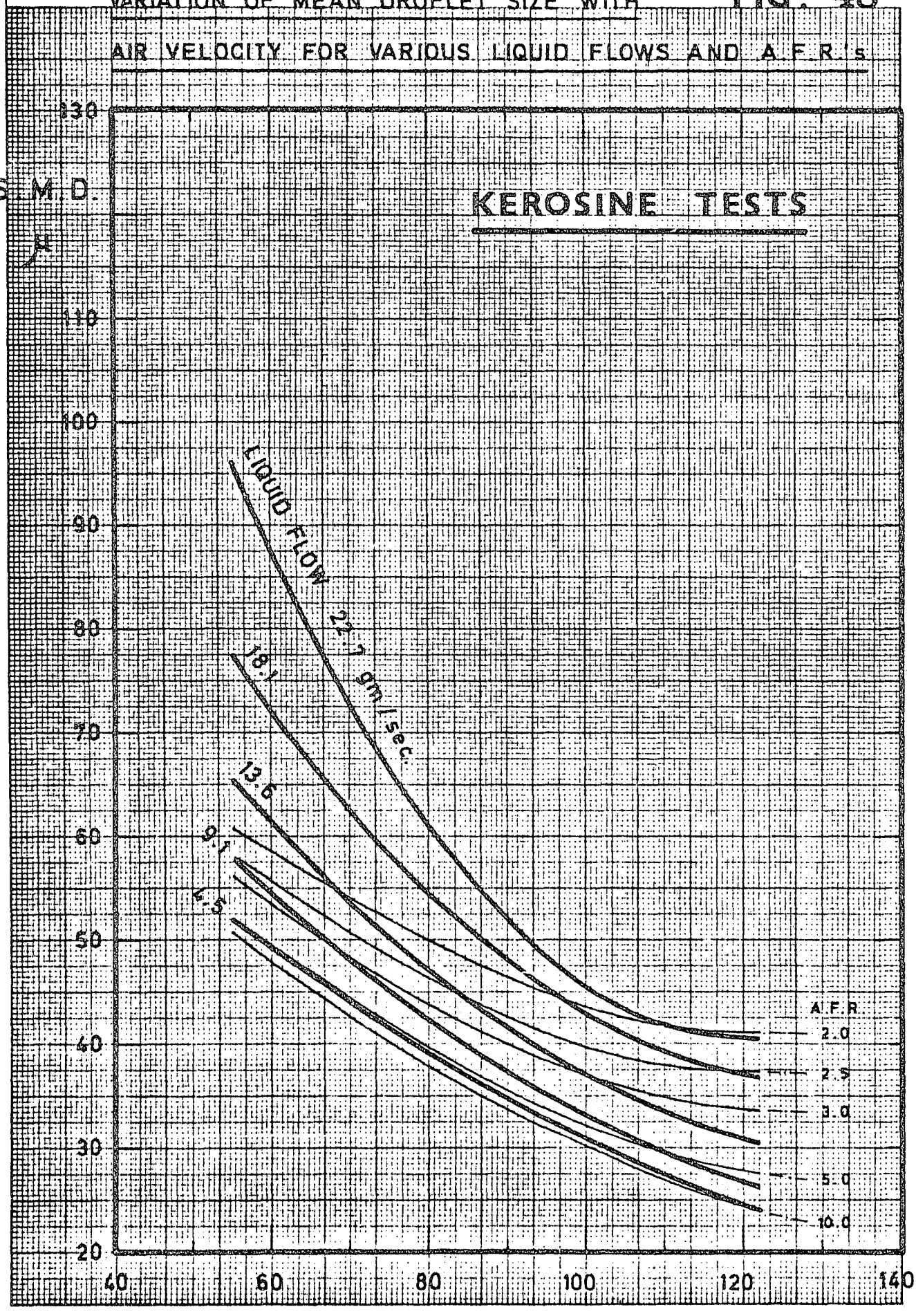

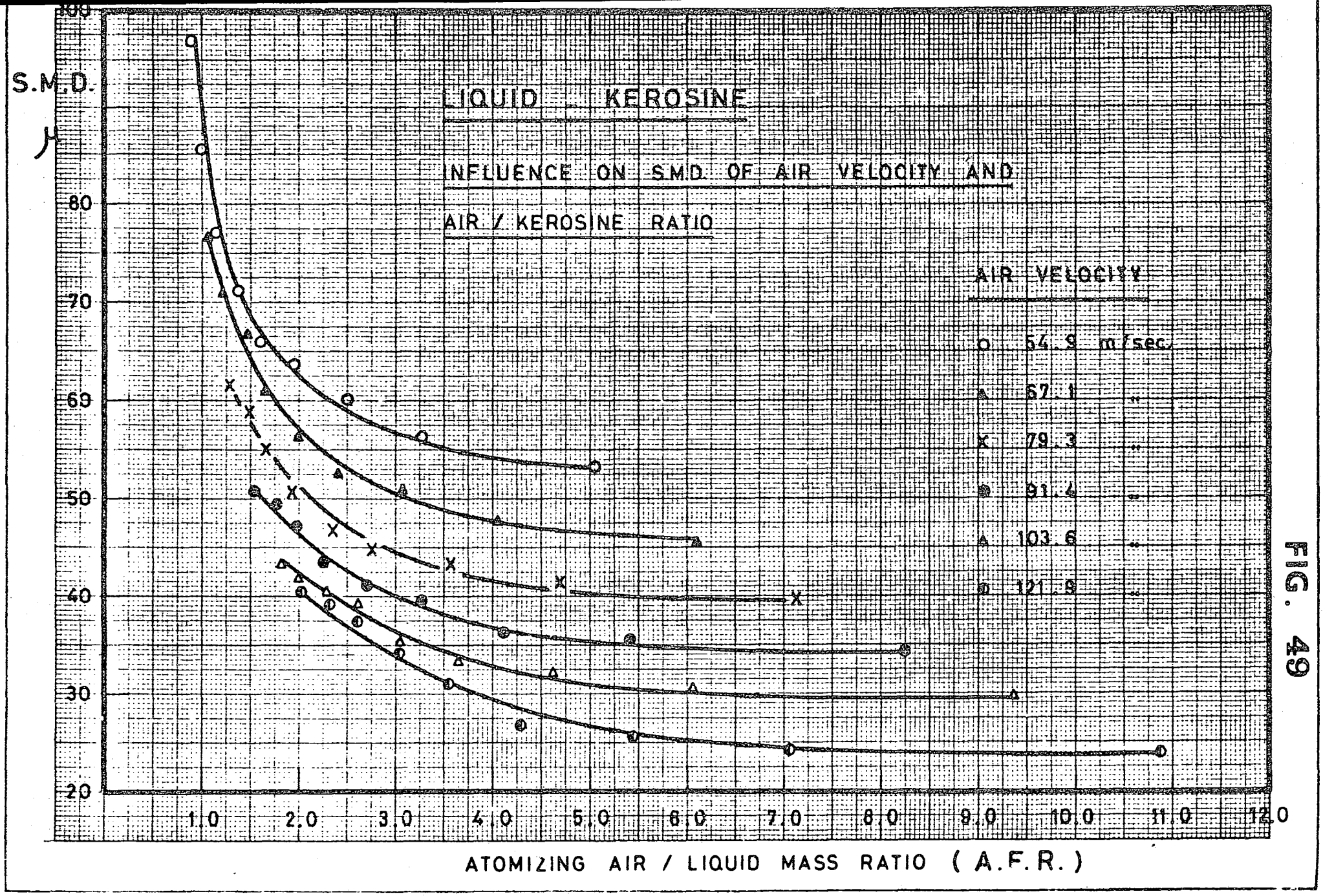
S.M.D.
μ
LIQUID : KEROSINE
INFLUENCE ON S.M.D. OF AIR VELOCITY AND
AIR / KEROSINE RATIO
AIR VELOCITY
54.9 m/sec.
67.1 "
79.3 "
91.4 "
103.6 "
121.9 "
100
90
80
70
60
50
40
30
20
1.0
2.0
3.0
4.0
5.0
6.0
7.0
8.0
9.0
10.0
11.0
12.0
ATOMIZING AIR / LIQUID MASS RATIO (A.F.R.)

FIG. 49

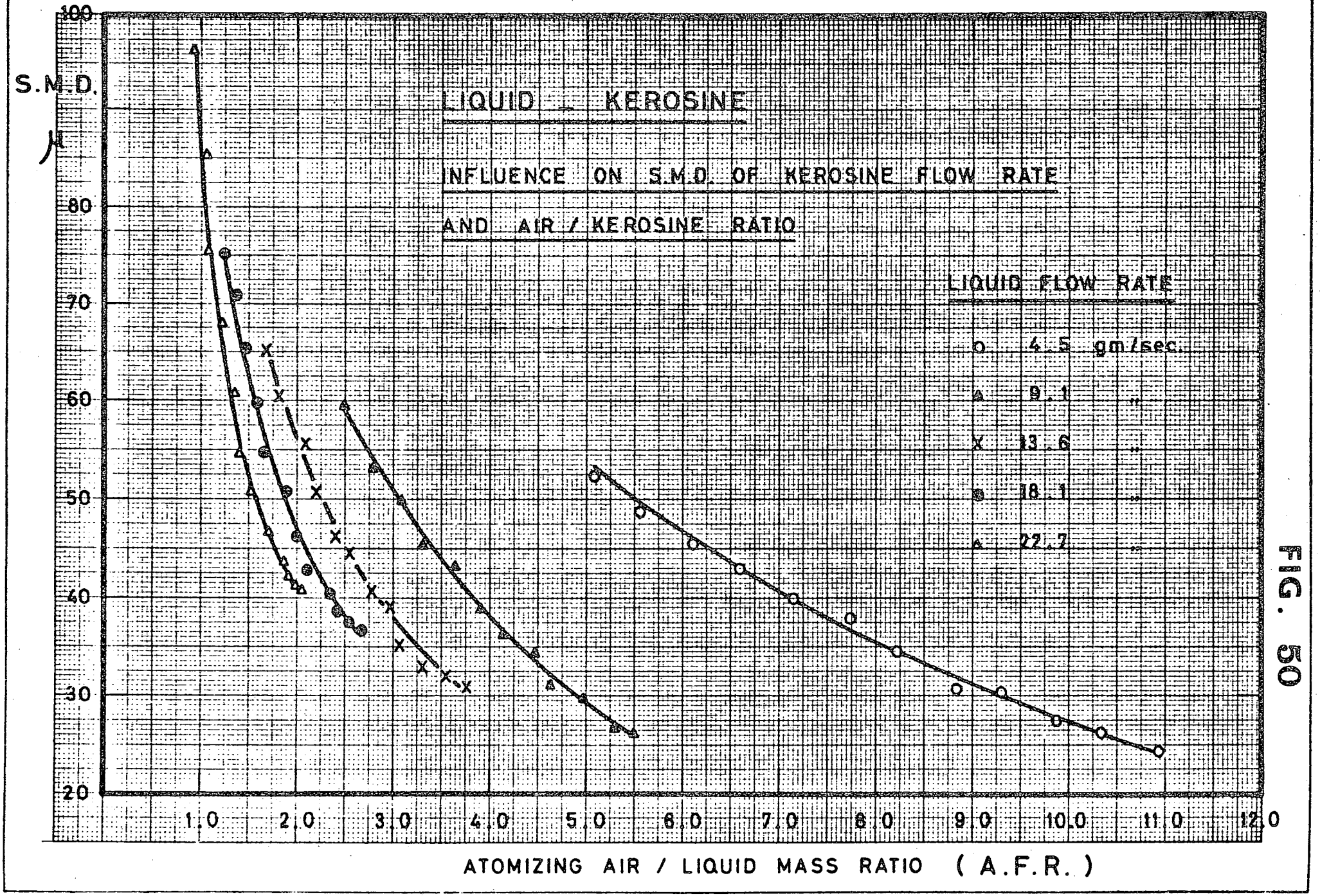
LIQUID - KEROSINE
INFLUENCE ON S.M.D. OF KEROSINE FLOW RATE
AND AIR / KEROSINE RATIO
S.M.D.
μ
LIQUID FLOW RATE
o 4.5 gm/sec.
Δ 9.1 "
X 13.6 "
● 18.1 "
▲ 22.7 "
100
80
70
60
50
40
30
20
1.0
2.0
3.0
4.0
5.0
6.0
7.0
8.0
9.0
10.0
11.0
12.0
ATOMIZING AIR / LIQUID MASS RATIO (A.F.R.)

FIG. 50

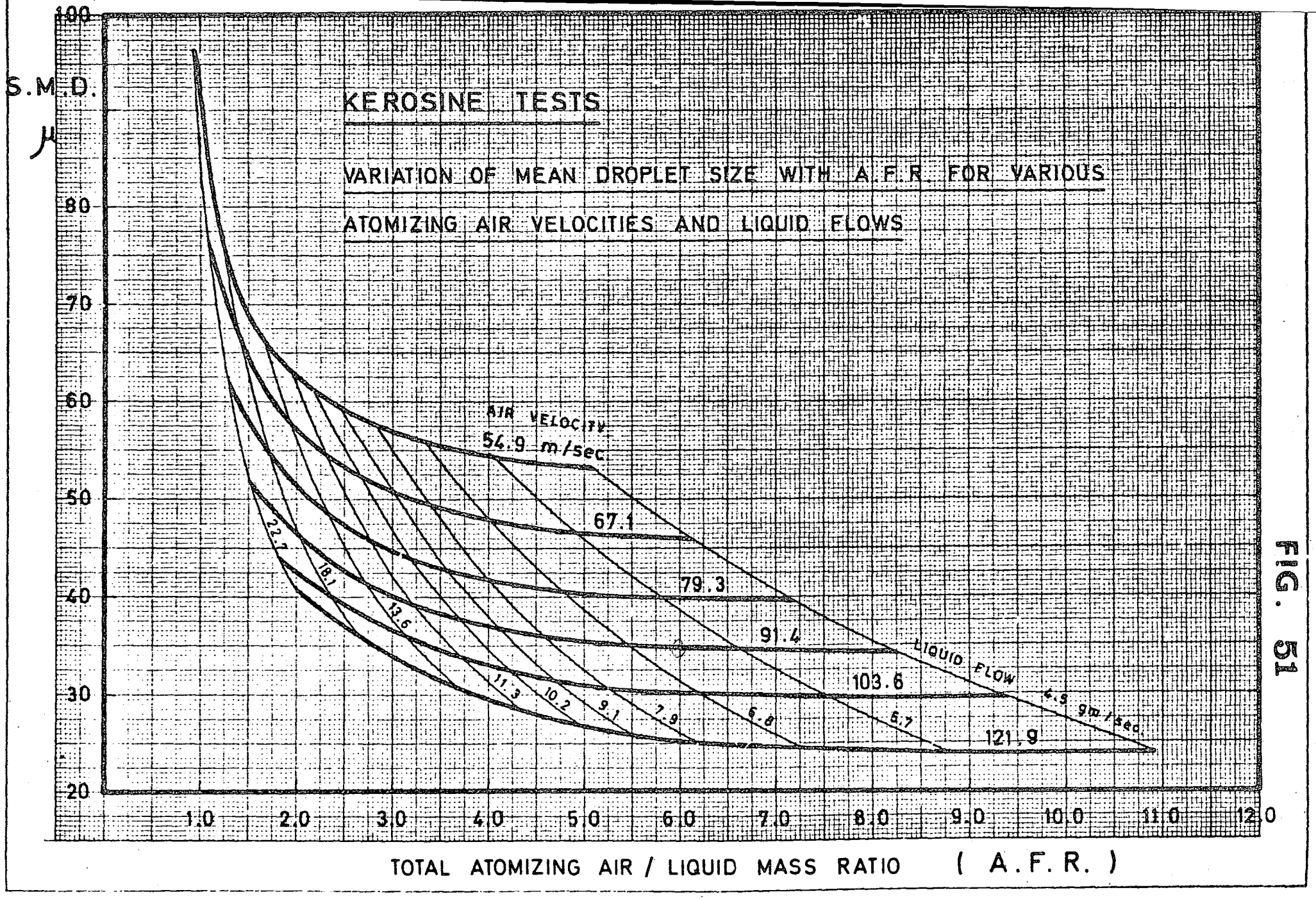
KEROSINE TESTS
VARIATION OF MEAN DROPLET SIZE WITH A.F.R FOR VARIOUS
ATOMIZING AIR VELOCITIES AND LIQUID FLOWS
S.M.D.
μ
100
80
70
60
50
40
30
20
1.0
2.0
3.0
4.0
5.0
6.0
7.0
8.0
9.0
10.0
11.0
12.0
TOTAL ATOMIZING AIR / LIQUID MASS RATIO (A.F.R.)
AIR VELOCITY
54.9 m/sec
67.1
79.3
91.4
103.6
121.9
LIQUID FLOW
6.9 gm/sec
6.7
6.8
7.9
9.1
10.2
11.3
13.6
18.1
22.7

FIG. 51

WATER TESTS

FIG. 52

EFFECT OF SHROUD AIR VELOCITY ON S.M.D.

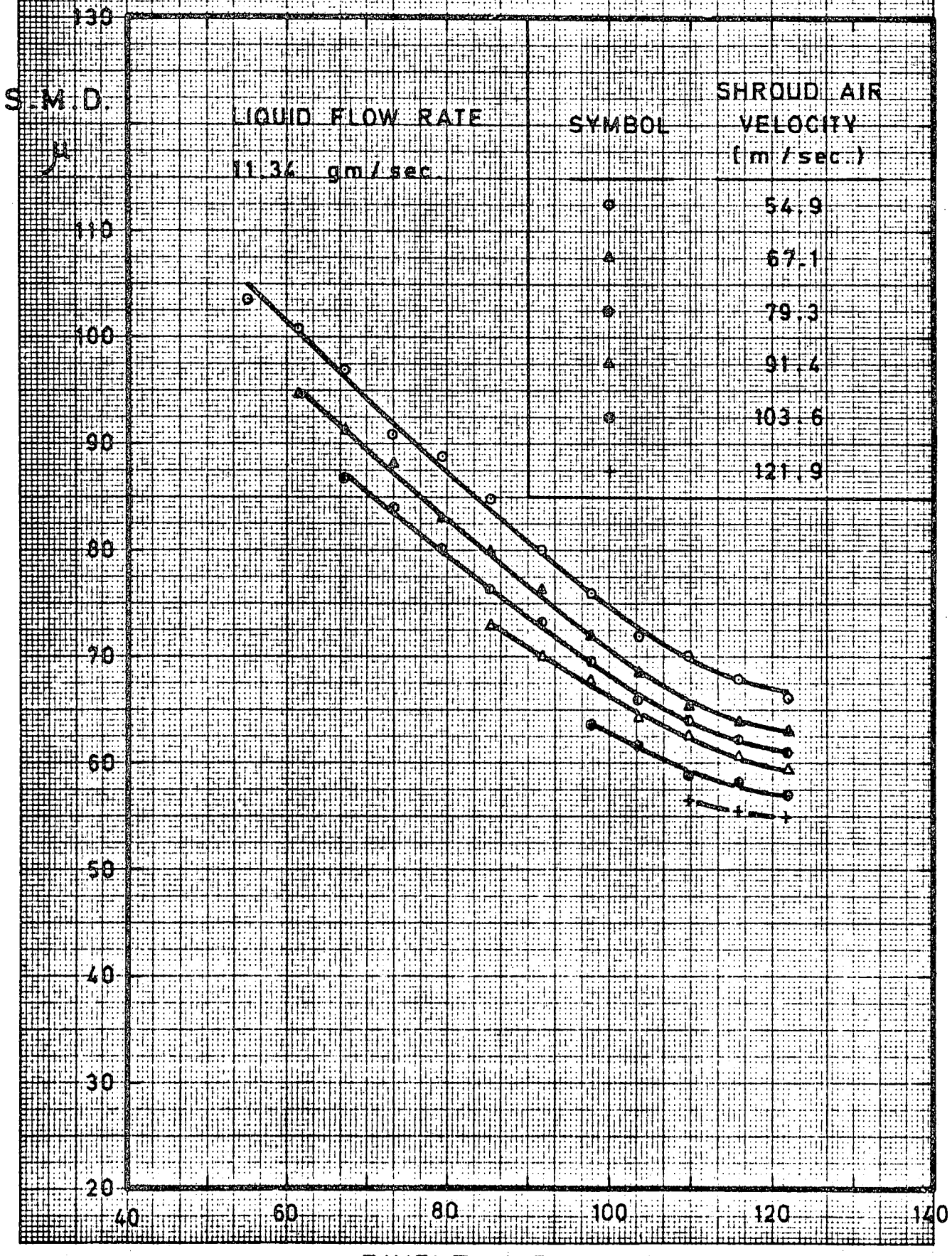

WATER TESTS

FIG. 53

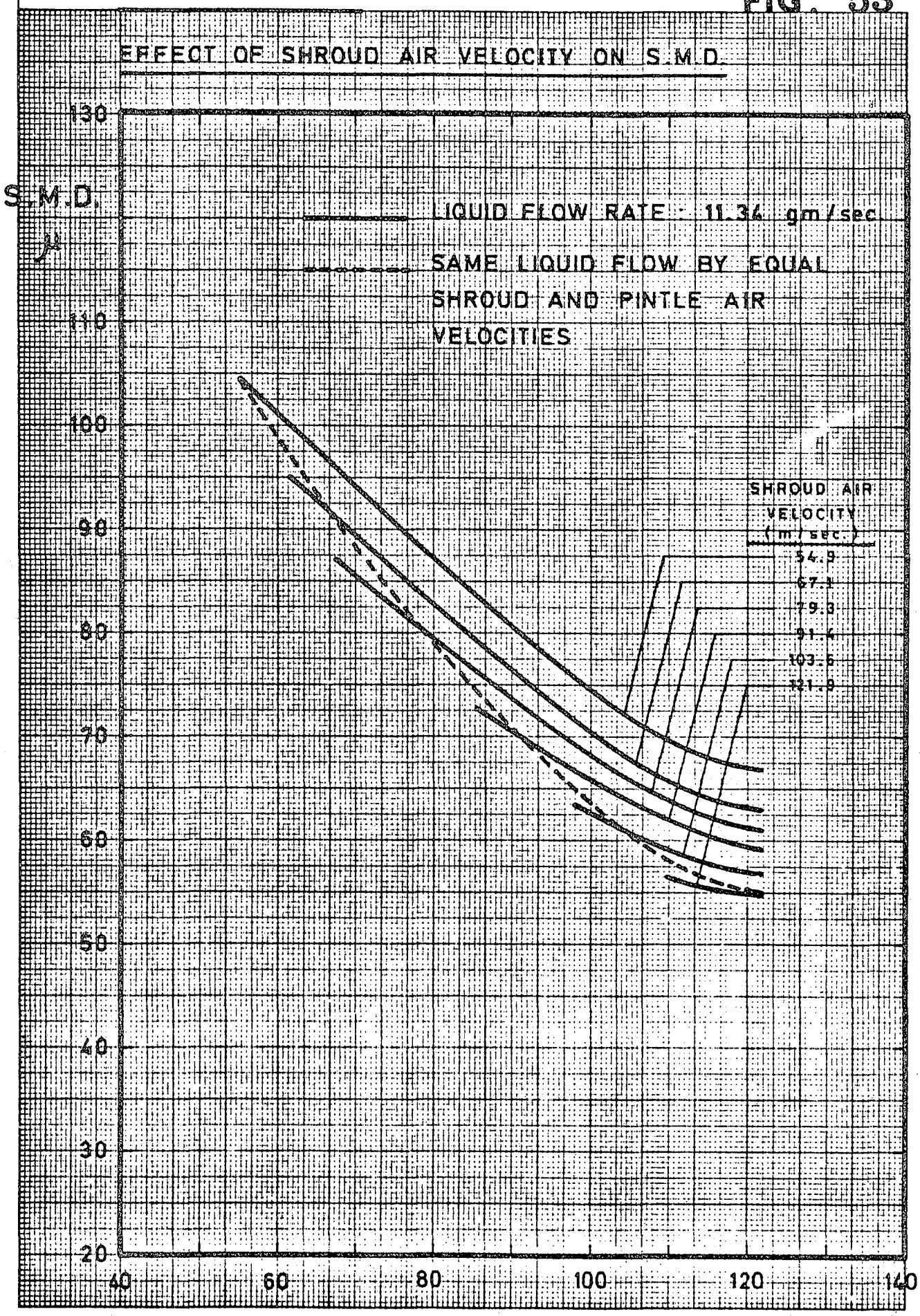

WATER TESTS

FIG. 54

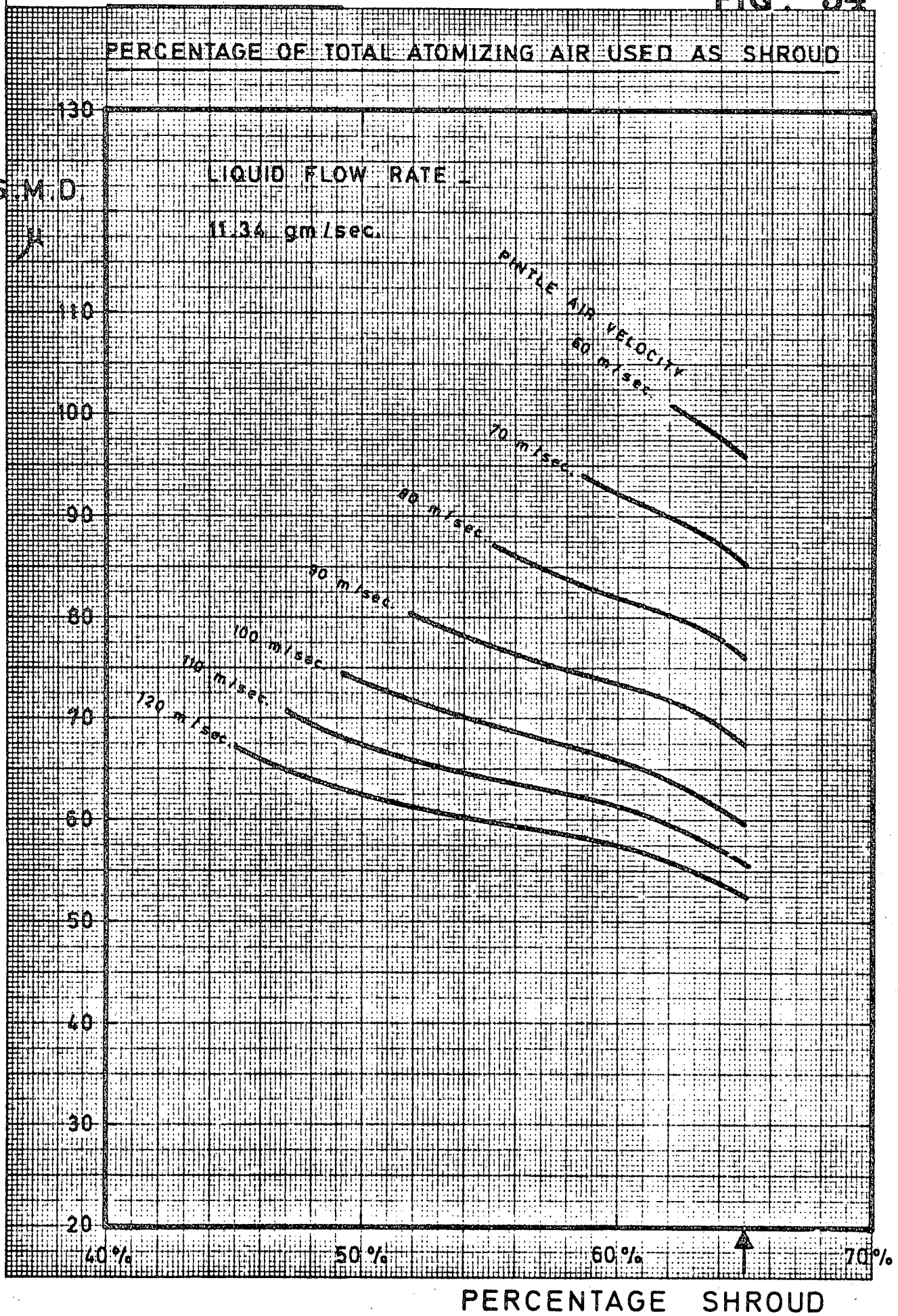

KEROSINE TESTS

FIG. 55

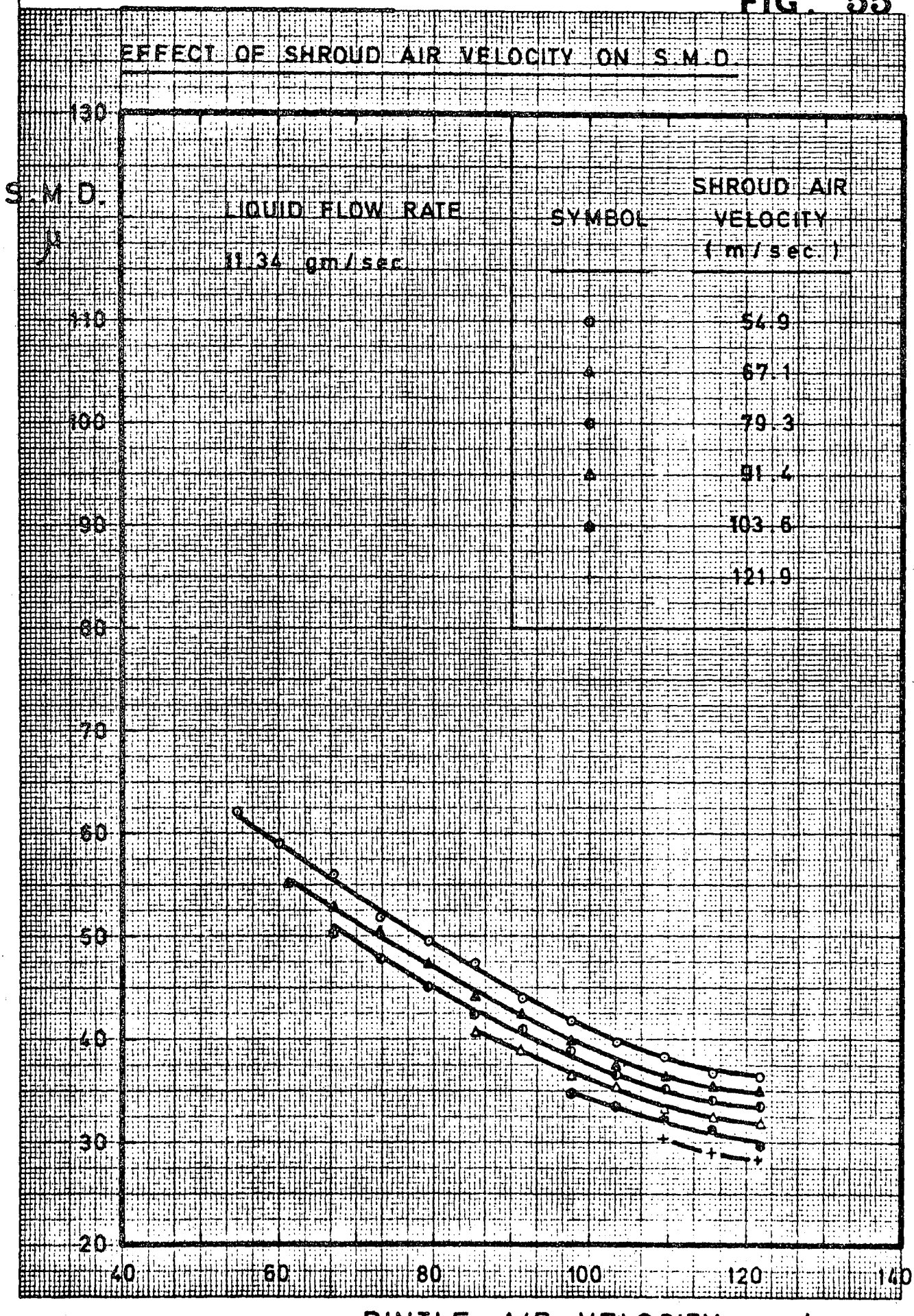

KEROSINE TESTS

FIG. 56

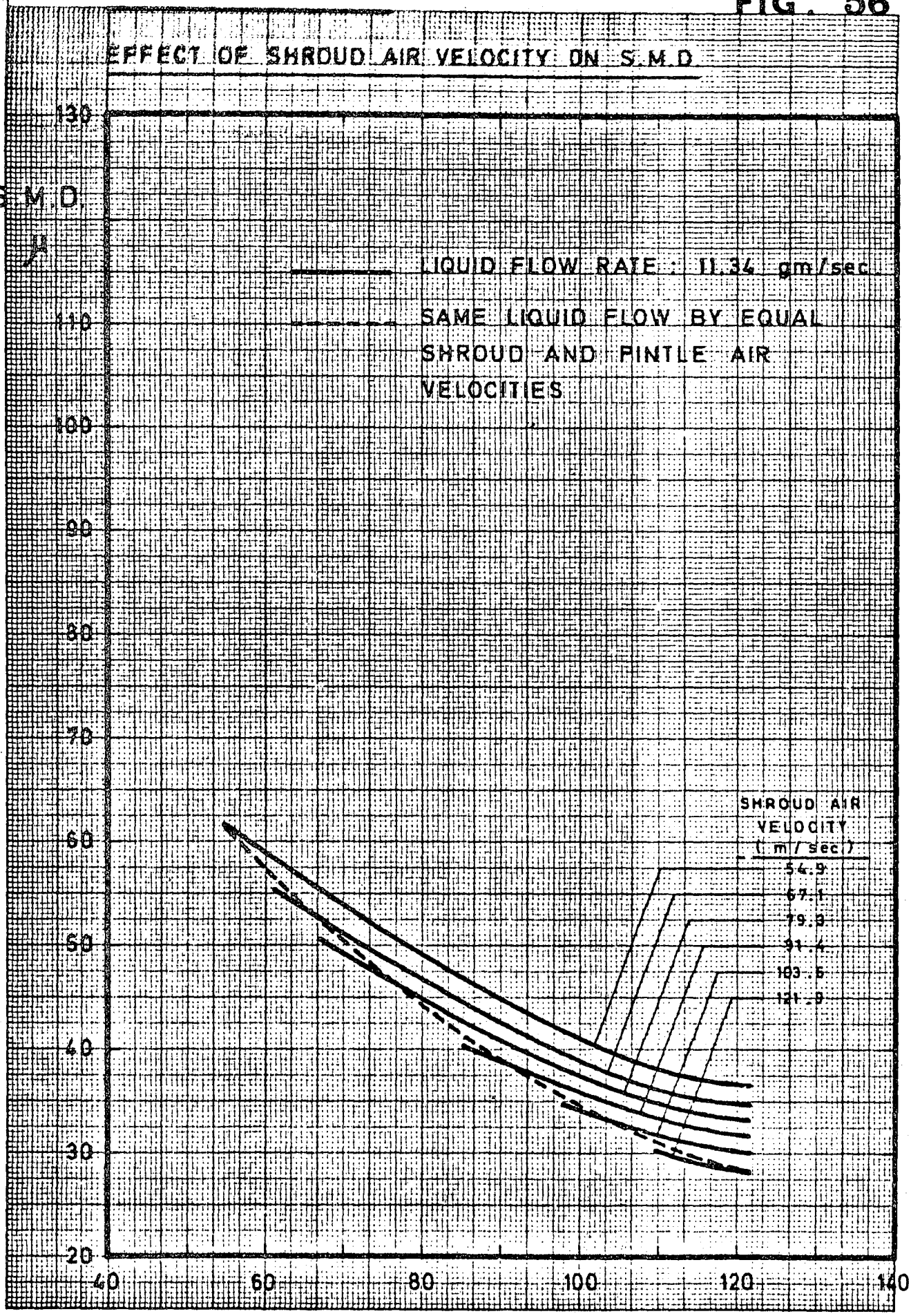

KEROSINE TESTS

FIG. 57

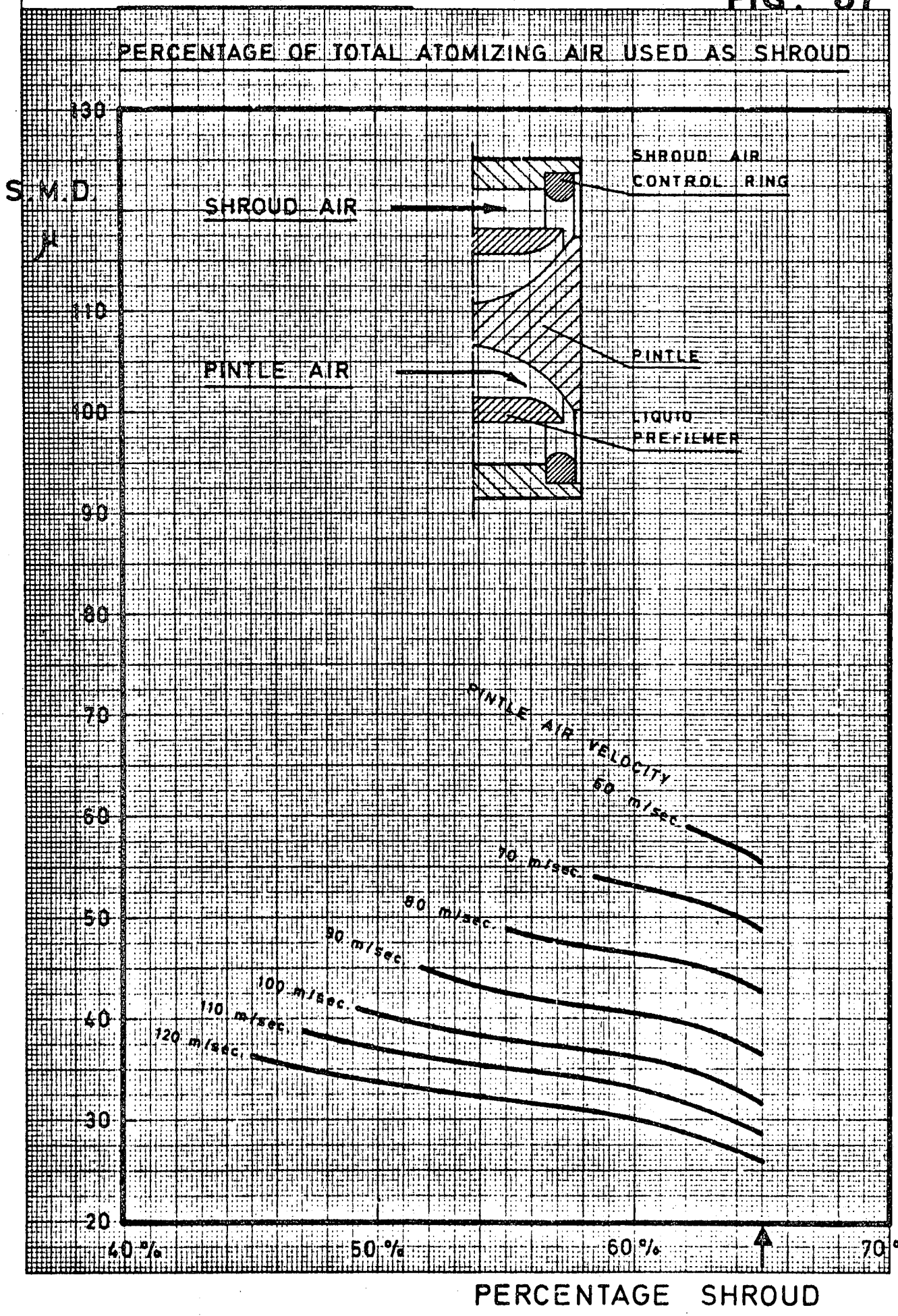

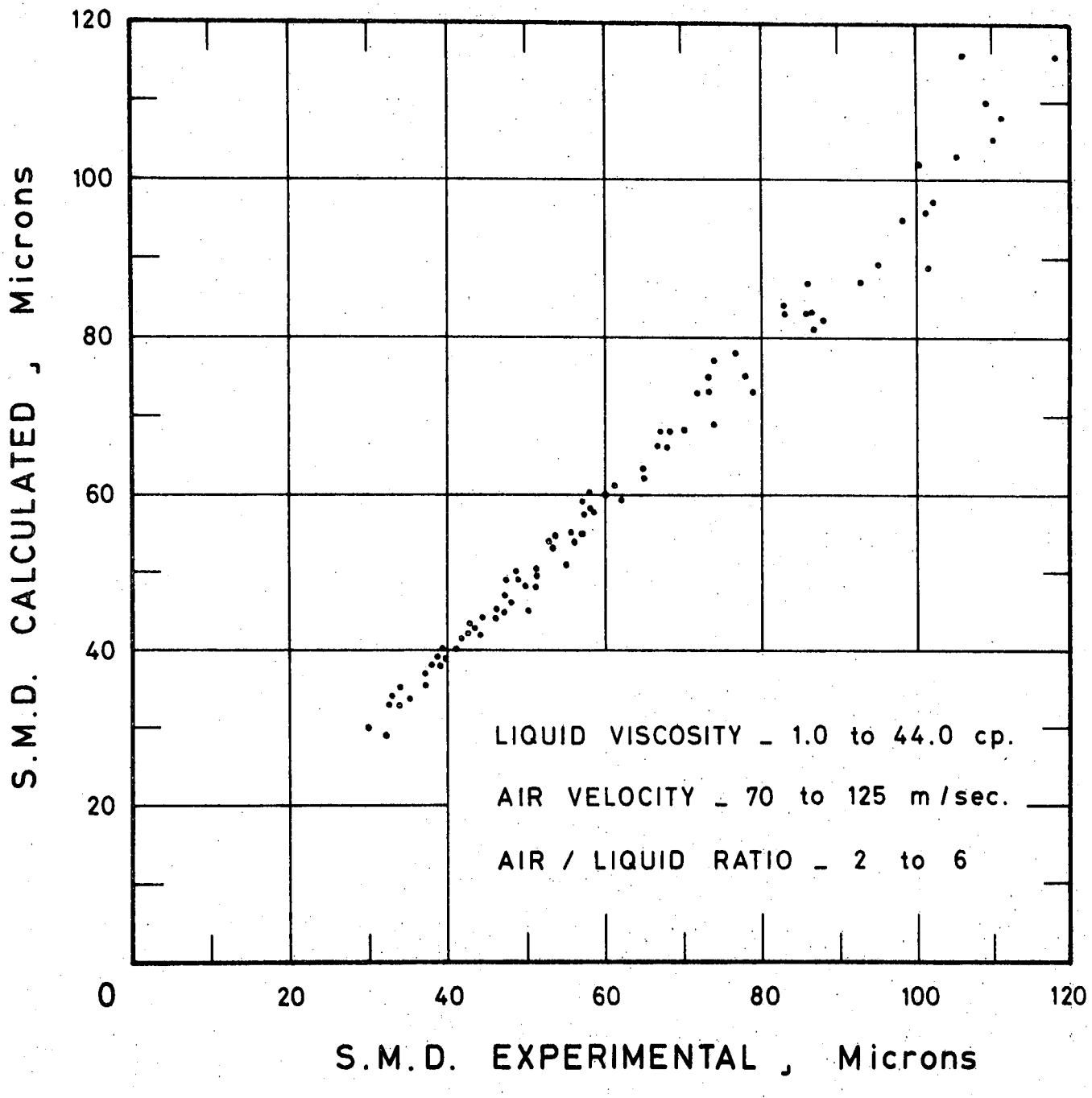

FIG. 58 COMPARISON OF CALCULATED AND EXPERIMENTAL VALUES OF S.M.D.

(LIQUID VISCOSITY DATA)

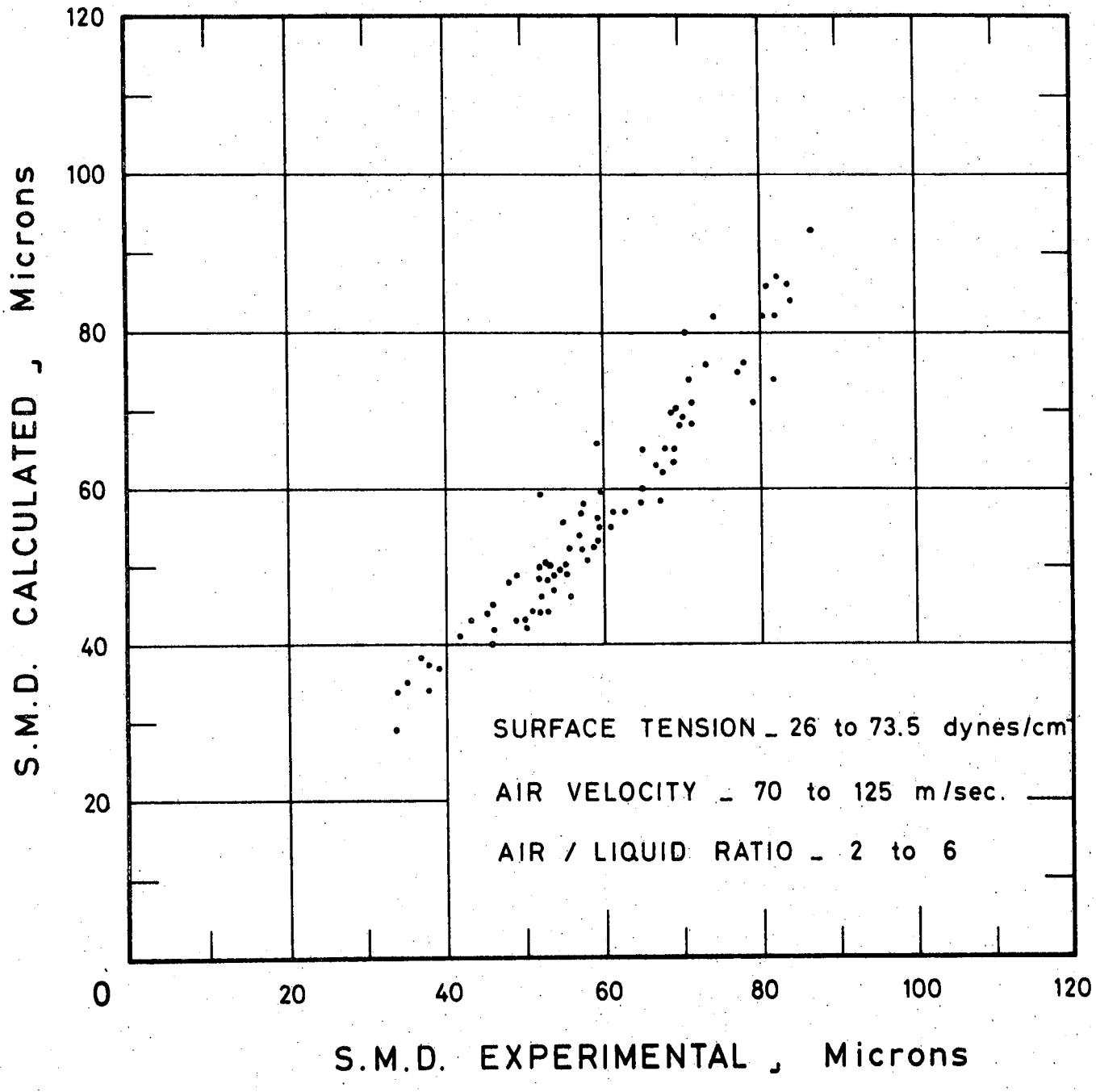

FIG. 59 COMPARISON OF CALCULATED AND EXPERIMENTAL VALUES OF S.M.D.

(SURFACE TENSION DATA)

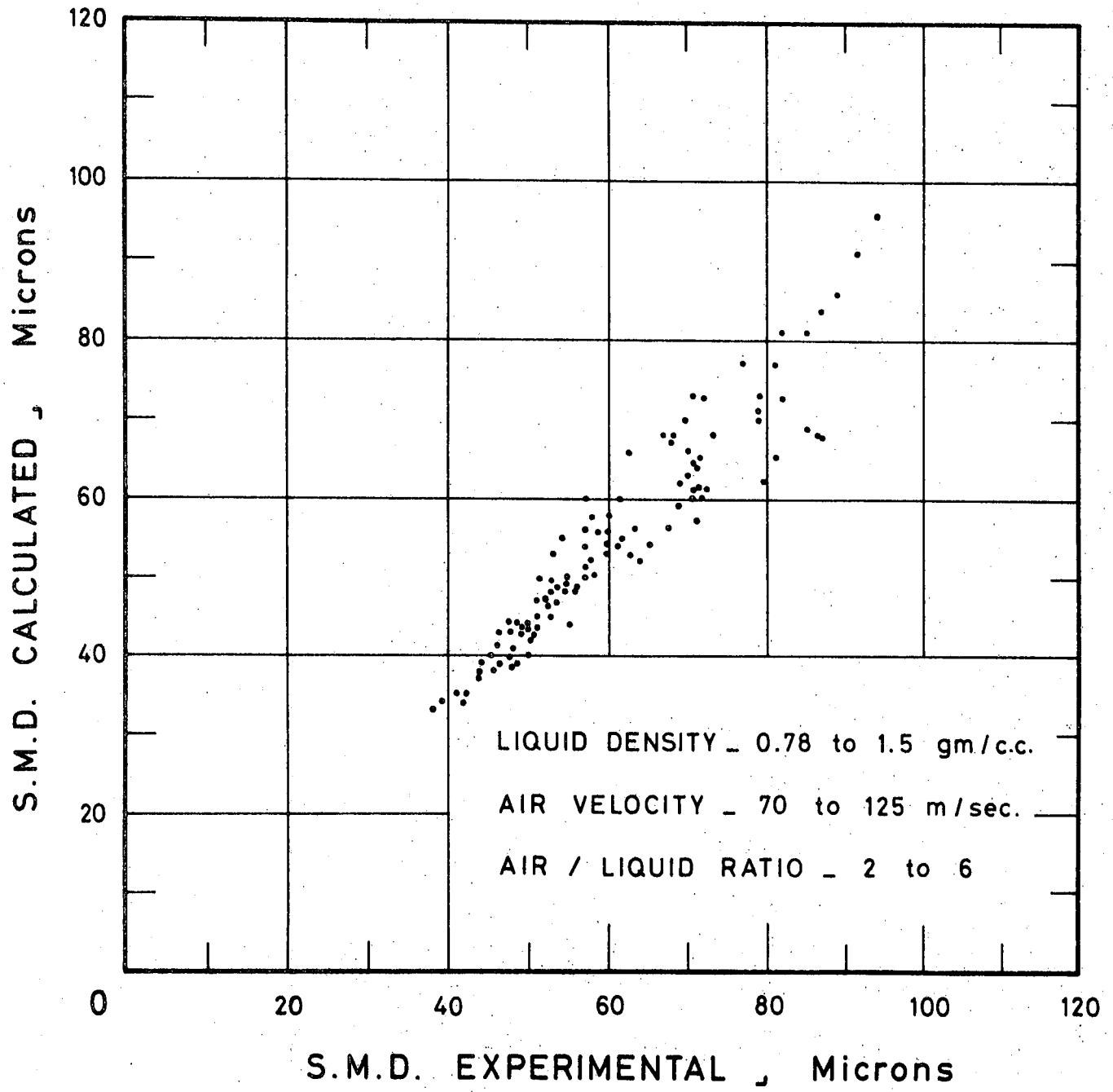

FIG. 60 COMPARISON OF CALCULATED AND EXPERIMENTAL VALUES OF S.M.D.

(LIQUID DENSITY DATA)

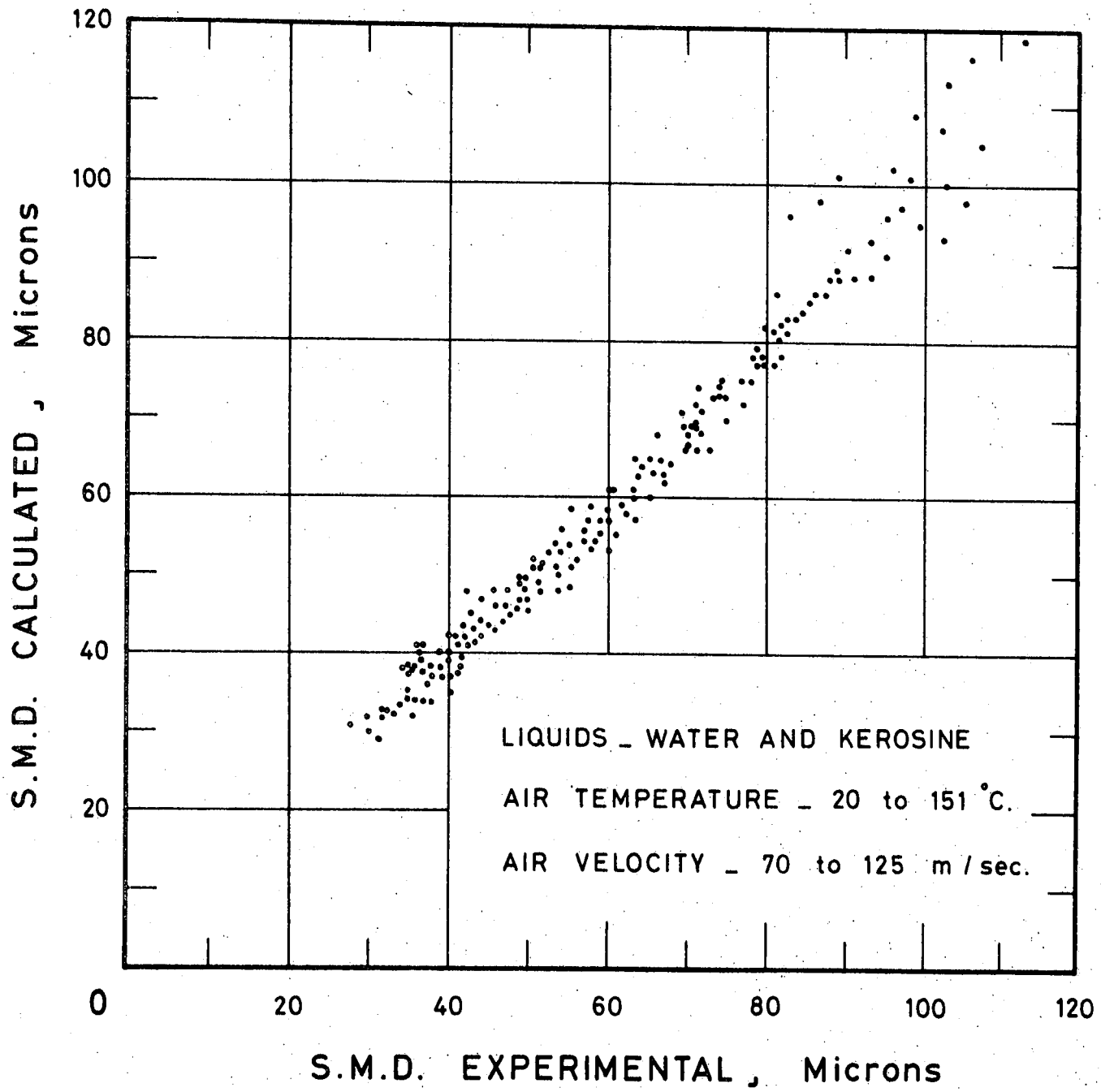

FIG. 61 COMPARISON OF CALCULATED AND EXPERIMENTAL VALUES OF S.M.D.

(MAIN VARIABLES _ AIR VELOCITY AND TEMP.)

FIG. 62

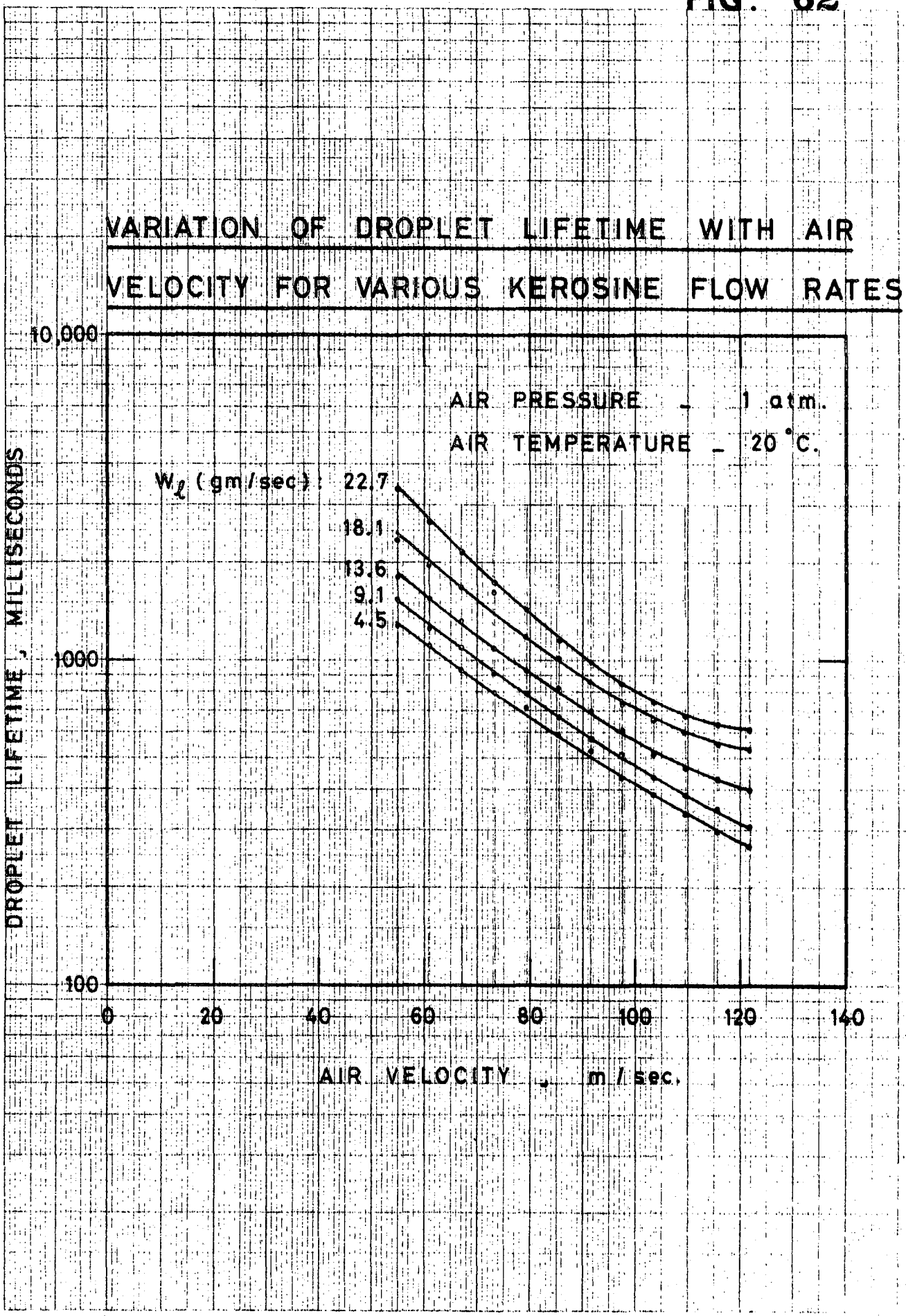
VARIATION OF DROPLET LIFETIME WITH AIR VELOCITY FOR VARIOUS KEROSINE FLOW RATES
AIR PRESSURE - 1 atm.
AIR TEMPERATURE - 20 °C.
W_l (gm/sec): 22.7
18.1
13.6
9.1
4.5
10,000
1000
100
DROPLET LIFETIME, MILLISECONDS
0
20
40
60
80
100
120
140
AIR VELOCITY - m/sec.

FIG. 63

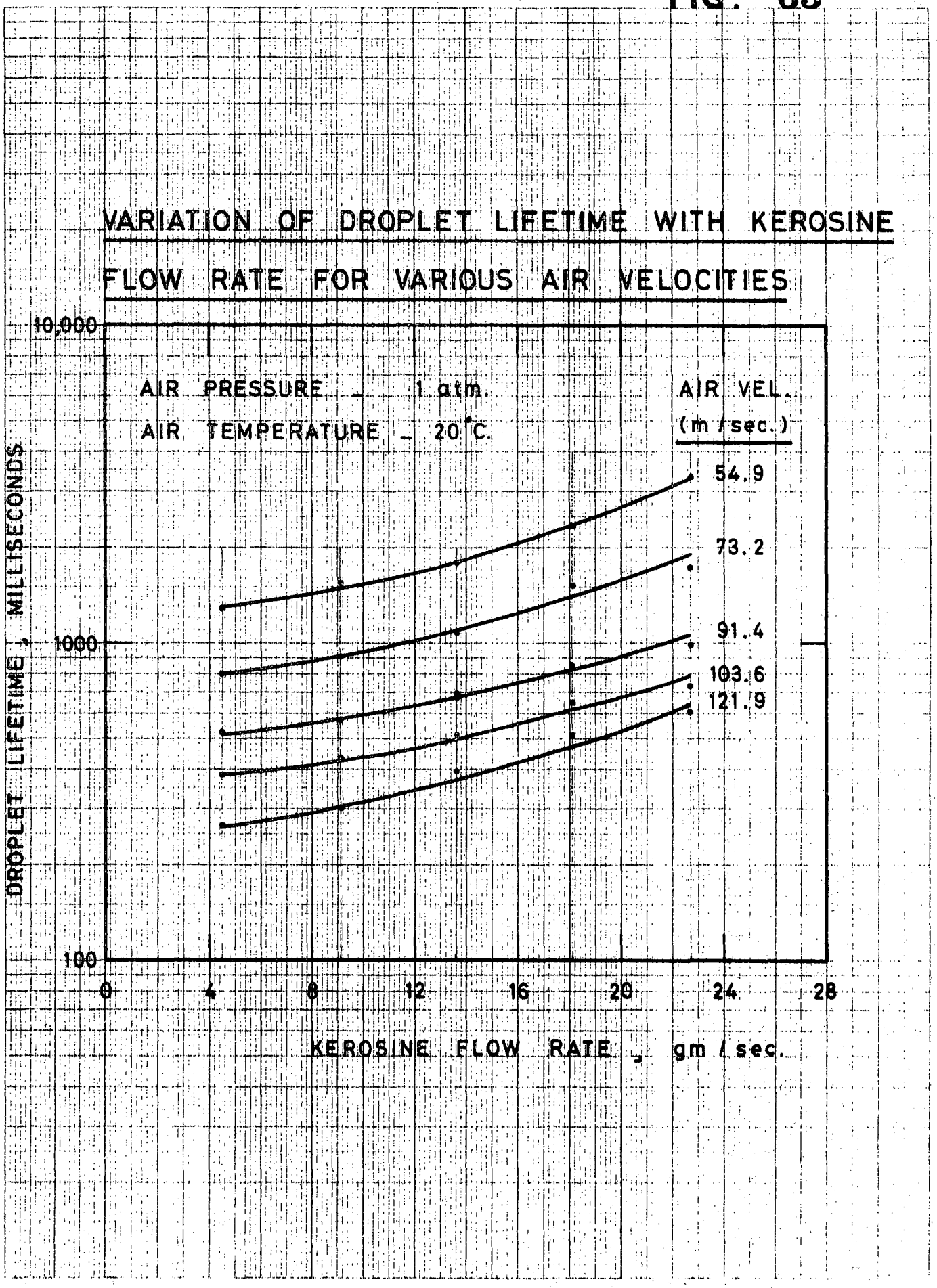
VARIATION OF DROPLET LIFETIME WITH KEROSINE FLOW RATE FOR VARIOUS AIR VELOCITIES
AIR PRESSURE - 1 atm.
AIR TEMPERATURE - 20°C.
AIR VEL. (m/sec.)
54.9
73.2
91.4
103.6
121.9
DROPLET LIFETIME, MILLISECONDS
10,000
1000
100
0
4
8
12
16
20
24
28
KEROSINE FLOW RATE, gm/sec.

FIG. 64

VARIATION OF DISTANCE THE DROPLETS MOVED DURING LIFETIME WITH AIR VELOCITY FOR VARIOUS KEROSINE FLOW RATES

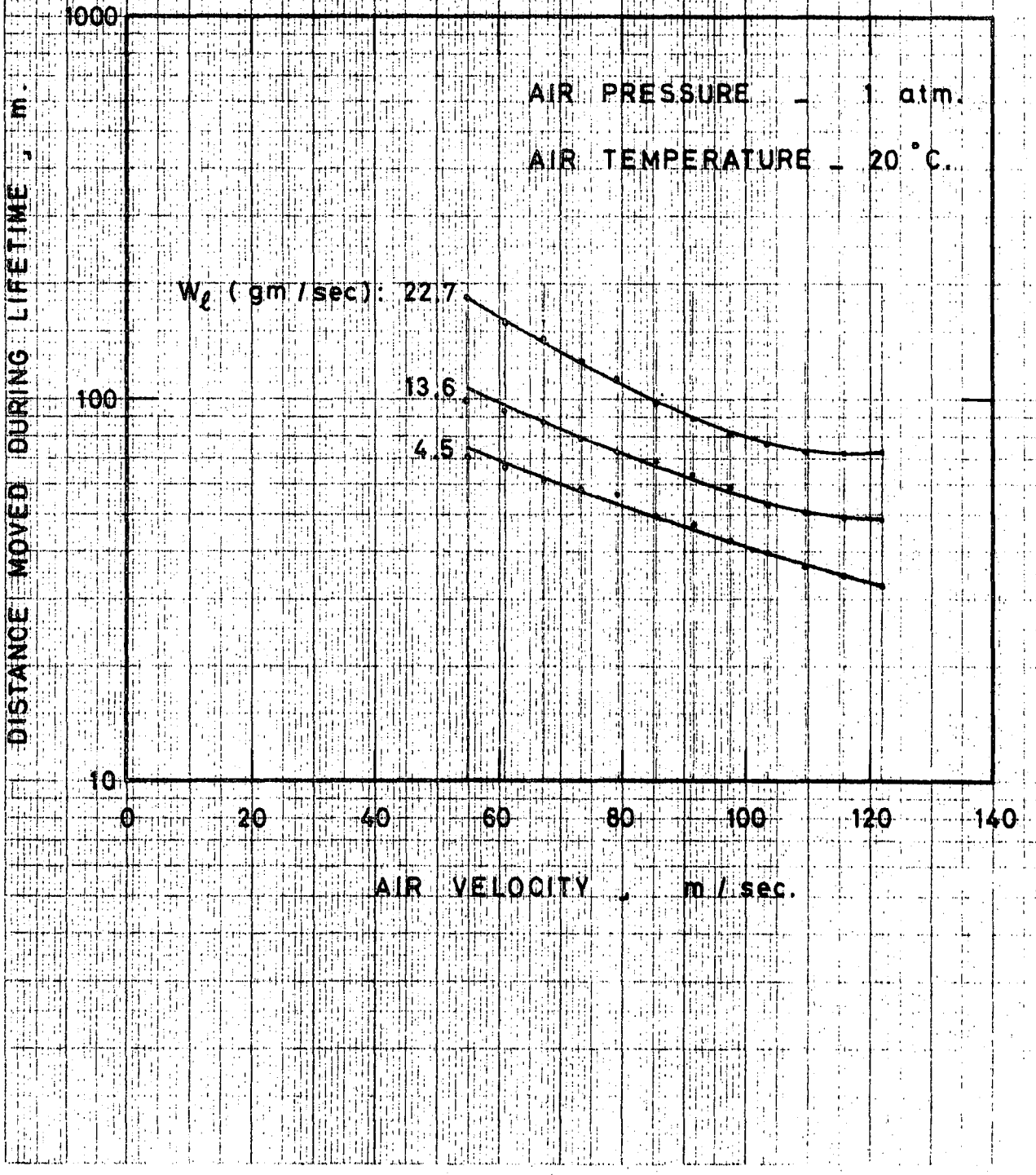

FIG. 65

VARIATION OF DISTANCE THE DROPLETS MOVED DURING LIFETIME WITH KEROSINE FLOW RATE FOR VARIOUS AIR VELOCITIES

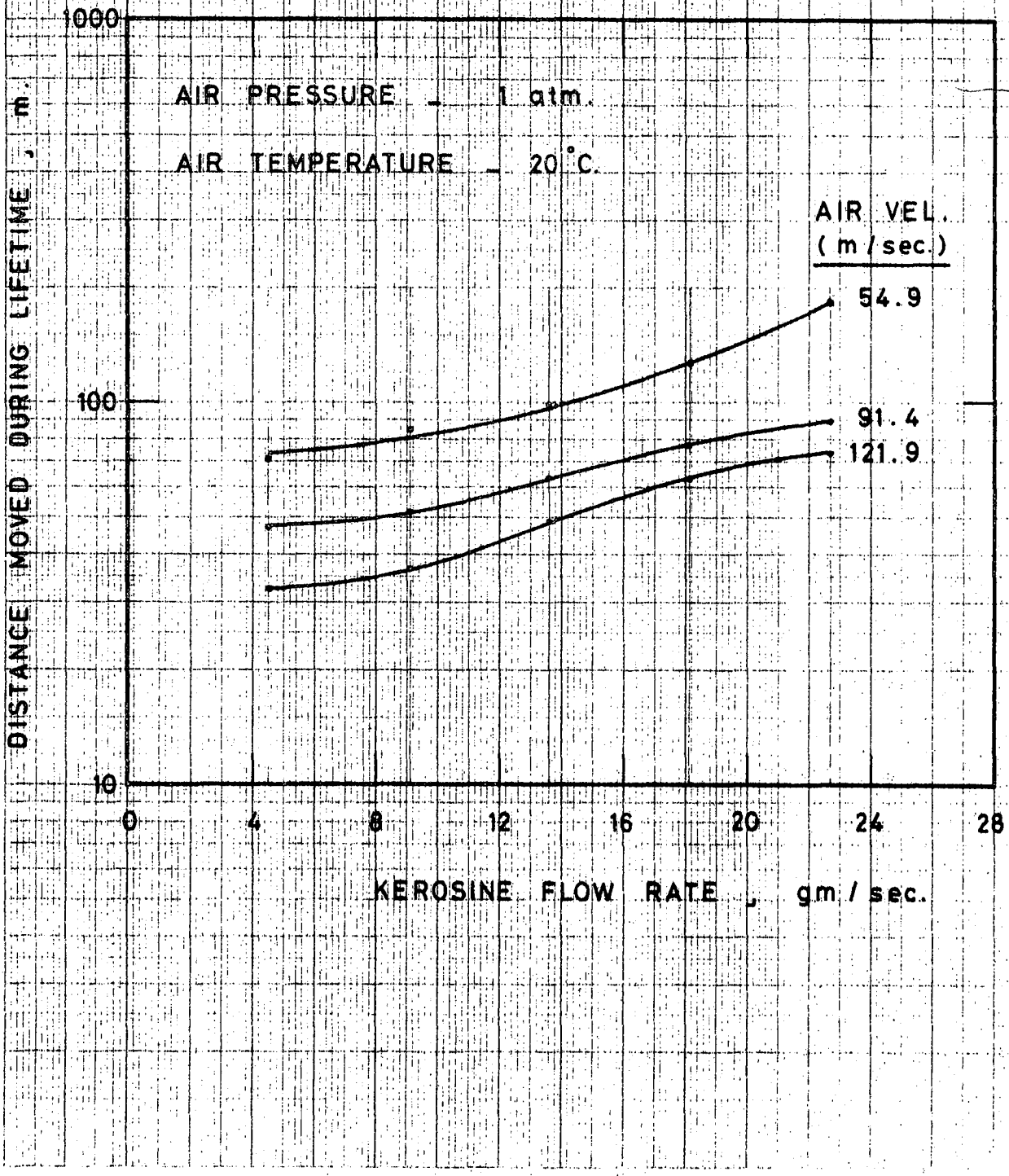

FIG. 66

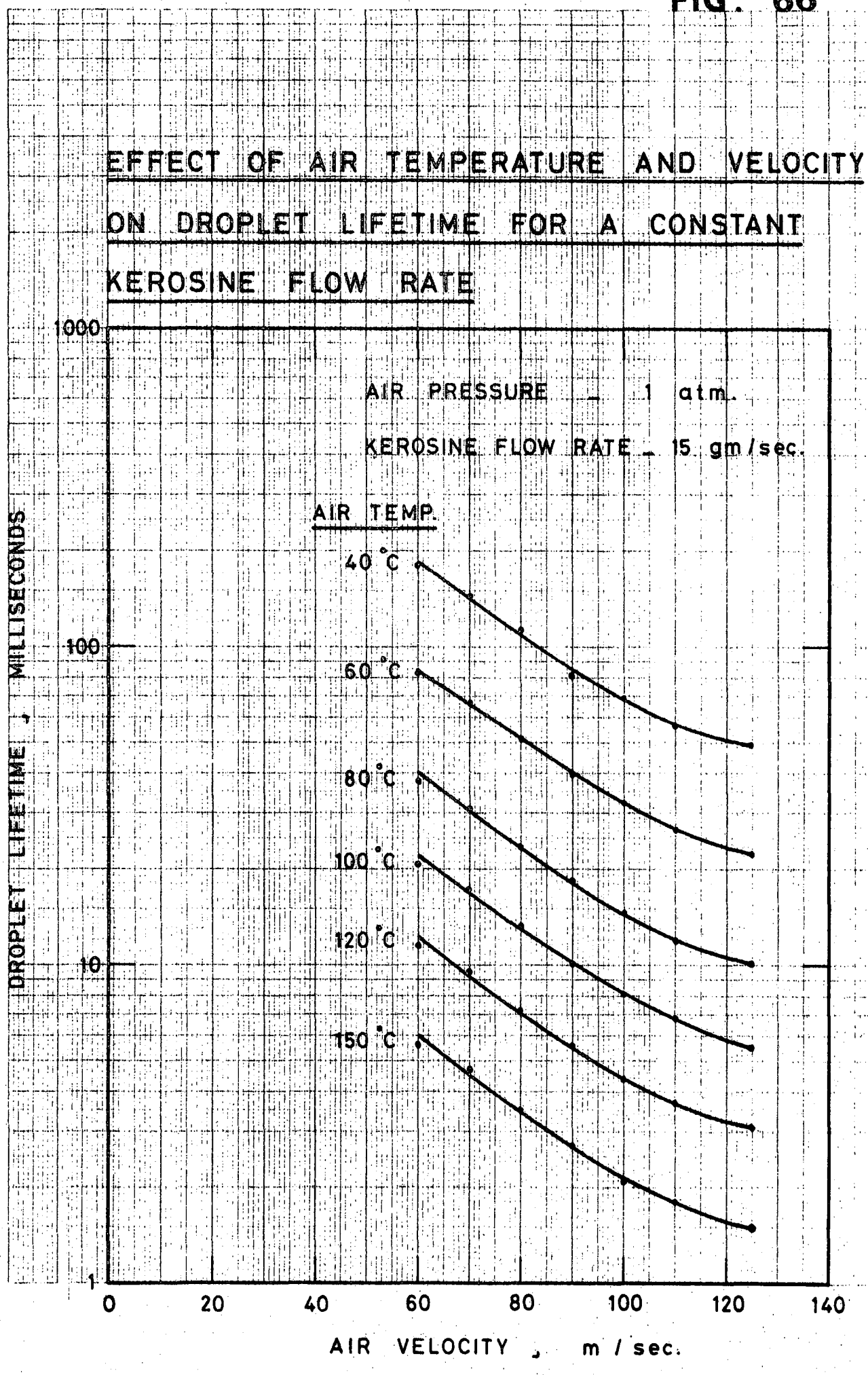
EFFECT OF AIR TEMPERATURE AND VELOCITY ON DROPLET LIFETIME FOR A CONSTANT KEROSINE FLOW RATE
AIR PRESSURE - 1 atm.
KEROSINE FLOW RATE - 15 gm/sec.
AIR TEMP.
40 °C
60 °C
80 °C
100 °C
120 °C
150 °C
DROPLET LIFETIME, MILLISECONDS
1000
100
10
1
0
20
40
60
80
100
120
140
AIR VELOCITY, m/sec.

FIG. 67

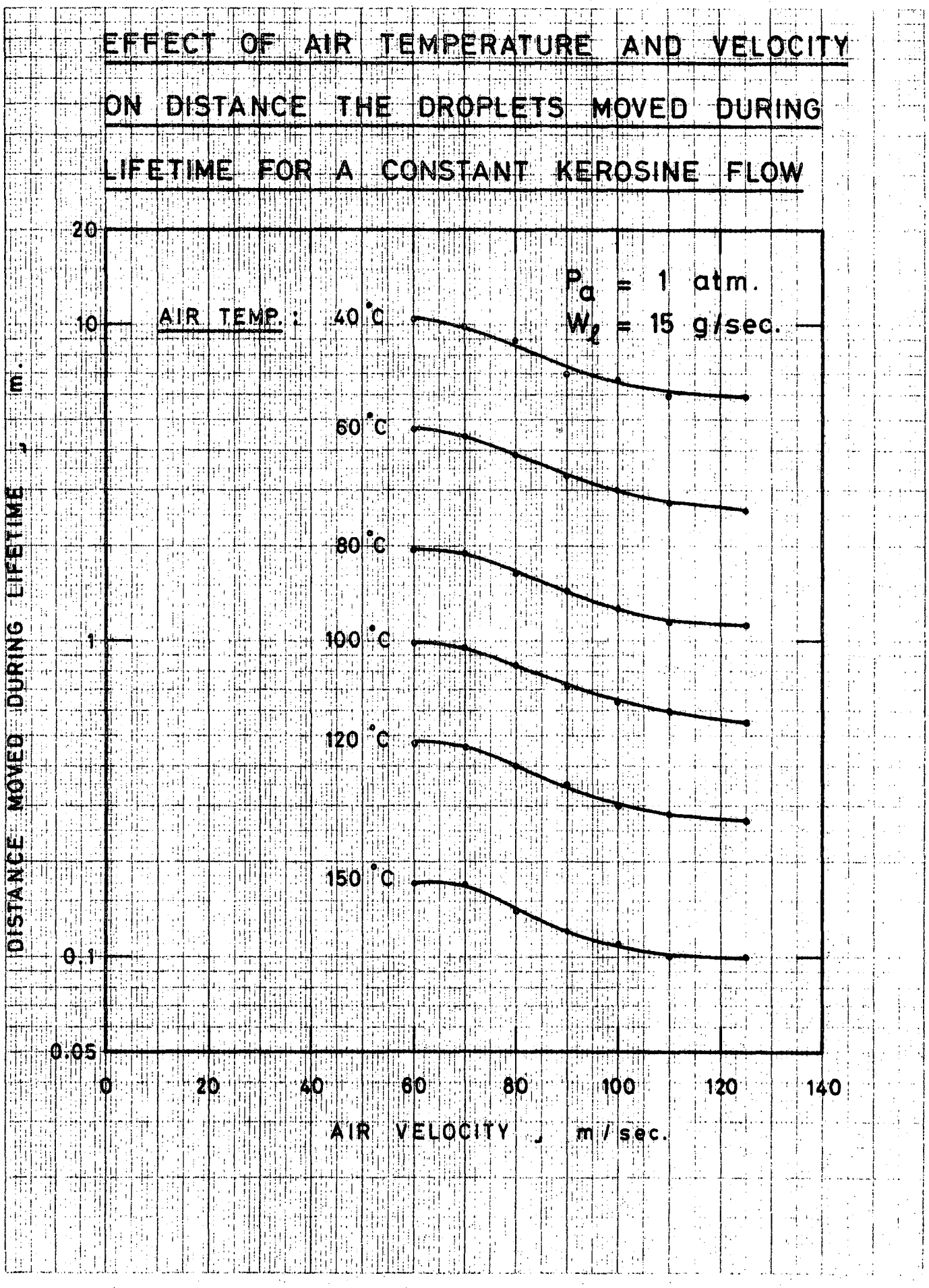
EFFECT OF AIR TEMPERATURE AND VELOCITY ON DISTANCE THE DROPLETS MOVED DURING LIFETIME FOR A CONSTANT KEROSINE FLOW
P_a = 1 atm.
W_l = 15 g/sec.
AIR TEMP. : 40 °C
60 °C
80 °C
100 °C
120 °C
150 °C
DISTANCE MOVED DURING LIFETIME , m.
20
10
1
0.1
0.05
0
20
40
60
80
100
120
140
AIR VELOCITY , m/sec.

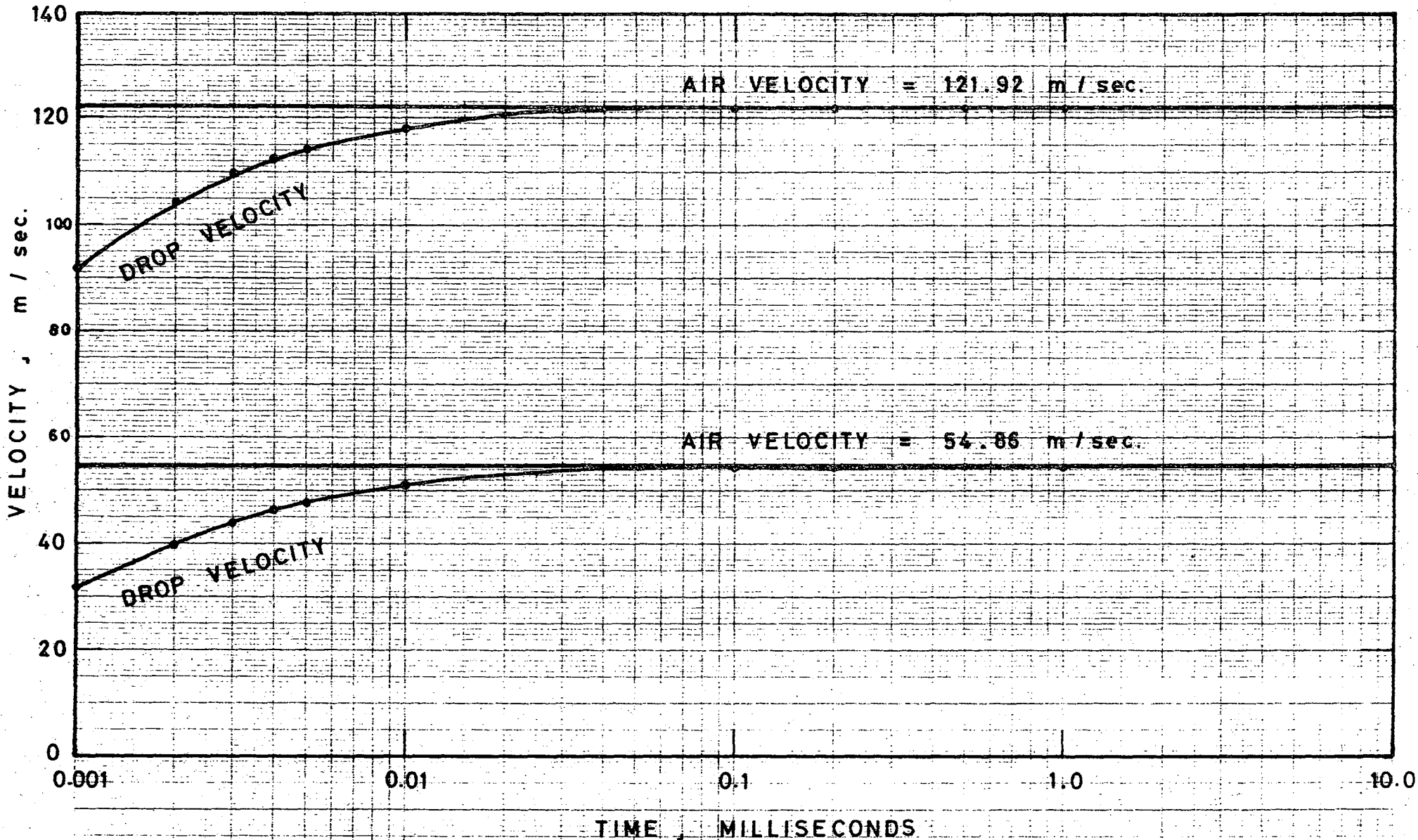

FIG. 68 GRAPHS ILLUSTRATING THE RELATIONSHIP BETWEEN THE ATOMIZING AIR VELOCITY AND THE DROP VELOCITY

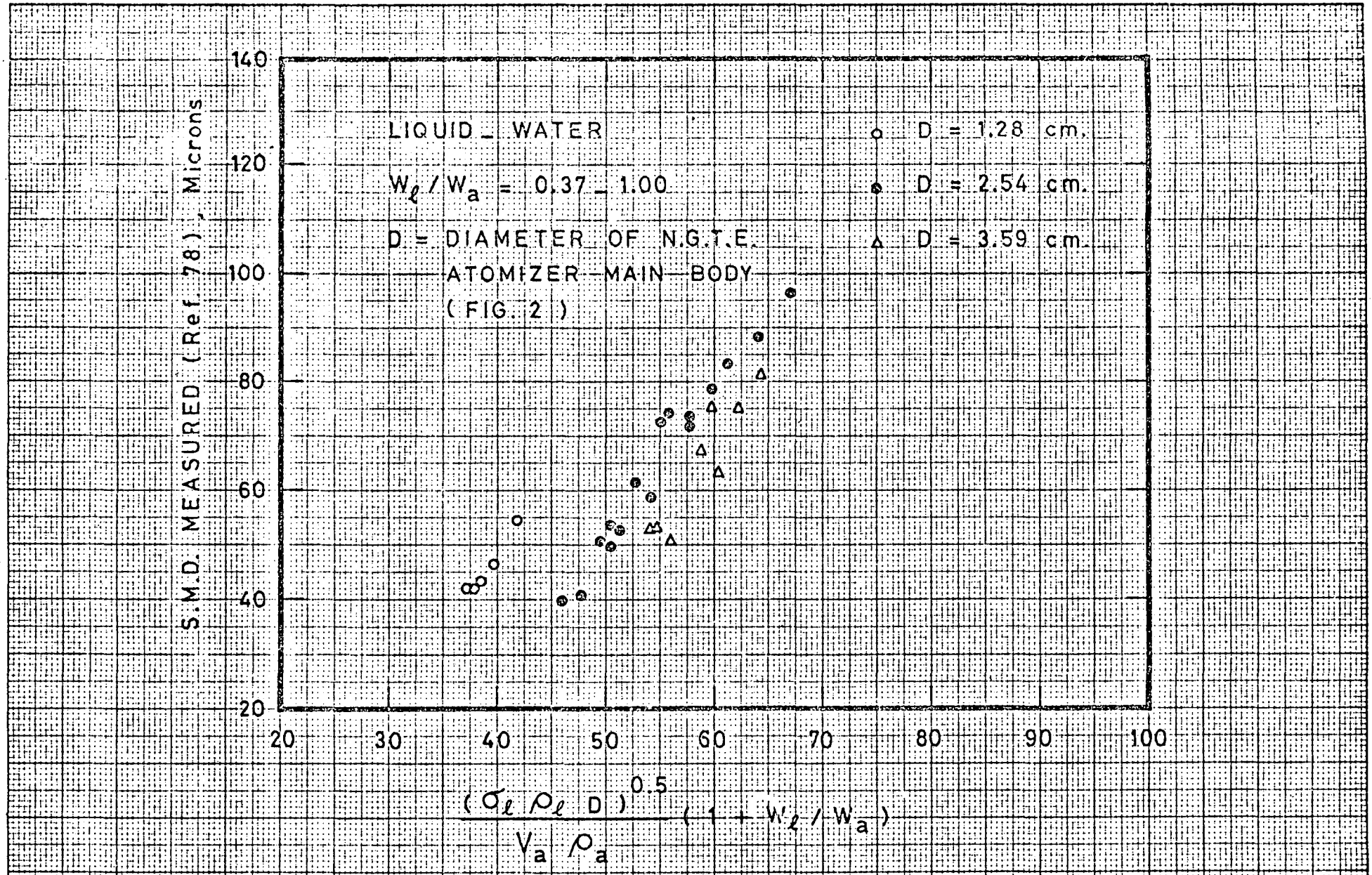

FIG. 69 COMPARISON OF MEASURED (Ref. 78) AND PREDICTED (Equation 15) VALUES OF S.M.D.

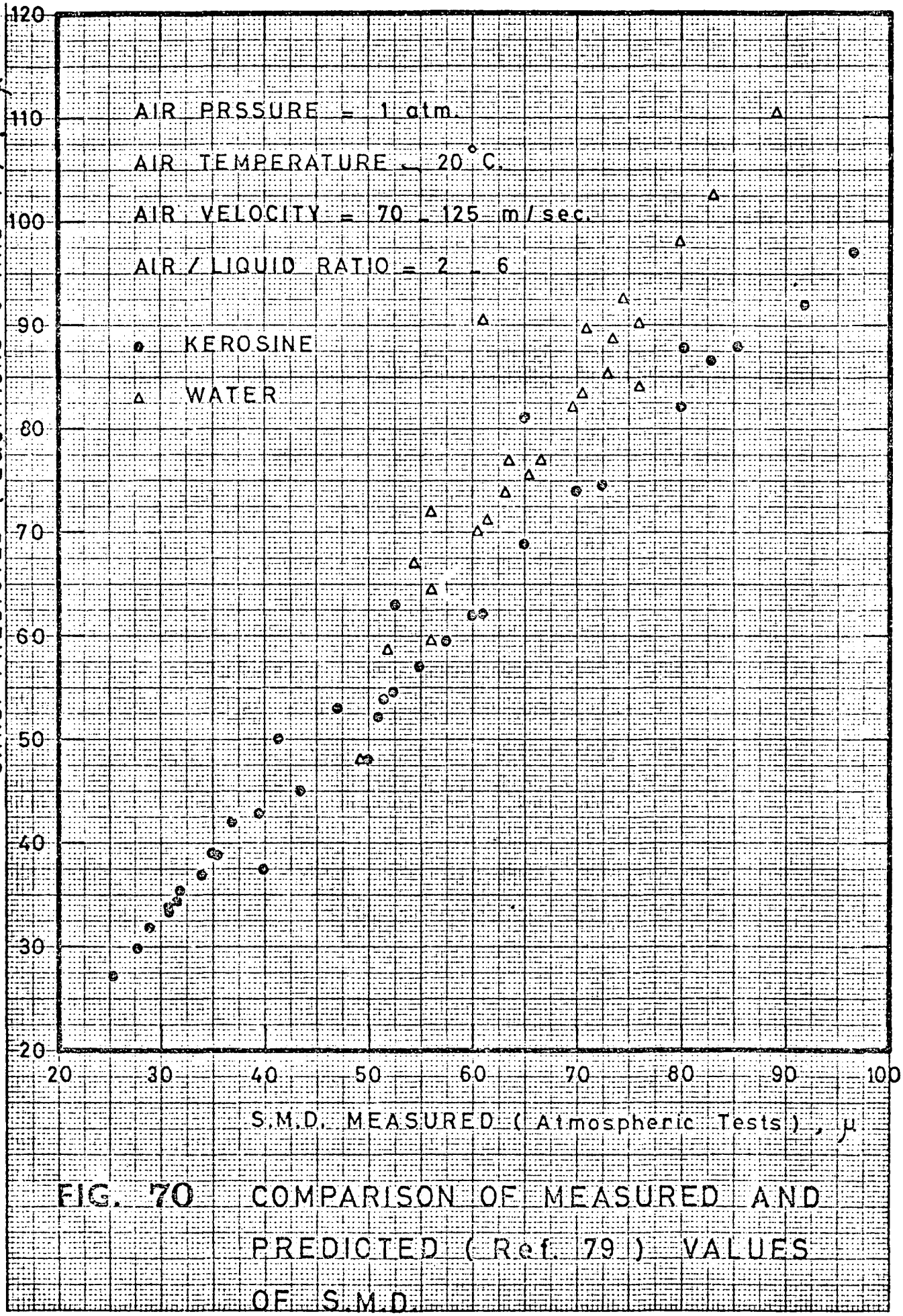

FIG. 70 COMPARISON OF MEASURED AND PREDICTED (Ref. 79) VALUES OF S.M.D.

PLATES

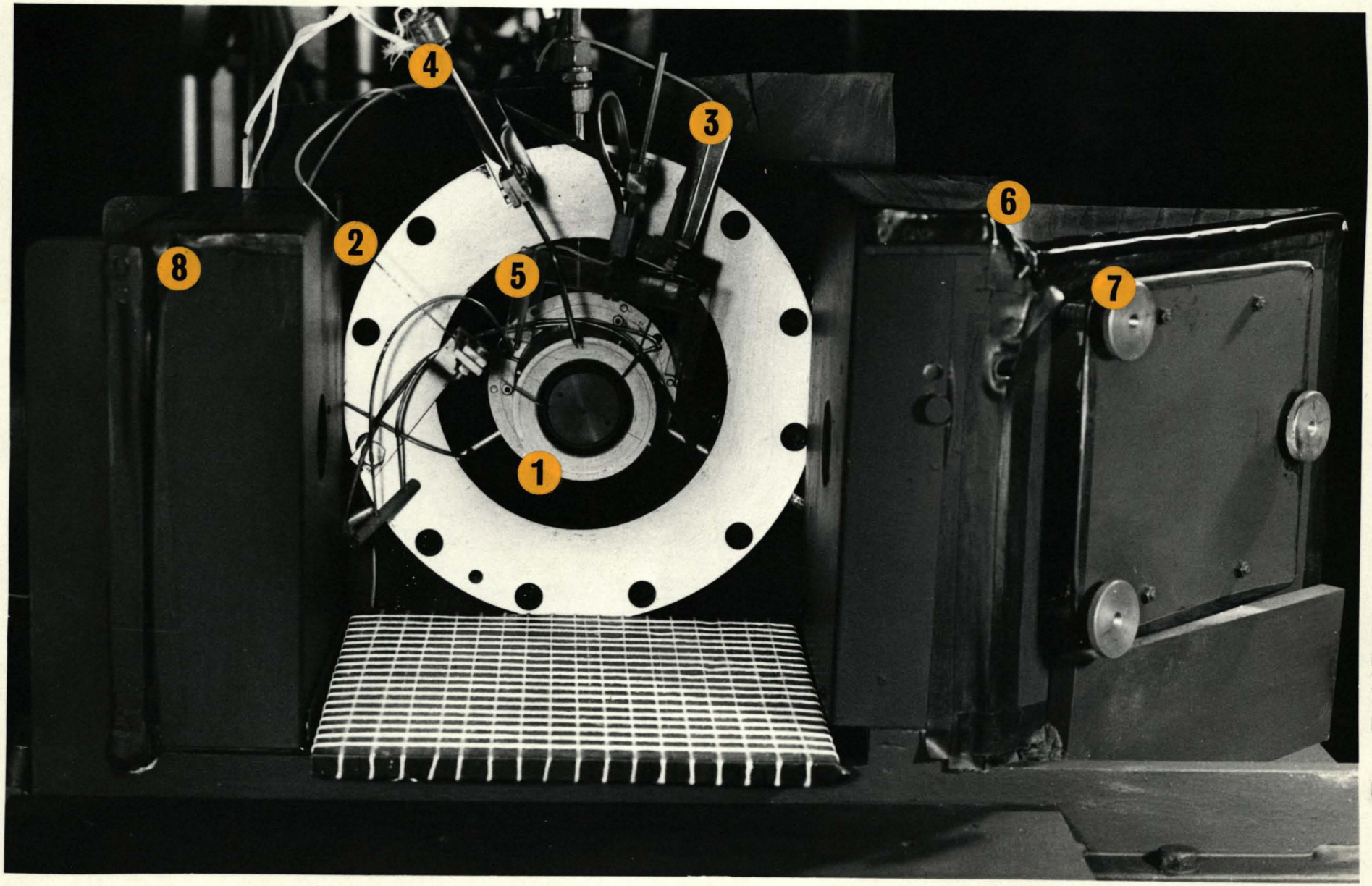

PLATE 1

1 _ AIRBLAST ATOMIZER HOUSING
2 _ SHROUD AIR PITOT TUBE
3 _ PINTLE AIR PITOT TUBE
4 _ THERMOCOUPLE (1)
5 _ THERMOCOUPLE (2)
6 _ PRISM BOX
7 _ PRISM ADJUSTING SCREWS
8 _ RECEIVER LENS BOX

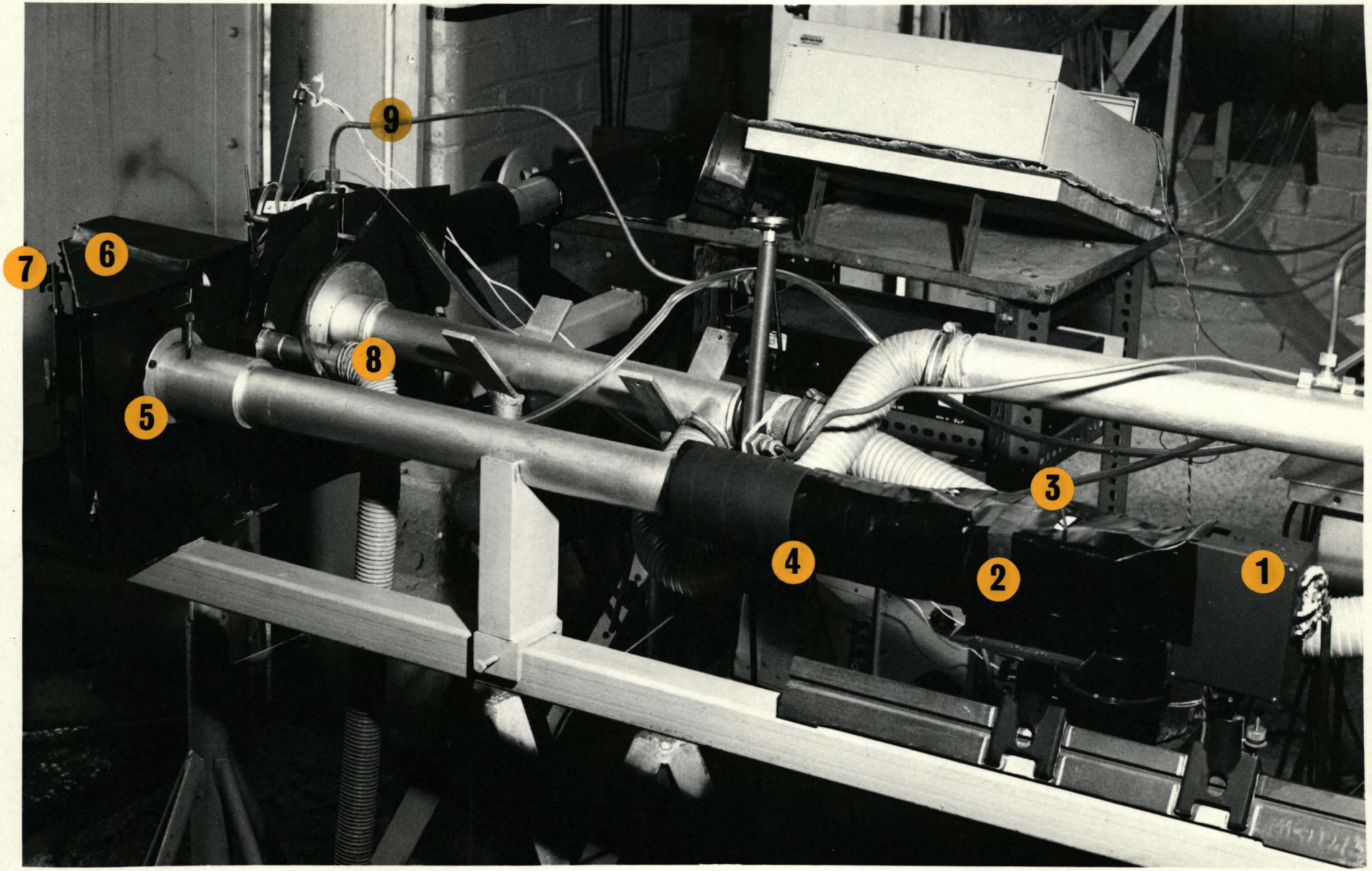

PLATE 2

1 _ LAMP HOUSING
2 _ CONDENSER BOX
3 _ IRIS DIAPHRAGM CONTROL
4 _ COLLIMATING APERTURE
5 _ COLLIMATOR LENS
6 _ PRISM MOUNT
7 _ PRISM ADJUSTING SCREWS
8 _ BLOWER TO PRISM MOUNT
9 _ LIQUID LINE

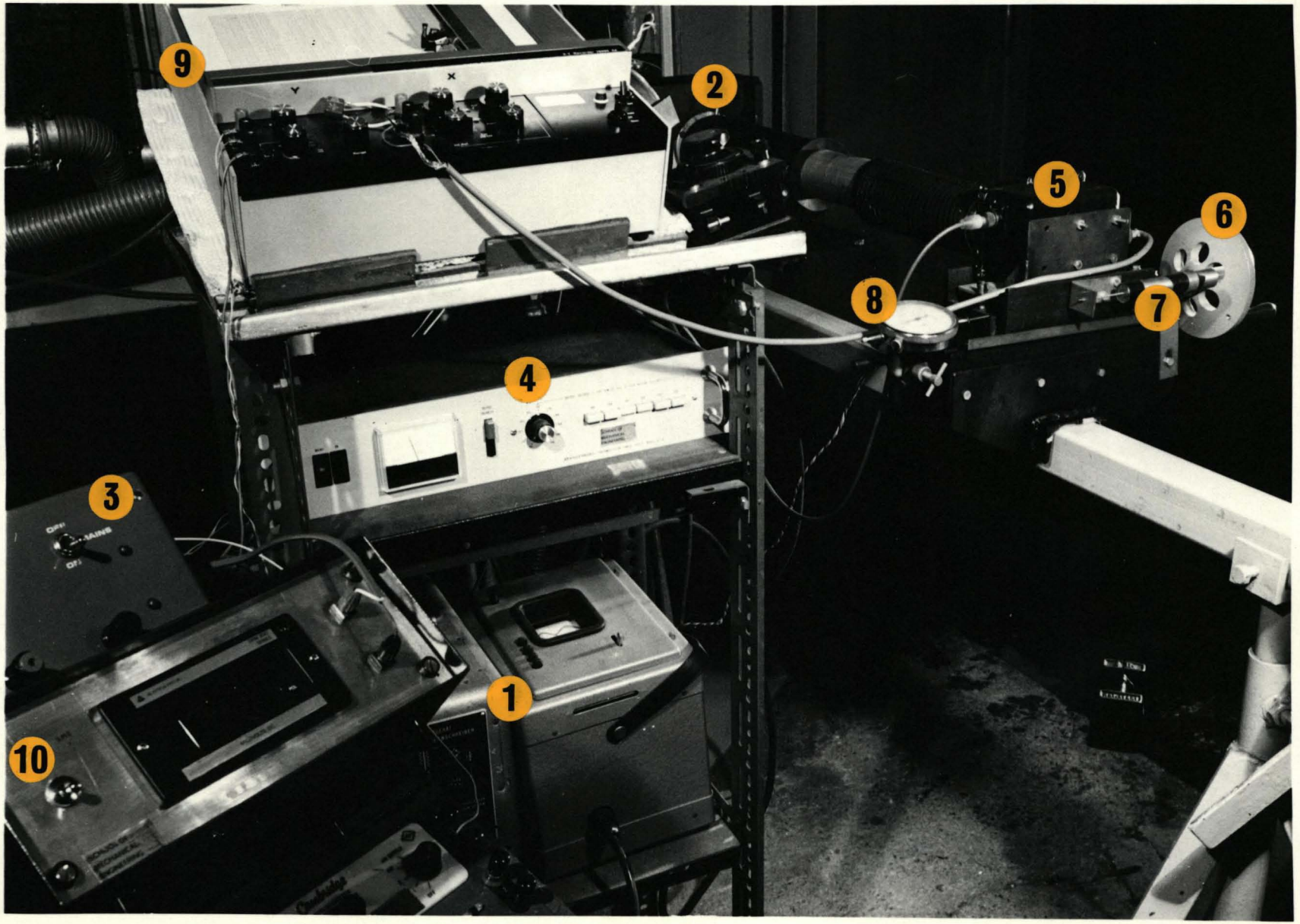

PLATE 3

1 _ LAMP POWER SUPPLY
2 _ RECEIVER LENS
3 _ X _ AXIS POWER SUPPLY
4 _ H. T. SUPPLY TO PHOTOMULTIPLIER
5 _ PHOTOMULTIPLIER BOX
6 _ TRAVERSING WHEEL
7 _ X _ AXIS TRANSDUCER
8 _ DIAL TEST INDICATOR
9 _ LOG. AMPLIFIER
10 _ DIGITAL VOLTMETER

PLATE 4

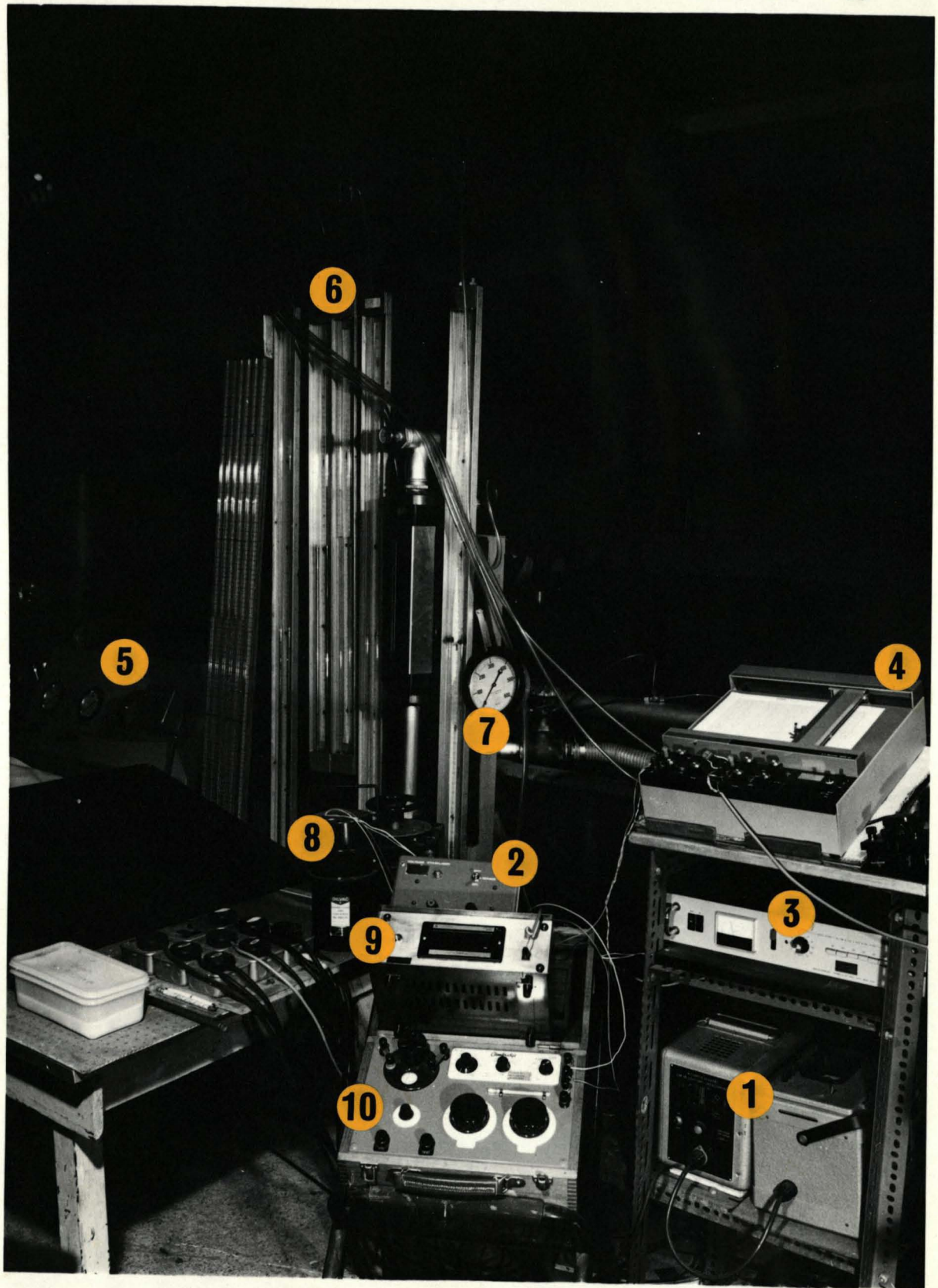

1 - LAMP POWER SUPPLY
2 - X-AXIS POWER SUPPLY
3 - H.T. SUPPLY TO PHOTOMULTIPLIER
4 - LOG. AMPLIFIER
5 - WATER PUMP
6 - MANOMETERS SET-UP
7 - LIQUID PRESSURE GAUGE
8 - THERMOCOUPLES COLD JUNCTION
9 - DIGITAL VOLTMETER
10 - GALVANOMETER

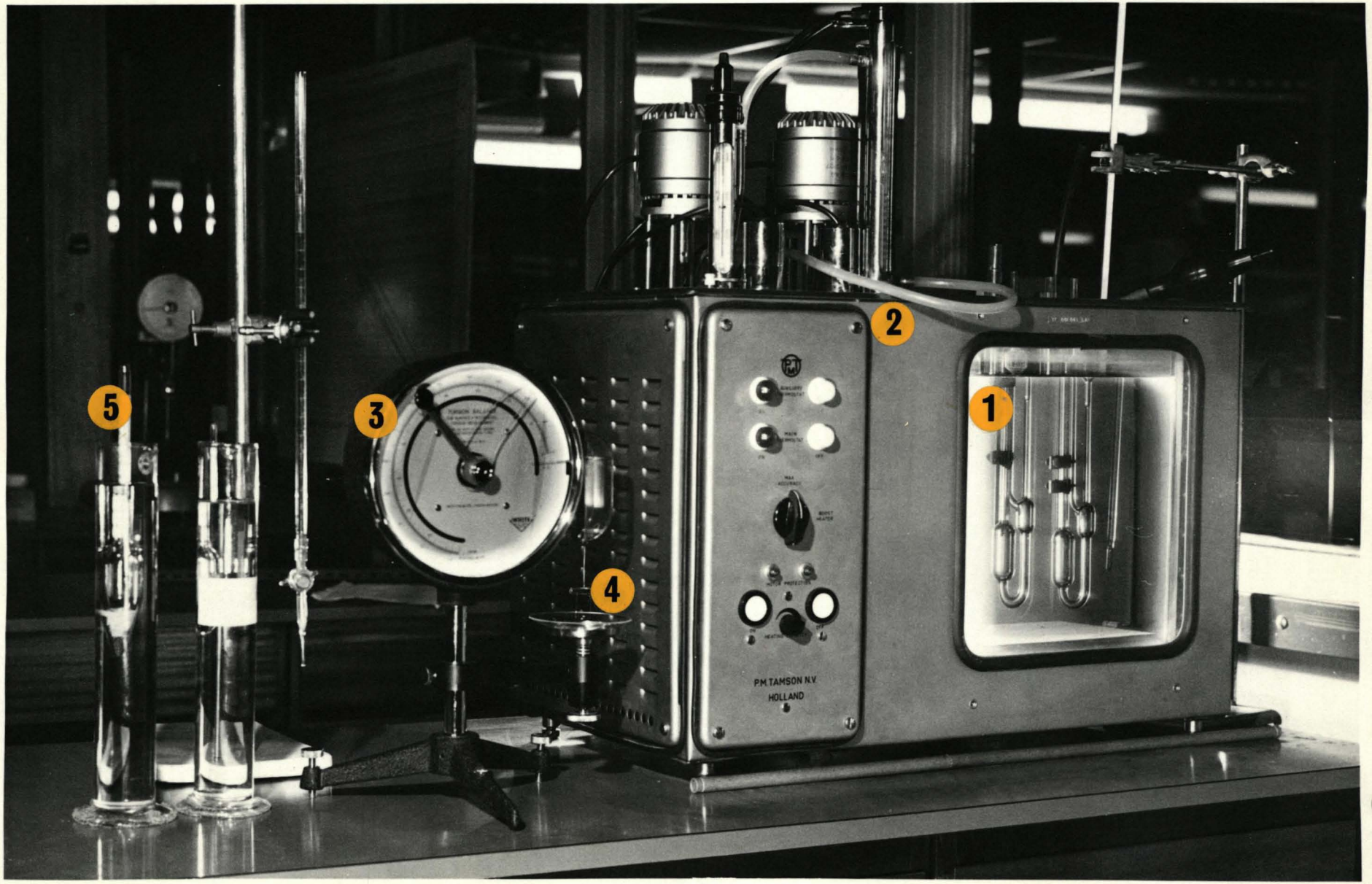

PLATE 5

1 _ PSL _ CALIBRATED SUSPENDED LEVEL VISCOMETER
2 _ THERMOSTATICALLY CONTROLLED VISCOMETER BATH
3 _ TORSION BALANCE
4 _ PLATINUM RING
5 _ RELATIVE DENSITY HYDROMETER

PLATE 6

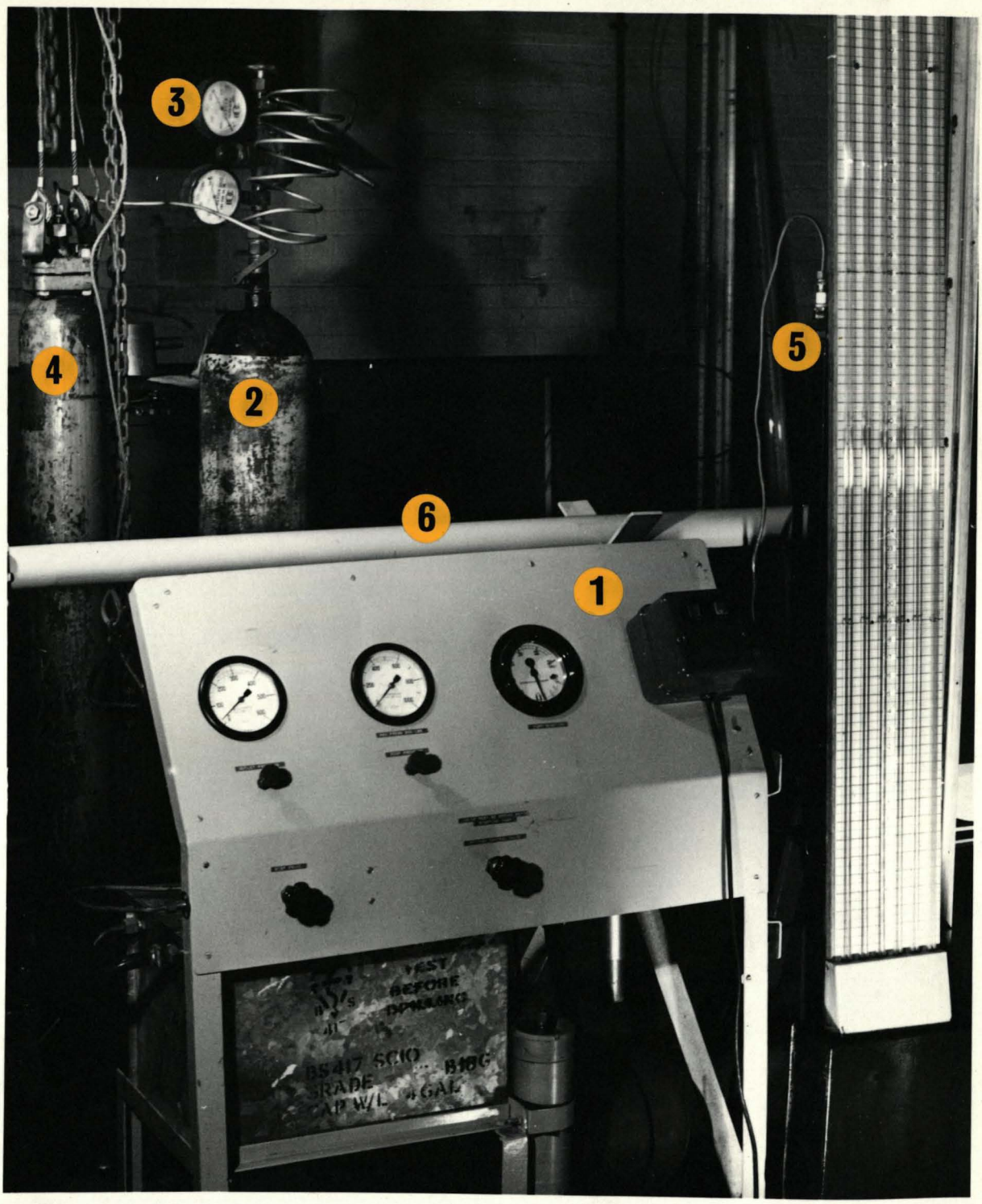

1 - WATER PUMP

2 - NITROGEN PRESSURIZING BOTTLE

3 - NITROGEN PRESSURE GAUGE

4 - LIQUID BOTTLE

5 - LIQUID FLOWMETER

6 - SHROUD AIR DUCT

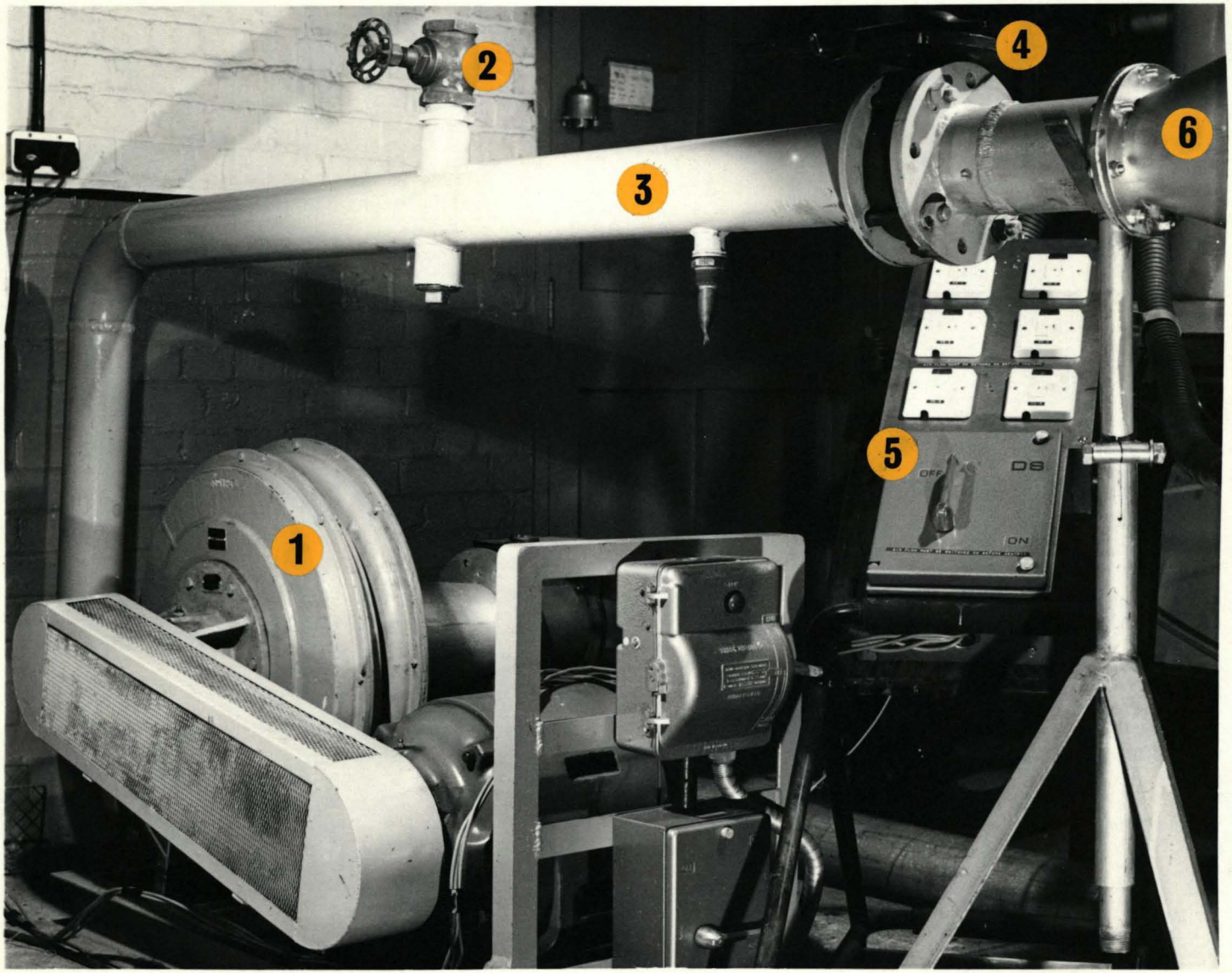

PLATE 7

1 _ AIR BLOWER
2 _ BLEEDING _ OFF VALVE
3 _ MAIN AIR DUCT
4 _ ISOLATION VALVE
5 _ AIR HEATERS SWITCHES
6 _ AIR HEATERS CASING

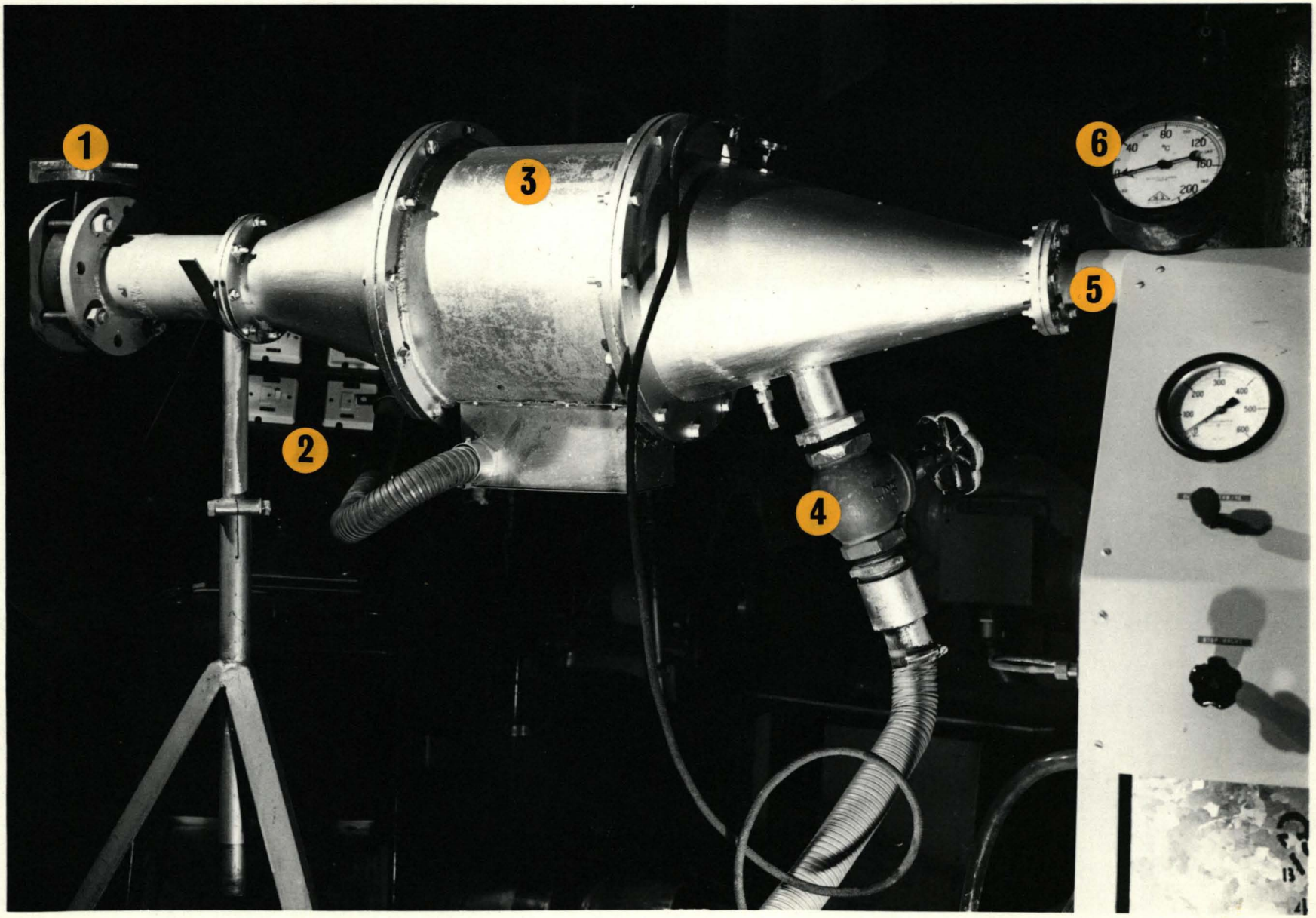

PLATE 8

1 _ ISOLATION VALVE
2 _ AIR HEATERS SWITCHES
3 _ AIR HEATERS CASING
4 _ PINTLE AIR BRANCH
5 _ SHROUD AIR DUCT
6 _ INITIAL AIR TEMPERATURE GAUGE

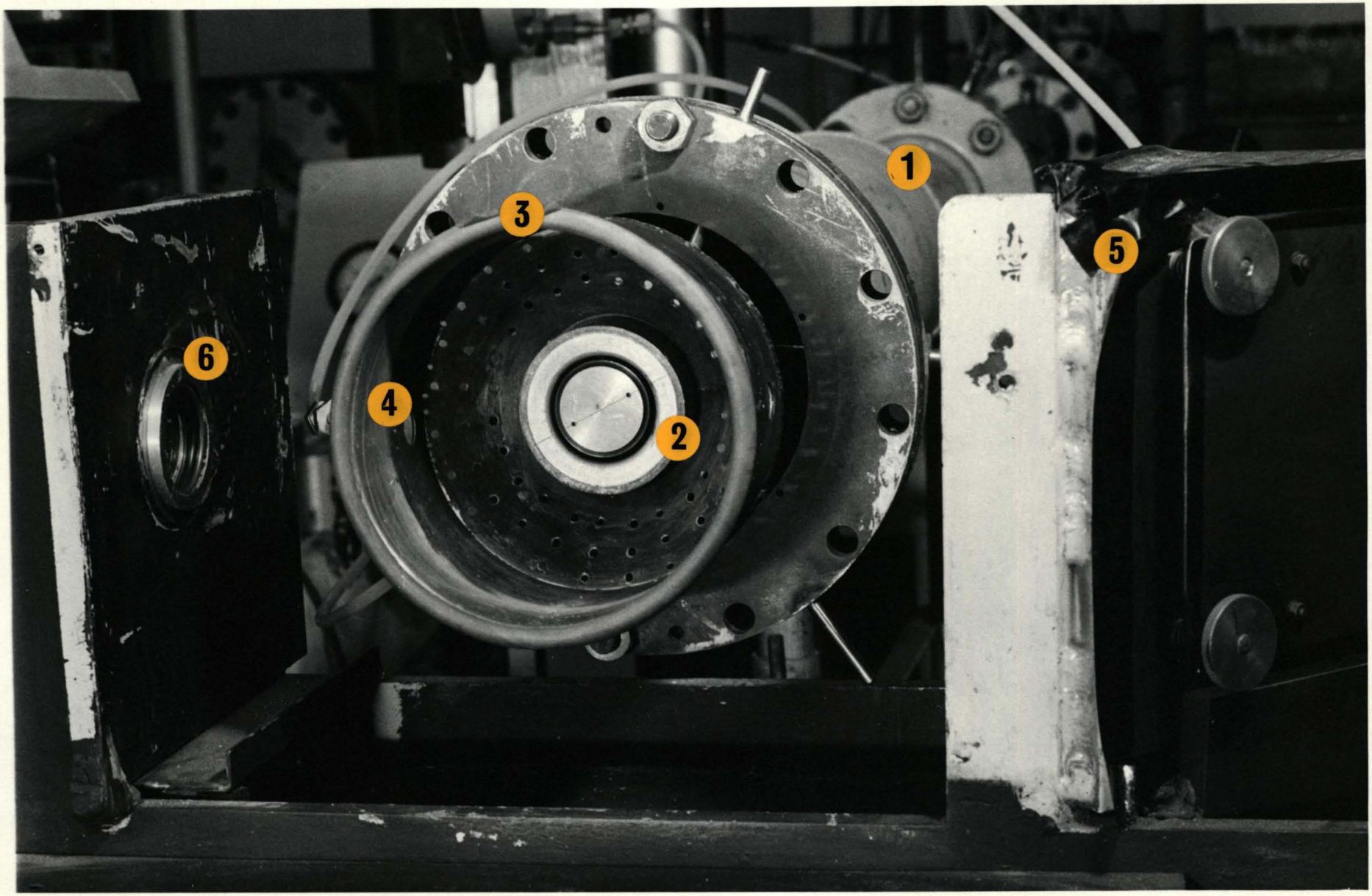

PLATE 9

1 _ H.P. AIR MAIN DUCT
2 _ AIRBLAST ATOMIZER HOUSING
3 _ FLAME TUBE
4 _ OBSERVATION HOLES
5 _ PRISM MOUNT
6 _ RECEIVER LENS

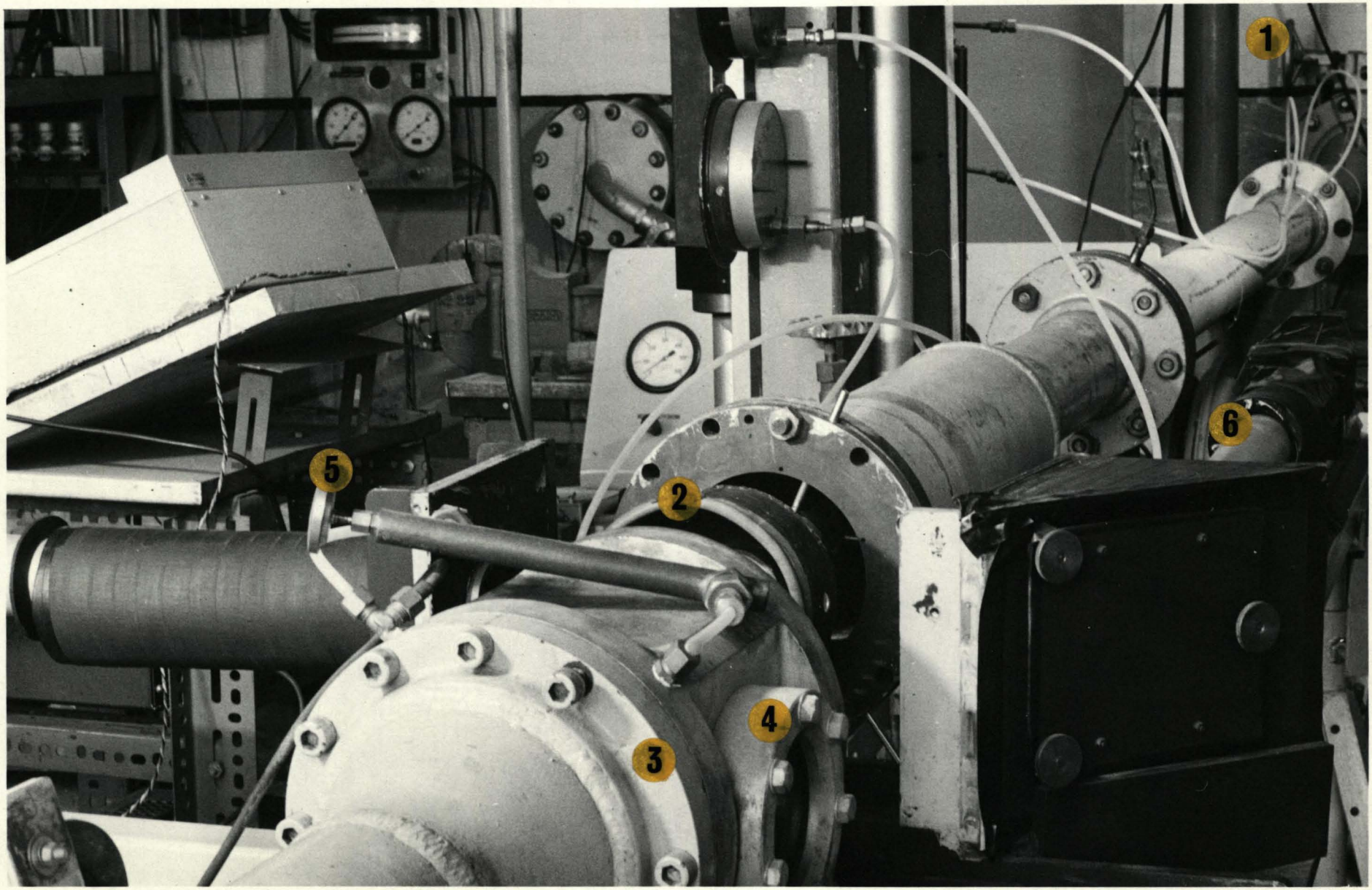

PLATE 10

1 _ H.P. AIR ISOLATION VALVE
2 _ FLAME TUBE
3 _ HIGH PRESSURE CHAMBER
4 _ OBSERVATION WINDOWS
5 _ TEMPERATURE GAUGE
6 _ THE OPTICAL BENCH

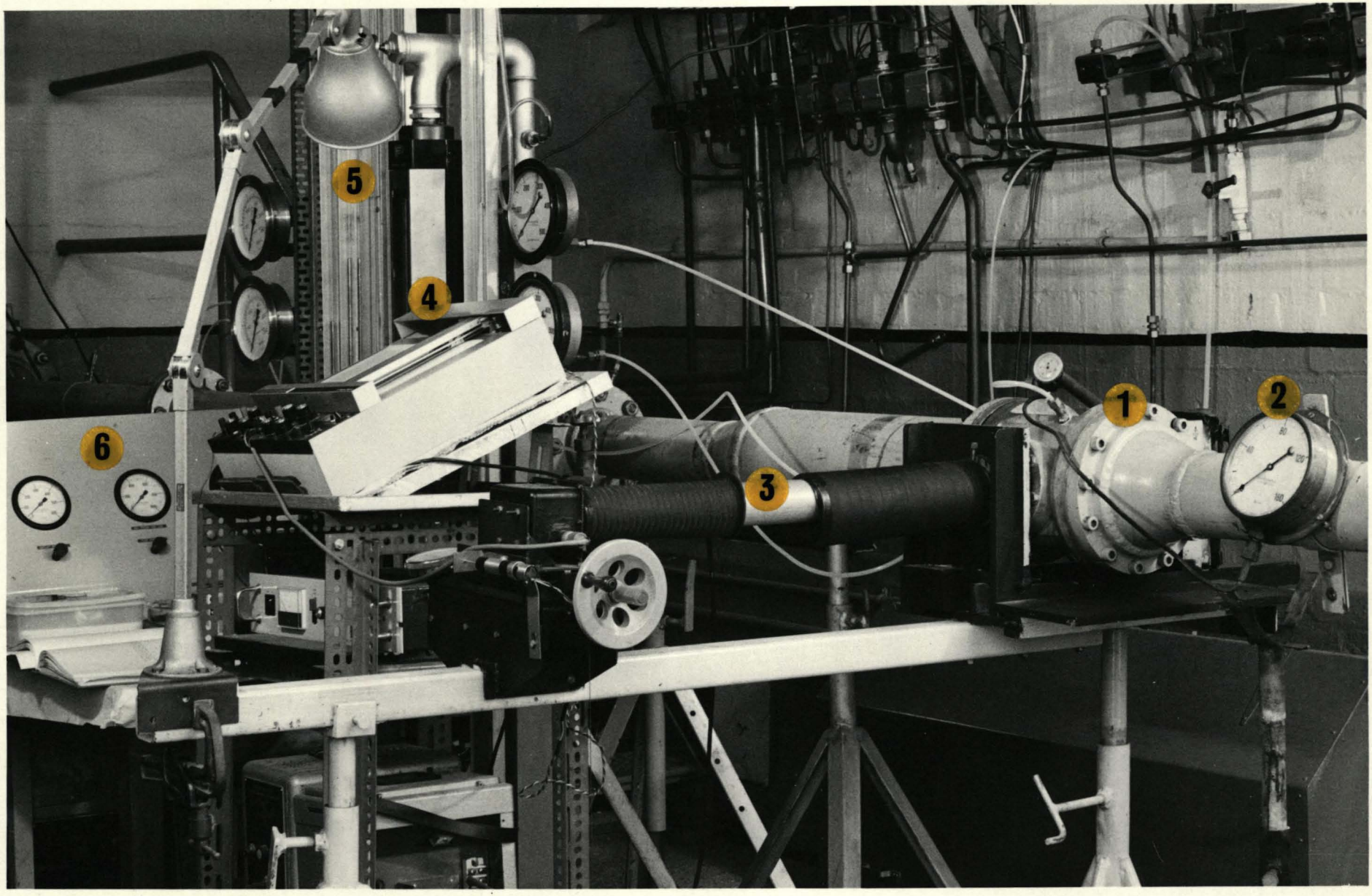

PLATE 11

1 _ HIGH PRESSURE CHAMBER
2 _ CHAMBER PRESSURE GAUGE
3 _ THE OPTICAL BENCH
4 _ LOGARITHMIC AMPLIFIER
5 _ INSTRUMENTATION PANEL
6 _ WATER PUMP